약학박사학위논문

LC-MS Based Targeted Isolation of Cyclopeptide Alkaloids and Triterpenoids from *Ziziphus jujuba* Roots with Development of Dereplication Methods

LC-MS 기반 대추나무 뿌리의 cyclopeptide alkaloids 및 triterpenoids 성분의 표적 분리 및 dereplication 방법 개발

2016 년 2 월

서울대학교 대학원

약학과 생약학전공

강 교 빈

Abstract

Ziziphus jujuba Mill. is the most economically important species in the family Rhamnaceae. Among hundreds of previously reported constituents, cyclopeptide alkaloids and ceanothane-type triterpenoids have been regarded as chemotaxonomic marker compounds of the Rhamnaceae species, and they have been focused as new drug candidates for their characteristic structures and bioactive potentials. The goal of this study was the development of targeted isolation strategy for bioactive cyclopeptide alkaloids and triterpenoids from *Z. jujuba*. UHPLC-qTOF-MS based dereplication-guided fractionation was selected as a main platform for this purpose. The analytical methods were optimized for LC-MS profiling of cyclopeptide alkaloids and triterpenic acids in MeOH extracts of *Z. jujuba* roots, twigs, leaves, and fruits. Based on UV, MS, and MS/MS spectral data, the dereplication methods were developed for cyclopeptide alkaloids and triterpenoids. Cyclopeptide alkaloids were hard to be fully predicted, but many triterpenoids could be tentatively identified with their spectra data. Based on these dereplication results, LC-MS profiles of extracts were compared for their potential as the isolation target. The root extract was selected to be a target for further separation, because of its abundance in both target compound classes. MS-guided fractionation resulted in the isolation of 9 cyclopeptide alkaloids (**1-9**), 37 triterpenoids (**10-46**), and 6 phenolic compounds (**47-52**) from the root extract. Among these 52 compounds, 5 cyclopeptide alkaloids (**1-5**) and 21 triterpenoids (**16-20**, **23**, **24**, **26**, **27**, **30**, **33**, and **35-43**) were isolated from nature for the first time. In-house LC-MS library was built with the retention time and spectral data of isolated compounds, and it was confirmed that tentatively predicted structures of triterpenoids were correctely matched to their real structures. In addition, it was suggested that dereplication method for cyclopeptide alkaloids could be developed in the further study. Bioactivity of isolated compounds were tested, and as a result, antiviral activity of cyclopeptide alkaloid compounds **2**, **3**, and **6** against PEDV (EC_{50} 4.49-3.41 μM) and cytotoxicity of triterpenic compounds **10**, **22**, **28-30**, **33**, **35**, **36**, and **41** against HepG2 cell line (IC_{50} 1.93-9.24 μM) were evaluated. In conclusion, it was demonstrated that developed UHPLC-qTOF-MS based derelication

method was an efficient strategy for the discovery of bioactive cyclopeptide alkaloids and triterpenoids from *Z. jujuba*.

Keyword: *Ziziphus jujuba*, UHPLC-qTOF-MS, cyclopeptide alkaloids, triterpenoids, dereplication

Student Number: 2012-30455

Table of Contents

List of Schemes

List of Tables

List of Figures

List of Abbreviations

$[\alpha]_D$: specific rotation

Ala: alanine

n-BuOH: *n*-butanol

CC: column chromatography

CD: circular dichroism

$CHCl_3$: chloroform

COSY: correlation spectroscopy

d: doublet

dd: doublet of doublet

dt: doublet of triplet

DMSO: dimethylsulfoxide

ESI: electron spray ionization

EtOAc: ethyl acetate

GITC: 2,3,4,6-tetra-*O*-acetyl-β-D-glucopyranosyl isothiocyanate

h: hours

HMBC: heteronuclear multi-bond correlation

HPLC: high performance liquid chromatography

HSQC: heteronuclear single quantum coherence

Hz: hertz

IC_{50}: the half maximal inhibitory concentration

Ile: isoleucine

IR: infrared spectroscopy

Leu: leucine

m: multiplet

me-HSQC: multiplicity-edited heteronuclear single quantum coherence

MeCN: acetonitrile

MeOH: methanol

mp: melting point

MS: mass spectrometry

MTT: 3-(4,5-dimethylthiozol-2-yl)-2,5-diphenyltetrazolium bromide

N-MeAla: *N*-methylalanine

NMR: nuclear magnetic resonance

N,N-diMeAla: *N,N*-dimethylalanine

NOESY: nuclear Overhauser enhancement spectroscopy

ODS: octadeca silica

PDA: photodiode array detector

PGME: phenylglycine methylester hydrochloride

q: quartet

qTOF: quadrupole - time of flight

ROESY: rotating-frame nuclear Overhauser effect correlation spectroscopy

rt: room temperature

s: singlet

t: triplet

td: triplet of doublet

TLC: thin layer chromatography

t_R: retention time

UHPLC: ultra high performance liquid chromatography

UV: ultraviolet absorption spectroscopy

Val: valine

Chapter 1. Introduction

1.1. Study background

1.1.1. The family Rhamnaceae and the species *Ziziphus jujuba*

The family Rhamnaceae is widely distributed in the world, inhabiting tropical, subtropical and temperate area. The family contains woody, herbaceous, and scandent species which could be characterized by flowers with cucullate, convolute or conchiform petals, antipetalous stamens, and a nectariferous disc internally enclosing the floral receptacles (de Lima and Giulietti, 2014). There are more than 900 species within about 60 genera in the family, and among them, fourteen species within seven genera of Rhamnaceae have been reported to occur in Korea (Mun and Jeong, 2006).

Ziziphus jujuba Mill. is a 5 - 8 m tall deciduous tree which is widely cultivated in South Europe and Asia, including Russia, India, the Middle East, and China (Outlaw et al., 2002). The genus *Ziziphus* is recognized as the most economically important genera in the Rhamnaceae family (Meng et al., 2013). More than 170 species of plants have been classified as the genus *Ziziphus,* and among them *Z. jujuba* is considered as the most important species for the fruit production (Gao et al., 2013). Fruits of *Z. jujuba*, commonly as dried fruits, have been utilized as food, food additive, and flavoring for thousands of years because of its high nutritional value (Li et al., 2007a). In addition to their food uses, they have been used in many traditional medicines. Their seeds are especially known for their sedative effect, which might be caused by their flavonoids (Jiang et al., 2007).

Due to its frequent usages of this plant in many traditional medicines, the chemical constituents of *Z. jujuba* have been widely studied, resulting in hundreds of reported compounds including triterpenic acids (Guo et al., 2010), flavonoids

(Pawlowska et al., 2009), phenolic acids (Gao et al., 2011), and alkaloids (Tripathi et al., 2001). Among these compounds, ceanothane-type triterpenoids and cyclopeptide alkaloids have been considered as chemotaxomonic marker constituents of Rhamnaceae species (Guo et al., 2011b; Tan and Zhou, 2006).

1.1.2. Cyclopeptide alkaloids

Cyclopeptide alkaloids are defined as basic compounds containing a *p*- or *m*-ansa 13, 14, or 15- membered ring structure that consists of a styrylamine moiety and two or three α-amino acid residues (Schmidt et al., 1985). In many cases, they possess one or two side-chain *N*-methyl or *N,N*-dimethyl α-amino acid residues. They are the largest subtype, type I, among the eight subtypes of plant cyclopeptides which have been discovered from higher plants. 455 cyclopeptides had been discovered in higher plants up to 2005, and among them, 185 belong to type I (Tan and Zhou, 2006). Except few cases, most of cyclopeptide alkaloids have been discovered in Rhamnaceae species. Therefore, cyclopeptide alkaloids are also called Rhamnaceae-type cyclopeptides.

Cyclopeptide alkaloids are divided into three types: Ia, Ib, or Ic, according to the size of a macro-ring structure, and type Ia also includes four subtypes Ia1, Ia2, Ia3, and Ia4, based on the β–hydroxyl amino acid residue (Figure 1). Because of their restricted natural availability (0.0002-1%), their biological properties have not been studied very well (Gournelis et al., 1998). However, some experimental evidences have been reported, which shows cyclopeptide alkaloids may function as ionophores in plants (Kawai et al., 1977; Lagarias et al., 1978). Sedative, antibacterial, antifungal, antiplasmodial, antimycobacterial, and antimalarial effects have been reported for some cyclopeptide alkaloids (Gournelis et al., 1998; Panseeta et al., 2011; Tan and Zhou, 2006).

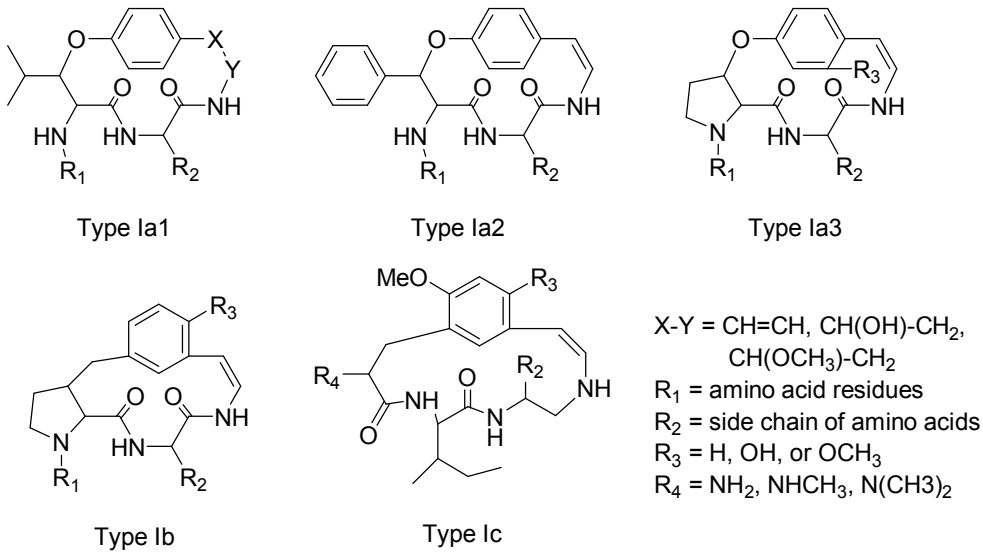

Figure 1. Types of cyclopeptide alkaloids (Tan and Zhou, 2006)

Although the fruit is the most widely used part of *Z. jujuba* for food, cyclopeptide alkaloids have been separated from other plant parts, especially from the stem bark. Four Ia-type (frangufoline, scutianine D, jubanine C, and mauritine A) and eight Ib-type cyclopeptide alkaloids (amphibine H, jubanine A, jubanine B, jubanine E, mucronine D, nummularine A, nummularine B, and zizyphine A) have been isolated and reported from the *Z. jujuba* stem bark (Devi et al., 1987; Pandey et al., 2008; Tripathi et al., 2001; Tschesche et al., 1976). Only one publication has reported cyclopeptide alkaloids from the *Z. jujuba* root, and these alkaloids are mauritine A and seven Ib-type cyclopeptide alkaloids: mucronine D, amphibine H, jubanine A, jubanine B, jubanine D, nummularine A, and nummularine B (Khokhar et al., 1994). Nothing has been reported about their bioactivities. However, other *Ziziphus* species such as *Z. abyssinica, Z. mucronata, Z. oenoplia, Z. sativa, Z. nummularia,* and *Z. mauritiana* have yielded so various cyclopeptide alkaloids, including every types of Ia1, Ia2, Ia3, Ib, and Ic. Therefore, *Z. jujuba* has

a great potential as a candidate for discovery of unknown cyclopeptide alkaloid entities.

1.1.3. Ceanothane-type triterpenoids

Triterpenoids with a five-membered A-ring have been rarely reported in the nature. However, some of them were isolated from the aerial and subterranean parts of plants used in traditional folk medicines as sedative, hypoglycemic, antibacterial, antifungal, antiviral, anticonvulsive, anti-inflammatory, and hemostatic agents in Asia, Africa, India, Australia, Europe, and North and South America, and exhibited valuable biological properties (Grishko et al., 2015). The most well-known natural triterpenoids with a five-membered A-ring are ceanothane-type triterpenoids. This name came from ceanothic acid, which was first isolated from the outer root bark of *Ceanothus americanus* in 1938 by Julian et al (Julian et al., 1938). Ceanothane-type triterpenoids possess the same structural characters with pentacyclic lupane-type triterpenoids, such as five-membered E-ring and the presence of isopropenyl moiety at C-19 position of the E-ring. Therefore, ceanothane-type triterpenoids have been considered to be biosynthesized by rearrangement of a six-membered A-ring of lupane-type triterpenoids. Biosynthetic pathway of this rearrangement has not been fully revealed, but several researchers proposed possible biosynthetic pathways. Most of them included selective 2,3-fragmentation of a six-membered

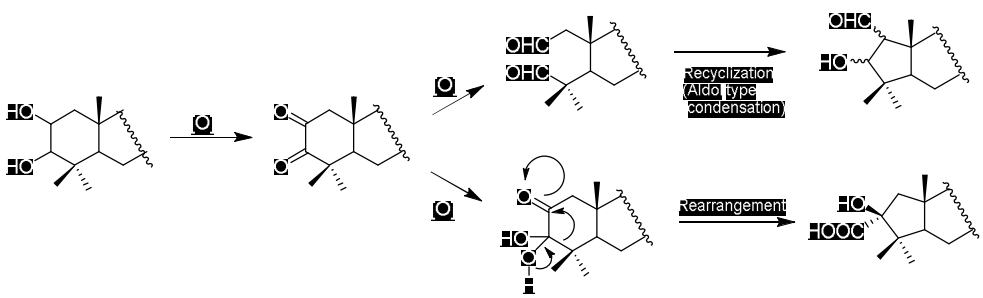

Figure 2. Proposed biosynthetic pathways of a five-membered A-ring (Grishko et al., 2015)

A-ring and subsequent recyclization forming a cyclopentanyl A-ring containing various functional groups at C-1 and C-3 (Figure 2). This could explain the variety in configurations of functional groups at C-1 and C-3 in previously reported ceanothane-type triterpenoids.

Since the first isolation of ceanothic acid, that compound was reported from various species of plants, and its derivatives were also described. Most of discovery of ceanothane-type triterpenes have been occurred in plants belonging to the family Rhamnaceae, except some of derivatives observed in separate species such as *Gleditsia sinensis* (Leguminosae), *Allophylus longipes* (Sapindaceae), *Breynia fruticose* (Phyllanthaceae), and *Dysoxylum hainanense* (Meliaceae). Chemical structures of previously reported natural ceanothane-type triterpenoids are shown in Figure 3, and their trivial names and sources of isolation are shown in Table 1.

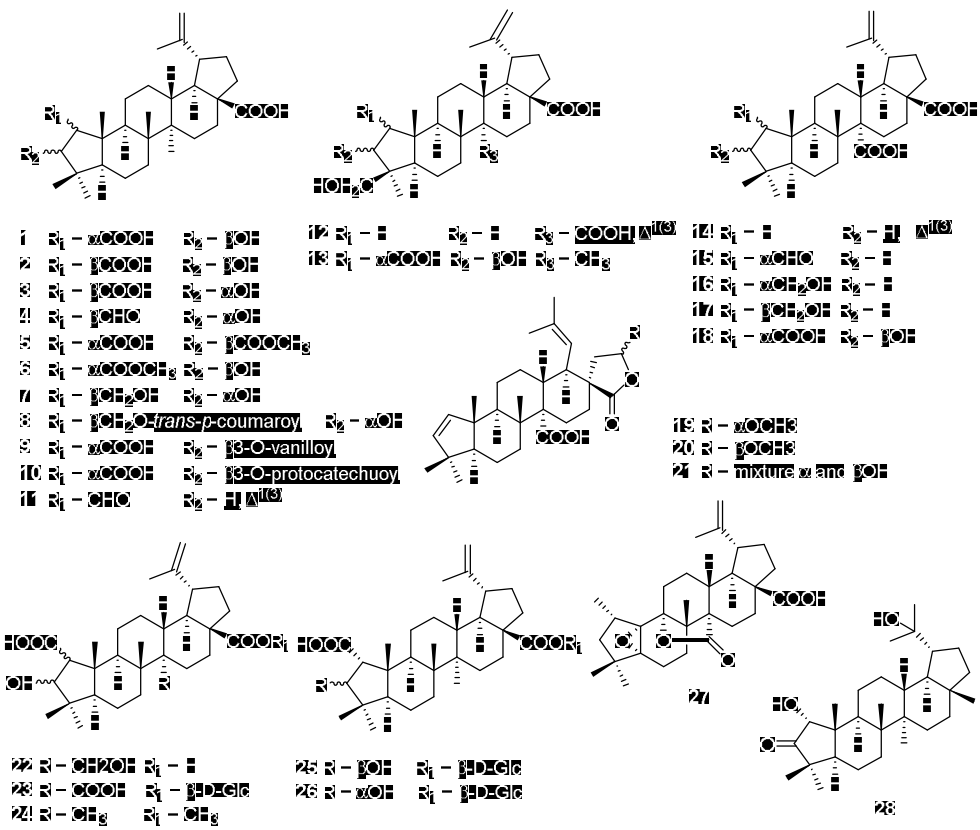

Figure 3. Chemical structures of previously reported natural ceanothane-type triterpenoids

Table 1. Distribution of ceanothane-type triterpenoids in plant species from Rhamnaceae, *Sapindaceae, **Leguminosae, ***Phyllanthaceae, and ****Meliaceae. Adapted from (Grishko et al., 2015) and modified

Compound	Plant source, plant part, reference
Ceanothic acid (**1**)	*Alphitonia philippinensis*: stems (Jou et al., 2004) *Ceanothus americanus*: root bark (Li et al., 1997) *Colubrina greggii* var. *yucatanensis*: root (Dominguez-Carmona et al., 2011) *Paliurus ramosissimu*: root, stem bark (Lee et al., 1992; Lee et al., 1991) *Ziziphus cambodiana*: root bark, leaves (Arai et al., 2008; Suksamrarn et al., 2006) *Ziziphus glabrata*: stem bark (Ganapaty et al., 2006) *Ziziphus jujuba*: bark, root, fruit, seeds (Fujiwara et al., 2011; Guo et al., 2010; Sekar et al., 1992) *Ziziphus jujuba* var. *spinosa*: root, fruit (Guo et al., 2011b) *Ziziphus mauritiana*: root (Ji et al., 2012) *Talguenea quinquenervia*: aerial parts and root (Quiroz et al., 2015)
Epiceanothic acid (**2**)	*Gleditsia sinensis***: thorns (Li et al., 2007b) *Zizyphus jujuba*: seeds and fruit (Fujiwara et al., 2011; Guo et al., 2010) *Zizyphus jujuba* var. *spinosa*: seeds and fruit (Guo et al., 2011b; Li et al., 2005)
Isoceanothic acid (**3**)	*Zizyphus xylopyrus*: stem wood (Jagadeesh et al., 2000)
Zizyberanalic acid (**4**)	*Ziziphus jujuba*: stem bark (Kundu et al., 1989) *Ziziphus jujuba*: fruit (Guo et al., 2009b; Yu et al., 2012) *Talguenea quinquenervia*: aerial parts and root (Quiroz et al., 2015)
3-*O*-acetylceanothic acid (**5**)	*Colubrina greggii* var. *yucatanensis*: root (Dominguez-Carmona et al., 2011)
Ceanothic acid 2-methyl ester (**6**)	*Ziziphus jujuba*: stems (Fujiwara et al., 2011)
Ceanothanolic acid (**7**)	*Paliurus hemsleyanus*: root (Lee et al., 1997) *Ziziphus cambodiana*: leaves (Arai et al., 2008)
2-*O*-*trans*-*p*-coumaroyl-ceanothanolic acid (**8**)	*Paliurus hemsleyanus*: root (Lee et al., 1997)
3-*O*-vanilloyl ceanothic acid (**9**)	*Ziziphus cambodiana*: root bark (Suksamrarn et al., 2006)
3-*O*-protocatechuoyl ceanothic acid (**10**)	*Ziziphus jujuba* var. *spinosa*: root (Lee et al., 1996)
Zizyberenalic acid (**11**)	*Allophylus longipes**: stems (Zhang et al., 2012) *Alphitonia philippinensis*: stems (Jou et al., 2004) *Paliurus hemsleyanus*: root (Lee et al., 1997) *Ziziphus cambodiana*: root bark (Suksamrarn et al., 2006) *Ziziphus jujuba*: fruit (Lee et al., 2003; Lee et al., 2004; Yu et al., 2012)

	Talguenea quinquenervia: aerial parts and root (Quiroz et al., 2015)
Gouanic acid B (**12**)	*Gouania ulmifolia* : aerial part (Giacomelli et al., 2007)
24-Hydroxyceanothic acid (**13**) (granulosic acid)	*Paliurus ramosissimus* : root (Lee et al., 1992) *Ziziphus glabrata*: leaves (Ganapaty et al., 2006)
Ceanothenic acid (**14**)	*Alphitonia philippinensis*: stems (Jou et al., 2004) *Colubrina greggii* var. *yucatanensis*: root (Dominguez-Carmona et al., 2011) *Ziziphus jujuba*: fruit (Yu et al., 2012) *Ziziphus mauritiana*: root (Ji et al., 2012)
Zizyberanal acid (**15**) (colubrinic acid)	*Allophylus longipes**: stems (Zhang et al., 2012) *Gleditsia sinensis***: thorns (Li et al., 2007b) *Paliurus hemsleyanus*: root (Lee et al., 1997) *Trevoa trinervis*: aerial part (Erazo et al., 1998) *Ziziphus cambodiana*: root bark, leaves (Arai et al., 2008; Suksamrarn et al., 2006) *Ziziphus jujuba*: fruit (Guo et al., 2009a; Lee et al., 2003; Lee et al., 2004; Yu et al., 2012)
Epigouanic acid A (**16**)	*Ziziphus joazeiro*: bark (Leal et al., 2010)
Gouanic acid A (**17**)	*Gouania ulmifolia* : aerial part (Giacomelli et al., 2007)
Ceanothetric acid (**18**)	*Ceanothus americanus*: root bark (Li et al., 1997) *Ziziphus cambodiana*: leaves (Arai et al., 2008)
Zizymauritic acid A (**19**)	*Ziziphus mauritiana*: root (Ji et al., 2012)
Zizymauritic acid B (**20**)	*Ziziphus mauritiana*: root (Ji et al., 2012)
Zizymauritic acid C (**21**)	*Ziziphus mauritiana*: root (Ji et al., 2012)
27-Hydroxyceanothic acid (**22**)	*Ceanothus americanus*: root bark (Li et al., 1997) *Paliurus ramosissimus*: root (Lee et al., 1992)
Hovetrichoside H (**23**)	*Hovenia trichocarea*: bark (Yoshikawa et al., 1998)
Ceanothic acid 28-methyl ester (**24**)	*Ziziphus joazeiro*: bark (Leal et al., 2010) *ziziphus jujuba*: seeds (Fujiwara et al., 2011)
Ceanothic acid 28-β-D-glucopyranoside (**25**)	*Paliurus ramosissimus* : root, stem bark (Lee et al., 1991)
Isoceanothic acid 28-β-D-glucopyranoside (**26**)	*Paliurus ramosissimus* : root, stem bark (Lee et al., 1991)
Breynceanothanolic acid (**27**)	*Breynia fruticosa****: root (Liu et al., 2011)
Dysoxyhainol (**28**)	*Dysoxylum hainanense*****: branches and leaves (He et al., 2009)

As written above, biological activities of ceanothane-type triterpenoids have turned many researchers' interests to themselves. Various biological activities were reported for compounds of this class, including cytotoxic, antibacterial, antiparasitic, anti-inflammatory, and antiviral activities, but the most important activities of these compounds are cytotoxicity and antiviral activity. Betulinic acid, the most abundant lupane-type triterpenic acid derivative in the plant world, has been well known for its potential as a chemotherapeutic for cancer and HIV infection (Cichewicz and Kouzi, 2004). Ceanothane-type triterpenoids are kinds of

structural derivatives of betulinic acids, so they have been expected to possess similar bioactivities. However, ceanothane-type triterpenoids with a saturated A-ring, such as ceanothic acid, isoceanothic acid, zizyberanalic acid, and ceanothanolic acid exhibited none of weak cytotoxicity according to several previous researches (Arai et al., 2008; Dominguez-Carmona et al., 2011; Fujiwara et al., 2011; Ji et al., 2012). Compounds with unsaturated A-ring, such as zizymauritic acids and zizyberanalic acid, exhibited significant cytotoxicity to various cancer cell lines [IC_{50} 5.50 (A549), 5.36 (HeLa), and 6.24 μg/mL (BGC-823) for zizymauritic acid A, and 43 μM (PANC1) for zizyberanalic acid] (Arai et al., 2008; Ji et al., 2012). Semi-synthetic approaches to ceanothane-type triterpenoids for enhancing their cytotoxicity against tumor cells have also tried. According to lee et al., 1-nor derivatives of ceanothic acid exhibited pronounced (IC_{50} 2.8-9.1 μg/mL) cytotoxicity against OVCAR-3 and HeLa cell lines (Lee et al., 1998). Epiceanothic acid and its synthetic intermediates from betulin were evaluated for cytotoxic activity against PC3, A549, MCF-7, HeLA, and BGC-823 cells by Zhang et al. (Zhang et al., 2011). Epiceanothic acid exhibited selective cytotoxicity against BGC-823 (IC_{50} 2.41 μM), while one of synthetic intermediate, 3-*O*-acetyl epiceanothic acid 2-methyl ester showed potent cytotoxicity against other cancer cell lines, A549 and MCF-7 with IC_{50} values of 0.89 and 0.33 μM, respectively. It has been rarely revealed about the biomolecular mechanism of ceanothane-type triterpenoids for their cytotoxicity. According to Arai et al., cytotoxicity against cancer cells by zizyberanalic acid would be caused by inhibition of the Hh/GLI signaling and of the expression the anti-apoptosis protein BCL12 (Arai et al., 2008). Epiceanothic acid has been also known as its antiviral activity against HIV-1 (EC_{50} < 0.064 μg/mL) (Li et al., 2007b). A-seco triterpenoids have been reported to have high levels of biological activities including antiviral effects against HIV-1 and influenza A virus, so semi-synthetic approaches have been performed (Grishko et al., 2014). However, almost nothing more has been reported about antiviral activities of natural ceanothane-type triterpenoids.

1.1.4. Dereplication of natural products

The more natural metabolites have been discovered by researchers, the harder it is getting to discover new chemical entities from natural products for the last several decades. Nowadays, for high productivity of natural product researches, a concept called ‘dereplication’ has been remarked by scientists. Dereplication is a process in which sample mixtures would be tested to differentiate novel constituents from active substances that have already been known (Koehn and Carter, 2005). According to a review paper written by Gaudencio and Pereira, the concept of dereplication was firstly reported in 1978 (Hanka et al., 1978), but it was started to be researched briskly after a paper published in 1993 (Beutler et al., 1990), due to advances of involved techniques such as biological screening processes, LC-MS techniques, MS libraries, and databases (Gaudencio and Pereira, 2015). Recent advances in analytical technologies have had the most important part for the advances of dereplication. Improvements in separation techniques such as ultra high performance liquid chromatography (UHPLC) have allowed rapid and reproductive chromatographic analysis with high sensitivity and resolution (Wolfender et al., 2015). Mass spectrometry (MS) has been more and more commonly used as a detector of chromatographic systems such as HPLC, gas chromatography (GC), or capillary electrophoresis (CE), because it could provide valuable information about chemical structures of separated metabolites. Dereplication strategies rely on analytical techniques and database searching to determine the identity of an active compound at the earliest possible stage in the discovery process (Gaudencio and Pereira, 2015), so the amount of structural information is the critical point for successful dereplication of natural products. Nowadays, hyphenated HPLC-PDA-MS has been the most selective analytical tool for identification and dereplication of natural products (Aldini et al., 2011), because of its plenty amount of structural information and large target metabolite window of HPLC separation and ESI-MS detection. Current MS techniques

provide information about not only molecular mass of metabolites, but molecular partial structures, which could be achieved by tandem MS techniques. In tandem MS, fragmentation patterns give additional information about partial structures of analytes. General dereplication process by LC-MS is facilitated by structural identification of chromatographic peaks by comparison of MS and tandem MS data with commercial or in-house database of natural products (Wolfender et al., 2015). Determining the identity of natural products in mixtures tentatively is becoming easier with advances in these analytical equipment and better compound databases (Nielsen et al., 2011).

1.2. Purpose of research

The purpose of this research was discovery of new bioactive chemical entities applying dereplication strategy. Two classes of chemotaxonomic marker metabolites of the family Rhamnaceae, cyclopeptide alkaloids and ceanothane-type triterpenoids, were selected as target compounds accounting their potential as new drug candidates. *Z. jujuba* was selected as target plant species, because it is the most well-known and widely cultivated plant species of Rhamnaceae, so it has large advantage in accessability. UHPLC-ESI-qTOF-MS was applied for the dereplication process. The schematic representation of dereplication-guided isolation strategy is shown in Scheme 1.

This thesis is organized as follows: In Chapter 2, development of specific analytical method for cyclopeptide alkaloids and targeted isolation based on LC-MS for them are described. None of previous studies have treated about profiling or dereplication these compounds, so partial dereplication strategy for cyclopeptide alklaoids was also developed based on isolated comounds and their spectral data. In Chapter 3, dereplication based isolation of triterpenoids is described. With the LC-MS profiles of *Z. jujuba* extracts, tentative identification for chromatographic

peaks was firstly performed. Based on UV, MS, and MS/MS spectral data, the dereplication method was developed for lupane- and ceanothane- type triterpenoids of Rhamnaceae plants. Based on these dereplication result, LC-MS guided isolation was performed to acquire target peaks as pure compounds and compare their structures with the predicted ones. Bioactivity of isolated chemical entities were evaluated in Chapter 4. Antiviral activity of cyclopeptide alkaloids were firstly evaluated. Triterpenoids were mainly evaluated for their cytotoxicity against HepG2, the human hepatocarcinoma cancer cell line. Experimental details of these works will be described in Chapter 5.

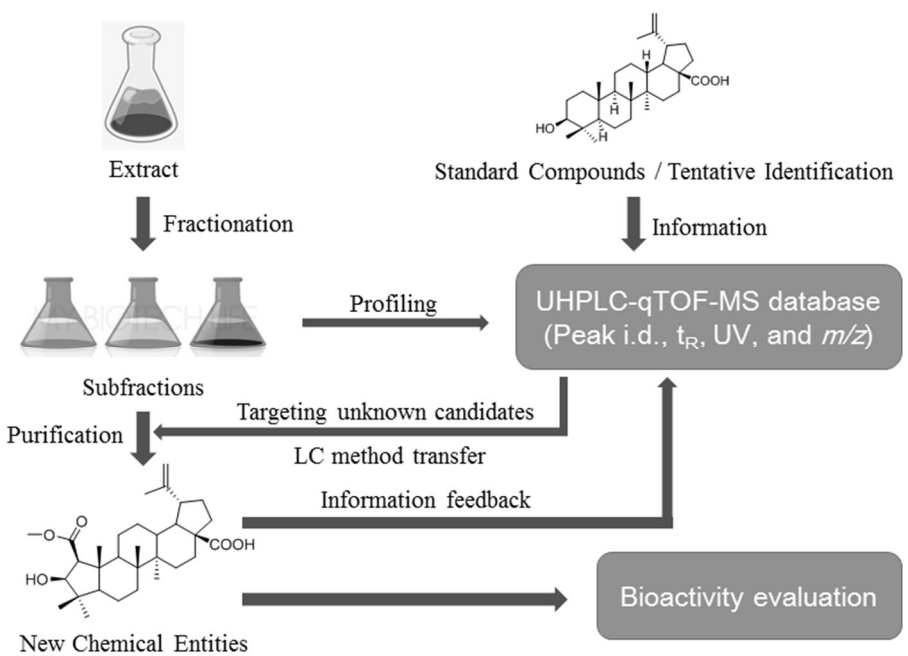

Scheme 1. Schematic representation of dereplication-guided isolation process

Chapter 2. Isolation of Cyclopeptide Alkaloids

2.1. LC-MS analysis of cyclopeptide alkaloids in extracts of *Z. jujuba* plant parts

Roots, twigs, leaves, and fruits of *Z. jujuba* were collected and analyzed by UHPLC-qTOF-MS for their cyclopeptide alkaloid constituents. For my best knowledge, there has not been any report about specific LC-MS analytical method for cyclopeptide alkaloids, so it had to be optimized first. At first, sample preparation method should be developed, considering the scarce amounts of cyclopeptide alkaloids in crude plants. Methanol was selected as an extraction solvent referring to previously reported publications about isolation of cyclopeptide alkaloids from Rhamnaceae species, (Giacomelli et al., 2001; Maldaner et al., 2011; Panseeta et al., 2011). Maceration was selected as an extraction method, in order to prevent any degradation which could be occurred physically or chemically in the extraction step. Macerated MeOH extracts of each plant parts were analyzed by UHPLC-qTOF-MS, but chromatographic peaks expected to contain nitrogen atoms were too small in their intensities, so the sample preparative method was further modified. MeOH extracts were fractionated with an acid-base fractionation method to afford basic $CHCl_3$ fractions, as described in the reference (Han et al., 2011). These alkaloid fractions were prepared to be 5 mg/mL in 50% aqueous MeOH, and were analyzed by UHPLC-qTOF-MS. Regarding the basicity of cyclopeptide alkaloids, ammonium formate was added to the gradient mixture mobile phase of aqueous acetonitrile, and positive ion mode was selected as the detection mode of ESI-qTOF-MS. The alkaloid fraction of root extract showed several major ion peaks with expected molecular formula with nitrogen, while the fractions of rest plant part extracts did not exhibited remarkable alkaloid chromatographic peaks (Figure 5-(a) for profile of root extracts. Chromatograms of other extracts are not

shown). Therefore, Root extract of *Z. jujuba* was selected as a target for further isolation of cyclopeptide alkaloids. Molecular formulas of major chromatographic peaks were calculated from their MS spectra. Peaks **g-y**, and **1-9** were estimated to be cyclopeptide alkaloids by their molecular formulae, but structural variety of cyclopeptide alkaloids and lack of analytical references made it impossible to putatively identify their chemical structures in this step.

Seeds of *Z. jujuba* var. *spinosa,* which is a well-known and widely-used material in traditional medicines as Zizyphi Semen, were analyzed for validation of developed analytical method. Those seeds have been reported to contain a significant amount of cyclopeptide alkaloids, so these were expected to be an appropriate validation sample for our analytical method. Alkaloid fraction was prepared and profiled as shown in Figure 5-(b). Many major peaks were detected, and most of them were expected to contain nitrogen atoms according to MS spectra (Table 2). Interestingly, *Z. jujuba* var. *spinosa* seeds showed several major chromatographic peaks of smaller alkaloids, such as peaks **a-d**, and **f**. The peak **b** with the largest intensity exhibited its pseudo-molecular ion at *m/z* 342.1714, which suggested molecular formula of $C_{20}H_{24}NO_4$. This molecular formula suggested **b** was magnoflorine, one of major constituents of Zizyphi Semen (Kim et al., 2014). For confirming this tentative identification, reference standards of major constituents of Zizyphi Semen, magnoflorine and spinosin, were injected. As a result, peaks **b** and **e** were confirmed to be peaks of magnoflorine and spinosin, respectively. Peaks **c** and **f** showed similar predicted molecular formulae containing one nitrogen atom. They were tentatively identified as sanjoine K and juzirine for their molecular formulae, respectively (Liu et al., 2007). However, it was not possible to acquire any information about strucrual identification of cyclopeptide alkaloids with the extract of *Z. jujuba* var. *spinosa* semen. Therefore, it was decided to perform targeted isolation of unknown cyclopeptide alkaloid peaks and structural elucidation. From isolated compounds, dereplication method for cyclopeptide alkaloids would be developed further.

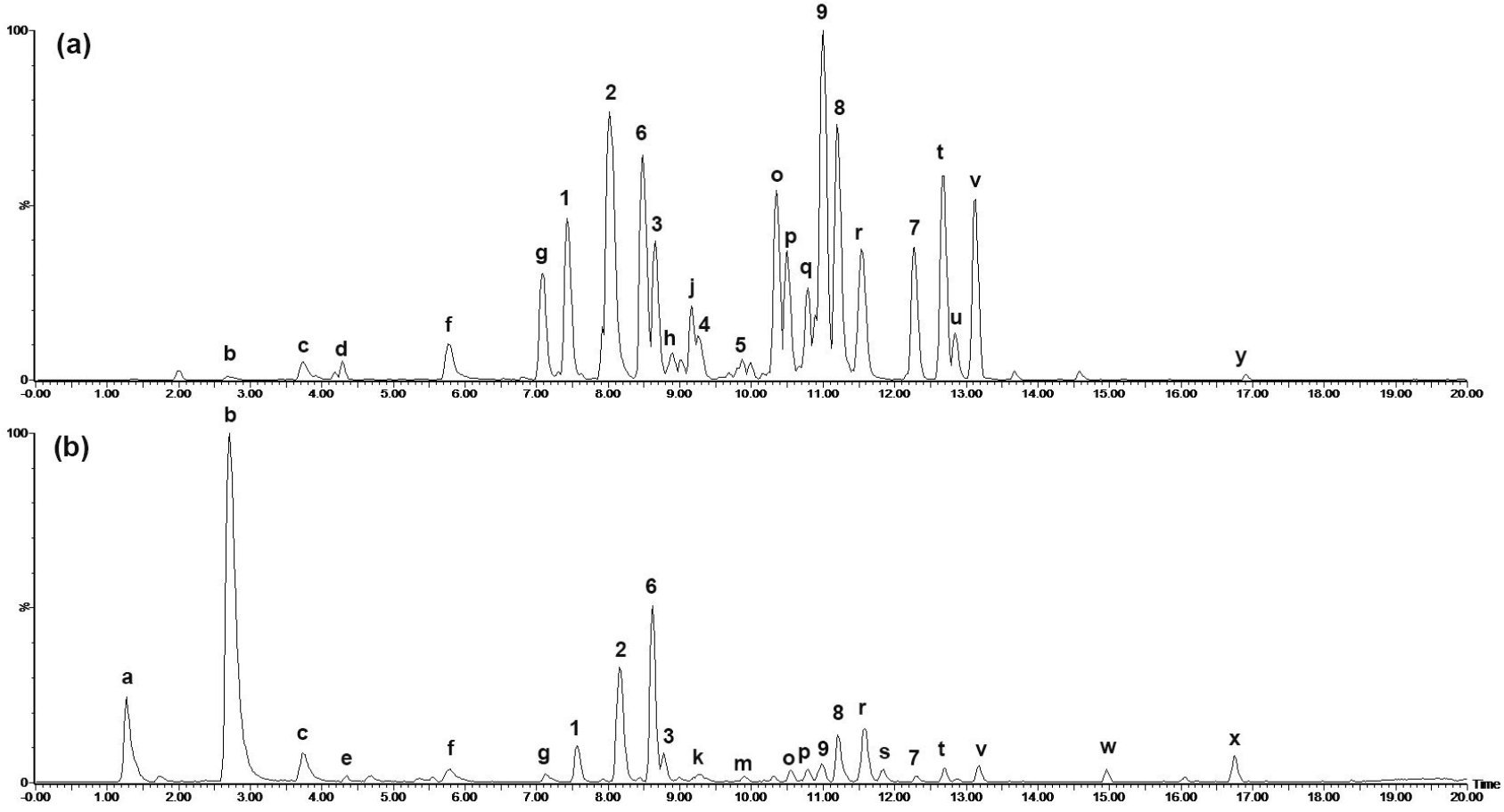

Figure 4. Base peak intensity chromatograms of alkaloid fractions of (a) *Z. jujuba* roots and (b) *Z. jujuba* var. *spinosa* seeds

Table 2. Peak identification of cyclopeptide alkaloid chromatographic profiles in Figure 4

Peak No.	Compounds identification	t_R (mins)	observed *m/z*	calculated *m/z*	Molecular formula $[M+H]^+$	MS/MS fragments (m/z)	UV (λmax, nm)
a		1.27	160.0945	160.0974	$C_7H_{13}NO_3$	114 $[M-CHO_2+H]^+$	
b	Magnoflorine [b]	2.71	342.1714	342.1705	$C_{20}H_{24}NO_4$ [a]	297 $[M-C_2H_7N]^+$	227, 273, 319
c	Sanjoine K	3.73	286.1411	286.1443	$C_{17}H_{20}NO_3$ [a]	269 $[M-NH_3]^+$	227, 283
d		4.29	298.1067	298.1079	$C_{17}H_{16}NO_4$		227, 256
e	Spinosin [b]	4.53	609.1823	609.1819	$C_{28}H_{33}O_{15}$	447 $[M-C_6H_{10}O_5+H]^+$	217, 271, 338
f	Juzirine	5.76	282.1132	282.1130	$C_{17}H_{16}NO_3$		236
g	Hemsine-D	6.23	507.2974	507.2971	$C_{29}H_{39}N_4O_4$	408 $[M-C_6H_{13}N+H]^+$	221
1	Jubanine F	6.39	544.3124	544.3135	$C_{28}H_{42}N_5O_6$	360 $[M-C_9H_{16}N_2O_2+H]^+$	269, 317
2	Jubanine G	7.05	558.3281	558.3292	$C_{29}H_{44}N_5O_6$	360 $[M-C_{10}H_{18}N_2O_2+H]^+$	269, 318
6	Nummularine B	7.60	592.3134	592.3135	$C_{32}H_{42}N_5O_6$	408 $[M-C_9H_{16}N_2O_2+H]^+$	269, 317
3	Jubanine H	7.77	572.3448	572.3448	$C_{30}H_{46}N_5O_6$	374 $[M-C_{10}H_{18}N_2O_2+H]^+$	269, 317
h		8.89	501.3082	501.3077	$C_{27}H_{41}N_4O_5$	374 $[M-C_7H_{13}NO+H]^+$	267, 320
i		9.22	543.2608	543.2607	$C_{31}H_{35}N_4O_5$		269, 317
j		9.16	487.3276	487.3284	$C_{27}H_{43}N_4O_4$	352 $[M-C_8H_9NO+H]^+$	232
4	Jubanine I	9.27	572.3448	572.3448	$C_{30}H_{46}N_5O_6$	374 $[M-C_{10}H_{18}N_2O_2+H]^+$	269, 317
k		9.48	558.3096	558.3080	$C_{32}H_{40}N_5O_4$		

l		9.69	499.3290	499.3284	$C_{28}H_{43}N_4O_4$		
5	Jubanine J	9.87	586.3622	586.3605	$C_{31}H_{48}N_5O_6$	374 $[M\text{-}C_{11}H_{20}N_2O_2+H]^+$	273, 319
m		9.99	644.4038	644.4023	$C_{34}H_{54}N_5O_7$		
n		10.10	519.2940	519.2971	$C_{30}H_{39}N_4O_4$		
o		10.34	501.3454	501.3441	$C_{28}H_{45}N_4O_4$		229
p	Paliurine-H	10.50	614.3900	614.3918	$C_{33}H_{52}N_5O_6$	374 $[M\text{-}C_{13}H_{24}N_2O_2+H]^+$	270, 319
q	Daechuine-S7	10.79	515.3235	515.3233	$C_{28}H_{43}N_4O_5$	374 $[M\text{-}C_8H_{15}NO+H]^+$	267, 319
9	Adouetine X	10.54	501.3444	501.3441	$C_{28}H_{45}N_4O_4$		229
8	Mucronine K	10.84	515.3235	515.3233	$C_{28}H_{43}N_4O_5$		267, 319
r		11.53	588.3191	588.3186	$C_{33}H_{42}N_5O_5$	457 $[M\text{-}C_9H_9N+H]^+$	272, 319
s		11.84	274.2751	274.2746	$C_{16}H_{36}NO_2$		
7	Deachuine-S3	12.28	628.4078	628.4074	$C_{34}H_{54}N_5O_6$	374 $[M\text{-}C_{14}H_{26}N_2O_2+H]^+$	270, 319
t		12.67	628.4077	628.4074	$C_{34}H_{54}N_5O_6$	374 $[M\text{-}C_{14}H_{26}N_2O_2+H]^+$	270, 319
u		12.84	662.3922	662.3918	$C_{37}H_{52}N_5O_6$	374 $[M\text{-}C_{17}H_{24}N_2O_2+H]^+$	267, 317
v		13.13	662.3912	662.3918	$C_{37}H_{52}N_5O_6$	374 $[M\text{-}C_{17}H_{24}N_2O_2+H]^+$	267, 317
w		14.96	520.3380	520.3387	$C_{28}H_{46}N_3O_6$		
x		16.75	522.3543	522.3543	$C_{28}H_{48}N_3O_6$		
y		16.92	532.3670	532.3710	$C_{25}H_{50}N_5O_7$		

[a] Pseudo-molecular peaks were detected in their form as $[M]^+$, instead of $[M+H]^+$.
[b] identified by comparison with authentic standard compounds.
Isolated compounds were annotated with numbers, and putatively predicted compounds were with letters.

2.2. Isolation of cyclopeptide alkaloids and development of dereplication method

Pulverized air-dried *Z. jujuba* roots (14.5 kg) were macerated with MeOH (2 × 60 L, for one week each) at rt. The alkaloid fraction (1.7 g) was prepared with an acid-base fractionation method from the crude extract (500.8 g). This alkaloid fraction was subjected to silica gel column chromatography to afford four subfractions, and the subfractions were further purified using Sephadex LH-20 and preparative HPLC. As a result, nine cyclopeptide alkaloids (compounds **1-9,** Figure 5) were isolated and chemically characterized. Compounds **1-5** were isolated from nature for the first time, and they were reported to scientific community by the author (Kang et al., 2015). The details for structural elucidation will be described in section 2.3.

Isolated nine cyclopeptide alkaloids were injected and analyzed by LC-MS for peak-picking in the alkaloid profile of root extract. As a result, retention time, UV absorption spectra, and MS spectra of compounds **1-9** were matched to nine major peaks of the root extract LC-MS profile (Figure 4 and Table 2). From these, several remarkable features for tentative identification of cyclopeptide alkaloids could be purposed. As the previous references described, type-Ib cyclopeptide alkaloids such as compounds **1-8** showed UV λ_{max} at 269 and 317 nm, while type-Ia such as compound **9** exhibited λ_{max} only at 229 nm. These absorption bands are caused by the characteristic styrylamine chromophore in 13-membered cyclopeptide alkaloids (Panseeta et al., 2011), and these absorption bands cannot be observed with 14-membered rings due to the ring system strain, except when there is a tryptophan moiety in the molecule (Gournelis et al., 1998). In most of type-Ib cyclopeptide alkaloids, the numbers of oxygen atoms are larger than the number of nitrogens in their molecular formulae. This is for the hydroxy or methoxy groups in their styrylamine moieties, but it cannot be generalized, because there are several

reported type-Ia structures with the hydroxyl in their styrylamine moieties such as ramosine-C (Lin et al., 2003). In addition, there were even other reported cyclopeptide alkaloids containing hydroxylated amino acid residues, such as scutianine-G (Tschesche and Hillebrand, 1977) and aralionine-C (Tschesche et al., 1977). Most of type-Ib cyclopeptide alkaloids exhibited MS fragments in which their intermediate and terminal amino acids were eliminated. For example, compound **1** showed MS/MS fragment peak at *m/z* 360 $[M\text{-}C_9H_{16}N_2O_2+H]^+$. This

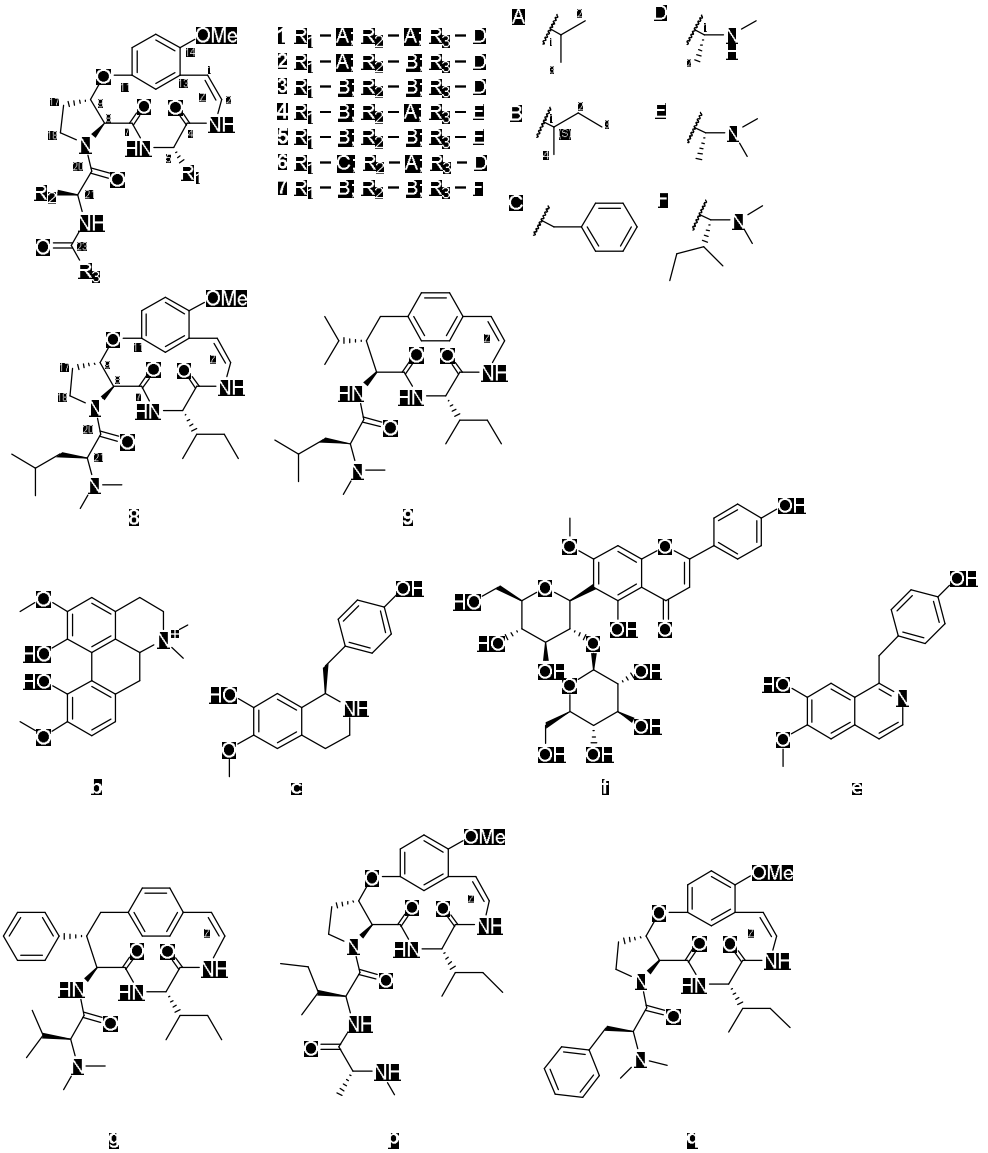

Figure 5. Chemical structures of compounds **1**-**9**, **b**, **c**, **e**-**g**, **p**, and **q**

fragment ion was formed by elimination of a smaller peptide formed by the intermediate valine and the terminal *N*-methylalanine. Therefore, MS/MS fragment patterns could provide evidences for the identification of cyclopeptide alkaloid peaks. However, different molecules could exhibit identical pseudo-molecular ions and fragment ions, like the case of compounds **3** and **4**. If a fragment ion in which only a terminal amino acid would be eliminated, then it could be used to distinguish chromatographic peaks of these compounds.

Based on these analytic results, limited dereplication could be performed for not-isolated peaks. For example, molecular formula of peak **g** could be identified as $C_{29}H_{38}N_4O_4$ by its MS spectrum. UV spectrum of **g** only showed its maximum absorption at 221 nm, suggesting **g** is a type-Ia cyclopeptide alkaloid. By searching chemical databases, the author could only one type-Ia cyclopeptide alkaloid having such a molecular formula, hemsine-D, which were isolated from roots of *Paliurus hemsleyanus* (Lin et al., 2003). It has a L-*N*-methylvaline as its terminal amino acid, so it was reasonable that peak **g** showed a MS/MS fragment ion of *m/z* 408, formed by loss of $C_6H_{13}N$. Another example is for peak **p**. Its UV spectra suggested that **p** is a type-Ib cyclopeptide alkaloids, and its molecular formula was suggested as $C_{33}H_{51}N_5O_6$ by MS spectrum. From chemical database, paliurine-H, which was reported from *Paliurus ramosissimus* (Lee et al., 2001), was matched to this molecular formula. Paliurine-H has a L-*N*-methyleucine and a L-leucine as its terminal amino acid and intermediate amino acid. Therefore, its MS/MS fragment ion with *m/z* 374, generated by the loss of $C_{13}H_{24}N_2O_2$, could be reasonable. However, further optimization of tandem MS condition should be performed to utilize this tentative identification method for cyclopeptide alkaloids.

2.3. Structural elucidation of cyclopeptide alkaloids

2.3.1. Compound **1**

Compound **1** was obtained as white amorphous powder with molecular formula $C_{28}H_{41}N_5O_6$, as indicated by ESI-qTOF-MS (*m/z* 544.3112 $[M+H]^+$, calcd. for $C_{28}H_{42}N_5O_6$, 544.3135). The UV spectrum of **1** showed absorption bands at around 276 and 323 nm, which indicated that compound **1** was a 13-membered cyclopeptide alkaloid, as written in section 2.2. Three aromatic protons of **1** [δ_H 6.70 (1H, *d*, *J* = 3.2 Hz, H-12), δ_H 6.87 (1H, *d*, *J* = 9.2 Hz, H-15), and δ_H 6.80 (1H, *dd*, *J* = 3.2, 9.2 Hz, H-16)] were observed in ^{1}H NMR spectrum of **1** (Figure 6). This suggests that compound **1** contains a *m*-oxystyrylamino moiety, which then suggests that **1** is 13-membered cyclopeptide alkaloid (Lin et al., 2000). From the analysis of ^{1}H, ^{13}C, HSQC, and ^{1}H-^{1}H COSY (Figure 7) NMR spectroscopic data, presences of two valines, one β-oxyproline, and one *N*-methylalanine moiety were suggested. The HMBC experiment exhibited following correlations: δ_H 8.42 (1H, *d*, *J* = 11.5 Hz, H-3) to δ_C 167.1 (C-4), δ_H 7.24 (1H, overlapped, H-6) to δ_C 170.4 (C-7), and δ_H 5.52 (1H, *td*, *J* = 3.2, 7.3 Hz, H-9) to δ_C 151.1 (C-11) (Figure 8). These signals repectively indicated linkages between a *m*-oxysyrylamine and a valine, the valine and a β-oxyproline, and the β-oxyproline and the *m*-oxystyrylamine. Thus, compound **1** was confirmed as an Ib-type cyclopeptide alkaloid (Tan and Zhou, 2006), which have a valine as a ringbound amino acid. A NOE signal between δ_H 4.23 (1H, m, H-18a) and δ_H 4.56 (1H, *dd*, *J* = 7.8, 9.2 Hz, H-21) suggested that the β-oxyproline was connected to another valine moiety (Figure 9). Thus, the valine and the *N*-methylalanine were confirmed as an intermediate and terminal amino acid, respectively. CD spectrum of **1** exhibited two negative Cotton effects at its UV λ_{max}, 265 and 321 nm (Figure 10). Only little have been studied about the relationship between CD spectra and absolute configurations of cyclopeptide

alkaloids, but every previously reported type-Ib cyclopeptide alkaloids with 5*S*, 8*S*, and 9*S*-configurations showed similar CD spectra (Schmidt et al., 1983). A weak vicinal coupling between H-8 and H-9 (J = 3.2 Hz) also supported the L-*erythro* (8*S*, 9*S*) orientation of them (Suksamrarn et al., 2005; Mostardeiro et al., 2013). To confirm the absolute configuration, acid hydrolysis of **1** was performed for advanced Marfey's method (Fujii et al., 1997). The hydrolysate of **1** was treated with the D-FDLA (Nα-(5-fluoro-2,4-dinitrophenyl)- D-leucinamide) or L-FDLA (Nα-(5-fluoro-2,4-dinitrophenyl)-L-leucinamide) and the reaction products were analyzed by LC-MS. D-FDLA derivatives are retained longer than the L-FDLA derivatives on C_{18} reverse phased HPLC, exhibiting amino acid residues of **1** as L-valine and L-*N*-methylalamine, respectively. As a result, the configuration of compound **1** was confirmed as 5*S*, 8*S*, 9*S*, 21*S*, and 1‴*S*. Compound **1** was isolated for the first time from nature and named jubanine F after its plant origin.

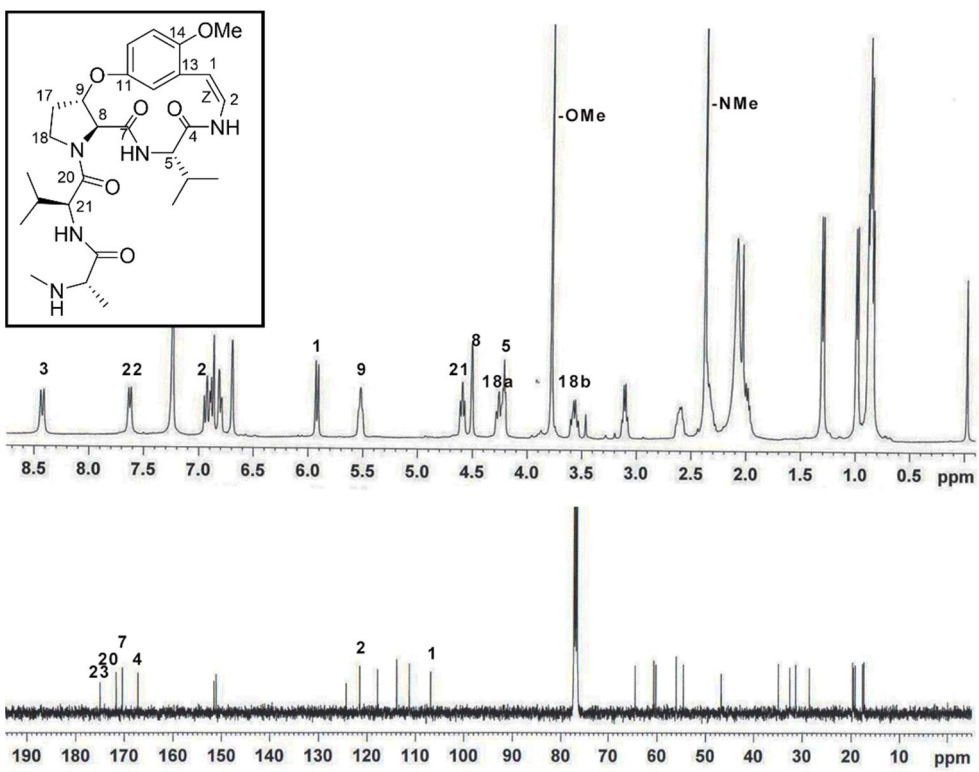

Figure 6. ^{1}H and ^{13}C NMR spectra of compound **1** (400 / 100MHz, $CDCl_3$)

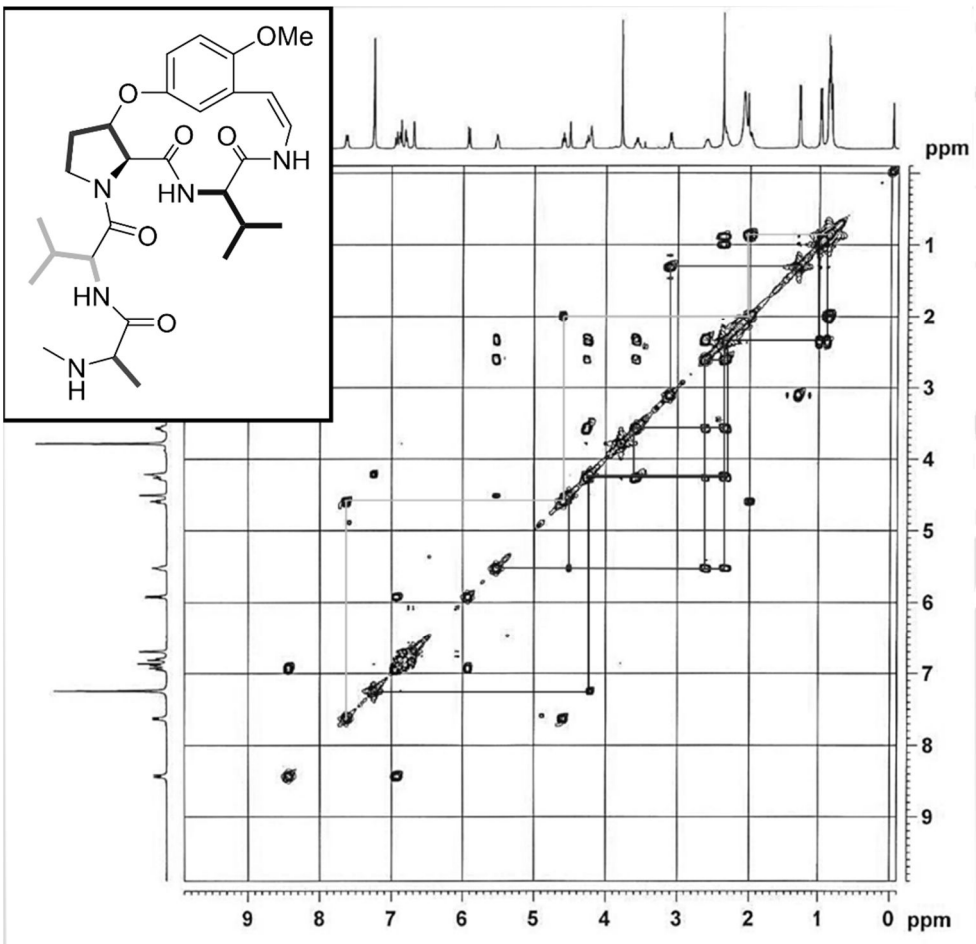

Figure 7. ^{1}H-^{1}H COSY spectrum of compound **1** (400 MHz, $CDCl_3$)

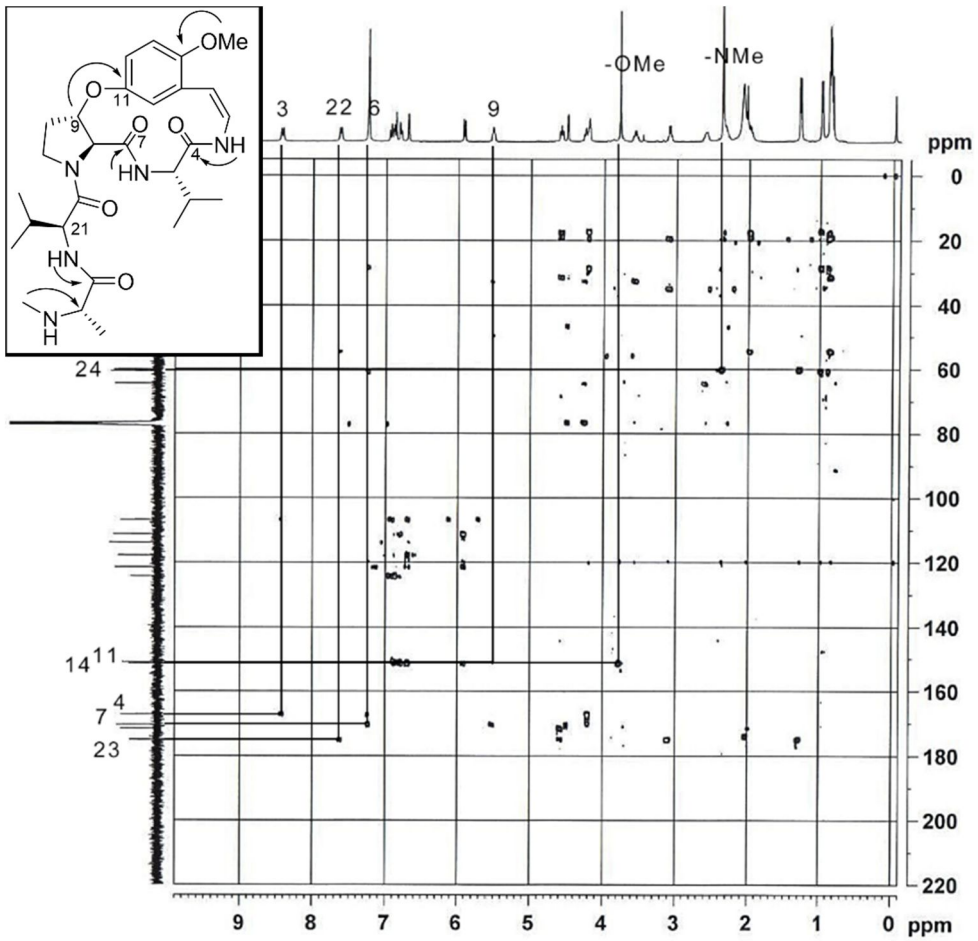

Figure 8. HMBC spectrum of compound **1** (400 MHz, $CDCl_3$)

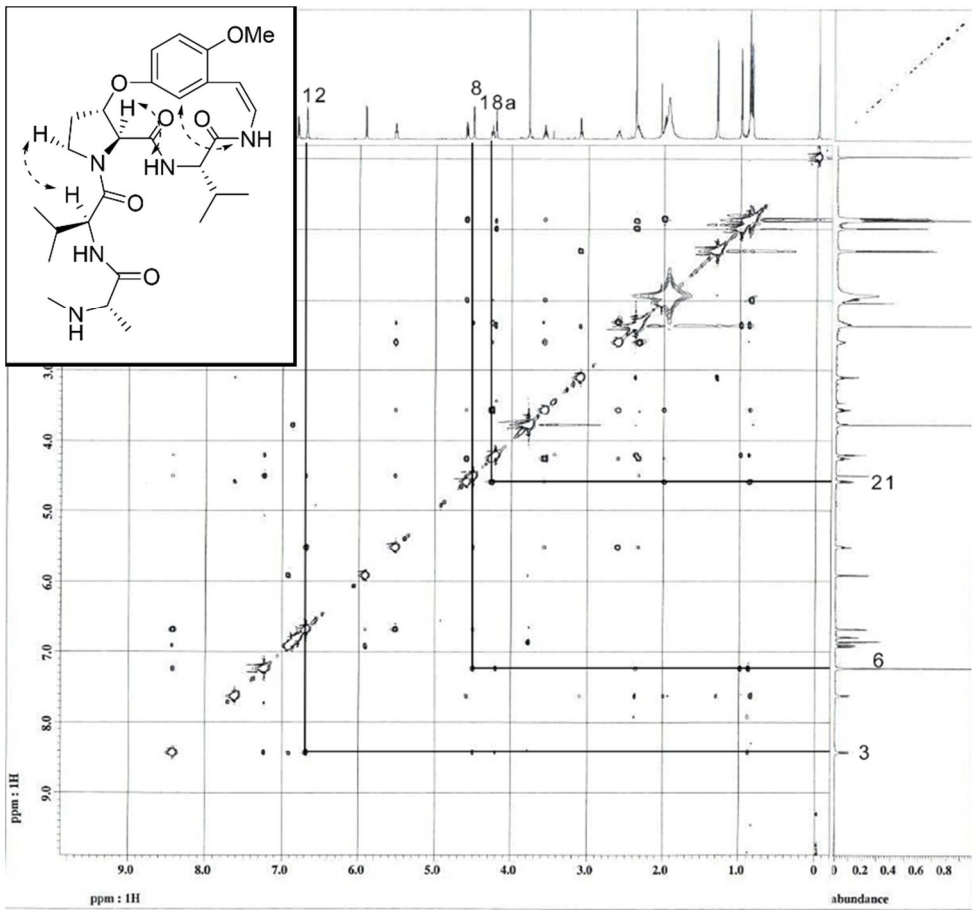

Figure 9. NOESY spectrum of compound **1** (400 MHz, $CDCl_3$)

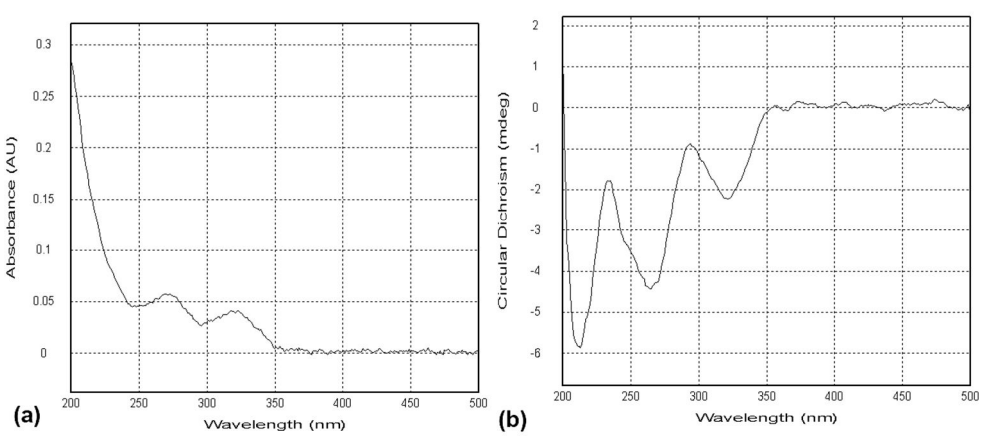

Figure 10. (a) UV and (b) CD spectra of compound **1**

2.3.2. Compounds **2** and **3**

The molecular formula of compound **2** was determined to be $C_{29}H_{43}N_5O_6$ by ESI-qTOF-MS (*m/z* 558.3296 $[M+H]^+$, calcd. for $C_{29}H_{44}N_5O_6$, 558.3292). ^1H- and ^{13}C-NMR spectrum of **2** was similar to one of **1** but slightly different (Figure 11). Two methyl (δ_C 10.8 and 15.1), one methylene (δ_C 24.5), and one methine (δ_C 37.4) signals were observed, instead of the intermediate valine. ^1H-^1H COSY analysis indicated that these comprised an isoleucine residue (Figure 12). The HMBC cross-peaks of H-3 to C-4, H-6 to C-7, and H-22 to C-23 indicated connections between a *m*-oxystyrylamino moiety with a valine, the valine with a β-oxyproline, and an isoleucine with a *N*-methylalanine, respectively (Figure 13). Thus, **2** was suggested as a cyclopeptide similar to **1**, having an isoleucine as the intermediate amino acid instead of the valine in **1**. The absolute configurations of C-5, C-8, C-9, C-21, and C-1‴ were identified as *S, S, S, S*, and *S* by CD spectrum and the advanced Marfey's method, as same for compound **1**. However, an absolute configuration of isoleucine cannot be determined by the advanced Marfey's method, because of the presence of its *allo* isomer. To determine the absolute configuration of the isoleucine residue, a GITC (2,3,4,6-tetra-*O*-acetyl-β-D-glucopyranosyl isothiocyanate) derivative of the hydrolysate was prepared and analyzed by LC-MS (Hess et al., 2004). The GITC derivatives of L-isoleucine and L-*allo*-isoleucine eluted very closely, so co-injection experiments were performed and it was proved that the configuration of the isoleucine residue was L-isoleucine (21*S*, 1″*S*) instead of L-*allo*-isoleucine (21*S*, 1″*R*). Compound **2** was also isolated for the first time from nature. Compound **2** was named jubanine G.

Compound **3** was obtained as a white amorphous powder. The molecular formula of compound **3** was determined as $C_{30}H_{45}N_5O_6$ by ESI-qTOF-MS (*m/z* 572.3451 $[M+H]^+$, calcd. for $C_{30}H_{46}N_5O_6$, 572.3448). Since it is similar to compounds **1** and **2**, it was determined that **3** is a type-Ib cyclopeptide alkaloid containing a *m*-oxystyrylamine, a β-oxyproline, and a terminal *N*-methylalanine by ^1H, ^{13}C (Figure

14), ^{1}H-^{1}H COSY (Figure 15), and HMBC (Figure 16) NMR spectra. From the COSY spectrum, it was also revealed that **3** has two isoleucine moieties as the ring bound amino acid and the intermediate amino acid residues, respectively. The absolute configurations of 5*S*, 8*S*, 9*S*, 21*S*, 1′*S*, 1″*S,* and 1‴*S* were identified by CD spectrum, the advanced Marfey's method, and the GITC analysis, as same for compounds **1** and **2**. Compound **3** was also isolated for the first time from nature, and was named jubanine H.

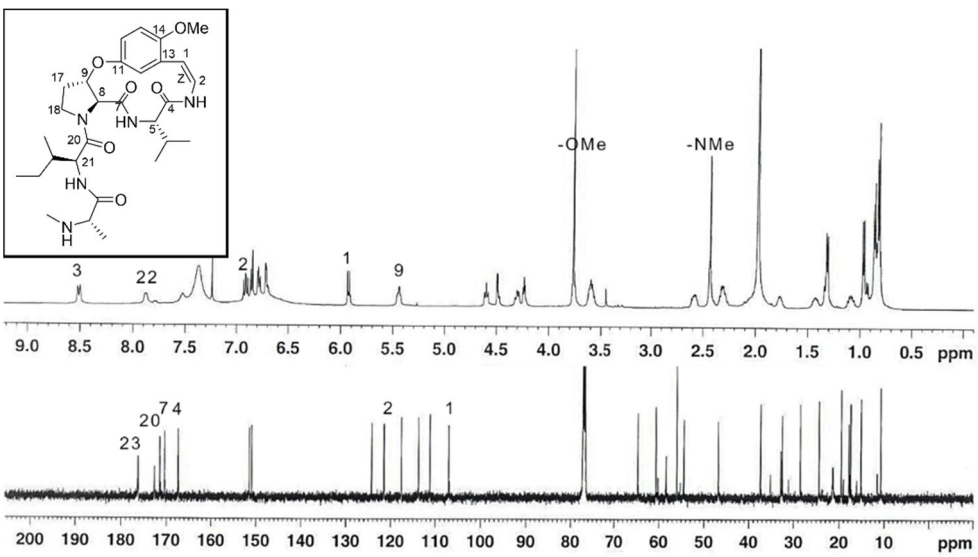

Figure 11. ^{1}H and ^{13}C NMR spectra of compound **2** (500 / 125MHz, $CDCl_3$)

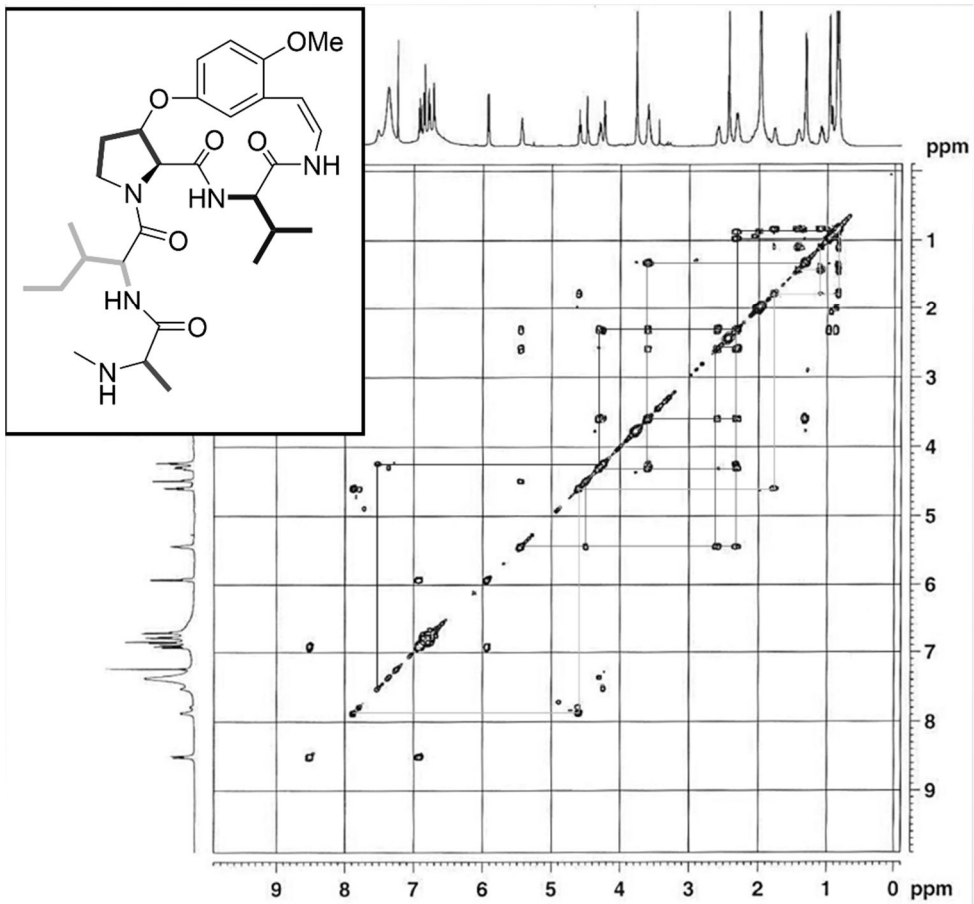

Figure 12. ^{1}H-^{1}H COSY spectrum of compound **2** (500 MHz, $CDCl_3$)

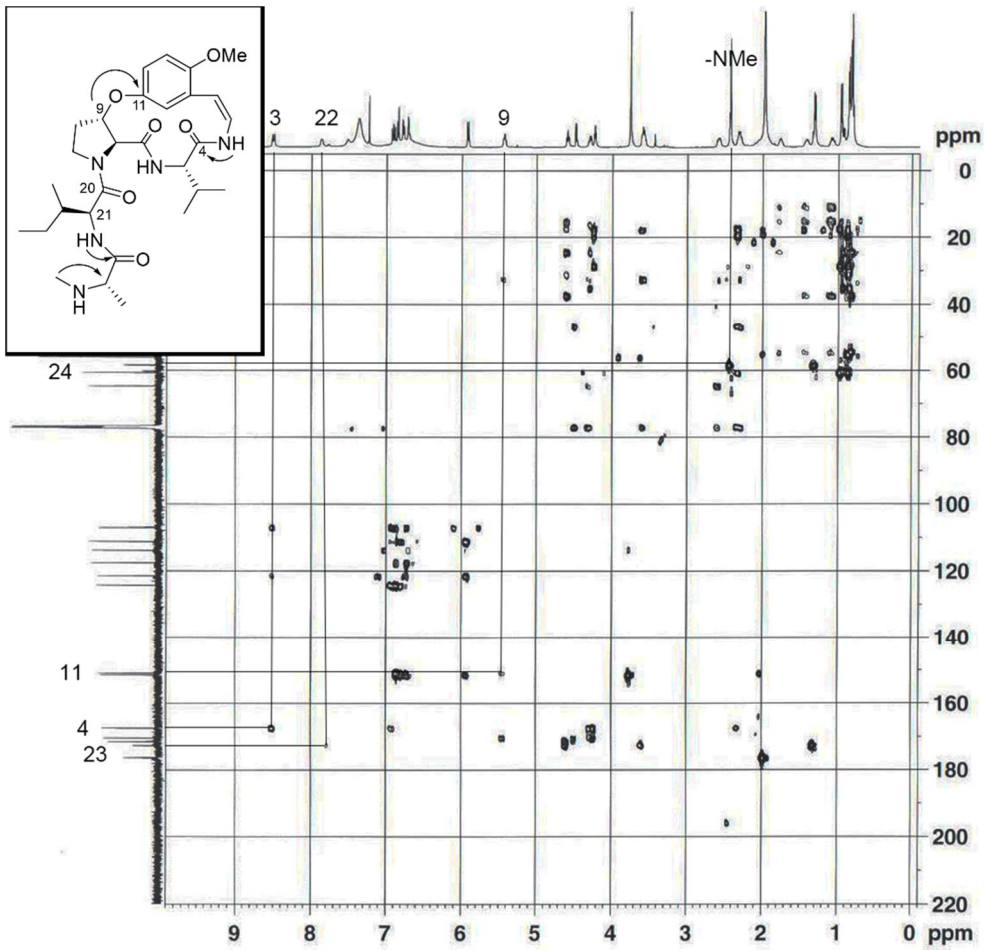

Figure 13. HMBC spectrum of compound **2** (500 MHz, $CDCl_3$)

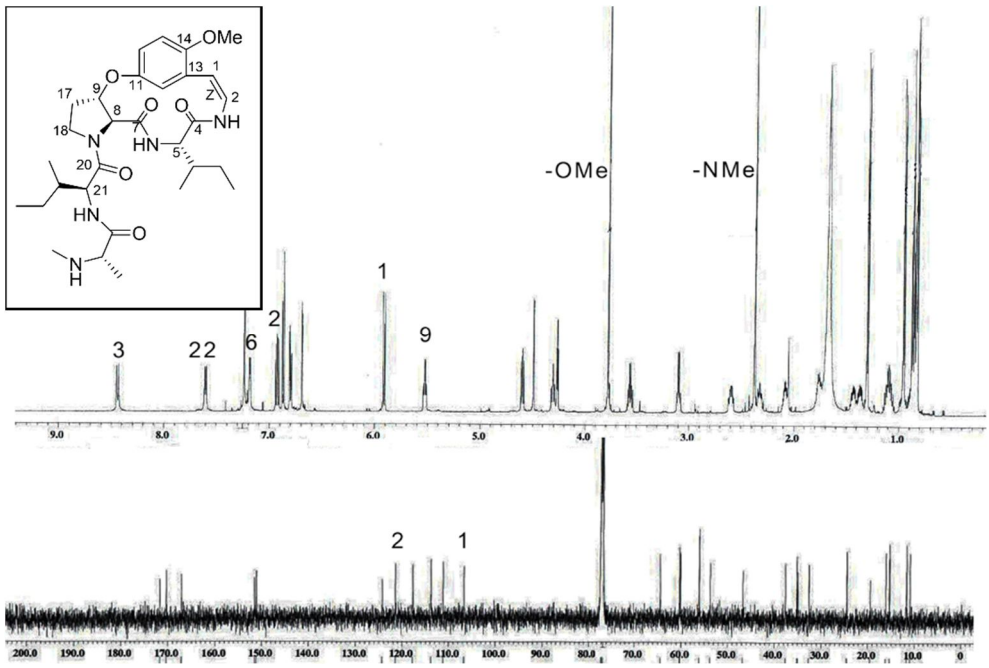

Figure 14. 1H and 13C NMR spectra of compound **3** (600 / 150 MHz, $CDCl_3$)

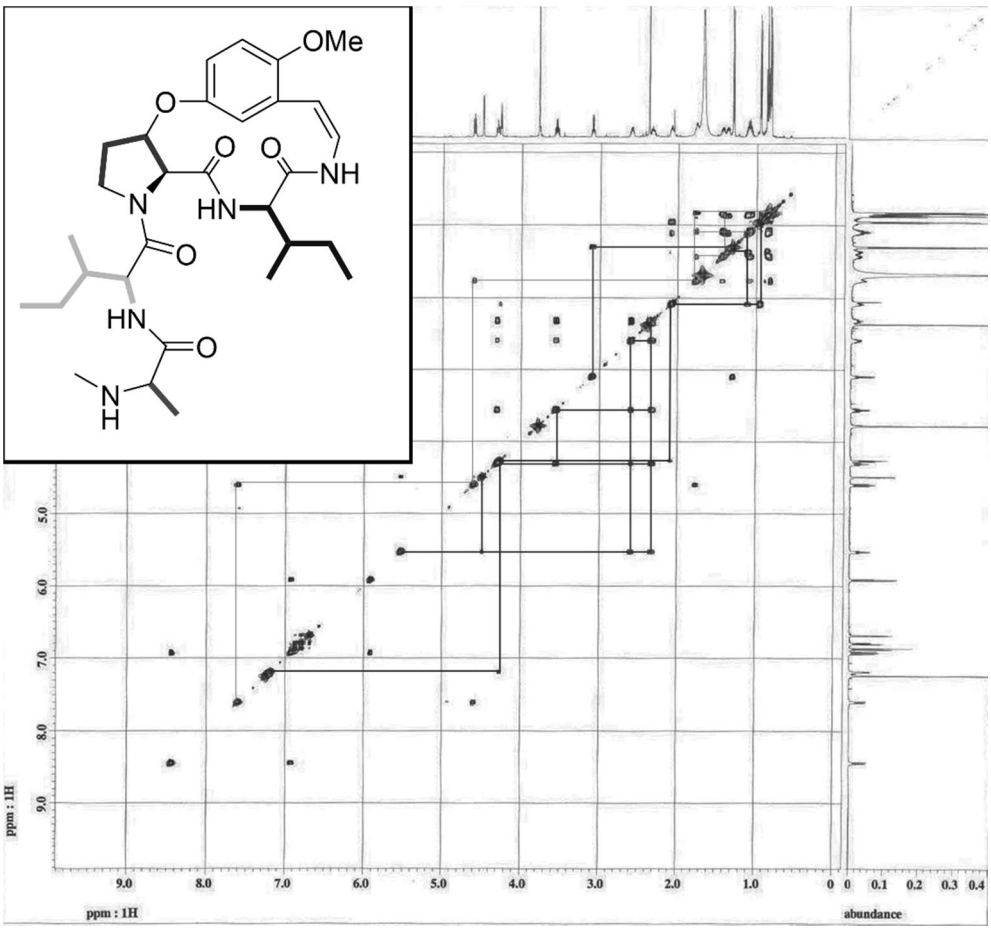

Figure 15. ^{1}H-^{1}H COSY spectrum of compound **3** (600 MHz, $CDCl_3$)

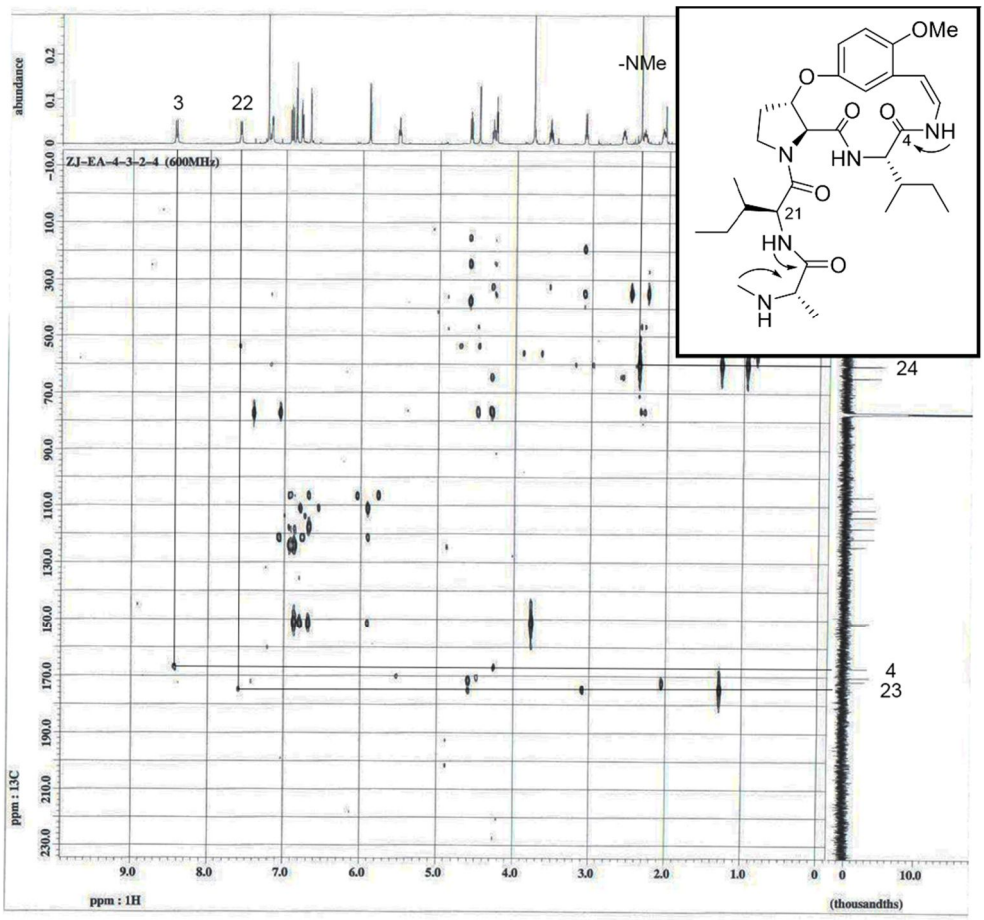

Figure 16. HMBC spectrum of compound **3** (600 MHz, $CDCl_3$)

2.3.3. Compounds **4** and **5**

Compound **4**, obtained as white amorphous powder, was determined its molecular formula as $C_{30}H_{45}N_5O_6$ by ESI-qTOF-MS (*m/z* 572.3451 $[M+H]^+$, calcd. for $C_{30}H_{46}N_5O_6$, 572.3448). Different to compounds **1-3**, *N*-methyl protons (δ_H 2.17, *s*) of **4** were equivalent to six protons in ^1H NMR spectrum (Figure 17). Thus, compound **4** was deduced to have a terminal *N,N*-dimethyl amino acid, instead of a mono-methyl substituted one. This terminal amino acid was determined as a *N,N*-dimethylalanine from ^1H-^1H COSY (Figure 19) and HMBC (Figure 20) NMR spectroscopic data. Additionally, the ringbound amino acid was determined as an

isoleucine, and the intermediate amino acid was determined as a valine. The absolute configurations of 5*S*, 8*S*, 9*S*, 21*S*, 1′*S,* and 1″*S* were identified by the same methods as used for the previous compounds **1-3**. However, the absolute configuration of *N,N*-dimethylalanine could not be determined by advanced Marfey's method, because *N,N*-dimethylalanine was not able to form FDLA derivatives due to the fully substituted nitrogen atom. Therefore, the absolute configuration of *N,N*-dimethylalanine was confirmed by derivatization of the *N,N*-dimethylalanine with phenylglycine methylester hydrochloride (PGME) amide coupling products (Um et al., 2013). The PGME derivatives of the synthetic *N,N*-dimethylalanine were analyzed by LC-MS, and the synthetic amides of L- and D-*N,N*-dimethylalanine exhibited retention times of 8.83 min and 10.24 min, respectively. The *N,N*-dimethylalanine-PGME amide derived from the hydrolysate of compound **4** was detected at 8.79 min. Thus, the absolute configuration of *N,N*-dimethylalanine in compound **4** was identified as L (*S*) and compound **4** was named jubanine I. It was firstly isolated from nature.

The molecular formula of compound **5** was determined to be for $C_{31}H_{47}N_5O_6$ utilizing ESI-qTOF-MS (*m/z* 586.3597 $[M+H]^+$, calcd. for $C_{31}H_{48}N_5O_6$, 586.3605). Similar to compound **4**, compound **5** was deduced to have a terminal *N,N*-dimethylalanine residue from ^{1}H NMR spectrum (Figure 18). Two isoleucine residues and their connectivity with *m*-oxystyrylamine, β-oxyproline, and terminal *N,N*-dimethylalanine moieties were inferred by COSY (Figure 21) and HMBC (Figure 22) correlations. The absolute configuration of the two isoleucine residues and a *N,N*-dimethylalanine residue in compound **5** were also determined by the chromatographic analysis on GITC and PGME derivatives of the hydrolysate. The absolute configurations of C-5, C-8, C-9, C-21, C-1′, C-1″ and C-1‴ of **5** were all identified as *S*. Compound **5** was named jubanine J and it was firstly isolated from nature.

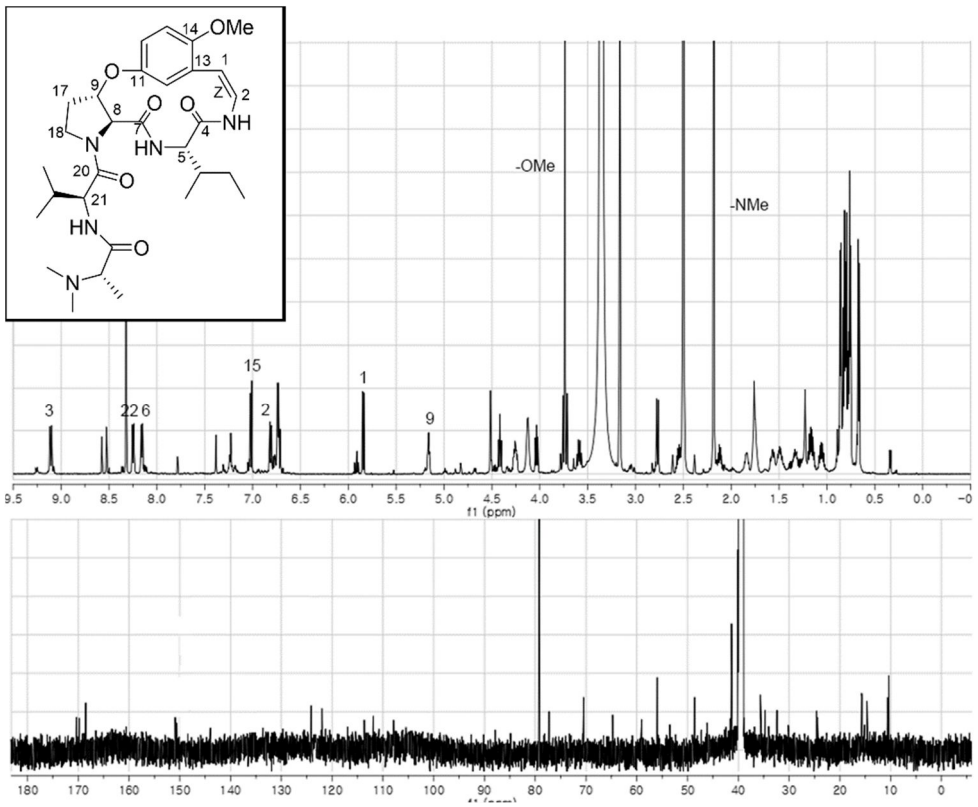

Figure 17. ^{1}H and ^{13}C NMR spectra of compound **4** (600 / 150 MHz, DMSO-d_6)

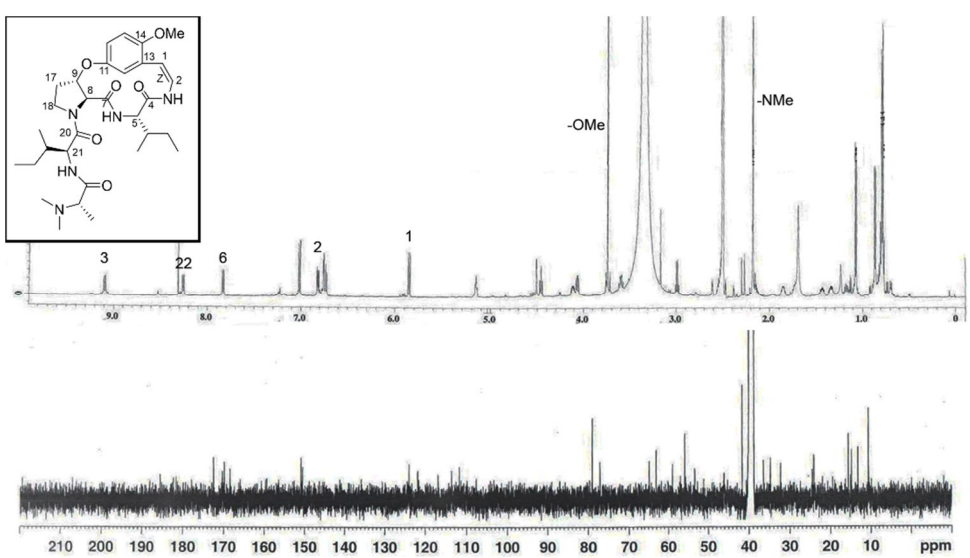

Figure 18. ^{1}H and ^{13}C NMR specra of compound **5** (600 / 150 MHz, DMSO-d_6)

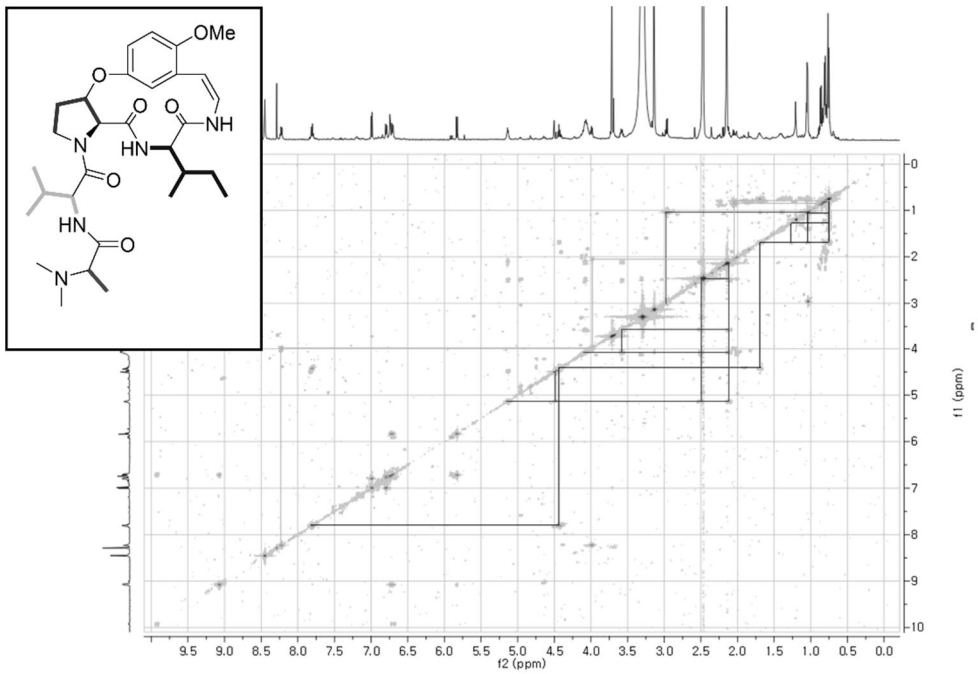

Figure 19. ^{1}H-^{1}H COSY spectrum of compound **4** (600 MHz, DMSO-d_6)

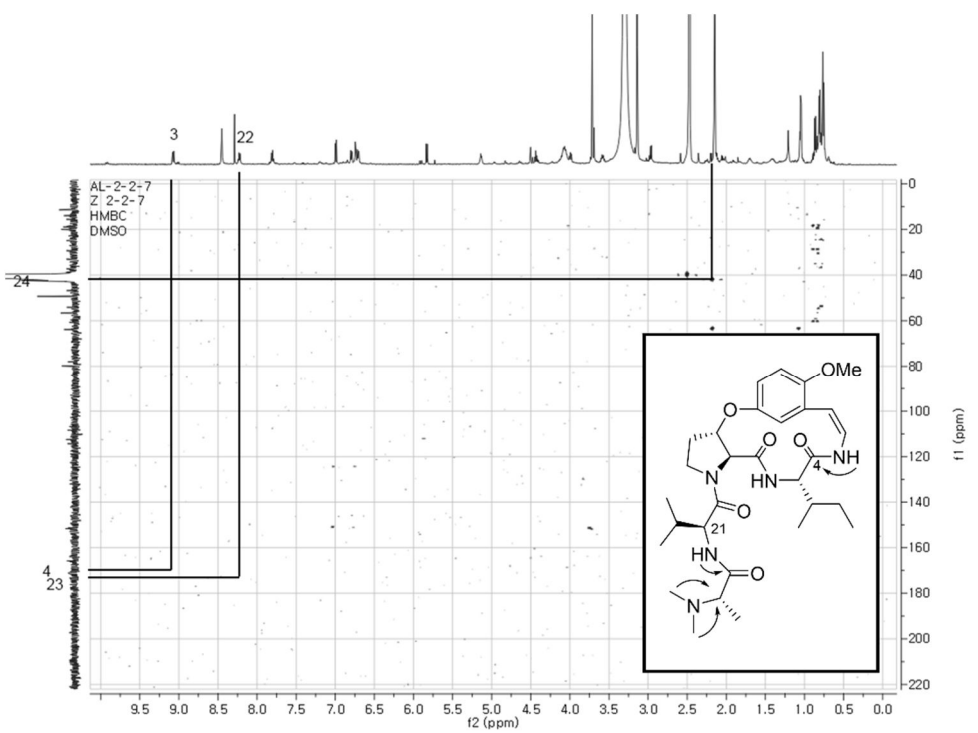

Figure 20. HMBC spectrum of compound **4** (600 MHz, DMSO-d_6)

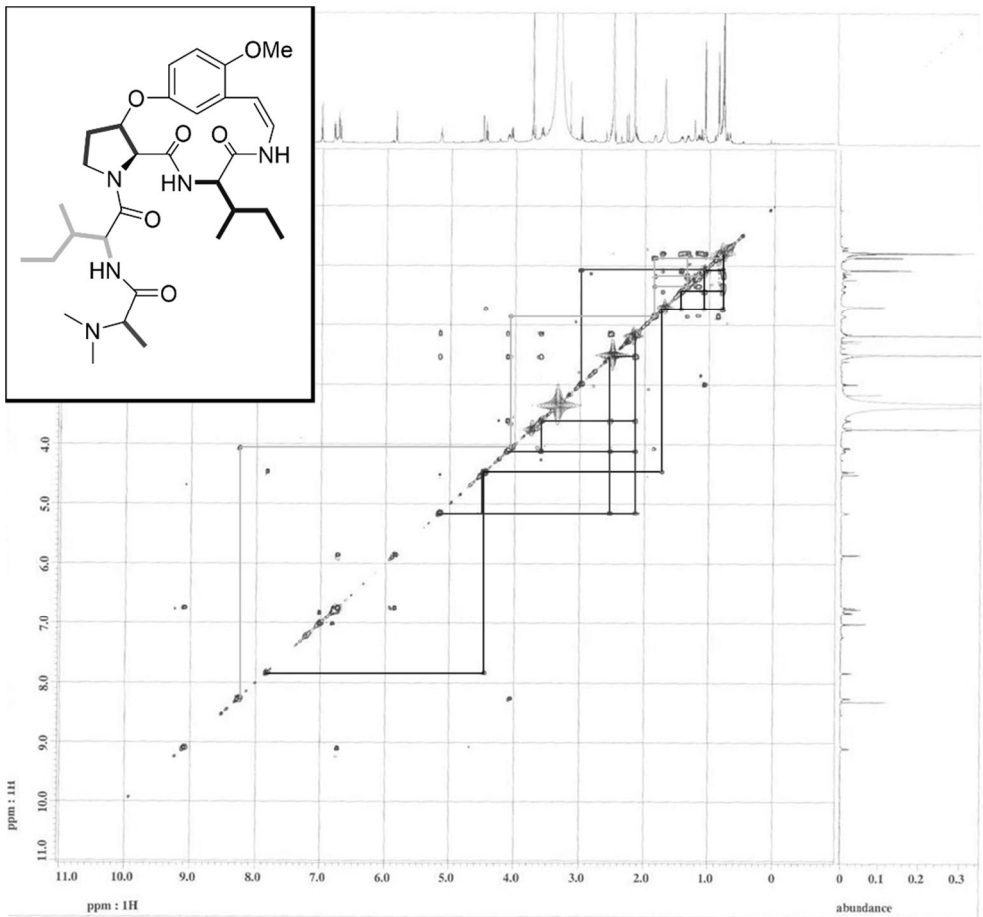

Figure 21. ^{1}H-^{1}H COSY spectrum of compound **5** (600 MHz, DMSO-d_6)

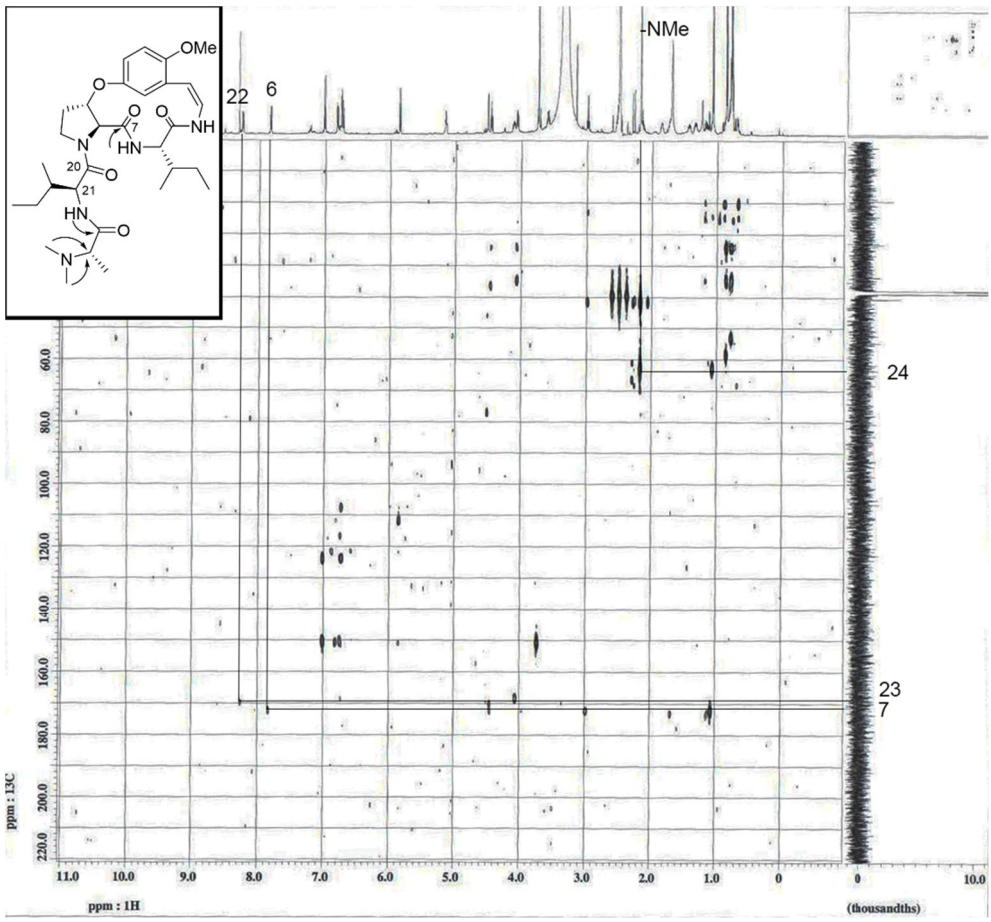

Figure 22. HMBC spectrum of compound **5** (600 MHz, DMSO-d_6)

2.3.4. Compound **6**

Compound **6** was obtained as white amorphous powder with molecular formula $C_{32}H_{43}N_5O_6$, as indicated by ESI-qTOF-MS. Similar to compounds **1-5**, compound **6** was determined as a type-Ib cyclopeptide alkaloid with a terminal *N*-methylalanine, by ^1H, ^{13}C, ^1H-^1H COSY, and HMBC NMR spectral analysis. In ^1H NMR spectrum, two doublet methyl signals at δ_H 0.59 and 0.66 (3H each, *d*, *J* = 6.7 for both) and several overlapped aromatic proton signals at δ_H. 7.20 to 7.29 were observed, and none of methylene proton was observed (Figure 23). These suggested that **6** has a valine and a phenylalanine moiety. From the HMBC NMR spectrum, it was determined that the phenylalanine was the ring bound amino acid and the valine was the intermediate amino acid residue. Comparing these results with the previous report, compound **6** was identified as nummularine B (Panseeta et al., 2011).

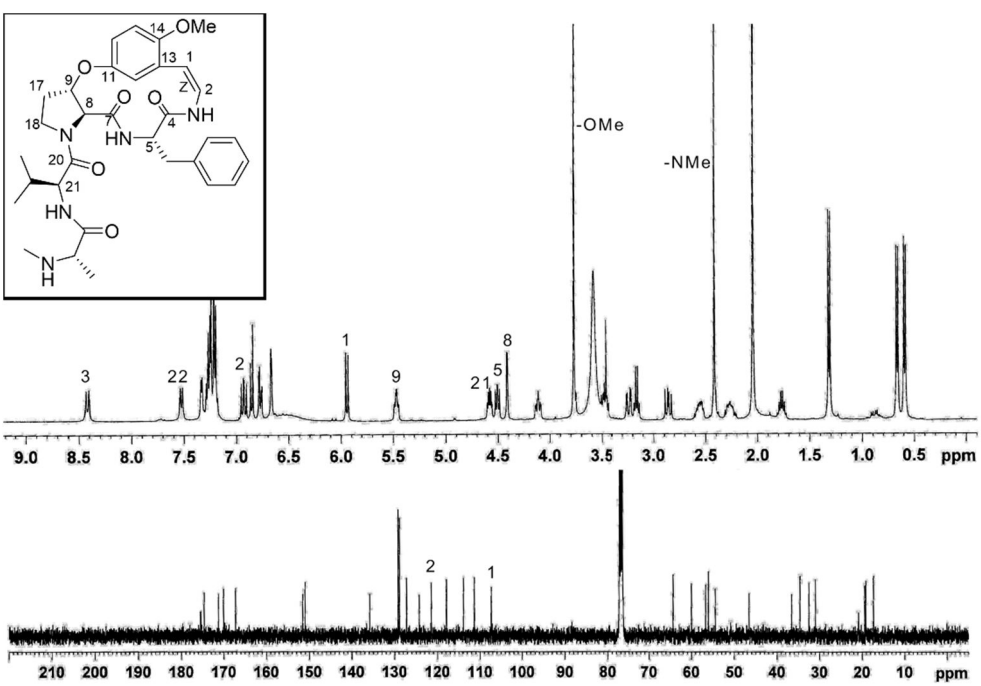

Figure 23. ^1H and ^{13}C NMR spectra of compound **6** (400 / 100MHz, $CDCl_3$)

2.3.5. Compound **7**

Compound **7**, obtained as white amorphous powder, was determined its molecular formula as $C_{34}H_{55}N_5O_6$ by ESI-qTOF-MS. Compound **7** was also determined as a type-Ib cyclopeptide alkaloid with a terminal *N*-methyl amino acid by 1D and 2D NMR spectral analysis. However, the downshifted methyl proton signal of glycine moiety was not observed in ^{1}H NMR spectrum of **7** (Figure 24). Instead, severely overlapped methyl proton signals were observed at δ_H 0.77 to 0.86 region. Analyzing the COSY spectrum of **7**, it was identified that all of ring bound, intermediate, and terminal amino acids have isoleucine side chains. Comparing these spectral inspections with the previously published paper, compound **7** was identified as daechuine-S3 (Lee et al., 2001).

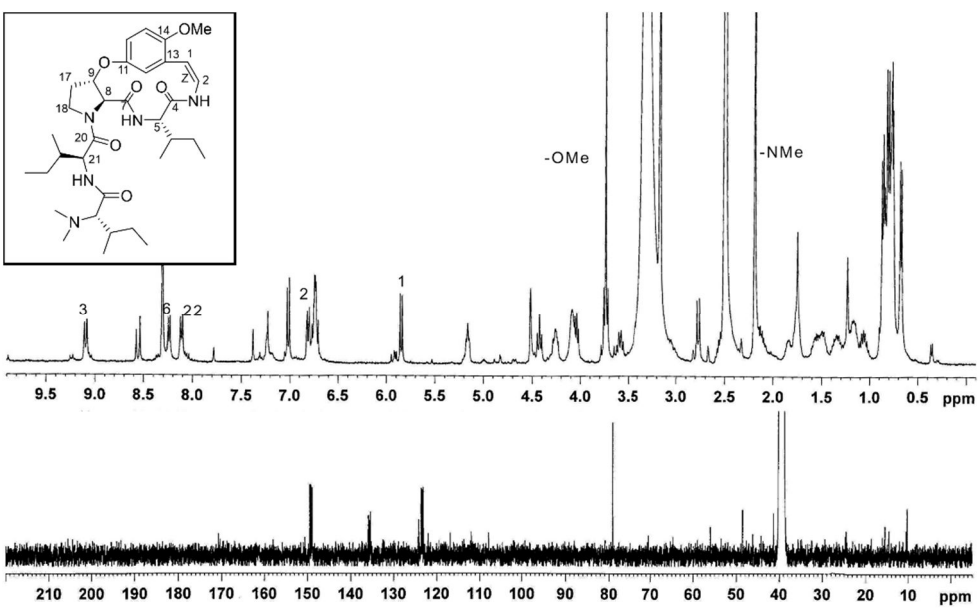

Figure 24. ^{1}H and ^{13}C NMR spectra of compound **7** (400 / 100 MHz, DMSO-d_6)

2.3.6. Compound **8**

Compound **8** was obtained as white amorphous powder. Molecular formula of **8**, $C_{28}H_{45}N_4O_5$ which was indicated by ESI-qTOF-MS, suggested that **8** consisted of three amino acid residues and an oxystyrylamino moiety, different to compounds **1-7**. Analyzing 1D and 2D NMR spectra, it was determined that the ring bound amino acid of **8** was an isoleucine and the terminal amino acid was a *N,N*-dimethylleucine (Figure 25). Comparing this with the previous report, chemical structure of compound **8** was identified as drawn in Figure 25 (Barboni et al., 1994). However, authors of the previous publication did not give compound **8** a trivial name. For convenience, compound **8** was named mucronine K, after the plant species name in which this compound was isolated firstly.

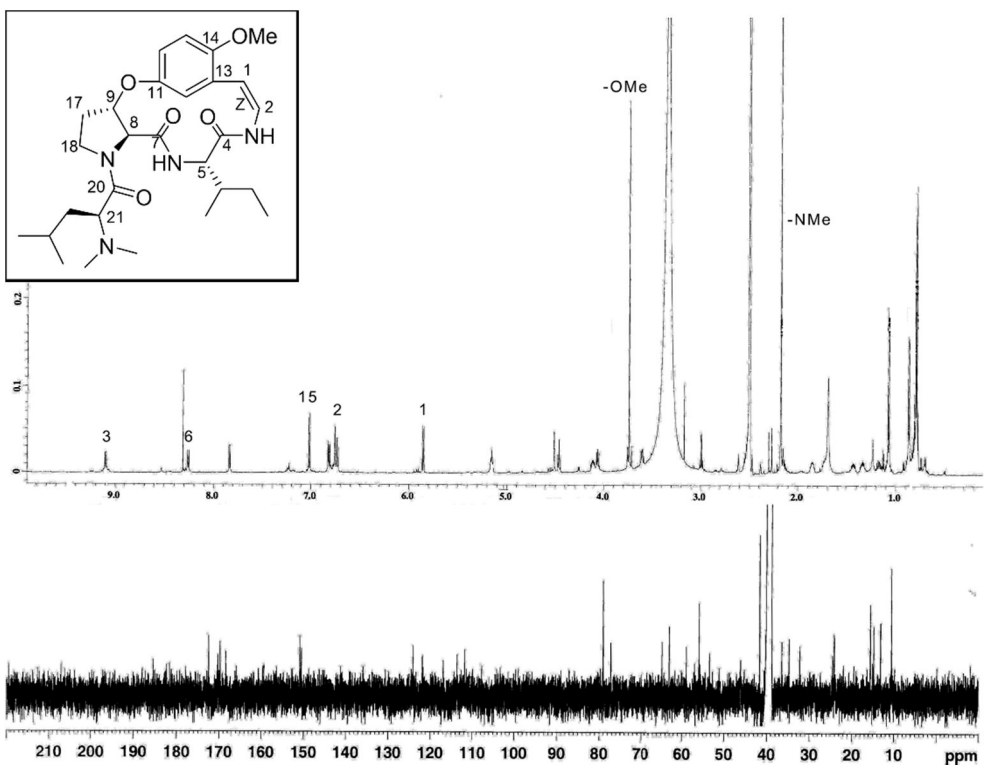

Figure 25. ^{1}H and ^{13}C NMR spectra of compound **8** (400 / 100 MHz, DMSO-d_6)

2.3.7. Compound **9**

Compound **9** was white amorphous powder. It had the molecular formula $C_{28}H_{44}N_4O_4$, as suggested by ESI-qTOF-MS pseudo-molecular peak at *m/z* 501.3444 $[M+H]^+$ (calcd. for $C_{28}H_{45}N_4O_4$, 501.3441). Four aromatic AA′BB′ proton NMR signals at δ_H 7.02, 7.04 (signal overlapped for these two protons), 7.11, and 7.17 (*dd*, *J* = 8.5, 2.2 for these two protons) suggested that **9** is a type-Ia cyclopeptide alkaloid possessing a 14-membered ring (Figure 26). Only one UV_{max} absorption band at λ 229 nm supported this assumption. From the ^1H-^1H COSY spectrum, the proton coupling systems of an isoleucine residue, a β-hydroxyvaline residue, and a leucine residue were confirmed. In the HMBC experiment, the leucine side chain was confirmed to be a part of the terminal *N,N*-dimethyl leucine, and the amide bonds of the *p*-oxystyrylamino moiety to the isoleucine, the isoleucine to β-hydroxyvaline, β-hydroxyvaline to *N,N*-dimethyl leucine. Based on these spectral data anlaysis and comparison with the previously reported reference, compound **9** was identified as adouetine X (Trevisan et al., 2009).

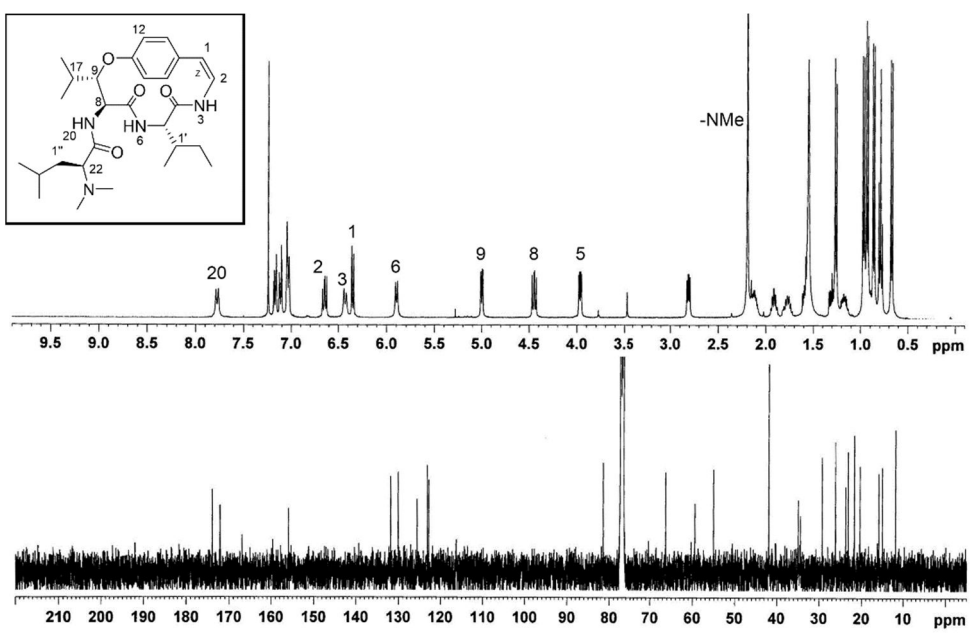

Figure 26. ^1H and ^{13}C NMR spectra of compound **9** (400 / 100 MHz, $CDCl_3$)

Chapter 3. Isolation of Triterpenoids

3.1. LC-MS analysis and dereplication of triterpenic acids in extracts of *Z. jujuba* plant parts

To maximize the amount of information about the chemical constituents of samples, the sample preparative conditions were optimized, such as solvent (methylene chloride, ethyl acetate, and aqueous methanol of different concentrations), extraction methods (maceration, refluxing, and ultrasonication), and extraction time (60, 90, and 120 min). The most important criteria of the optimization were the total amount of extracts and the number of major peaks in chromatogram. As a result, the extraction procedure was optimized as the ultrasonication with MeOH for 120 min. To achieve excellent resolution of chromatograms, ACQUITY BEH C18 column (100 mm × 2.1 mm, 1.7 μm) was selected as a stationary phase column. Regarding the acidity of triterpenic acids, mobile phase was selected as the gradient mixture system of 0.1% aqueous formic acid and acetonitrile. For the mass detection, the negative ion mode was considered to be more suitable because of acidity of triterpenic acids. Both positive and negative ion modes were investigated, and it was confirmed that negative ion modes showed much better sensitivities for triterpenic acid peaks.

Under these optimized analytical conditions, extracts of *Z. jujuba* roots, twigs, leaves, and fruits were analyzed by UHPLC-qTOF-MS. The total ion chromatograms of extracts are shown in Figure 27. Under this chromatographic condition, 52 major peaks were observed and annotated in total ion chromatograms of *Z. jujuba* extracts. Dereplication for these peaks were performed based on their UV, MS, and MS/MS spectra. At first, Triterpenic acids which are abundant in most of plant species, betulinic acid (**KK**), oleanolic acid (**NN**), ursolic acid (**OO**), and maslinic acid (**P**) were obtained commercially and analyzed for peak picking in

LC-MS profiles. Based on these, other triterpenic peaks **G**, **J**, **M-Q**, **T**, **BB**, **CC**, **EE**, **GG**, **JJ**, **MM**, **UU**, **WW**, **XX**, and **ZZ**, were tentatively identified based on their retention times and molecular formulae. These peaks have reported from HPLC profiles of *Z. jujuba* in the previous references (Guo et al., 2009a; Guo et al., 2010; Guo et al., 2011a; Guo et al., 2011c; Plastina et al., 2012), so they were easily identified with relative retention time. The qTOF-MS provided accurate molecular weights of chromatographic peaks with errors smaller than 5.0 ppm, so molecular formulae could be predicted from their MS spectra. Based on these considerations, those peaks were predicted as ceanothic acid (**G**), pomonic acid (**J**), alphitolic acid (**M**), zizyberanal acid (**N**), 2α-hydroxy ursolic acid (**O**), zizyberanalic acid (**Q**), epiceanothic acid (**T**), 3-*O*-*trans*-*p*-coumaroyl alphitolic acid (**BB**), ceanothenic acid (**CC**), 3-*O*-*trans*-*p*-coumaroyl maslinic acid (**EE**), 3-*O*-*cis*-*p*-coumaroyl maslinic acid (**GG**), 2-*O*-*trans*-*p*-coumaroyl alphitolic acid (**JJ**), 2-*O*-*cis*-*p*-coumaroyl alphitolic acid (**MM**), betulonic acid (**UU**), oleanonic acid (**WW**), ursonic acid (**XX**), and zizyberenaliic acid (**ZZ**), respectively.

Several characteristic spectral pattern could be found from spectral data of these tentatively predicted compounds (Table 2). At first, aromatic ester derivatives of altphiolic acid and maslinic acid, commonly exhibited MS/MS fragment ions of *m/z* 453, as shown in cases of peaks **BB**, **EE**, **GG**, **JJ**, and **MM**. However, this ion was not observed in MS/MS spectrum of **M** or **P** themselves. This *m/z* value was deduced to be a fragment ion of $[C_{30}H_{48}O_4\text{-}H_2O\text{-}H]^-$, while $C_{30}H_{48}O_4$ was the molecular formula of **M** and **P**. Considering these facts, this fragment was suggested to be formed by the McLafferty rearrangement occurred between the aromatic ester and H-3 of maslinic or alphitolic acid. The shematic mechanism of this rearrangement is shown in Scheme 2.

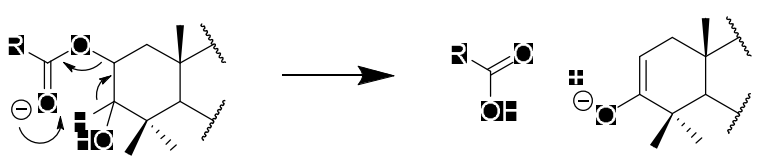

Scheme 2. McLafferty rearrangement in alphitolic acid 2-*O*-ester derivatives

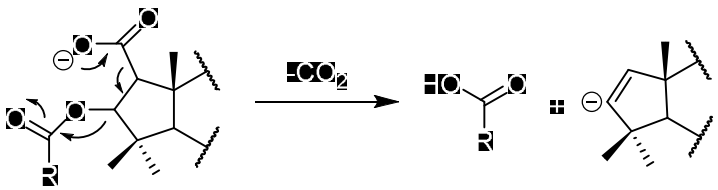

Scheme 3. Suggested fragmentation mechanism of ceanothane-type triterpene 3-*O*-ester derivatives

On the other hand, peaks **G** and **T** exhibited common MS/MS fragment ions of *m/z* 423. It were already reported that this *m/z* 423 ion could be generated from ceanothic acid by the loss of a carboxyl and a H_2O molecule (Yang et al., 2013). However, other chromatographic peaks such as **L** and **RR** showed this fragment ions. These peaks were estimated as aromatic ester derivatives of triterpenic acids, based on MS spectra and predicted molecular formulae of these peaks. The *m/z* 423 fragment ions were thought to be generated by mechanism shown in Scheme 3. Therefore, this ion was predicted to be specific marker MS/MS pattern for ceanothane-type triterpenoids, while *m/z* 453 fragment ions were markers for lupane- or oleanane-type triterpenoids. Peaks **L** and **RR** were estimated to be aromatic esters of ceanothic acid or epiceanothic acid, because they exhibited the *m/z* 423 fragments.

Aromatic ester derivatives provided MS/MS fragment ions of the aromatic moiety, additionally. Peaks **BB**, **EE**, **GG**, **JJ**, and **MM** commonly exhibited fragment ions at *m/z* 145, which was estimated to be a pseudo-molecular ion of *p*-coumaric acid ($C_9H_8O_3$). Other fragmentation pattern for different moieties were also observed, for example, *m/z* 153 ions for peaks **L**, **W**, and **PP** were estimated to be generated by protocatechuic acid ($C_7H_6O_4$) moiety. Based on this consideration and their MS/MS fragment ions of *m/z* 423 and 453, peaks **L** and **W** were tentatively identified as 3-*O*-protocatechuoyl ceanothic acid (**L**) and 2-*O*-protocatechuoyl alphitolic acid (**W**), respectively. Both of these compounds were reported from *Z. jujuba* (Lee et al., 1996), so chemotaxonomic consideration also

supported this putative identificaion. UV absorption spectra provided information about the identification of aromatic ester moieties. Peaks **BB**, **EE**, **GG**, **JJ**, and **MM** showed λ_{max} at 309 nm, which was identical to λ_{max} values of *p*-coumaroyl acid (Gomez-Romero et al., 2010). The presence of protocatechuoyl moieties for **L** and **W** was also enhanced by their λ_{max} at 262 and 292 nm, same as protocatechuic acid (Tadic et al., 2012).

Applying these spectral features of UV, MS, and MS/MS detector, structures of more peaks could be predicted tentatively. Peaks **R** and **S** in Figure 27, which were major peaks of the *Z. jujuba* twig extract, showed their pseudo-molecular peaks at *m/z* 633, which indicated their molecular formula as $C_{39}H_{63}O_7$. Both of them provided fragment ions at *m/*z 453, so they could be deduced to be ester derivatives of alphitolic acid. From fragment ions at *m/z* 179 and UV λ_{max} at 250 and 325 nm, the presence of caffeoyl moiety ($C_9H_8O_4$) could be deduced. Therefore, peaks **R** and **S** are supposed to be 2-*O*-(*trans*/*cis*)-caffeoyl alphitolic acids (Shao et al., 2002), although these compounds have not been isolated from *Z. jujuba* species yet. Similarly, peaks **RR** and **YY** were predicted as 3-*O*-benzoyl ceanothic acid and 2-*O*-benzoyl alphitolic acid, respectively. Peak **C** was predicted as ziziphin, one of major anti-sweetening triterpene glycoside constituents of *Z. jujube* leaves (Kurihara et al., 1988). It was supported by MS/MS fragmentation pattern showing successive loss of arabinose and rhamnose. The results of these dereplication process are summarized in Table 3.

Although major triterpenic acids which are found commonly in most plant species such as betulinic acid or oleanolic acid were found in every parts of the plant, there were many differences between the triterpenic acid constituents of each plant parts. Ceanothane-type triterpenes and their derivatives with five-membered A-ring were more abundant in roots and leaves, rather than twigs and fruits. In twigs extract, most of observed major peaks were tentatively assigned as alphitolic acid and its phenolic ester derivatives (peaks **M**, **R**, **S**, **W**, **BB**, **EE**, and **JJ** in figure 27-(b)). The major target of this experiment was ceanothane-type triterpenic acids, so twigs

were considered to be not suitable for isolation of these type compounds. Among other plant parts, roots showed the most various distribution of unknown triterpenic acids, such as peaks **E**, **I**, **K**, **Y**, **Z**, and **TT**, which could be excellent candidates for novel compound structural discovery. Therefore, the roots extract was chosen to be the target for the isolation of ceanothane-type triterpenic acids of *Z. jujuba*.

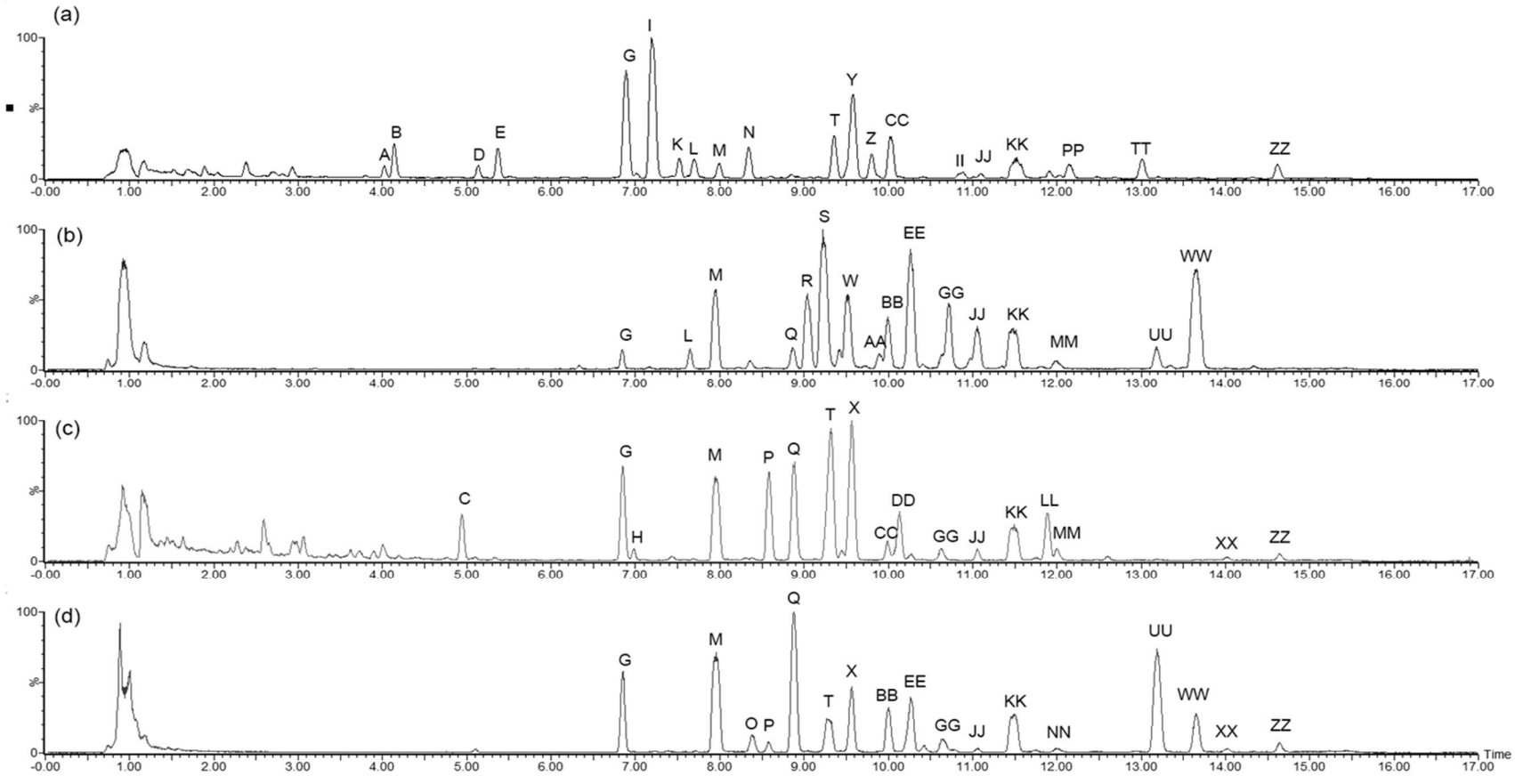

Figure 27. Total ion chromatograms of *Z. jujuba* (a) roots, (b) twigs, (c) leaves, and (d) fruits MeOH extracts in negative ion mode ESI-qTOF-MS detection.

Table 3. Triterpenic acids identified from the total ion chromatograms of *Z. jujuba* extracts.

No	Compounds identification	t_R (mins)	observed *m/z*	calculated m/z	Molecular formula $[M-H]^-$	MS/MS fragments (*m/z*)	UV (λmax, nm)	Peak detected in				References
								Root	Twig	Leaf	Fruit	
A		4.02	501.3221	501.3216	$C_{30}H_{45}O_6$			O				
B		4.14	515.3017	515.3009	$C_{30}H_{43}O_7$			O				
C	ziziphin	4.94	979.5247	979.5266	$C_{51}H_{79}O_{18}$	877, 749, 603				O		
D		5.14	501.3221	501.3216	$C_{30}H_{45}O_6$	471, 427, 409		O	O		O	
E		5.36	529.3163	529.3165	$C_{31}H_{45}O_7$	485		O				
F		6.32	501.3221	501.3216	$C_{30}H_{45}O_6$				O			
G	ceanothic acid	6.84	485.3279	485.3267	$C_{30}H_{45}O_5$	423		O	O	O	O	(Plastina et al., 2012)
H		6.99	501.3221	501.3216	$C_{30}H_{45}O_6$			O		O		
I		7.19	499.3064	499.3060	$C_{30}H_{43}O_6$	437, 409		O				
J	pomonic acid	7.44	469.3334	469.3318	$C_{30}H_{45}O_4$					O		(Plastina et al., 2012)
K		7.52	483.3108	483.3110	$C_{30}H_{43}O_5$			O				
L	3-*O*-protocatechuoyl ceanothic acid	7.70	621.3430	621.3427	$C_{37}H_{49}O_8$	423, 153	262, 297	O	O			
M	alphitolic acid	7.95	471.3476	471.3474	$C_{30}H_{47}O_4$			O	O	O	O	(Plastina et al., 2012)
N	zizyberanal acid	8.34	483.3125	483.3110	$C_{30}H_{43}O_5$	439, 421		O			O	(Guo et al., 2009a)
O	2α-hydroxy ursolic acid	8.37	471.3470	471.3474	$C_{30}H_{47}O_4$					O	O	(Guo et al., 2011c)
P	maslinic acid [a]	8.59	471.3477	471.3474	$C_{30}H_{47}O_4$			O		O	O	(Plastina et al., 2012)
Q	zizyberanalic acid	8.89	469.3317	469.3318	$C_{30}H_{45}O_4$				O	O	O	(Guo et al., 2011a)
R	2-*O*-*trans*-caffeoyl alphitolic acids	9.04	633.3788	633.3791	$C_{39}H_{53}O_7$	453, 179, 161	250, 325		O			
S	2-*O*-*cis*-caffeoyl alphitolic acids	9.22	633.3779	633.3791	$C_{39}H_{53}O_7$	453, 179, 161	246, 325		O			

T	epiceanothic acid	9.36	485.3266	485.3267	$C_{30}H_{45}O_5$	423		O		O	O	(Plastina et al., 2012)
U		9.42	467.3158	467.3161	$C_{30}H_{43}O_4$				O			
V		9.46	471.3479	471.3474	$C_{30}H_{47}O_4$					O		
W	2-*O* -protocatechuoyl alphitolic acid	9.52	607.3626	607.3635	$C_{37}H_{51}O_7$	497, 453, 153	260, 298		O			
X		9.57	469.3315	469.3318	$C_{30}H_{45}O_4$					O	O	
Y		9.58	513.3215	513.3216	$C_{31}H_{45}O_6$	469		O				
Z		9.80	529.3535	529.3529	$C_{32}H_{49}O_6$	485		O				
AA	2-*O* -*trans*- caffeoyl maslinic acid	9.89	633.3787	633.3791	$C_{39}H_{53}O_7$	453, 179, 161	250, 325		O			
BB	3-*O*-*trans* -*p*- coumaroyl alphitolic acid	10.00	617.3837	617.3842	$C_{39}H_{53}O_6$	453, 145	308		O		O	(Plastina et al., 2012)
CC	ceanothenic acid	10.03	453.3009	453.3005	$C_{29}H_{41}O_4$	409		O		O		(Guo et al., 2011c)
DD		10.13	499.3420	499.3423	$C_{31}H_{47}O_5$					O		
EE	3-*O*-*trans* -*p*- coumaroyl maslinic acid	10.26	617.3837	617.3842	$C_{39}H_{53}O_6$	453, 145	311		O	O	O	(Plastina et al., 2012)
FF		10.41	471.3484	471.3474	$C_{30}H_{47}O_4$				O			
GG	3-*O*-*cis* -*p*- coumaroyl maslinic acid	10.63	617.3829	617.3842	$C_{39}H_{53}O_6$	453, 145	259, 311		O	O	O	(Plastina et al., 2012)
HH		10.71	471.3485	471.3474	$C_{30}H_{47}O_4$				O			
II		10.89	453.3008	453.3005	$C_{29}H_{41}O_4$			O				
JJ	2-*O* -*trans*-*p*- coumaroyl alphitolic acid	11.06	617.3834	617.3842	$C_{39}H_{53}O_6$	453, 281,	311	O	O	O	O	(Plastina et al., 2012)
KK	betulinic acid [a]	11.48	455.3519	455.3525	$C_{30}H_{47}O_3$			O	O	O	O	(Plastina et al., 2012)
LL		11.91	499.3430	499.3423	$C_{31}H_{47}O_5$	423, 281		O		O		
MM	2-*O*-*cis*-*p*- coumaroyl alphitolic acid	11.98	617.3847	617.3842	$C_{39}H_{53}O_6$	453, 281, 145	310	O	O	O	O	(Plastina et al., 2012)
NN	oleanolic acid [a]	12.00	455.3519	455.3525	$C_{30}H_{47}O_3$			O	O	O	O	(Guo et al., 2010)
OO	ursolic acid [a]	12.10	455.3519	455.3525	$C_{30}H_{47}O_3$						O	(Guo et al., 2010)
PP		12.15	635.3571	635.3584	$C_{38}H_{51}O_8$	535, 437, 153	263, 299	O				
QQ		12.48	439.3207	439.3212	$C_{29}H_{43}O_3$			O				

RR	3-*O*-benzoyl ceanothic acid	12.60	589.3530	589.3529	$C_{37}H_{49}O_6$	423, 245, 121	227			O		
SS		12.67	483.3469	483.3474	$C_{31}H_{47}O_4$	281		O				
TT		13.01	483.3475	483.3474	$C_{31}H_{47}O_4$			O				
UU	betulonic acid	13.18	453.3365	453.3369	$C_{30}H_{45}O_3$	407		O	O	O	O	(Guo et al., 2011a)
VV		13.41	483.3483	483.3474	$C_{31}H_{47}O_4$			O				
WW	oleanonic acid	13.65	453.3366	453.3369	$C_{30}H_{45}O_3$	407			O		O	(Guo et al., 2010)
XX	ursonic acid	13.99	453.3383	453.3369	$C_{30}H_{45}O_3$	407		O	O	O	O	(Guo et al., 2010)
YY	2-*O*-benzoyl alphitolic acid	14.33	575.3759	575.3736	$C_{37}H_{51}O_5$	453, 281, 121	227	O	O			
ZZ	*zizy*berenalic acid	14.62	451.3214	451.3212	$C_{30}H_{43}O_3$	281, 116	252	O		O	O	(Guo et al., 2011a)

[a] identified by comparison with authentic standard compounds.

3.2. MS-guided isolation of triterpenoids

Pulverized air-dried roots of *Z. jujuba* (7.5 kg) were extracted in sonication with MeOH (2 × 30 L, for 3 h each) at rt. The crude extract (630.4 g) was fully evaporated *in vacuo*. The drided extract was suspended into water, and the suspension was sequentially fractionated with $CHCl_3$, EtOAc, and BuOH. LC-MS analysis showed that most of triterpenic acids were abundant in $CHCl_3$ and EtOAc fractions, so these two fractions were decided to be further fractionated. According to Lee et al., triterpenic acids and esters are not readily separated by silica gel column chromatography because of their acidities and similar polarities (Lee et al., 1996). LC-MS profiles suggested they could be separated efficiently with reversed phase HPLC eluted H_2O-MeCN solvent system modified with formic acid. However, they could not be subjected to reversed phased HPLC in the early stage of separation because of their poor solubility in MeOH. Thus, $CHCl_3$ fraction (103.5 g) and EtOAc fraction (75.0 g) were respectively subjected to silica gel column chromatography to afford subfractions of each. Subfractions were analyzed by UHPLC-qTOF-MS for dereplication, and the subfractions which exhibited LC-MS peaks of unknown compounds were selected as targets of further purification process. Selected fractions were subjected to other preparative techniques such as Sephadex LH-20 or preparative HPLC. When the targeted compound was finally purified, its chemical structure was elucidated by NMR analysis. With this strategy, 37 triterpenoids (compounds **10**-**46**) and 6 phenolic compounds (**47**-**51**) were isolated from $CHCl_3$ and EtOAc fractions, and chemically characterized. Among the 37 triterpenoids, eleven lupane-type, one oleanane-type, and one ursane-type triterpenoids were isolated, and the rest of them were ceanothane-type triterpenic acids. Especially, compound **42**-**44** were characterized as compounds with a novel backbone which has C-C bond linkage between catechin and A-ring of ceanothane-type triterpene, and they were named epicatechinoceanothic acid A-C. The

chemical structures of isolated triterpenoids (**10-46**) are shown in Figure 28, while phenolic compounds **47-52** are shown in Figure 29. The details about the structural elucidation will be described in section 3.3 and 3.4.

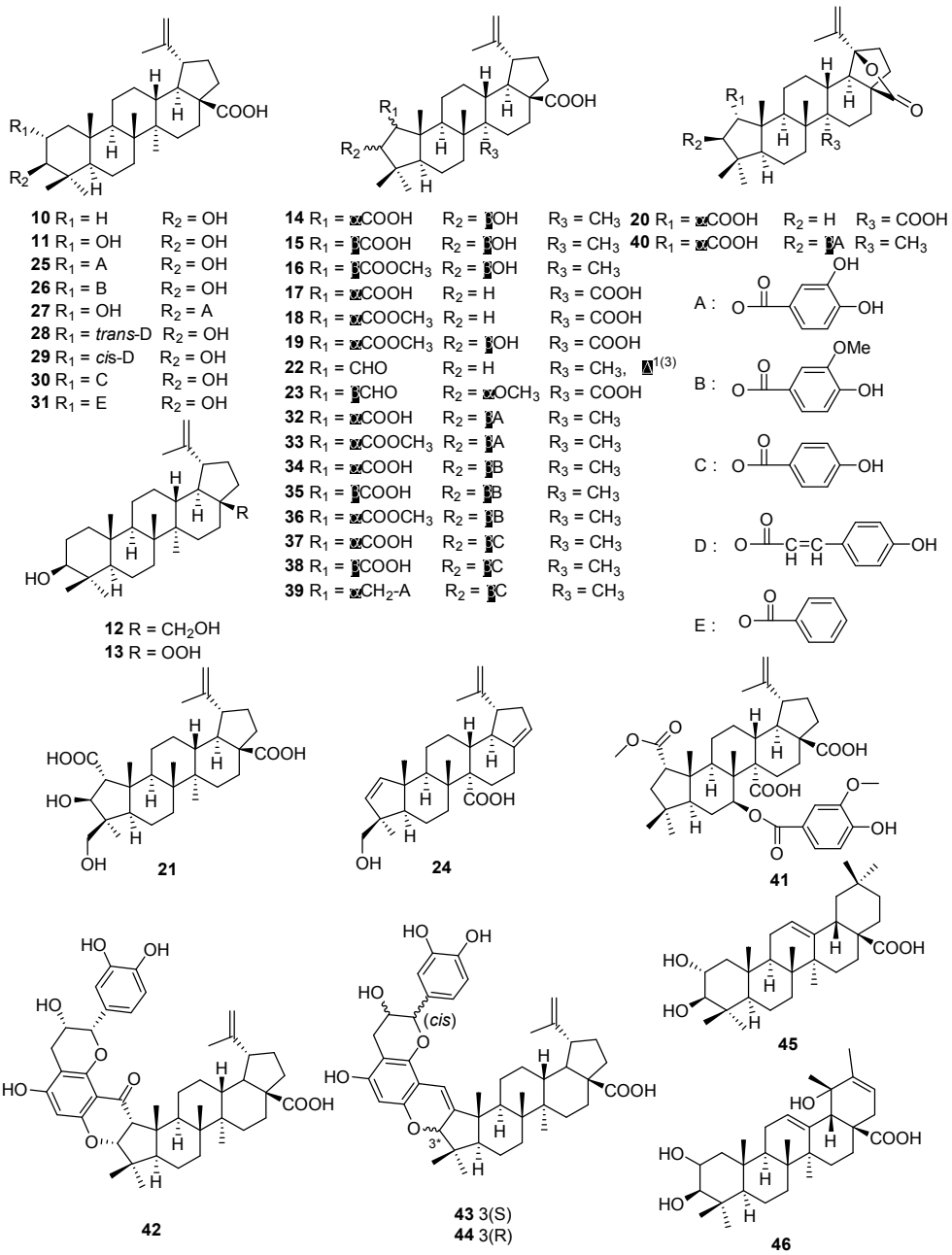

Figure 28. Chemical structures of isolated triterpenoid compounds **10-46**

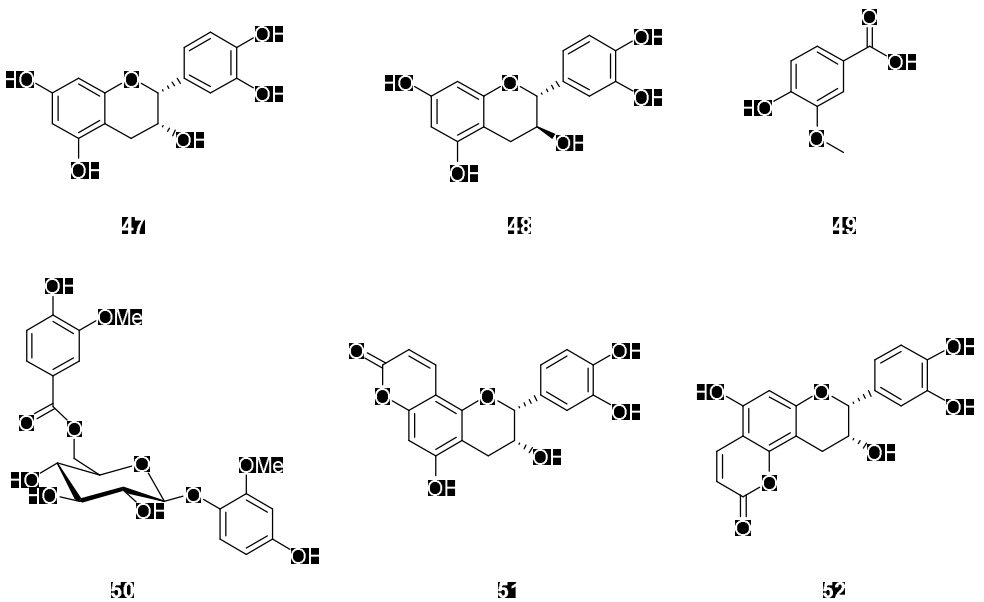

Figure 29. Chemical structures of isolated phenolic compounds **47-52**

The mixture of compound **10-41** and **45-46** were analyzed by UHPLC-qTOF-MS, except compounds **12** and **13** for their detectability problems in negative mode MS because of the lack of carboxylic acid function. The total ion chromatograms of the mixture and the crude root extract are shown in Figure 30. The in-house dereplication library for isolated triterpenic acids, containing t_R, observed MS *m/z* values, MS/MS fragmentational patterns, and UV λ_{max} was built based on this LC-MS data, as shown in Table 4. Most of major chromatographic peaks of root extract were successfully isolated with the MS-guided isolation. Peaks **G**, **L**, **M**, **P**, **T**, **W**, **JJ**, **KK**, **MM**, **YY** and **ZZ** showed that their predicted structures matched perfectly with isolated compounds as ceanothic acid (**14**), 3-*O*-protocatechuoyl ceanothic acid (**32**), alphitolic acid (**11**), maslinic acid (**45**), epiceanothic acid (**15**), 2-*O*-protocatechuoyl alphitolic acid (**25**), 2-*O*-*trans*-*p*-coumaroyl alphitolic acid (**28**), betulinic acid (**10**), 2-*O*-*cis*-*p*-coumaroyl alphitolic acid (**29**), 2-*O*-benzoyl alphitolic acid (**31**), and zizyberenalic acid (**22**), respectively. Additionally, chromatographic peaks of which structural identification was unknown before were

also purified and structurally elucidated. Peaks **D**, **E**, **I**, **Y**, **LL**, **PP**, and **TT** exhibited moderate to high ion intensities in the total ion chromatograms of the extracts, but their identification was unrevealed. Those peaks were successfully purified, and determined to be 24-hydroxy ceanothic acid (**21**), ceanothetric acid 2-methyl ester (**19**), 3-dehydroxy ceanothetric acid (**17**), 3-dehydroxy ceanothetric acid 2-methyl ester (**18**), epiceanothic acid 2-methyl ester (**16**), 3-*O*-protocatechuoyl ceanothic acid 2-methyl ester (**33**), and 3-*O*-methyl-zizyberanalic acid (**23**), by MS and NMR spectral analysis. Among these compounds, **16**-**19**, **23**, and **33** were first isolated from nature. Compounds **20**, **24**, **26**, **27**, **30**, **35**-**41** were also newly isolated compounds, although their chromatographic peaks had too small intensities in the LC-MS profile of the crude extract. Their chemical structures were elucidated, and named 3-dehydroxy-ceanotha-27α-carboxy-28β,19β-olide (**20**), 1,28-dinor-24-hydroxy-lup-2,17(22)-diene-27-oic acid (**24**), 2-*O*-vanilloyl alphitolic acid (**26**), 3-*O*-protocatechuoyl alphitolic acid (**27**), 2-*O*-*p*-hydroxybenzoyl alphitolic acid (**30**), 3-*O*-vanilloyl epiceanothic acid (**35**), 3-*O*-vanilloyl ceanothic acid 2-methyl ester (**36**), 3-*O*-*p*-hydroxybenzoyl ceanothic acid (**37**), 3-*O*-*p*-hydroxybenzoyl epiceanothic acid (**38**), 2-*O*-protocatechuoyl isoceanothanolic acid (**39**), 3-*O*-protocatechuoyl ceanotha-28β,19β-olide (**40**), 7-*O*-vanilloyl 3-dehydroxy ceanothetric acid 2-methyl ester (**41**).

From these isolated compound library, it was validated that the developed dereplication process was suitable for most triterpenoids. Aromatic ester derivatives of alphitolic acid (**11**), suck as compounds **25**-**31**, exhibited common MS/MS fragment ion peaks at *m/z* 453, while ceanothane-type compounds such as **14**, **15**, **32**, **35**, **37**, **37**, and **40** showed *m/z* 423. Aromatic moieties also exhibited their own characteristic fragmentation patterns, for example, *m/*z 153 in **32** and **40** for protocatechuic acid ($C_7H_6O_4$), *m/z* 137 in **37** and **38** for *p*-hydroxybenzoic acid ($C_7H_6O_3$), and *m/z* 167 in **35** for vanillic acid ($C_8H_7O_4$). However, when 2-carboxyl of ceanothanes was substituted to a methyl ester, the fragment of *m/z* 423 did not occur as shown in compounds **16**, **19**, **33**, and **36**. 3-dehydroxy derivatives such as

17, **18**, and **41** also did not provide this fragmentation pattern. UV absorption spectra also provided information about the identification of aromatic ester moieties. Protocatechuoyl and vanilloyl ester derivatives showed λ_{max} at 262 and 292 nm, *p*-hydroxybenzoyl ester derivatives at 260 nm, benzoyl ester derivative at 228 nm, and (*trans* or *cis*)-*p*-courmaroyl ester derivatives at 309 nm. These λ_{max} values were similar to those of protocatechuic acid (Tadic et al., 2012), vanillic acid (Kang et al., 2014), *p*-hydroxybenzoic acid (He et al., 2014), benzoic acid and *p*-coumaroyl acid (Gomez-Romero et al., 2010), respectively. Therefore, the dereplication method for triterpenoids of *Z. jujuba* was proven to be effective for prediction of Rhanmaceae triterepenoids including lupane- and ceanothane-types.

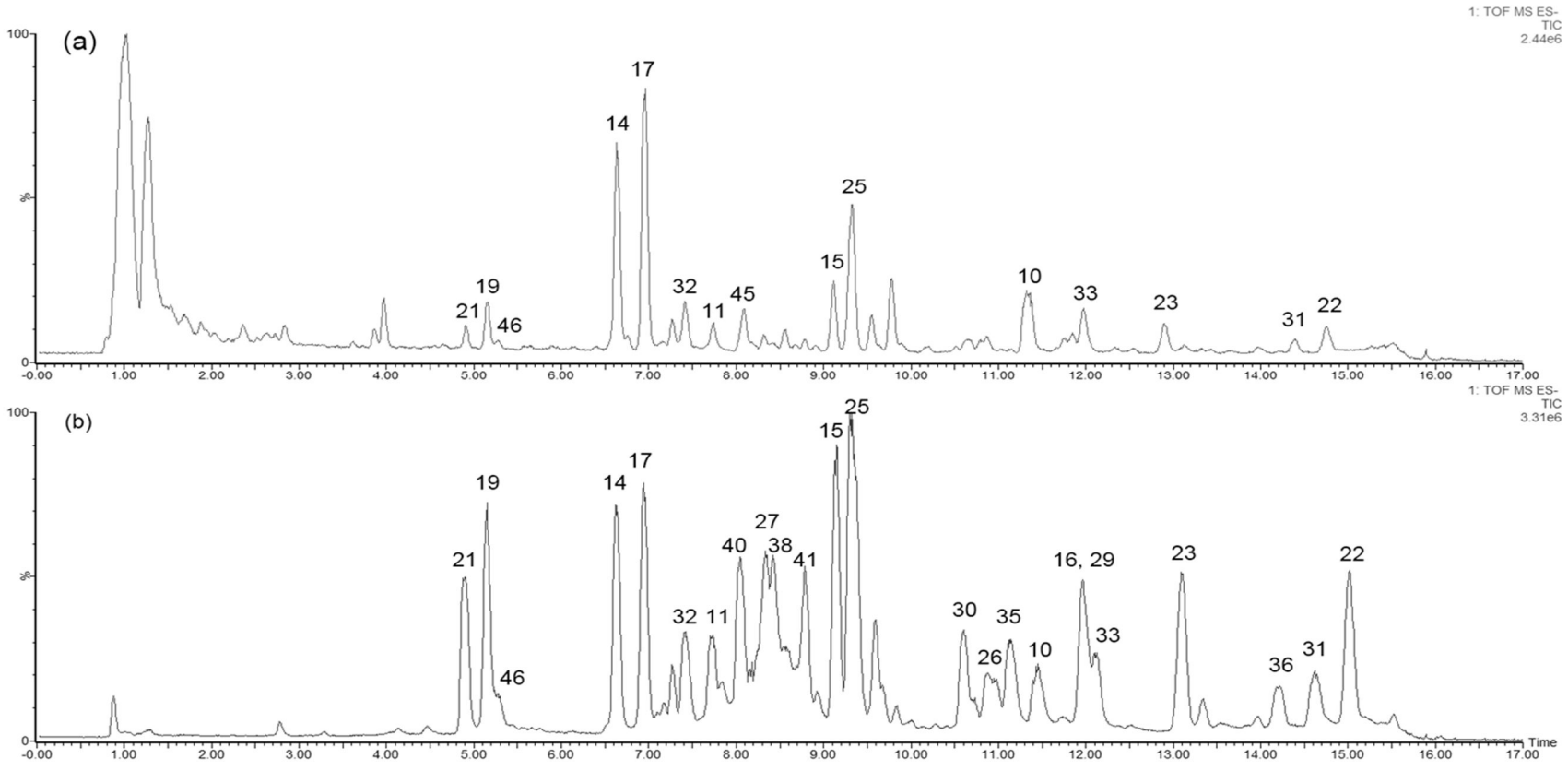

Figure 30. Total ion chromatograms of (a) *Z. jujuba* roots MeOH extract (b) mixtures of isolated compounds **10**, **11**, **14-41**, **45**, and **46** in negative ion mode ESI-qTOF-MS detection.

Table 4. In-house library for triterpenoids isolated from *Z. jujuba* root extract

Peak No.	Compound No.	Compounds identification	t_R (mins)	observed *m/z*	calculated *m/z*	Molecular formula $[M-H]^-$	MS/MS fragments (*m/z*)	UV (λmax, nm)
D	**21**	24-hydroxy ceanothic acid	4.90	501.3221	501.3216	$C_{30}H_{45}O_6$	471, 427	
E	**19**	ceanothetric acid 2-methyl ester	5.15	529.3157	529.3165	$C_{31}H_{45}O_7$	485	
	46	euscaphic acid	5.28	487.3429	487.3423	$C_{30}H_{47}O_5$	407	
G	**14**	ceanothic acid	6.84	485.3262	485.3267	$C_{30}H_{45}O_5$	423	
I	**17**	3-dehydroxy ceanothetric acid	6.94	499.3071	499.3060	$C_{30}H_{43}O_6$		
L	**32**	3-*O*-protocatechuoyl ceanothic acid	7.42	621.3430	621.3427	$C_{37}H_{49}O_8$	423, 153	262, 297
M	**11**	alphitolic acid	7.73	471.3478	471.3474	$C_{30}H_{47}O_4$		
	40	3-*O*-protocatechuoyl-ceanotha-28β,19β-olide	8.04	619.3265	619.3271	$C_{37}H_{47}O_8$	153	262, 296
P	**45**	maslinic acid	8.19	471.3470	471.3477	$C_{30}H_{47}O_4$		
	39	2-*O*-protocatechuoyl isoceanothanolic acid	8.28	607.3630	607.3635	$C_{37}H_{51}O_7$	423, 153	258
	27	3-*O*-protocatechuoyl alphitolic acid	8.34	607.3634	607.3635	$C_{37}H_{51}O_7$	453, 153	262
	38	3-O-p-hydroxy benzoyl epiceanothic acid	8.42	607.3627	607.3635	$C_{37}H_{51}O_7$	485, 423, 137	260
	34	3-*O*-vanilloyl ceanothic acid	8.58	635.3582	635.3584	$C_{38}H_{51}O_8$	423, 167	264, 295
	37	3-*O-p*-hydroxybenzoyl ceanothic acid	8.69	605.3480	605.3468	$C_{37}H_{49}O_7$	485, 423, 137	260
	41	7-*O*-vanilloyl 3-dehydroxy ceanothetric acid 2-methyl ester	8.78	679.3499	679.3482	$C_{39}H_{51}O_{10}$	511, 167	263, 295
T	**15**	epiceanothic acid	9.14	485.3273	485.3267	$C_{30}H_{45}O_5$	423	
	20	3-dehydroxy-ceanotha-27α-carboxy-28β,19β-olide	9.30	497.2914	497.2903	$C_{30}H_{41}O_6$		
W	**25**	2-*O*-protocatechuoyl alphitolic acid	9.37	607.3651	607.3635	$C_{37}H_{51}O_7$	453, 153	260, 295

Y	**18**	3-dehydroxy ceanothetric acid 2-methyl ester	9.37	513.3270	513.3216	$C_{31}H_{45}O_6$	469	
	24	1,28-dinor-24-hydroxy-lup-2,17(22)-diene-27-oic acid	10.19	423.2901	423.2889	$C_{28}H_{40}O_3$		
	30	2-*O*-*p* -hydroxybenzoyl alphitolic acid	10.60	591.3693	591.3686	$C_{37}H_{51}O_6$	547, 453, 137	256
	26	2-*O* -vanilloyl alphitolic acid	10.86	621.3787	621.3791	$C_{38}H_{53}O_7$	453, 167	261, 294
JJ	**28**	2-*O* -*trans*-*p* -coumaroyl alphitolic acid	10.98	617.3843	617.3842	$C_{39}H_{53}O_6$	453, 145	311
	35	3-*O* -vanilloyl epiceanothic acid	11.12	635.3591	635.3584	$C_{38}H_{51}O_8$	485, 423, 167	261, 294
KK	**10**	betulinic acid	11.46	455.3536	455.3525	$C_{30}H_{47}O_3$		
LL	**16**	epiceanothic acid 2-methyl ester	11.96	499.3419	499.3423	$C_{31}H_{47}O_5$		
MM	**29**	2-*O* -*cis*-*p* -coumaroyl alphitolic acid	12.00	617.3832	617.3842	$C_{39}H_{53}O_6$	453, 145	307
PP	**33**	3-*O* -protocatechuoyl ceanothic acid 2-methyl ester	12.12	635.3580	635.3584	$C_{38}H_{51}O_8$	153	260, 298
TT	**23**	3-*O* -methyl-zizyberanalic acid	13.13	483.3464	483.3474	$C_{31}H_{47}O_4$		
	36	3-*O* -vanilloyl ceanothic acid 2-methyl ester	14.22	649.3746	649.3740	$C_{39}H_{53}O_8$	167	262, 294
YY	**31**	2-*O* -benzoyl alphitolic acid	14.62	575.3740	575.3736	$C_{37}H_{51}O_5$	453, 121	228
ZZ	**22**	zizyberenalic acid	15.02	451.3236	451.3212	$C_{30}H_{43}O_3$		244

3.3. Structural elucidation of isolated triterpenoids

3.3.1. Compounds **10**, **11**, and **12**

Compound **10** was obtained as a white amorphous powder with molecular formula $C_{30}H_{48}O_3$, as indicated by ESI-qTOF-MS (*m/z* 455.3524 $[M-H]^-$, calcd. for $C_{30}H_{47}O_3$, 455.3525). The exo-methylene carbons at δ_C 151.3 (C-20) and 109.9 (C-29) and protons at δ_H 4.77 and 4.95 (each *s*, C-29) were the characteristic signals of an isopropenyl group, which could be found in a lupane-type triterpenoid, not an oleanane- or ursane-type (Fotie et al., 2006) (Figure 31). The carbon signals at δ_C 178.9 (C-28) and 78.1 (C-3) showed that compound **10** bear a carboxylic and a hydroxyl moiety, respectively. Based on the HMBC correlation between δ_H 3.46 (1H, *t*, *J* = 7.8 Hz, H-3) and δ_C 28.7 (C-23) / 16.4 (C-24), the location of the hydroxyl moiety was confirmed to be at C-3. The carboxyl acid was also confirmed to be at C-28 by the HMBC analysis. Basis on these spectral data, compound **10** was identified as betulinic acid (Yili et al., 2009).

Compound **11** was a white amorphous powder, and its molecular formula was determined as $C_{30}H_{48}O_4$ by ESI-qTOF-MS (*m/z* 471.3472 $[M-H]^-$, calcd. for $C_{30}H_{47}O_4$, 471.3471). The ^1H and ^{13}C NMR spectra of compound **11** were similar to those of compound **10**, except for the signals at δ_H/δ_C 4.14 (1H, *m*, H-2)/69.2 (C-2) (Figure 32). In the HMBC analysis, the H-2 correlated with the carbons of δ_C 48.6 (C-1) and 84.1 (C-3), so this hydroxyl moiety was determined to be located at C-2. The coupling constant of the doublet at δ_H 3.42 (*J* = 9.4 Hz) established 2α-configuration (Kojima and Ogura, 1989). Consequently, these spectral data showed compound **11** was alphitolic acid (Hao et al., 2009).

Compound **12** was isolated as a white amorphous powder. ESI-qTOF-MS pseudo-molecular ion peak at *m/z* 443.3885 $[M+H]^+$ (calcd. for $C_{30}H_{51}H_2$, 443.3889) indicated that the molecular formula of **12** was $C_{30}H_{50}H_2$. The ^1H and ^{13}C NMR

spectra of **12** were also similar to those of **10**, but there was no carboxyl carbon signal, and the proton signal of H-19 was upshifted from to δ_H 3.54 to 2.65, which means the deshielding effect by carboxylic acid of C-28 does not exist in compound **12** (Figure 33). Instead, a primary alcohol at δ_H/δ_C 3.69 and 4.12 (1H each, *d*, *J* = 10.7 Hz, H-28)/59.8 (C-28) was observed. The location of this –CH_2OH was established by the HMBC correlations of H-16/H-18/H-22 to C-28. Thus, compound **12** was confirmed as betulin, in comparison with previously reported literature (Wei et al., 2013).

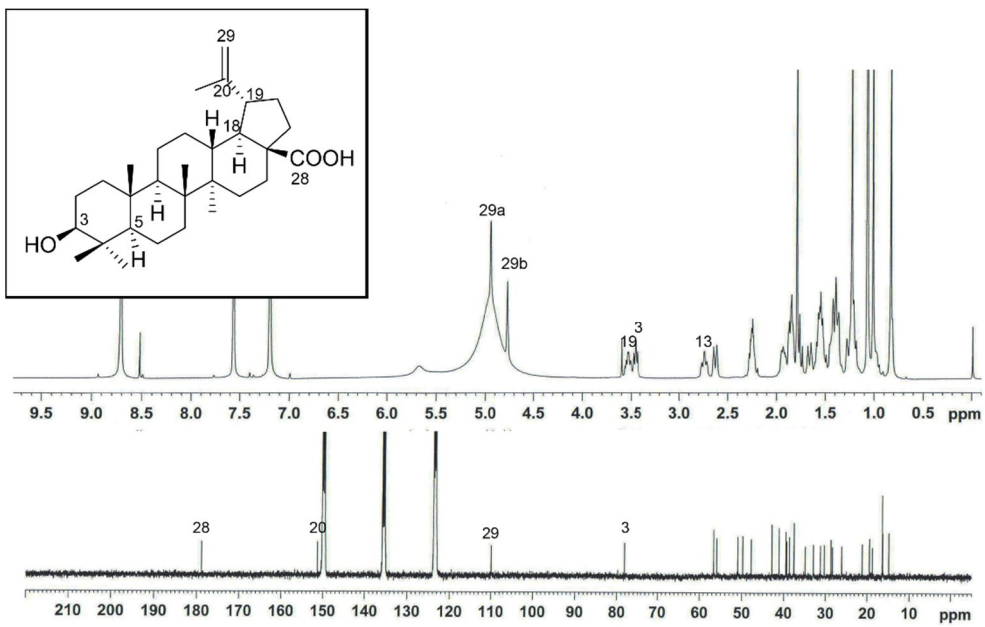

Figure 31. ^{1}H and ^{13}C NMR spectra of compound **10** (400 / 100 MHz, pyridine-d_5)

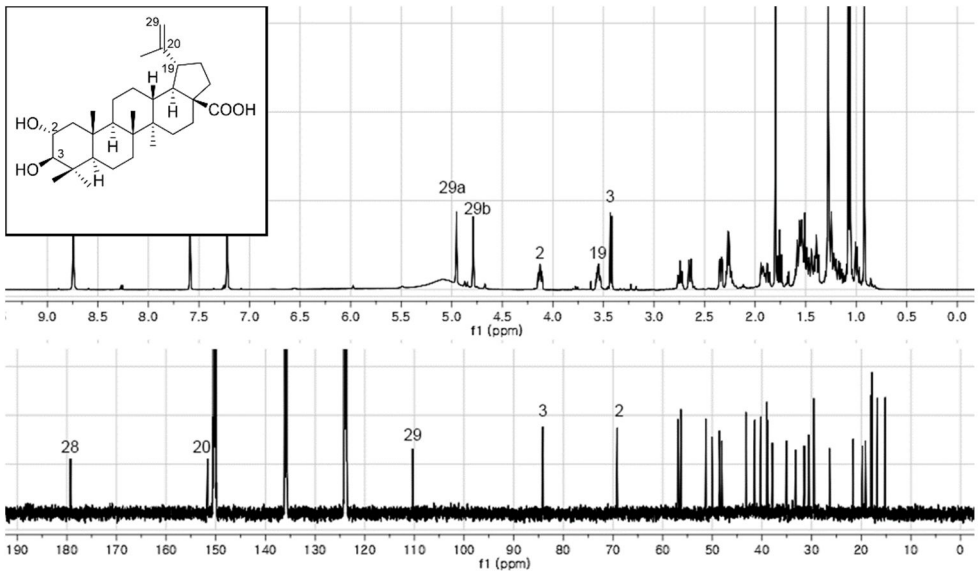

Figure 32. ^{1}H and ^{13}C NMR spectra of compound **11** (400 / 100 MHz, pyridine-d_5)

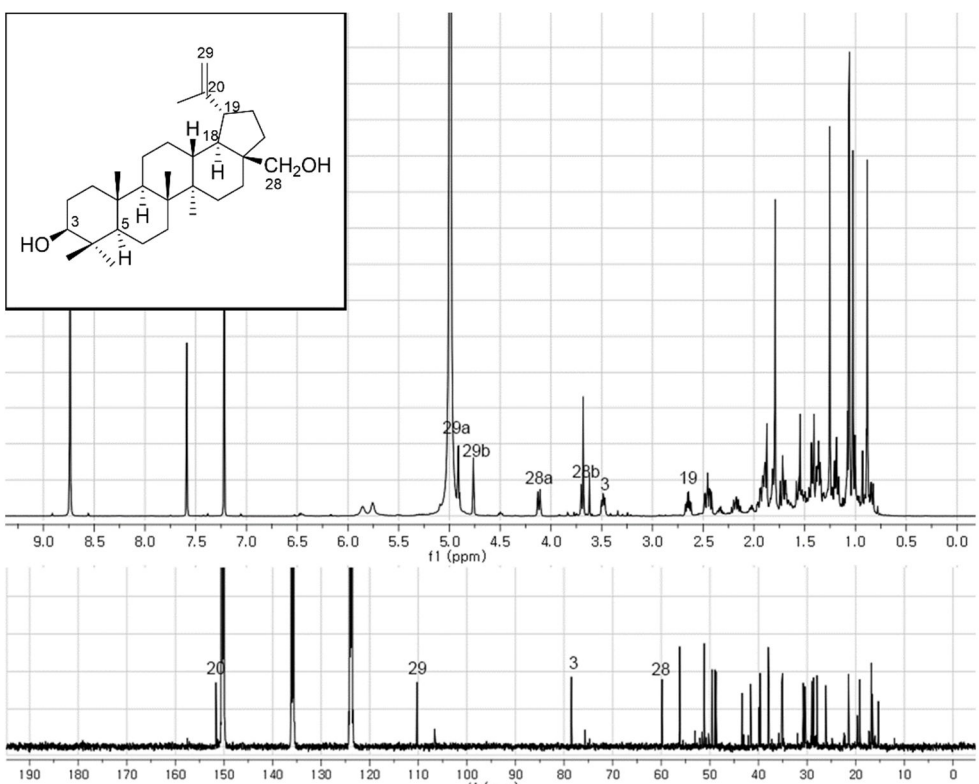

Figure 33. ^{1}H and ^{13}C NMR spectra of compound **12** (600 / 150 MHz, pyridine-d_5)

3.3.2. Compound **13**

Compound **13** was obtained as a colorless amorphous sold. Its molecular formula $C_{29}H_{48}O_3$, indicated by ESI-qTOF-MS (*m/z* 445.3678 $[M+H]^+$, calcd. for $C_{29}H_{49}O_3$, 445.3682 $[M+H]^+$) and its ^1H and ^{13}C NMR spectrum suggested that **13** is a norlupane derivative (Figure 34). The ^{13}C and HSQC NMR spectra of **13** showed a quaternary carbon signal at δ_C 91.6. This carbon was assigned to C-17, based on HMBC correlations from H-18 (δ_H 1.67, *m*) and H-22b (δ_H 2.15, *m*). Thus, compound **13** was to be a 28-norlupane derivative with C-17 hydroperoxy substituent. The β-configuration of C-17 was suggested by ^{13}C NMR data comparison with the previously reported publication (Abdel Bar et al., 2008). Abdel Bar et al. isolated both of C-17-epimeric analogues of 3β-hydroxy-28-norlup-20(29)-ene-17-hydroperoxide and confirmed there were significant differences in the chemical shifts of C-13 and C-19 between two analogues. By comparison with this data, compound **13** was confirmed as 3β-hydroxy-28-norlup-20(29)-ene-17β-hydroperoxide.

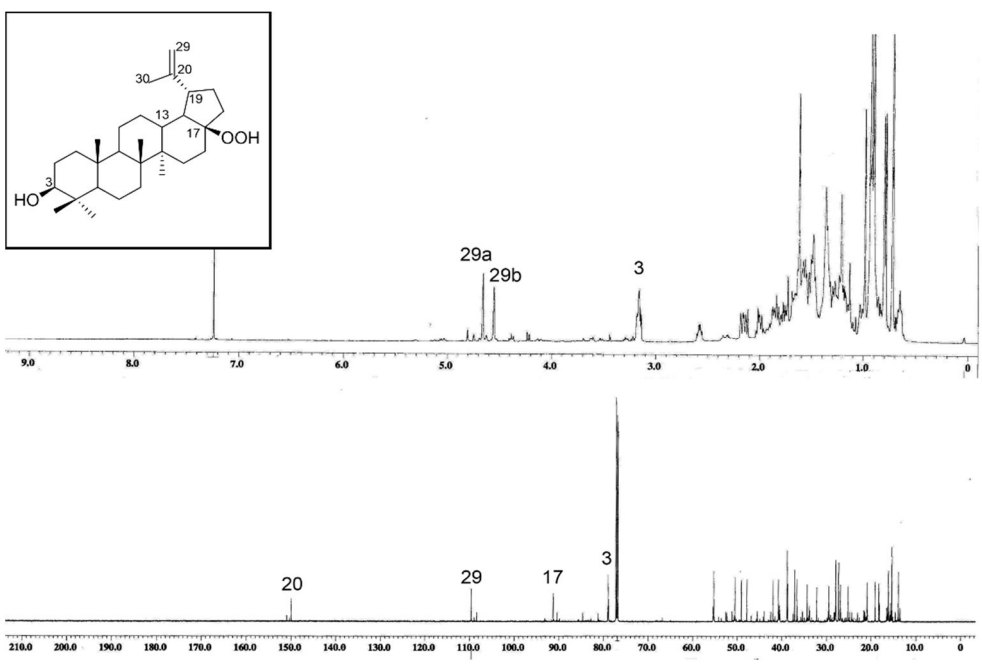

Figure 34. ^1H and ^{13}C NMR spectra of compound **13** (600 / 150 MHz, $CDCl_3$)

3.3.3. Compounds **14** and **15**

Compound **14** was obtained as pale yellowish powder with molecular formula $C_{30}H_{46}O_5$, indicated by ESI-qTOF-MS (*m/z* 485.3268 $[M-H]^-$, calcd. for $C_{30}H_{45}O_5$, 485.3267). The characteristic signals of the isopropenyl moiety, exo-methylene protons and carbons at δ_H/δ_C 4.63 and 4.83 (1H each, *s*, H-29)/109.7 (C-29) and 151.1 (C-20) were also shown in the ^1H and ^{13}C NMR spectra (Figure 35). However, different to compounds **10** and **11**, two proton singlets at δ_H 3.18 (H-1) and 4.79 (H-3) were observed in the ^1H NMR spectrum, and they exhibited ^1H-^1H COSY correlations to each other. Additionally, there was another carboxyl carbon signal at δ_C 178.0 (C-2), and those two proton singlets showed correlations to this carboxyl carbon in HMBC spectrum. Consequently, these spectral data showed that compound **14** is a ceanothane-type triterpene, which has a rearranged cyclopentanyl A-ring. The *trans* relationship between H-1β and H-3α was deduced from their singlet shape signals in ^1H NMR spectrum. It has been reported that only H-1β and H-3α orientation exhibits two singlet signals like these ones (Eade et al., 1967). Consequently, compound **14** was identified as ceanothic acid (Li et al., 1997).

Compound **15** was acquired as pale yellowish powder, and ESI-qTOF-MS determined its molecular formula as $C_{30}H_{46}O_5$, which was indicated by *m/z* value of 485.3268 $[M-H]^-$ (calcd. for $C_{30}H_{45}O_5$, 485.3267). Its ^1H and ^{13}C NMR spectra was similar to those of compound **14**, but proton signals of H-1 (δ_H 2.89) and H-3 (δ_H 4.66) were shown as doublets with J = 7.3 Hz, instead of singlets in **14** (Figure 36). This suggested that H-2 and H-3 would be in *cis* orientation. Methyl protons of H-25 were significantly downshifted than ones of compound **14** (δ_H 1.67 in **15**, δ_H 1.36 in **14**), while H-23 were upshifted (δ_H 1.12 in **15**, δ_H 1.40 in **14**). Additionally, chemical shifts of H/C-5 (δ_H/δ_C 1.08/62.7) showed significant differences to those of compound **14** (δ_H/δ_C 2.20/57.0). These differences were supposed to be caused by spatial effects of C-2 carboxyl group. The α-oriented carboxyl group in **14**

caused downshifts of α-oriented H-5 and H-23, on the other hands, C-5 was observed in more upfielded region because of the shielding effect by H-5. Therefore, compound **15** was determined to be a C-1 epimer of compound **14**, epiceanothic acid (Li et al., 2005).

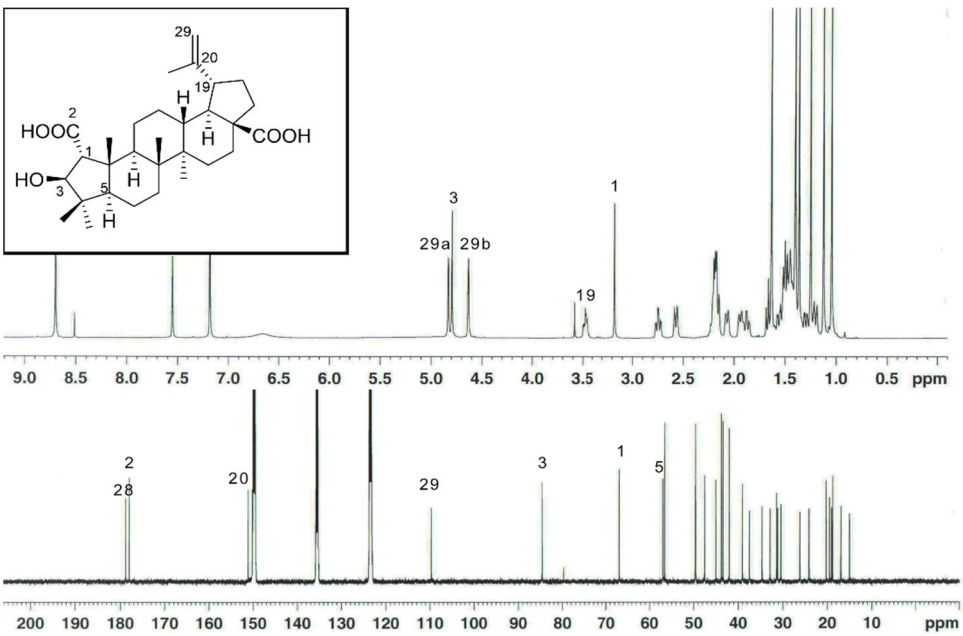

Figure 35. ^{1}H and ^{13}C NMR spectra of compound **14** (500 / 125 MHz, pyridine-d_5)

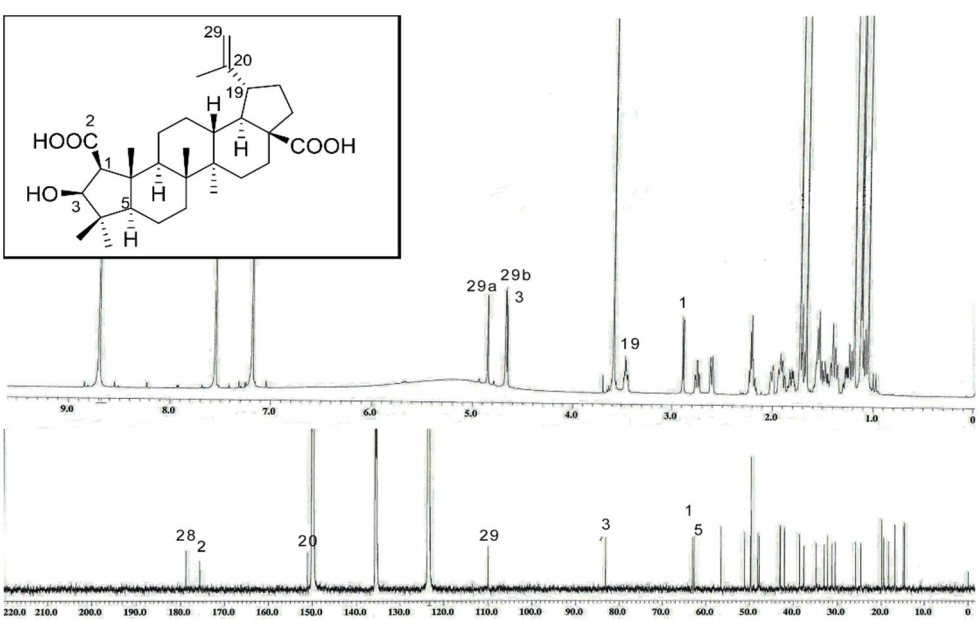

Figure 36. ^{1}H and ^{13}C NMR spectra of compound **15** (600 / 150 MHz, pyridine-d_5)

3.3.4. Compound **16**

Compound **16** was acquired as a white amorphous powder. Its molecular formula of $C_{31}H_{48}O_5$ was established by the pseudo-molecular ion peak at *m/z* 499.3417 $[M-H]^-$ (calcd. for $C_{31}H_{47}O_5$, 499.3423) in ESI-qTOF-MS. The ^1H and ^{13}C NMR spectra of compound **16** were similar to those of **15**, epiceanothic acid (Figure 37). The only difference was the presence of signals of a methoxy function (δ_H/δ_C 3.62, 51.2). The position of this methoxy group was confirmed by HMBC correlation to C-2 (δ_C 173.6) (Figure 38). Consequently, compound **16** was determined as epiceanothic acid 2-methyl ester, and it was firstly isolated from nature.

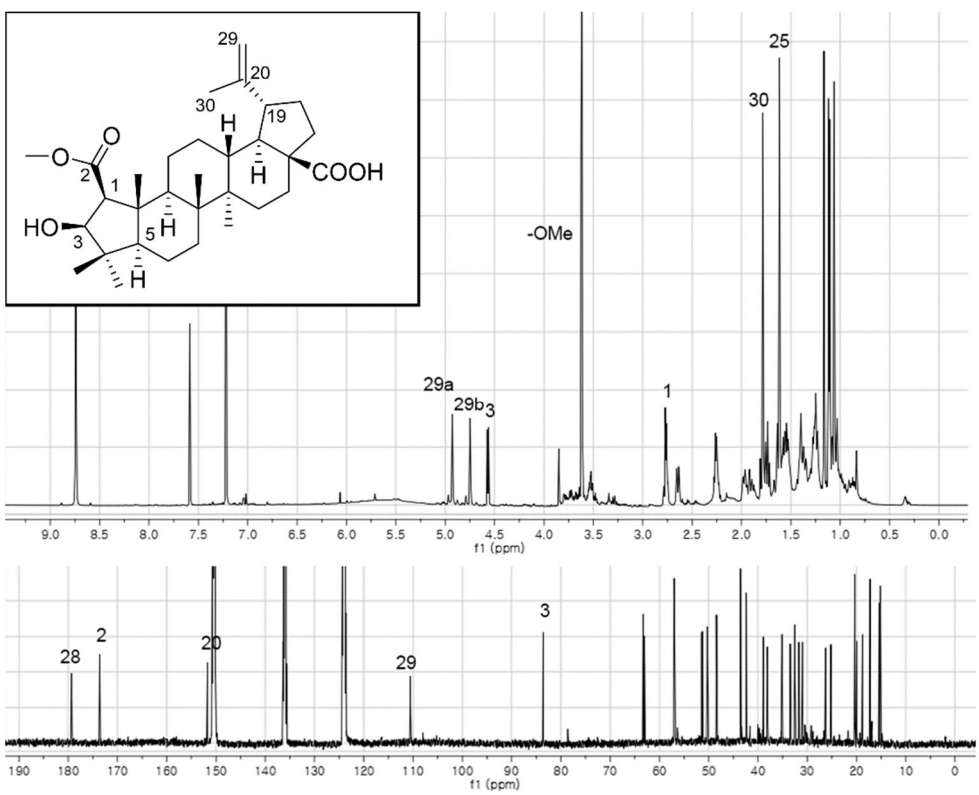

Figure 37. ^1H and ^{13}C NMR spectra of compound **16** (600 / 150 MHz, pyridine-d_5)

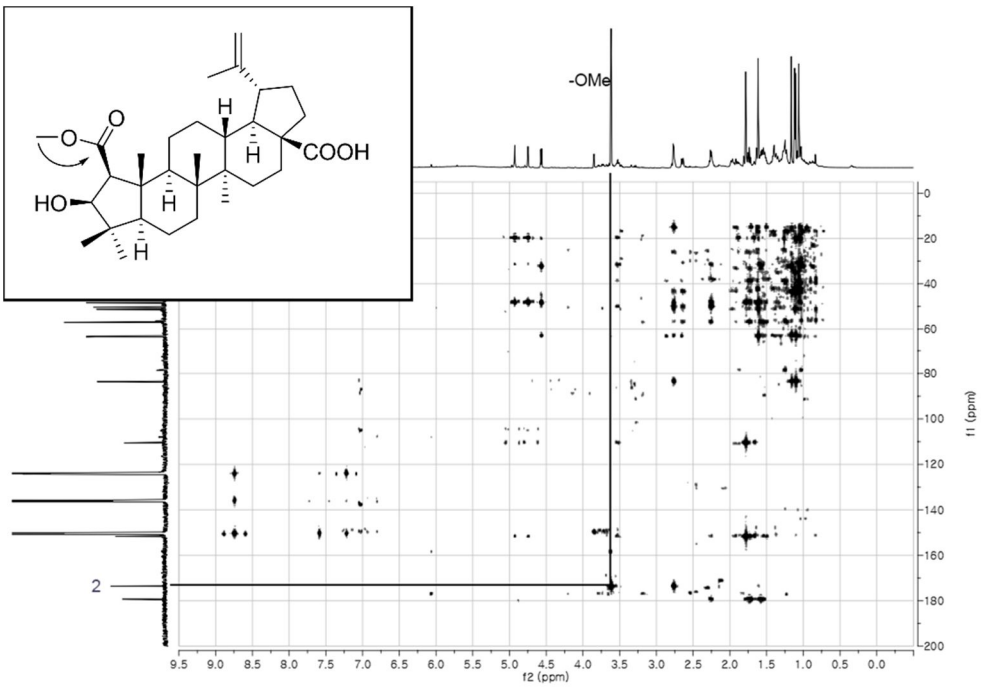

Figure 38. HMBC spectrum of compound **16** (600 MHz, pyridine-d_5)

3.3.5. Compounds **17** and **18**

Compound **17** was obtained as a white amorphous powder with a molecular formula $C_{30}H_{44}O_6$, which was indicated by ESI-qTOF-MS (*m/z* 499.3062 $[M-H]^-$, calcd. for $C_{30}H_{43}O_6$, 499.3060). ^1H NMR spectrum of **17** showed an isopropenyl group (δ_H 4.70, 5.03, 1.87), four additional singlet methyl protons (δ_H 0.94, 0.98, 1.23, and 1.24), and several methine protons (δ_H 2.06, 2.21, 2.65, 3.01, 3.70), which seems similar to other lupane- or ceanothane-type triterpenes. However, it lacked one methyl function to other triterpenes such as compounds **10-16**, and ^{13}C NMR spectrum of **17** showed three carboxyl carbon signals at δ_C 179.0, 179.1, and 179.8 (Figure 39). Thus, it was deduced that one of six methyl groups found in lupane- or ceanothane-type triterpenes was substituted to a carboxyl group in compound **17**. For confirming the position of the carboxyl groups, HMBC experiment was performed. Correlations of H-23 (δ_H 1.24) and H-24 (δ_H 0.94) with

C-3 (δ_C 43.2), C-4 (δ_C 38.8), and C-5 (δ_C 56.7), and of H-25 (δ_H 0.98) with C-1 (δ_C 56.3), C-5, C-9 (δ_C 46.7) and C-10 (δ_C 51.6) were observed. From the multiplicity-edited HSQC and ^{1}H-^{1}H COSY spectrum, it was found that H-1 (δ_H 2.88, *d*, *J* = 7.3) correlated with methylene protons H-3 (δ_H 1.88 and 2.06, *m*). From the HMBC correlations of H-1, H-3, and H-24 with C-2 (δ_C 179.1), it was determined that compound **17** has a cyclopentanyl A-ring system as compound **14** and **15**, but 3-hydroxy group is absent (Figure 40). H-26 (δ_H 1.23) showed HMBC couplings with C-7 (δ_C 38.3), C-8 (δ_C 41.9), C-9, and C-14 (δ_C 60.8). The downshifted chemical shift of C-14 suggested that an electron-withdrawing moiety attached to it. HMBC correlations of H-13 (δ_H 3.01) and H-15 (δ_H 1.95 and 2.54) with C-27 (δ_C 179.0) confirmed connection between the carboxyl group of C-27 and C-14. The position of carboxyl C-28 (δ_C 197.8) was confirmed by the HMBC coupling with H-18 (δ_H 2.21, *dd*, *J* = 10.9, 11.2). The stereochemistry at C-1 as deduced from the ROESY spectrum (Figure 41). A spatial correlation between H-1 and H-25 was observed, so H-1β configuration was determined under comparison with the previously reported reference (Leal et al., 2010). Additionally, ^{1}H and ^{13}C NMR chemical shifts of H/C-5 (δ_H/δ_C 2.06/56.7) were similar to those of compound **14**, rather than compound **15**. Considering all of the above described spectroscopic data, compound **17** was determined to be 3-dehydroxy-ceanotha-27-oic acid, and it was same as a 3-dehyroxy form of ceanothetric acid (Li et al., 1997). Thus, compound **17** was name 3-dehydroxy ceanothetric acid, and it was firstly isolated from nature.

Compound **18** was isolated as a white amorphous powder, and its molecular formula was indicated as $C_{31}H_{44}O_6$ by ESI-qTOF-MS (*m/z* 513.3208 $[M-H]^-$, calcd. for $C_{31}H_{43}O_6$, 513.3216). ^{1}H and ^{13}C NMR spectra of **18** were similar to those of compound **17**, but signals of a methoxy group was observed (δ_H/δ_C 3.78/51.7) (Figure 42). Thus, compound **18** was deduced to be a methyl ester derivative of **17**, and the position of the methoxy substituent was confirmed by the HMBC correlation of methoxy protons and C-2 (δ_C 176.8) (Figure 43). Its H-1β orientation was also confirmed by ROESY spectrum (Figure 44). Consequently, compound **18**

was elucidated to be 3-dehydroxy ceanothetric acid 2-methyl ester. It was also isolated for the first time from nature.

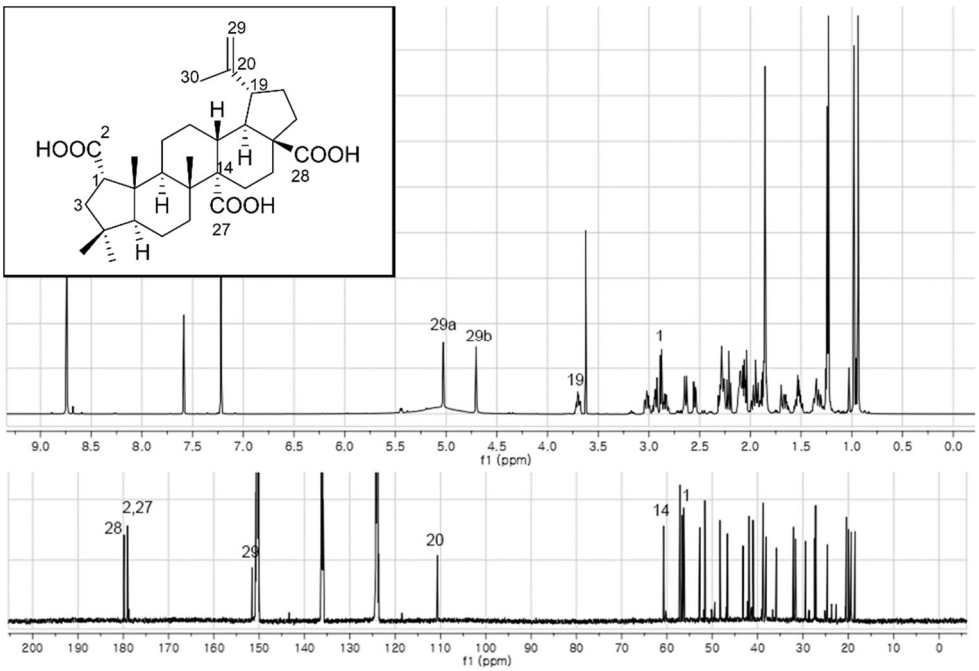

Figure 39. ^{1}H and ^{13}C NMR spectra of compound **17** (600 / 150 MHz, pyridine-d_5)

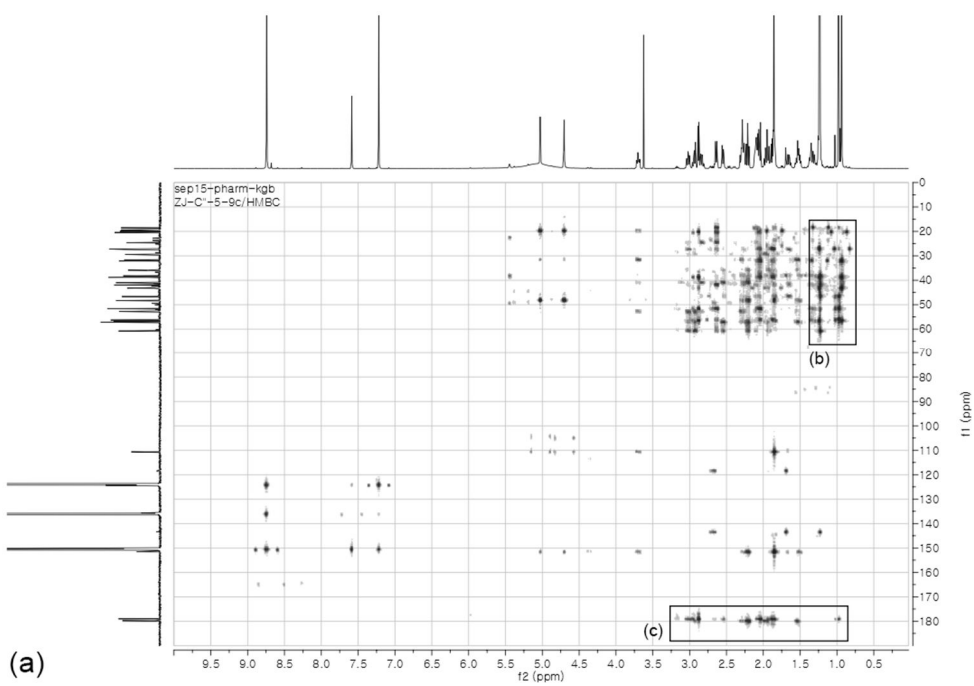

(continued)

(continued)

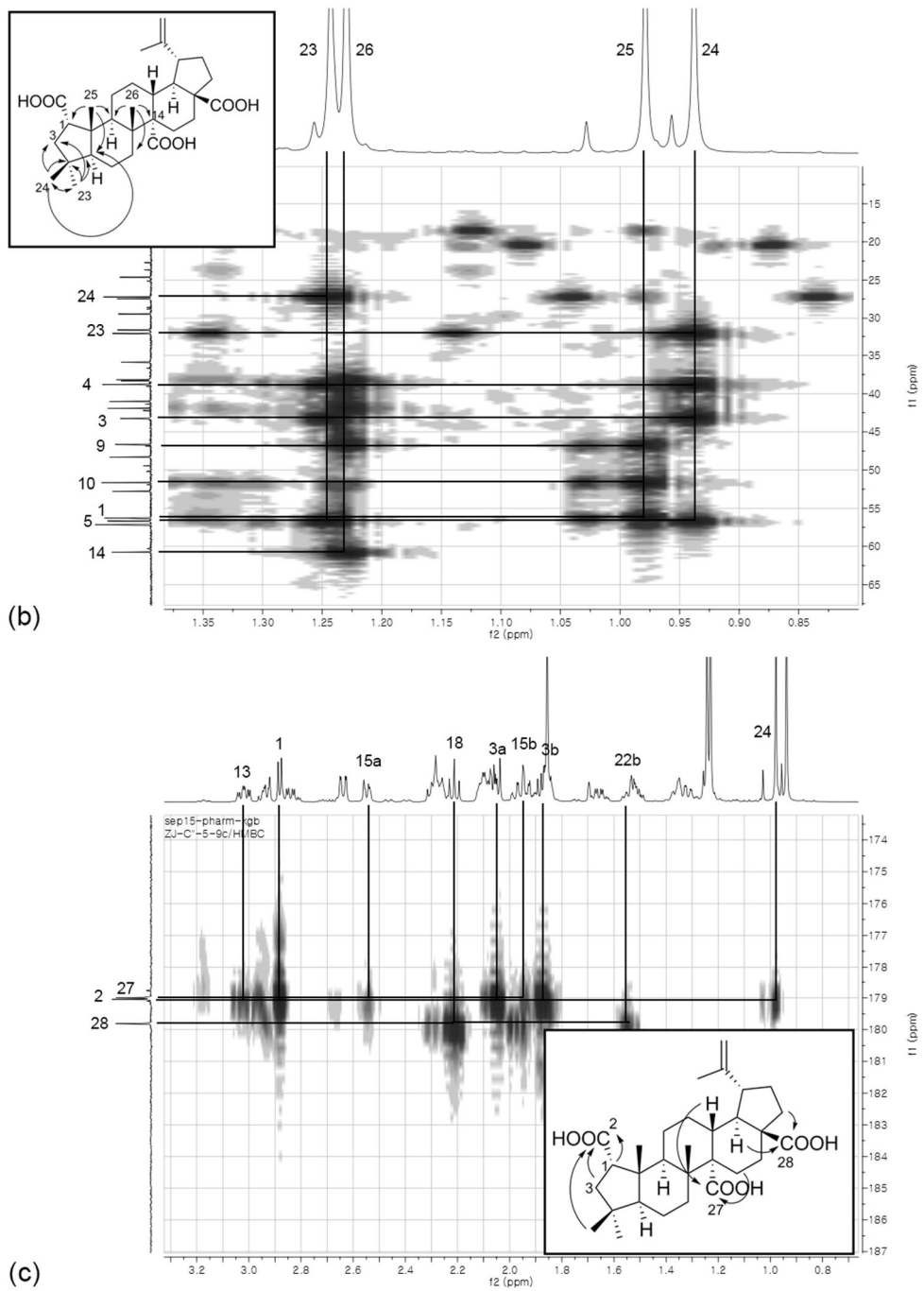

Figure 40. HMBC spectrum of compound **17** (600 MHz, pyridine-d_5)

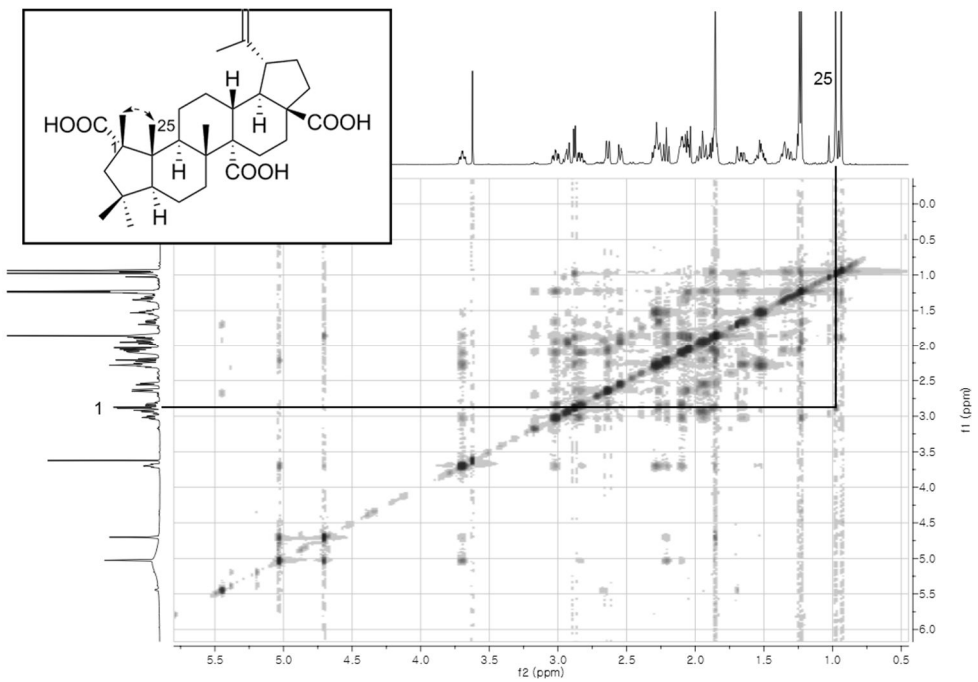

Figure 41. ROESY spectrum of compound **17** (600 MHz, pyridine-d_5)

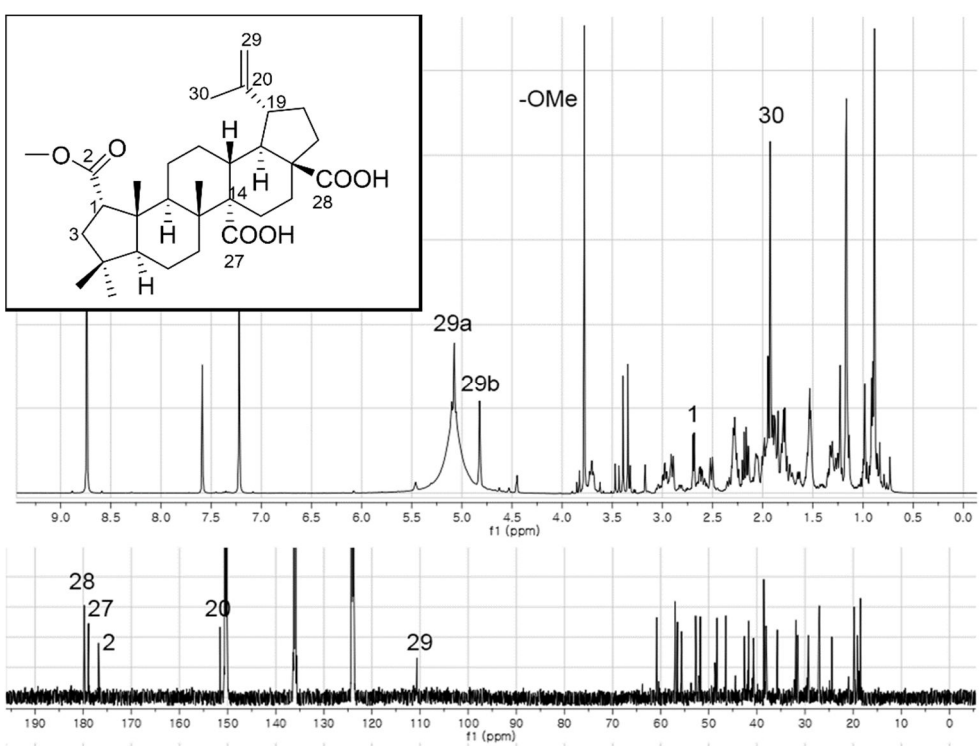

Figure 42. ^{1}H and ^{13}C NMR spectra of compound **18** (600 / 150 MHz, pyridine-d_5)

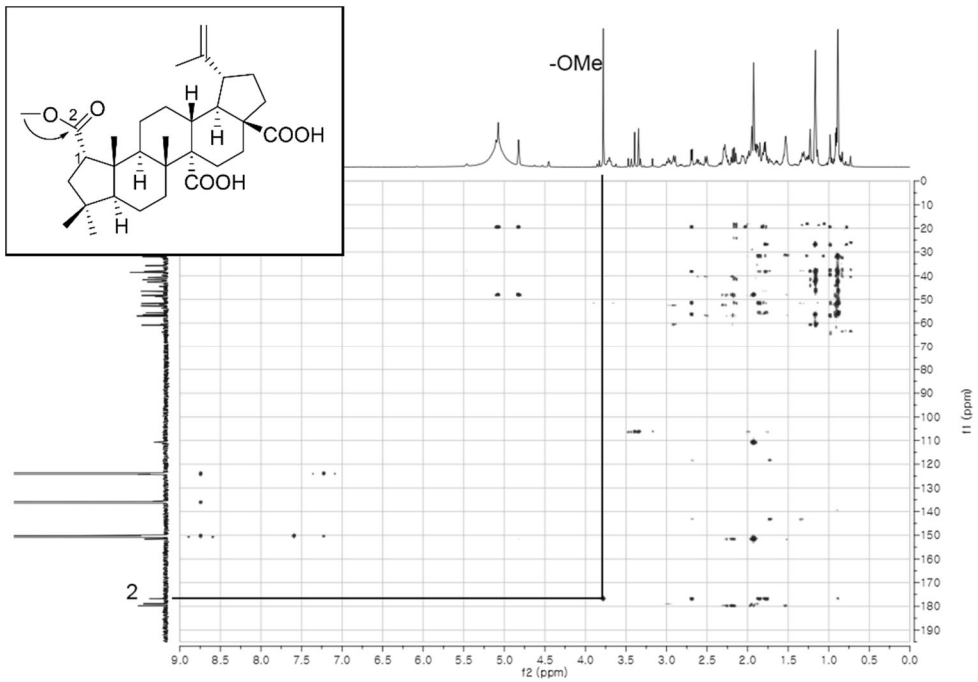

Figure 43. HMBC spectrum of compound **18** (600 MHz, pyridine-d_5)

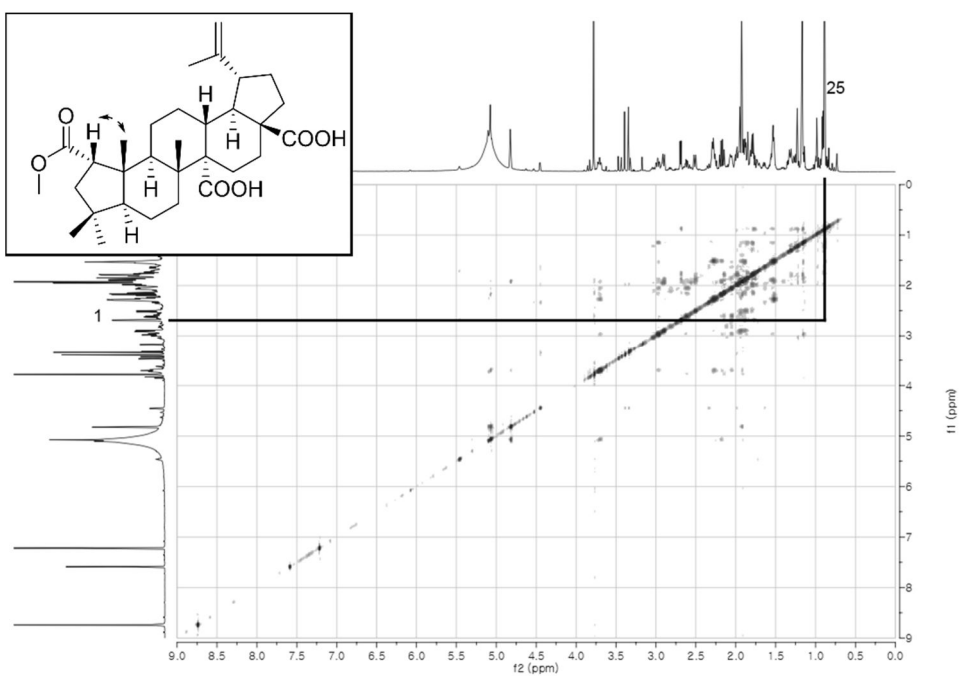

Figure 44. ROESY spectrum of compound **18** (600 MHz, pyridine-d_5)

3.3.6. Compound **19**

Compound **19** was acquired as a white amorphous powder, of which molecular formula was determined to be $C_{31}H_{46}O_7$ by ESI-qTOF-MS (*m/z* 529.3165 $[M-H]^-$, calcd. for $C_{31}H_{45}O_7$, 529.3165). In ^1H NMR spectrum of **19**, an isopropenyl group (δ_H 1.90, 4.80, 5.05), two singlet methine protons at δ_H 3.06 (H-1) and 4.62 (H-3), four additional methyl signals at δ_H 1.19 (H-24), 1.21 (H-26), 1.22 (H-23), and 1.37 (H-25), and one methoxy group at δ_H 3.74 were observed, and in ^{13}C NMR spectrum, three carboxyl carbons at δ_C 175.7 (C-2), 178.4 (C-27), and 179.3 (C-28) were observed (Figure 45). These suggested that compound **19** is a methyl ester derivative of a ceanothic acid with three carboxyl group similar to **17** and **18**. The HMBC experiment was performed to confirm positions of carboxyl carbons as C-2, C-27, and C-28, and also showed the correlation between methoxy protons and carboxyl C-2, which indicated that the methoxy signal exists as a methyl ester at the C-2 position (Figure 46). Based on these data, compound **19** was determined to be ceanothetric acid 2-methyl ester, and it was firstly isolated from nature.

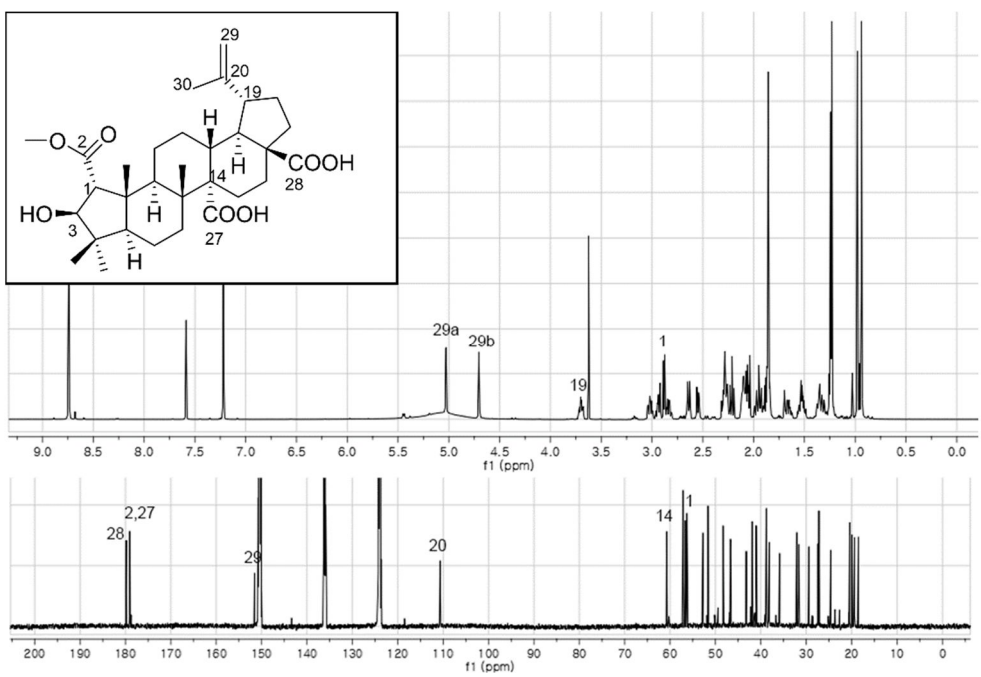

Figure 45. ^1H and ^{13}C NMR spectra of compound **19** (500 / 125 MHz, pyridine-d_5)

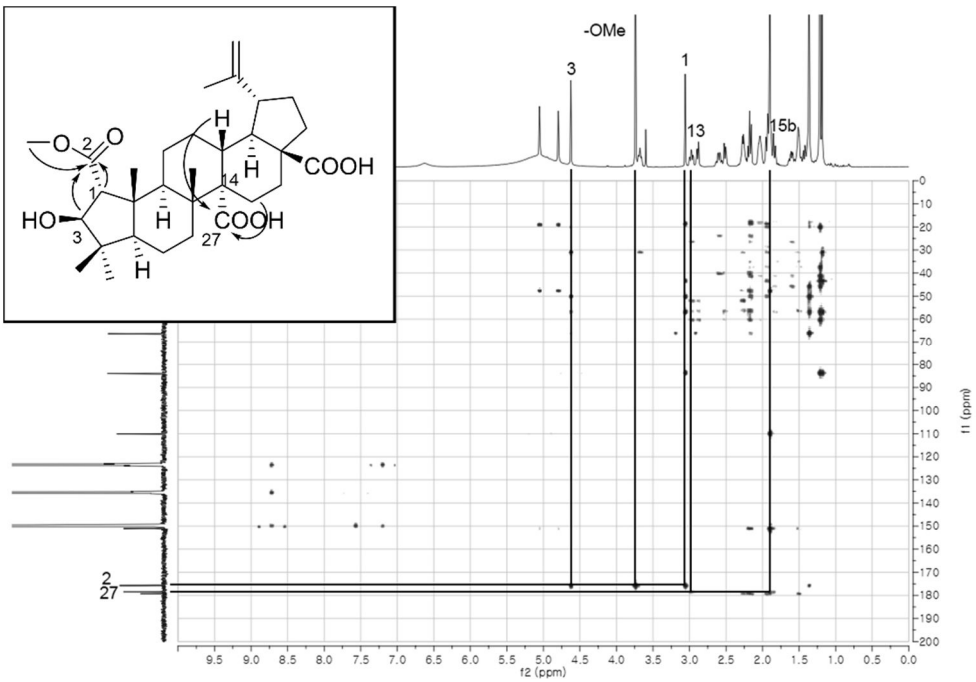

Figure 46. HMBC spectrum of compound **19** (500 MHz, pyridine-d_5)

3.3.7. Compound **20**

Compound **20** was isolated as a pale yellow solid. ESI-qTOF-MS indicated the molecular formula of **20** as $C_{30}H_{42}O_6$ (*m/z* 497.2897 $[M-H]^-$, calcd. for $C_{30}H_{41}O_6$, 497.2903). ^1H and ^{13}C NMR spectra of **20** was many common features to those of 16, such as isopropenyl proton signals, additional four methyl proton signals, none of oxygenated methine proton, and three carboxy carbon signals (Figure 47). However, significant differences were also observed. At first, methylene protons of isopropenyl group were significantly downshifted (δ_H 5.54 and 5.02, H-29a and H-29b, respectively), and one of them (H-29a) and the methyl signal of the isopropenyl group (δ_H 1.72, H-30) were observed in broad singlet shaped. Additionally, the characterstic doublet of triplet proton of H-19 was missing in ^1H NMR spectrum of **20**. In ^{13}C NMR spectrum, an unusual carbon signal was observed at δ_C 92.9 (C-17), which was identified as a tertiary carbon by

multiplicity-edited HSQC. From these NMR spectral data and IR absorption band at 1780 cm^{-1}, the presence of γ-lactone was deduced. The HMBC correlations of C-17 with H-29b and H-30 confirmed the position of the lactone bridge at C-17 (Figure 48). The α-orientation of C-2 carboxy at C-1 was confirmed by ROESY NMR spectrum (Figure 49). Thus, **20** was determined to be 3-dehydroxy-ceanotha-27α-carboxy-28β,19β-olide, and it was firstly isolated from nature. Ceanothane-type triterpenic acids containing γ-lactone bridge substructure have been reported only once before, the case of alphitexolide (Branch et al., 1972).

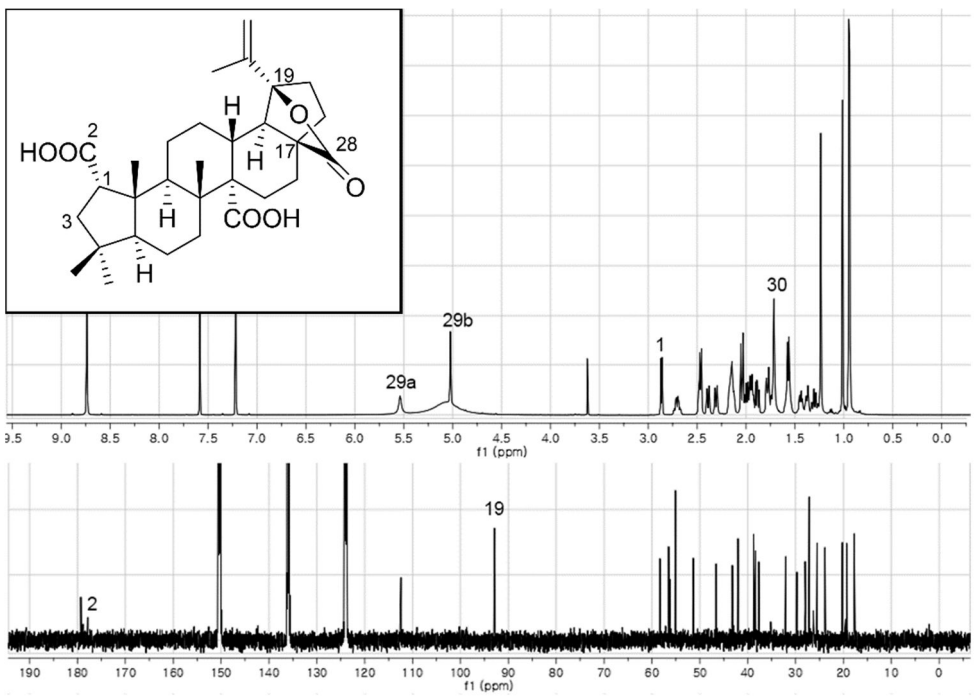

Figure 47. ^{1}H and ^{13}C NMR spectra of compound **20** (600 / 150 MHz, pyridine-d_5)

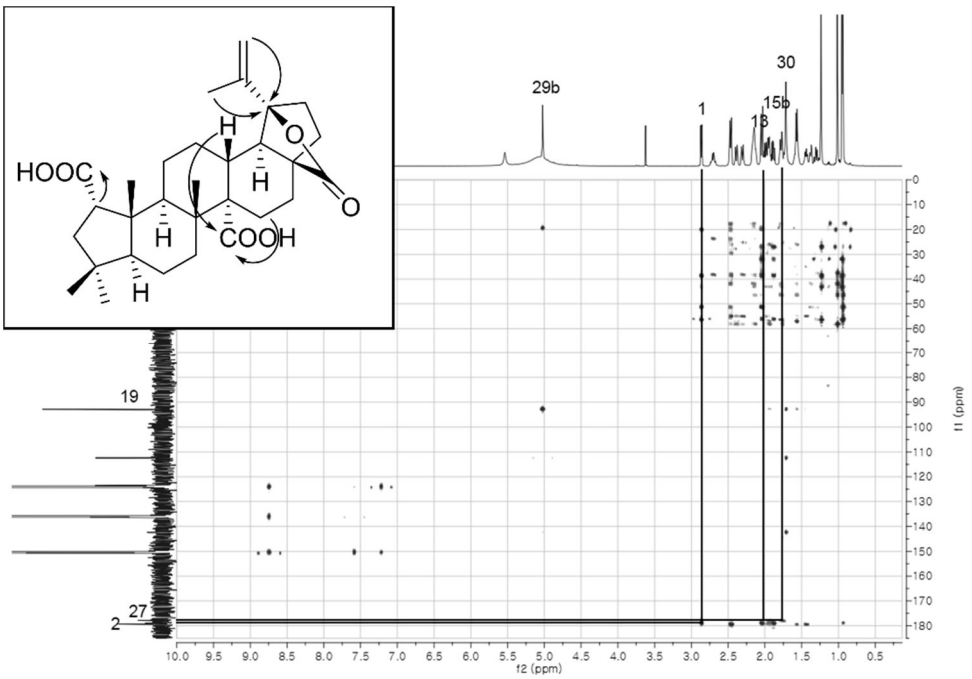

Figure 48. HMBC spectrum of compound **20** (600 MHz, pyridine-d_5)

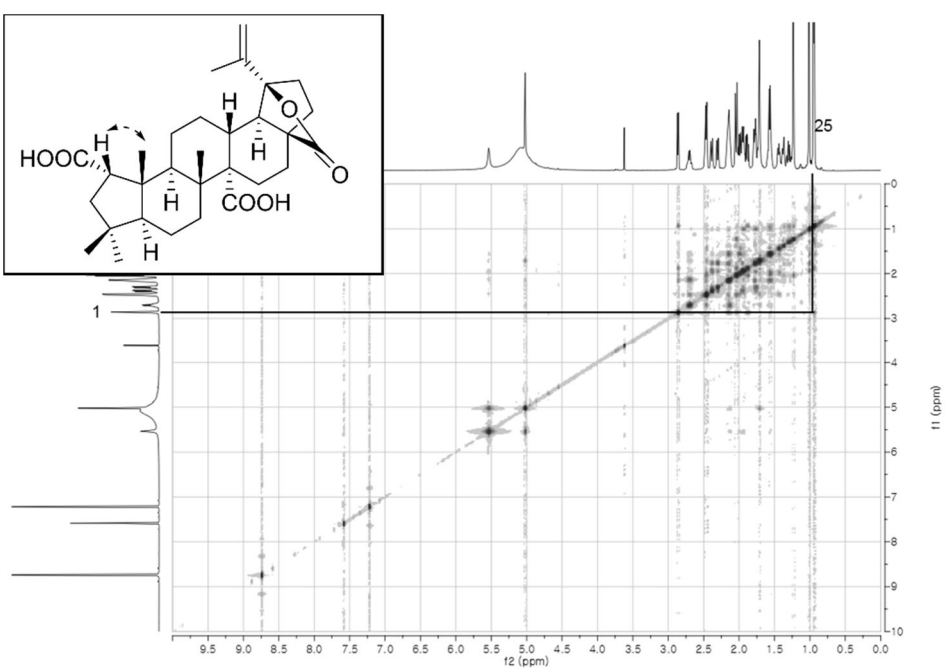

Figure 49. ROESY spectrum of compound **20** (600 MHz, pyridine-d_5)

3.3.8. Compound **21**

Compound **21** was purified as a white amorphous powder with molecular formula $C_{30}H_{46}O_6$, indicated by ESI-qTOF-MS (*m/z* 501.3221 $[M-H]^-$ (calcd. for $C_{30}H_{45}O_6$, 501.3216). ^1H NMR spectrum of **21** showed an isopropenyl group signal (δ_H 4.79, 4.60, and 1.59), four additional methyl singlets at δ_H 1.73 (H-23), 1.30 (H-25), 1.05 (H-26), and 0.98 (H-27), two methine singlets at δ_H 3.18 (H-1) and 4.87 (H-3), and a hydroxymethyl group at δ_H 3.62 and 4.56 (*d*, *J* = 10.6 Hz, H-24) (Figure 50). These features suggested that **21** was a hydroxylated derivative of compound **14**. HMBC correlations between the hydroxymethyl protons and carbons at δ_C 25.5 (C-23) and 85.6 (C-3) confirmed that hydroxylmethyl protons were H-24s. The relative configurations at A-ring were determined by correlation peaks of H-1/H-25, H-3/H-5, H-3/H-23, and H-24/H-25 in the ROESY spectrum. Based on these spectral data, compound **21** was concluded to be 24-hydroxyceanothic acid, also known as granulosic acid (Ganapaty et al., 2006).

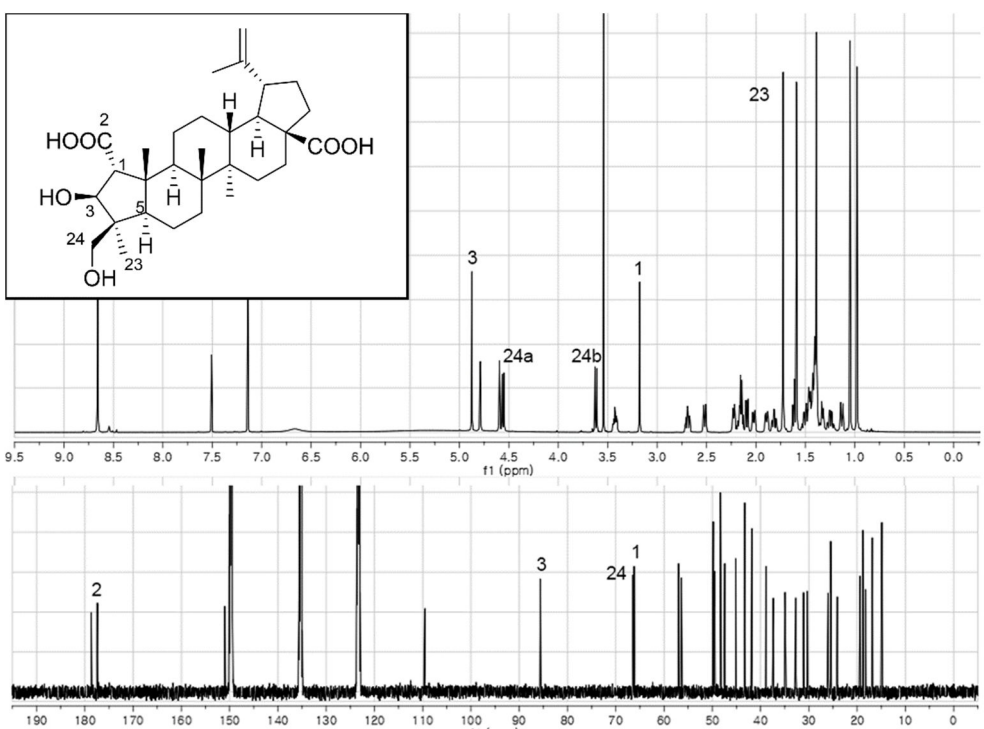

Figure 50. ^1H and ^{13}C NMR spectra of compound **21** (600 / 150 MHz, pyridine-d_5)

3.3.9. Compounds **22** and **23**

Compound **22** was obtained as a white amorphous powder with molecular formula $C_{30}H_{44}O_3$, indicated by pseudo-molecular peak *m/z* 451.3207 $[M-H]^-$ (calcd. for $C_{30}H_{43}O_3$, 451.3212) in ESI-qTOF-MS. UV, IR, ^1H NMR, and ^{13}C NMR spectra of **22** suggested it contained an α, β-unsaturated aldehyde function (UV λ_{max} 235 nm; IR 2865, 1685 cm^{-1}; δ_H 9.86 *s*, H-2; 6.51 *s*, H-3; δ_C 158.2, C-1; 164.2, C-3; 191.7, C-2) (Figure 51). It was confirmed by HMBC correlations of H-2 with C-1 and C-3, and H-1 with C-1, C-2, C-4 (δ_C 44.2), C-5 (δ_C 63.9), and C-10 (δ_C 52.9). Considered by these spectral data and comparison with previously reported reference, compound **22** was identified as zizyberenalic acid (Lee et al., 1997).

Compound **23** was isolated as a white amorphous powder. ESI-qTOF-MS indicated its molecular formula as $C_{31}H_{48}O_4$ (*m/z* 483.3484 $[M-H]^-$, calcd. for $C_{31}H_{47}O_4$, 483.3474). ^1H NMR spectrum of **23** was similar to those of **22**, but instead of two singlets of α, β-unsaturated aldehyde, an unconjugated aldehyde proton at δ_H 10.12 (*d*, *J* = 4.0, H-2) and two oxygenated methine protons at δ_H 2.53 (*dd*, *J* = 8.7 and 4.0, H-1) and δ_H 4.03 (*d*, *J* = 8.7, H-3) were observed (Figure 52). These chemical shifts and coupling constant values suggested that compound **23** is a saturated derivative of **22**, and it was supported by multiplicity-edited HSQC, in which these protons were coupled with carbons at δ_C 205.6 (C-2), 72.4 (C-1), and 91.4 (C-3), respectively. A methoxy signal (δ_H/δ_C 3.30/60.0) was also observed in ^1H and ^{13}C NMR spectra, and its position was determined by the HMBC correlation with C-3 (Figure 53). Doublet-shaped correlations between H-1 and H-3 have been shown in H-1β and H-3β orientation such as compounds **15** and **16**, but $J_{1,3}$ of **23** was significantly larger than those of **15** and **16**. For confirming the configurations at C-1 and C-3, ROESY experiment was performed. Interestingly, H-1 showed spatial correlations with H-5 (δ_H 1.32), H-9 (δ_H 1.75), and H-23 (δ_H 1.06), while a correlation of H-3 and H-25 (δ_H 0.94) was observed (Figure 54). These suggested H-1α and H-3β orientation of **23**. Eade et al. proved protons at 1α

and 3β exhibit coupling constants around 9.0 Hz (Eade et al., 1967), and previously reported NMR spectral data of H-1α and H-3β derivatives of ceanothane-type triterpenoids shown similar coupling constants values; 8.9 Hz in zizyberanalic acid (Kundu et al., 1989); 8.7 Hz in isoceanothic acid (Jagadeesh et al., 2000); 8.6 Hz in ceanothanolic acid (Lee et al., 1997). Thus, configurations at C-1 and C-3 of **23** were confirmed as H-1α and H-3β orientation. Consequently, compound **23** was determined to be 3-*O*-methyl-zizyberanalic acid. It was isolated for the first time from nature.

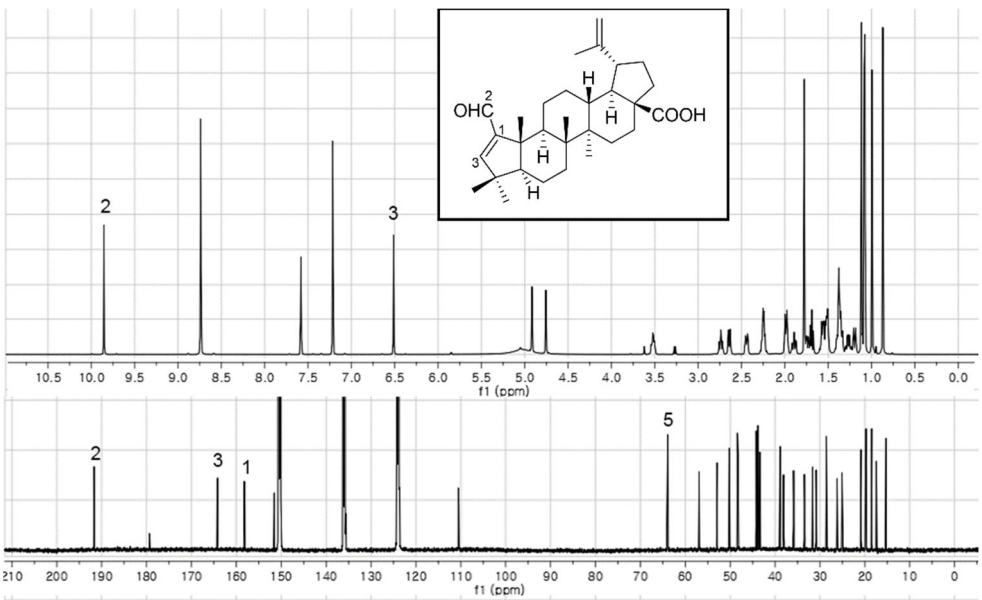

Figure 51. ^{1}H and ^{13}C NMR spectra of compound **22** (600 / 150 MHz, pyridine-d_5)

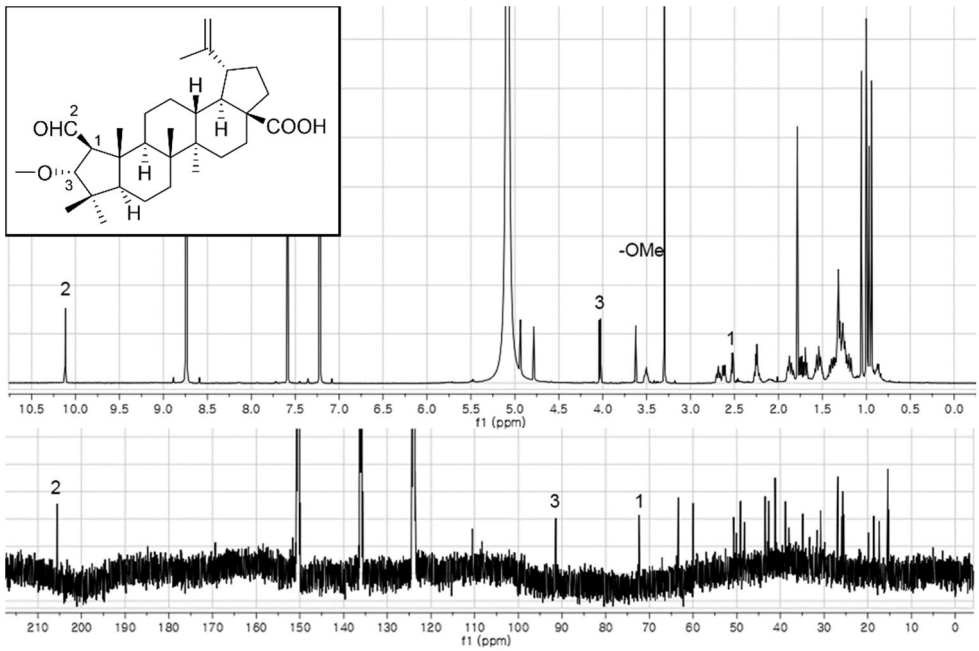

Figure 52. ^{1}H and ^{13}C NMR spectra of compound **23** (600 / 150 MHz, pyridine-d_5)

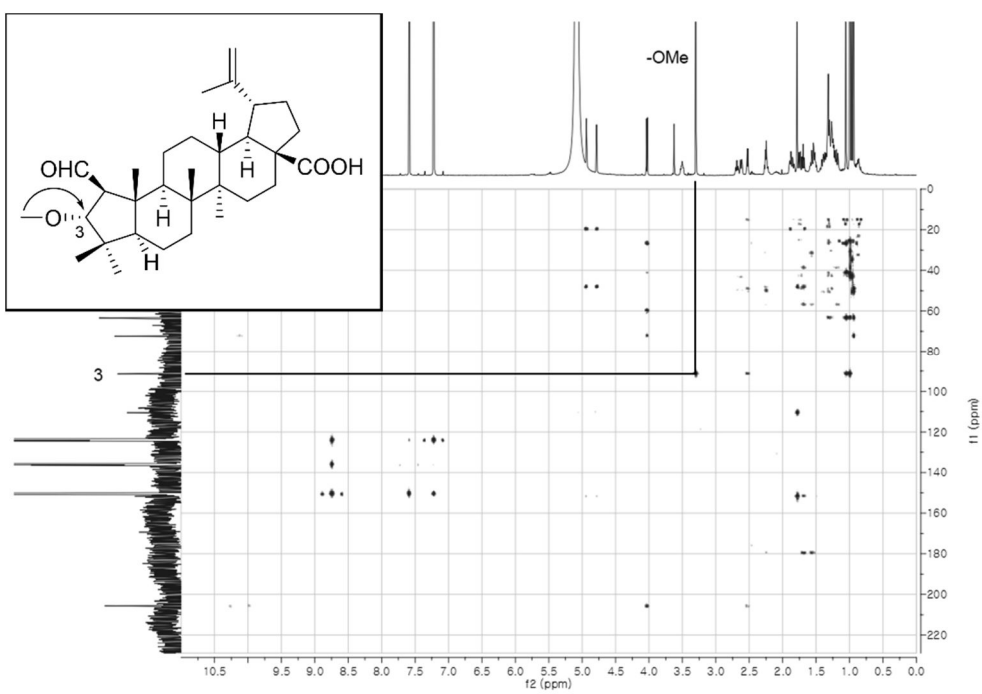

Figure 53. HMBC spectrum of compound **23** (600 MHz, pyridine-d_5)

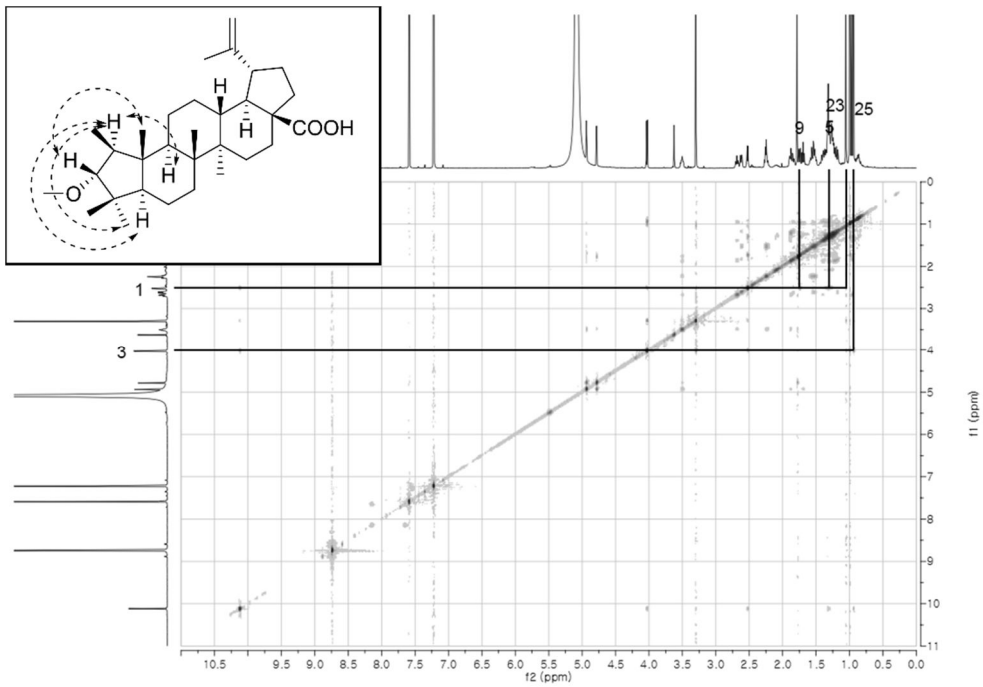

Figure 54. ROESY spectrum of compound **23** (600 MHz, pyridine-d_5)

3.3.10. Compound **24**

Compound **24** was obtained as a colorless solid. Its molecular formula $C_{28}H_{40}O_3$, which was indicated by ESI-qTOF-MS (*m/z* 423.2901 [M-H]-, calcd. for $C_{28}H_{39}O_3$, 423.2889), and ^{13}C NMR spectrum suggested that **24** has a dinortriterpene backbone. It was deduced to be dinorlupane-type, from the presence of the isopropenyl group protons in ^1H NMR spectrum of **24** (Figure 55). Additionally, three olefinic protons at δ_H 6.24 (*d*, *J* = 5.7 Hz, H-2), δ_H 5.85, (*d, J* = 5.7 Hz, H-3), and δ_H 5.33 (*s*, H-22), two hydroxymethyl protons at δ_H 3.84 and 4.03 (*d, J* = 10.6 Hz, H-24), and four methyl singlets at δ_H 1.16 (H-25), 1.16 (H-26), 1.31 (H-23), and 1.79 (H-30) were observed in the ^1H NMR spectrum. HMBC correlations between methyl protons and olefinic carbons, such as H-25/C-2 (δ_C 143.4) and H-23/C-3 (δ_C 137.7), indicated that **24** is a 1-nor-lupane-type triterpene possessing a cyclopentenyl A-ring (Figure). The hydroxymethyl protons exhibited HMBC correlations with C-2, C-3, and C-23 (δ_C 25.3), which suggested that the hydroxy function is at C-24, same as compound **21** (Figure 56). The elimination of the carboxy C-28 was deduced by upfielded chemical shift of β-oriented H-19 (δ_H 2.77, *dd*, *J* = 16.6, 8.4). The olefinic singlet at δ_H 5.33 correlated with C-17 (δ_C 146.1), C-18 (δ_C 51.5), C-19 (δ_C 54.3), and C-21 (δ_C 39.7) in the HMBC spectrum. From these correlations, elimination of C-28 and cyclopentenyl E-ring were confirmed. Uncommon doublet of doublet coupling of H-19 (doublet of triplet in cyclopentanyl E-ring of typical lupane-type triterpenes) and singlet shape of H-22 could be explained by the presence of cyclopentenyl E-ring, which has different conformation from a cyclopentanyl ring. Downshifted chemical shift of α-oriented H-18 (3.01, *dd*, *J* = 8.4, 8.6) suggested C-27 was the carboxy carbon, and it was confirmed by HMBC correlations from H-13 (δ_H 1.60, *m*) and H-15 (δ_H 1.48, *m*) to the carboxy carbon at δ_C 178.5 (C-27). Configuration at C-4 was confirmed by spatial correlation of H-24/H-25, and H-5/H-23 in the NOESY spectrum (Figure 57). Based on these spectral analysis, compound **24** was determined to be 1,28-

dinor-24-hydroxy-lup-2,17(22)-diene-27-oic acid. This compound was firstly isolated from nature.

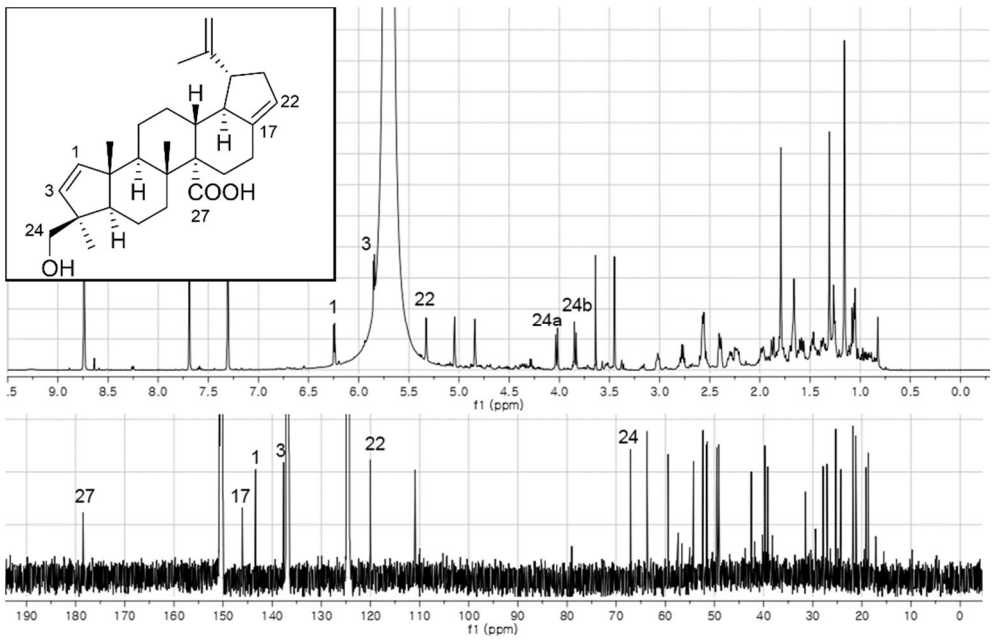

Figure 55. ^{1}H and ^{13}C NMR spectra of compound **24** (600 / 150 MHz, pyridine-d_5)

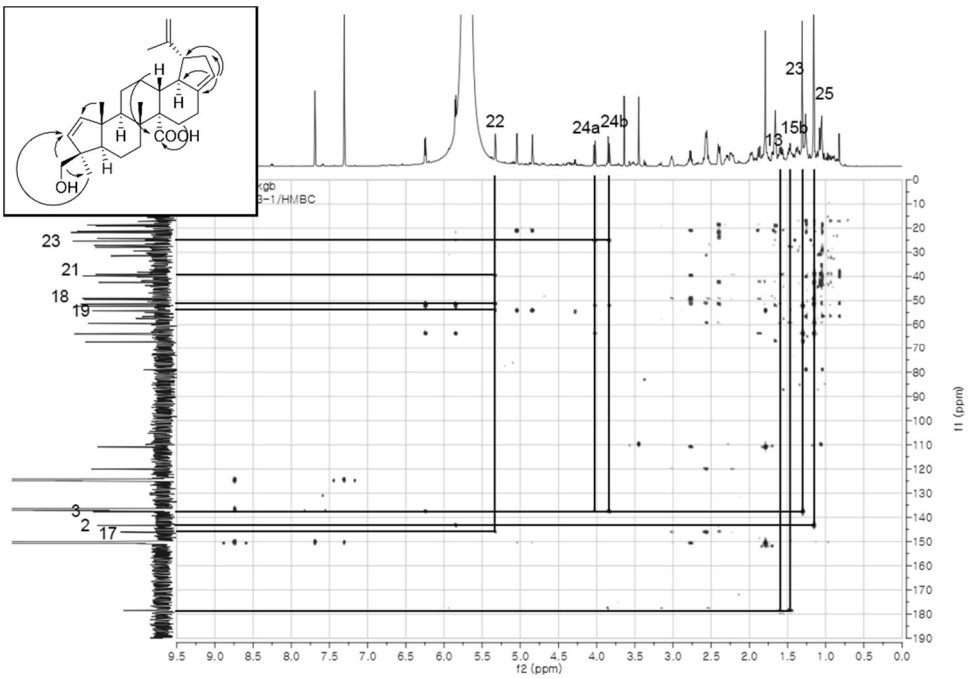

Figure 56. HMBC spectrum of compound **24** (600 MHz, pyridine-d_5)

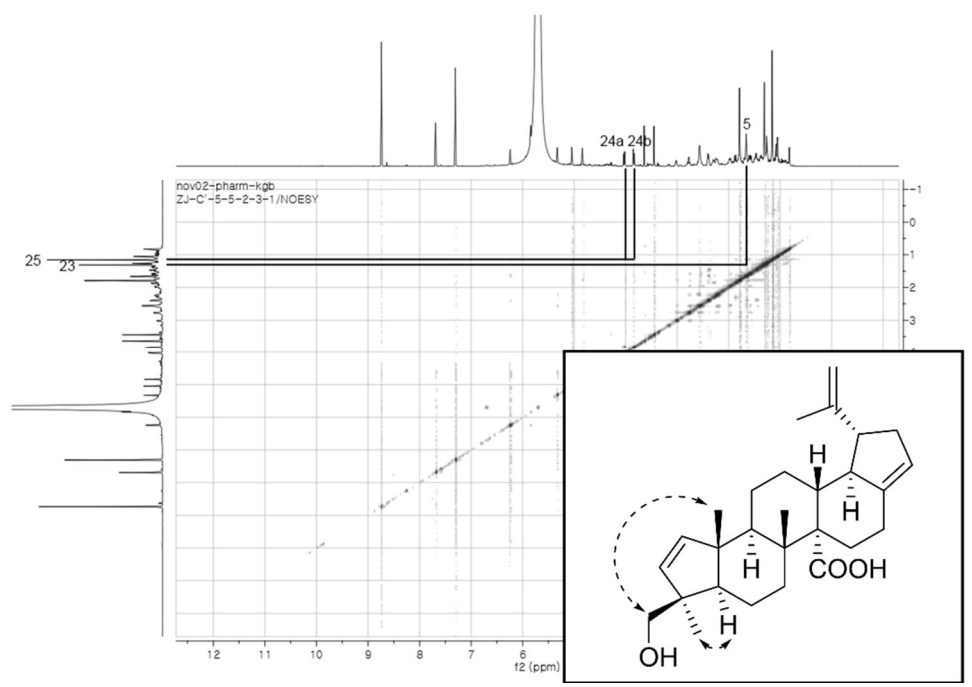

Figure 57. NOESY spectrum of compound **24** (600 MHz, pyridine-d_5)

3.3.11. Compounds **25**, **26**, and **27**

Compound **25** was a white amorphous powder. It has the molecular formula $C_{37}H_{52}O_7$, indicated by ESI-qTOF-MS (*m/z* 607.3644 $[M-H]^-$, calcd. for $C_{37}H_{51}O_7$, 607.3635). In its ^1H NMR spectrum, Compound **25** exhibited an isopropenyl group signal (δ_H 4.82, 4.97 and 1.83), five additional methyl singlets (δ_H 1.00, 1.09, 1.11, 1.13, and 1.30), and two oxygenated methine protons at δ_H 3.68 (*d, J* = 9.9, H-3) and δ_H 5.72 (*td, J* = 12.3, 4.5, H-2) (Figure 58). ^1H-^1H COSY showed a correlation between these methine protons, therefore, **25** was suggested as a derivative of compound **11**. The ^1H NMR spectrum also revealed aromatic protons in an AMX system, δ_H 7.30 (*d, J* = 8.2), δ_H 7.97 (*dd*, *J* = 8.2, 1.7), and δ_H 8.29 (*d, J* = 1.7) for a 3,4-disubstitueted benzoyl moiety. The multiplicity-edited HSQC and HMBC experiments confirmed the carbons of a protocatechuoyl moiety. The HMBC correlations of H-2 and C-7′ (δ_C 167.4) revealed the ester linkage between C-2 and the protocatechuoyl moiety, and the relatively downfield chemical shift of H-2 supported that. Based on these spectral data, compound **25** was identified as 2-*O*-protocatecuoyl alphitolic acid (Lee et al., 1996).

Compound **26** was a white amorphous powder with the molecular formula of $C_{38}H_{42}O_7$, indicated by ESI-qTOF-MS (*m/z* 621.3787 $[M-H]^-$, calcd. for $C_{38}H_{41}O_7$, 621.3791). ^1H and ^{13}C NMR spectra of **26** was almost identical to those of **25**, but one methoxy singlet (δ_H 3.72) was observed, and the chemical shifts of the aromatic protons were differed a little (Figure 59). The HMBC spectrum **26** confirmed the attachment of aromatic methoxy group at C-3′ (δ_C 113.9), and also confirmed the ester bonding between C-2 and C-7′ (δ_C 167.2) (Figure 61). Therefore, compound **26** was determined to be 2-*O*-vanilloyl alphitolic acid, and it was isolated for the first time from nature.

Compound **27**, obtained as a yellowish solid, was determined its molecular formula as $C_{37}H_{52}O_7$ by ESI-qTOF-MS (*m/z* 607.3630 $[M-H]^-$, calcd. for $C_{37}H_{51}O_7$, 607.3635). ^1H spectrum of **27** was also close to that of **25**, including the aromatic

proton signals of the protocatechuoyl moiety (Figure 60). However, two hydroxy methine protons of H-2 and H-3 showed differences in their chemical shifts, H-2 was observed more upfielded (δ_H 4.31), while H-3 downfielded (δ_H 5.34). From these chemical shift differences, it could be deduced that compound **25** has its protocatechuoyl ester at C-3 rather than at C-2. The HMBC correlation of H-3 and C-7′ (δ_C 167.8) confirmed this (Figure 62). Because of its scarce amount (1.0 mg), ^{13}C NMR spectrum of **27** could not be obtained, so chemical shifts of carbons were obtained using multiplicity-edited HSQC and HMBC. ^{13}C NMR chemical shifts of carbons were very similar to those of **25**. Consequently, compound **27** was confirmed as 3-*O*-protocatechuoyl alphitolic acid, and it was firstly isolated from nature.

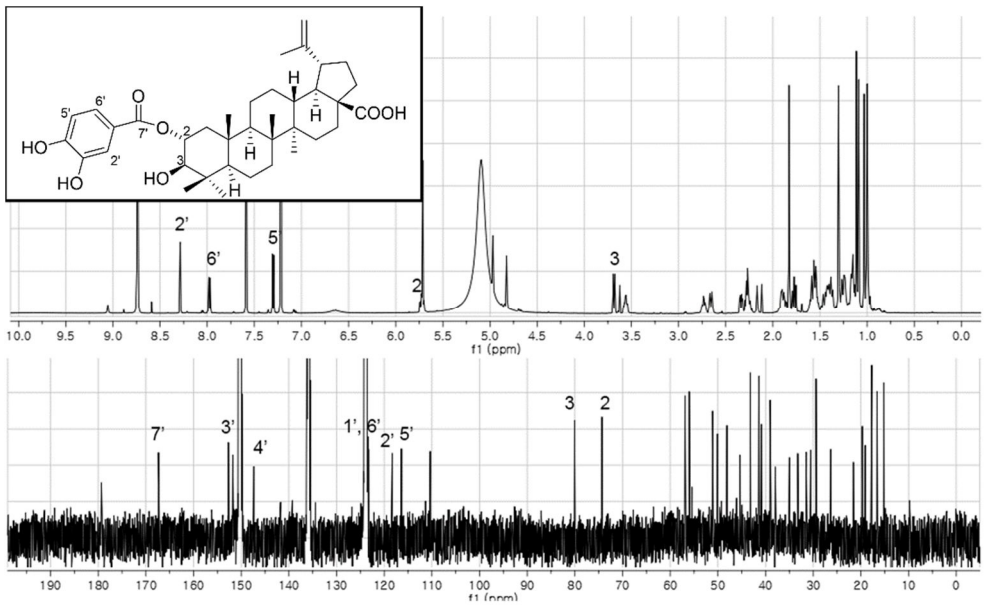

Figure 58. ^{1}H and ^{13}C NMR spectra of compound **25** (600 / 150 MHz, pyridine-d_5)

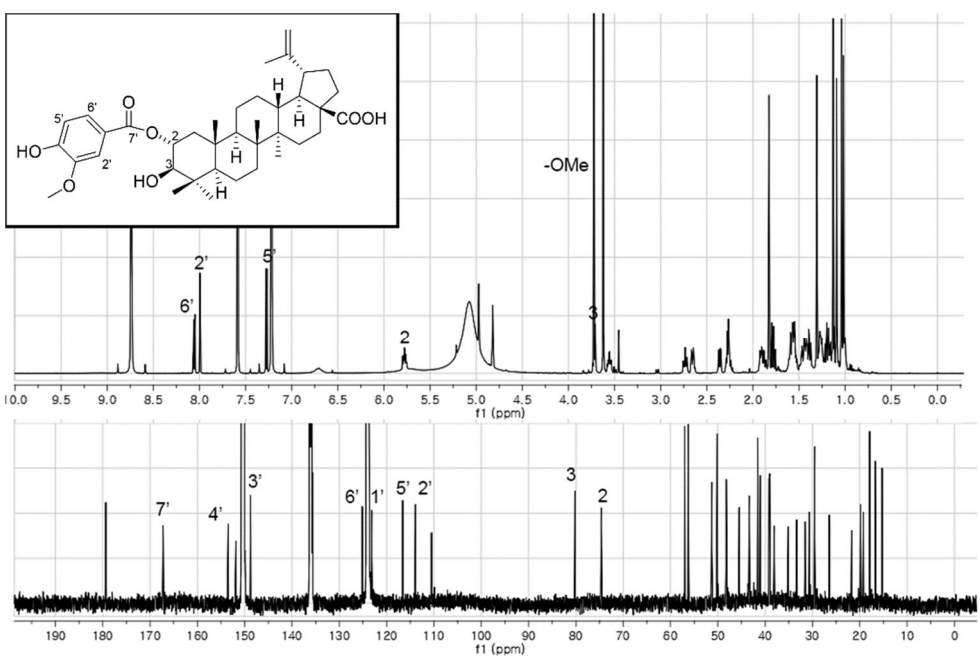

Figure 59. ^{1}H and ^{13}C NMR spectra of compound **26** (600 / 150 MHz, pyridine-d_5)

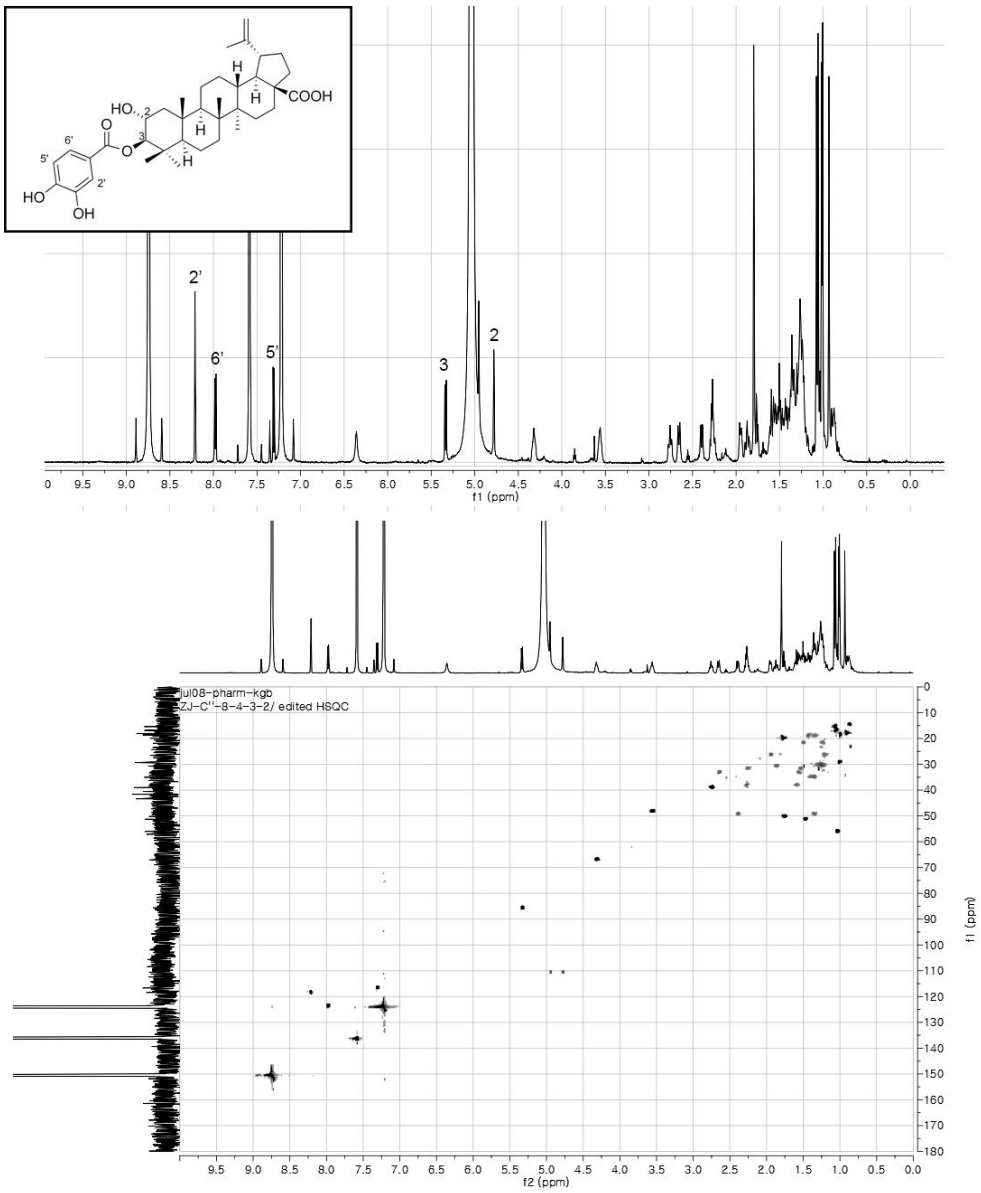

Figure 60. ^{1}H NMR and HSQC spectra of compound **27** (600 MHz, pyridine-d_5)

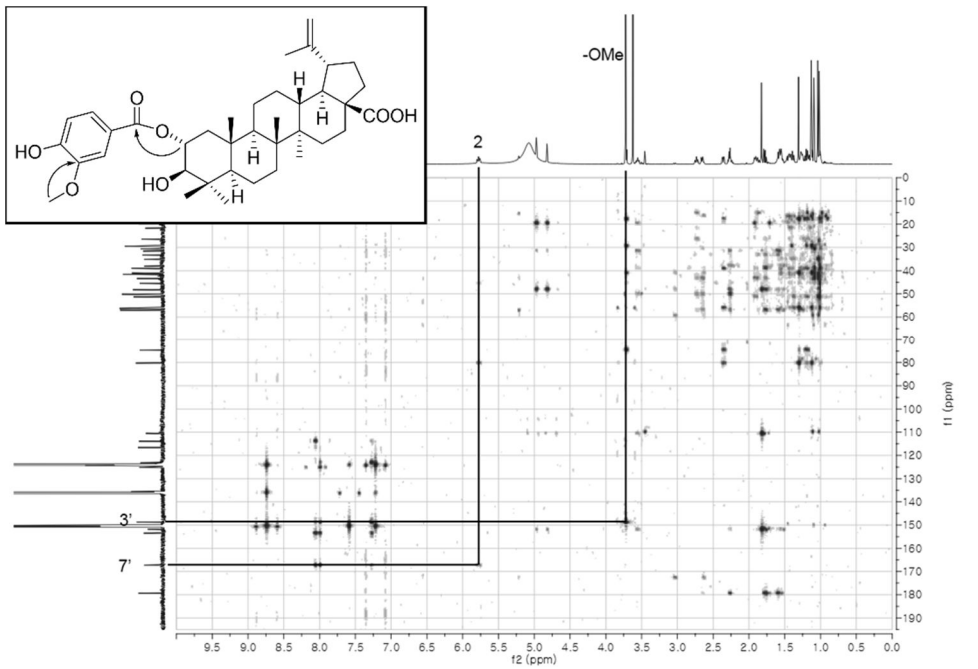

Figure 61. HMBC spectrum of compound **26** (600 MHz, pyridine-d_5)

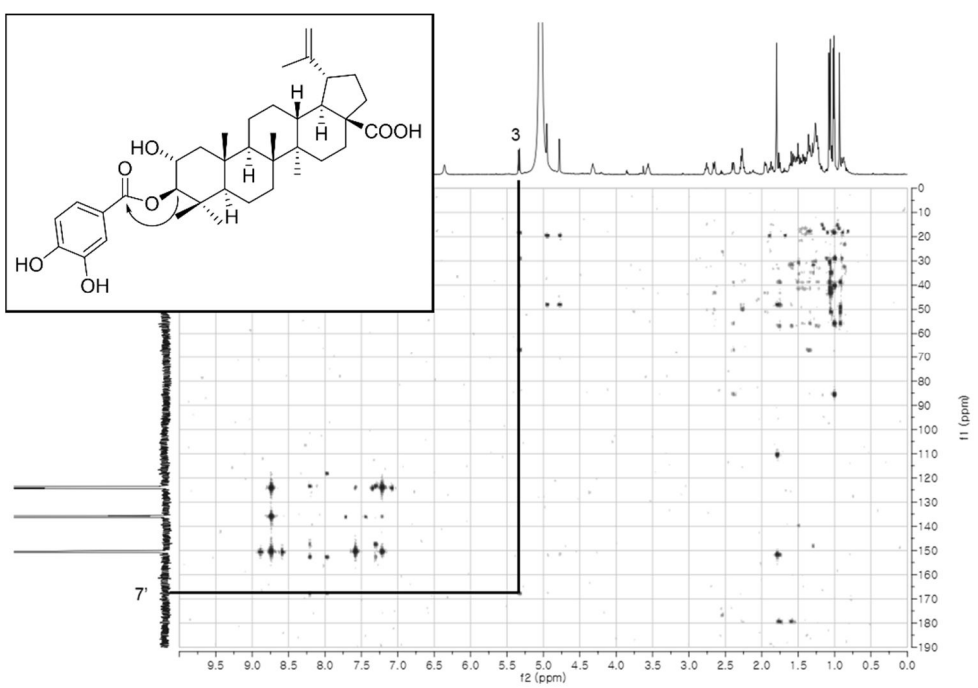

Figure 62. HMBC spectrum of compound **27** (600 MHz, pyridine-d_5)

3.3.12. Compounds **28** and **29**

Compound **28** was a white amorphous powder with the molecular formula $C_{39}H_{54}O_6$, indicated by its ESI-qTOF-MS pseudo-molecular peak (*m/z* 617.3848 $[M-H]^-$, calcd. for $C_{39}H_{53}O_6$, 617.3842). Compound **28** also showed the major characteristic features of lupane-type triterpenes, such as an isopropenyl group signal and five additional methyl singlets in its ^1H NMR spectrum (Figure 63). Two oxygenated methine protons at δ_H 3.60 (*d, J* = 9.9, H-3) and δ_H 5.59 (*td, J* = 11.1, 4.6, H-3) suggested that **28** is a derivative of **11** which has an ester moiety at C-2 position. In the aromatic region, two proton doublets were observed at δ_H 7.10 (2H, *d*, *J* = 8.6) and δ_H 7.50 (2H, *d*, *J* = 8.6), and additionally, *trans* conjugated olefinic protons at δ_H 6.58 (*d*, *J* = 15.9) and δ_H 7.98 (*d*, *J* = 15.9). From these signals, the presence of a *trans-p*-coumaroyl moiety was deduced. The attachment position of this moiety was confirmed by the HMBC correlation of H-2 and C-9′. Based on these spectral data and comparison with the previously reported references, compound **28** was identified as 2-*O*-*trans*-*p*-coumaroyl alphitolic acid (Lee et al., 2004; Yagi et al., 1978).

Compound **29** was obtained as a white amorphous powder, and its molecular formula was same with one of **28**, $C_{39}H_{54}O_6$ (ESI-qTOF-MS *m/z* 617.3848 $[M-H]^-$, calcd. for $C_{39}H_{53}O_6$, 617.3842). ^{13}C NMR of **29** was almost identical to one of **28**, but chemical shifts of *p*-coumaroyl protons showed differences (Figure 64). ^1H NMR signals of H-2′ and H-6′ were observed at lower field (δ_H 8.16), and olefinic protons showed the signals of *cis* conjugated protons (δ_H 6.07, *d*, *J* = 12.9, δ_H 6.92, *d, J* = 12.9) instead of *trans*. Consequently, Compound **29** was deduced to be 2-*O*-*cis*-*p*-coumaroyl alphitolic acid, and it was confirmed by comparison with the previously reported reference (Lee et al., 2004).

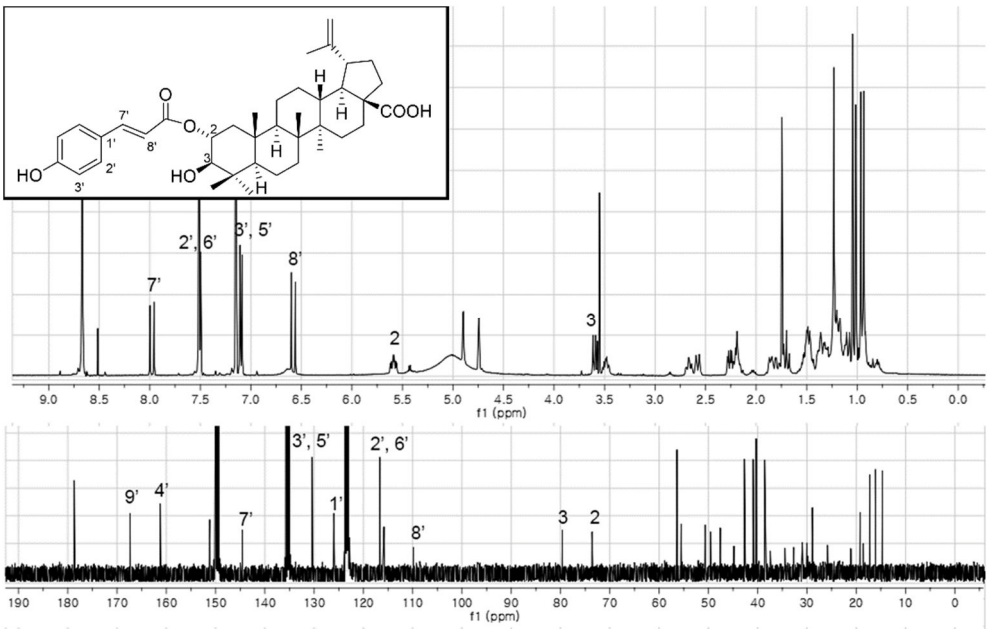

Figure 63. ^{1}H and ^{13}C NMR spectra of compound **28** (600 / 150 MHz, pyridine-d_5)

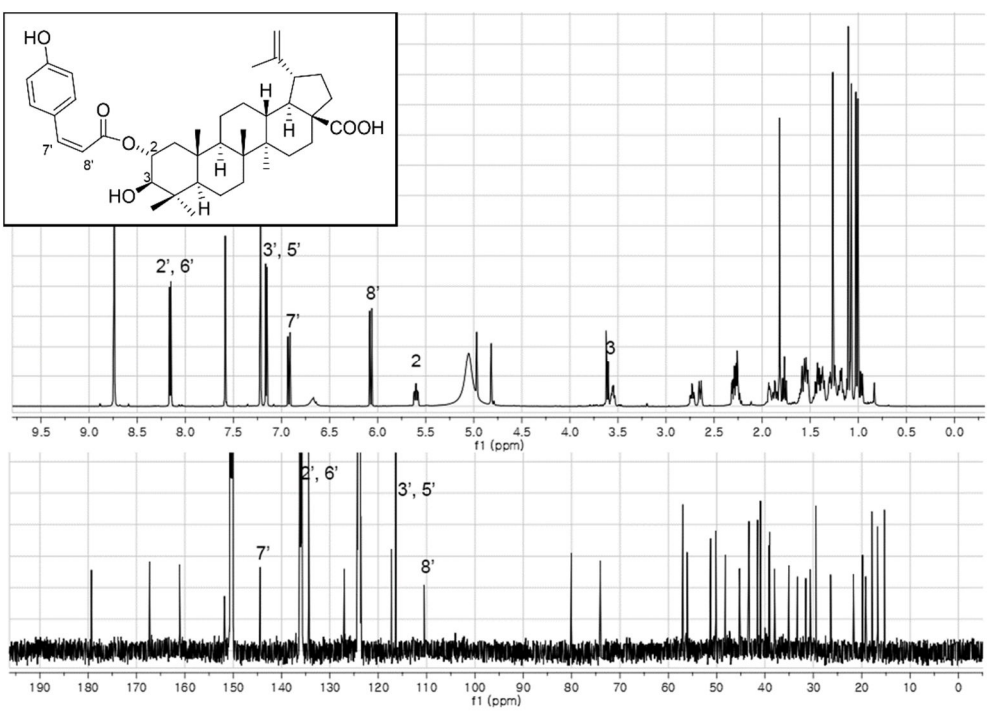

Figure 64. ^{1}H and ^{13}C NMR spectra of compound **29** (600 / 150 MHz, pyridine-d_5)

3.3.13. Compounds **30** and **31**

Compound **30** was obtained as a white amorphous powder with a molecular formula $C_{37}H_{52}O_6$, which was indicated by ESI-qTOF-MS (*m/z* 591.3678 $[M-H]^-$, calcd. for $C_{37}H_{51}O_6$, 591.3686). ^1H and ^{13}C spectra of **30** was similar to compounds **25**, **26**, **28**, and **29**, which suggested that compound **30** was also a derivative of compound **11**, which has an aromatic ester substituent at C-2 position (Figure 65). From the two proton doublets in AB system at δ_H 7.21 (2H, *d, J* = 8.6 Hz) and δ_H 8.34 (2H, *d, J* = 8.6 Hz) indicated the presence of a *p*-hydroxybenzoyl moiety. The position of this *p*-hydroxybenzoyl moiety was deduced by the downfield chemical shift of H-2 (δ_H 5.34, *td, J* = 11.1, 4.7), and confirmed by the HMBC correlation between H-2 and C-7′ (δ_C 167.2) (Figure 67). Based on these spectral data, compound **30** was determined to be 2-*O*-*p*-hydroxybenzoyl alphitolic acid, and it was firstly isolated from nature.

Compound **31** was also acquired as a white amorphous powder. The molecular formula of **31** was deduced as $C_{37}H_{52}O_5$ by ESI-qTOF-MS pseudo-molecular ion peak *m/z* 575.3735 $[M-H]^-$ (calcd. for $C_{37}H_{51}O_5$, 575.3736). ^1H and ^{13}C NMR spectra of **31** was almost identical to those of **30**, except the presence of an aromatic signal at δ_H 7.52 (1H, *t*, *J* = 7.4*),* doublet of doublet splitting of protons peak of C-3 ′ and C-5 ′ (δ_H 7.42, 2H, *dd*, *J* = 7.4, 7.1), and upshifted chemical shift of C-4′ at δ_C 132.2 (δ_C 163.9 for compound **30**) (Figure 66). These differences suggested that compound **31** has a benzoyl ester moiety at its C-2 position, instead of the *p*-hydroxybenzoyl moiety of **30**. From these spectral data and comparison with the previously reported reference, compound **31** was identified as 2-*O*-benzoyl alphitolic acid (Chen et al., 2015).

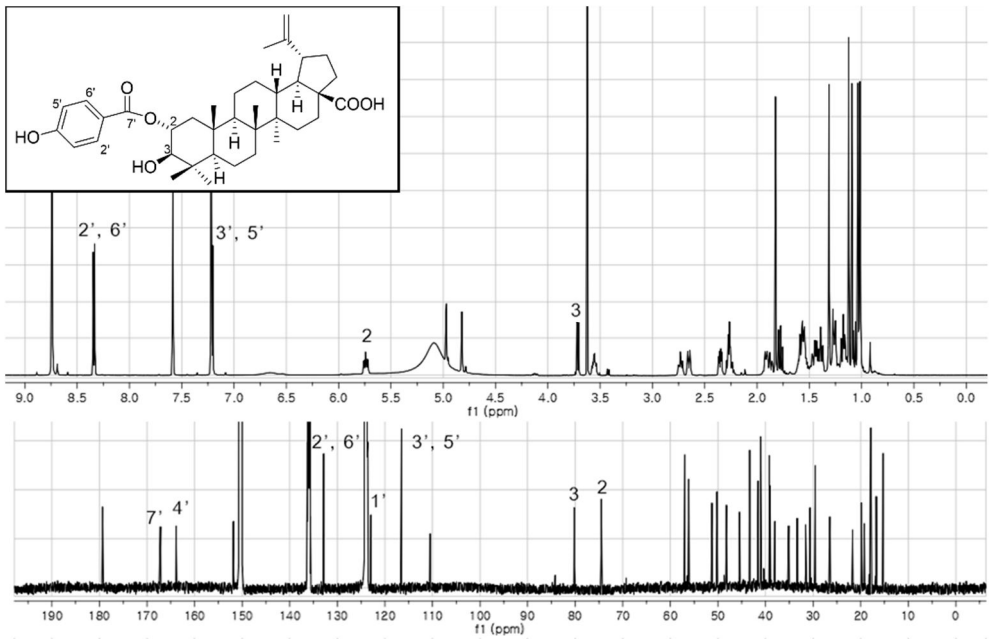

Figure 65. ^{1}H and ^{13}C NMR spectra of compound **30** (600 / 150 MHz, pyridine-d_5)

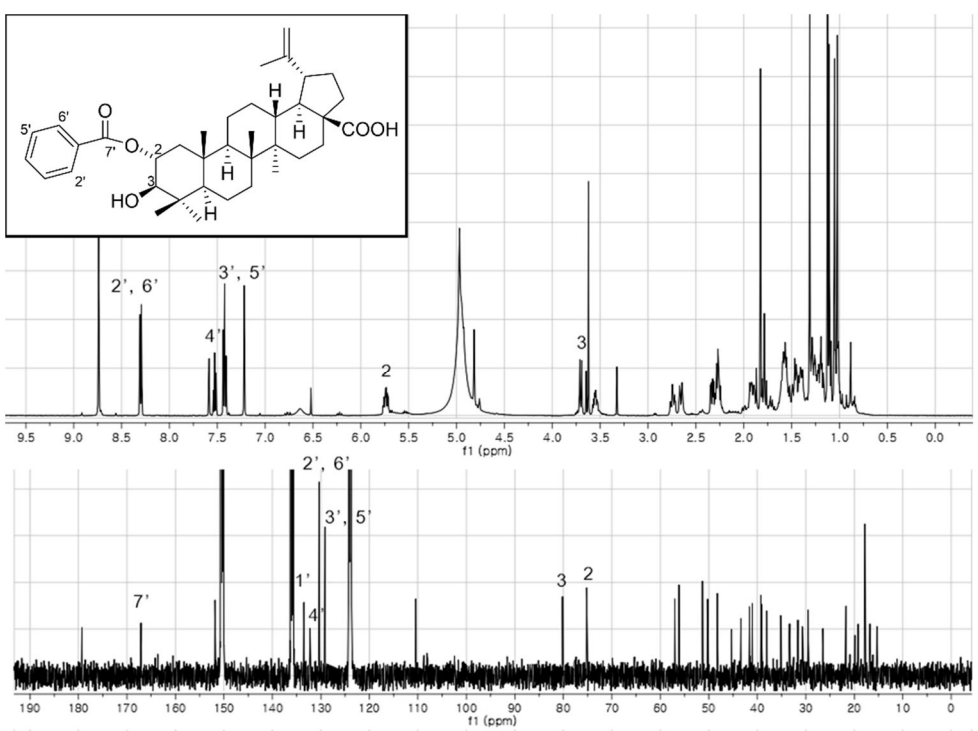

Figure 66. ^{1}H and ^{13}C NMR spectra of compound **31** (600 / 150 MHz, pyridine-d_5)

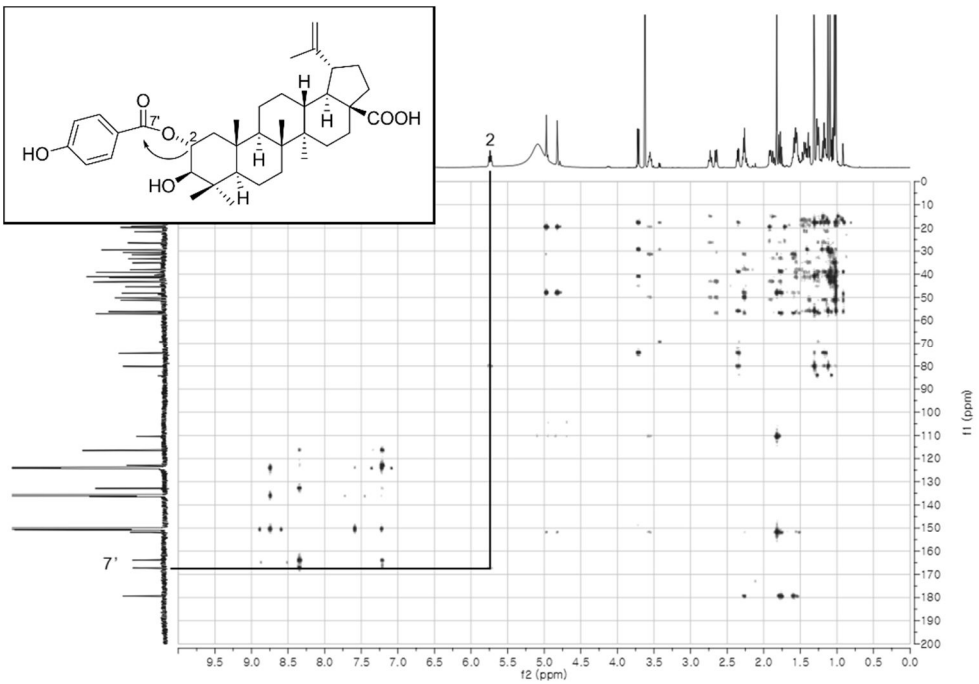

Figure 67. HMBC spectrum of compound **30** (600 MHz, pyridine-d_5)

3.3.14. Compounds **32** and **33**

Compound **32** was isolated as yellowish powder with molecular formula $C_{37}H_{50}O_8$, indicated by ESI-qTOF-MS (*m/z* 621.3442 $[M-H]^-$, calcd. for $C_{37}H_{49}O_8$, 621.3427). In ^1H NMR spectrum of **32**, an isopropenyl group signal (δ_H 4.83, 4.63, and 1.65), five additional methyl singlets (δ_H 1.03, 1.05, 1.12, 1.14, and 1.50), and two methine singlets at δ_H 3.09 and 5.82 were observed, which suggested that **32** is a derivative of compound **14** (Figure 68). Three aromatic protons at δ_H 7.29 (*d, J* = 8.2), δ_H 7.88 (*dd, J* = 8.2, 2.3), and δ_H 8.08 (*d, J* = 2.3) suggested the presence of a protocatechuoyl moiety. The downfielded chemical shift of H-3 (δ_H 5.82) suggested the position of the protocatechuoyl ester as C-3, and it was confirmed by the HMBC experiment. Therefore, compound **32** was deduced to be 3-*O*-protocatechuoyl ceanothic acid, and it was confirmed by comparison with the previously reported reference (Lee et al., 1996).

Compound **33** was obtained as pale yellowish powder, and its molecular formula was suggested to be $C_{38}H_{52}O_8$ by ESI-qTOF-MS (*m/z* 635.3580 $[M-H]^-$, calcd. for $C_{38}H_{51}O_8$, 635.3584). ^1H and ^{13}C NMR spectra of **33** were almost identical to those of **32**, but one methoxy signal was observed additionally at δ_H/δ_C 3.72/51.4 (Figure 69). However, chemical shifts of aromatic protons did not differ to those of **32**, not as the case of compound **25** and **26**, so the possibility for the presence of vanilloyl moiety was excluded. On the other hand, it was supposed to be a methyl ester substituent on the carboxyl positions, such C-2 or C-28. The HMBC experiment was performed to determine the position of this methyl ester, and the correlation of methoxy protons and C-2 (δ_C 176.5) confirmed the position (Figure 70). Therefore, compound **33** was determined to be 3-*O*-protocatechuoyl ceanothic acid 2-methyl ester, and it was isolated for the first time from nature.

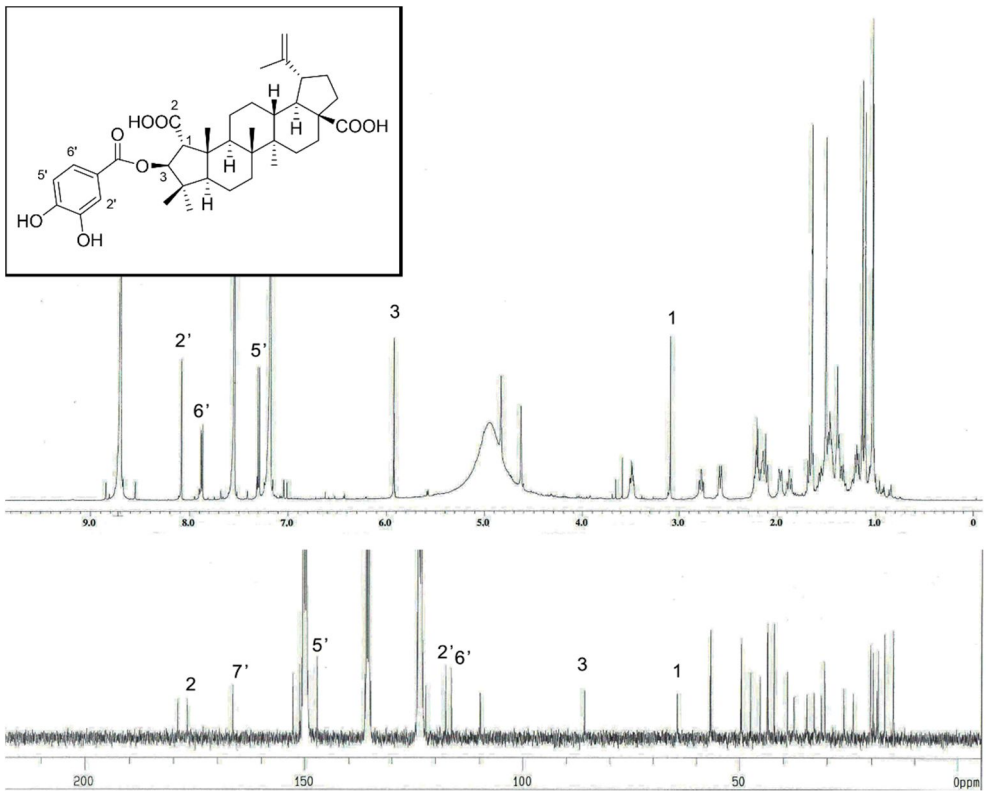

Figure 68. ^{1}H and ^{13}C NMR spectra of compound **32** (300 / 75 MHz, pyridine-d_5)

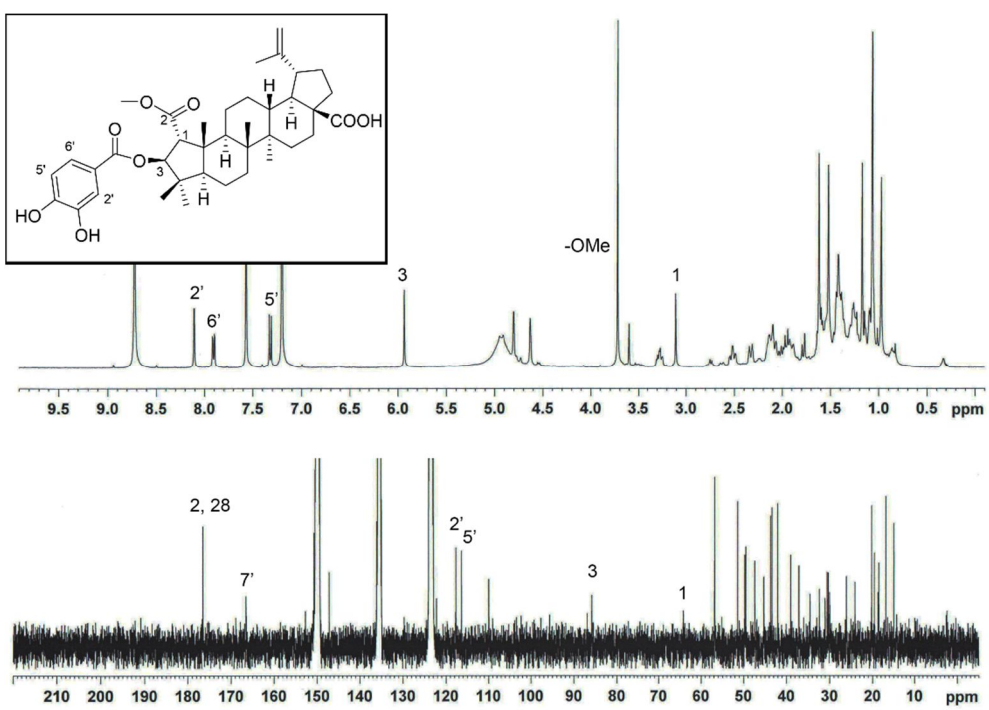

Figure 69. ^{1}H and ^{13}C NMR spectra of compound **33** (400 / 100 MHz, pyridine-d_5)

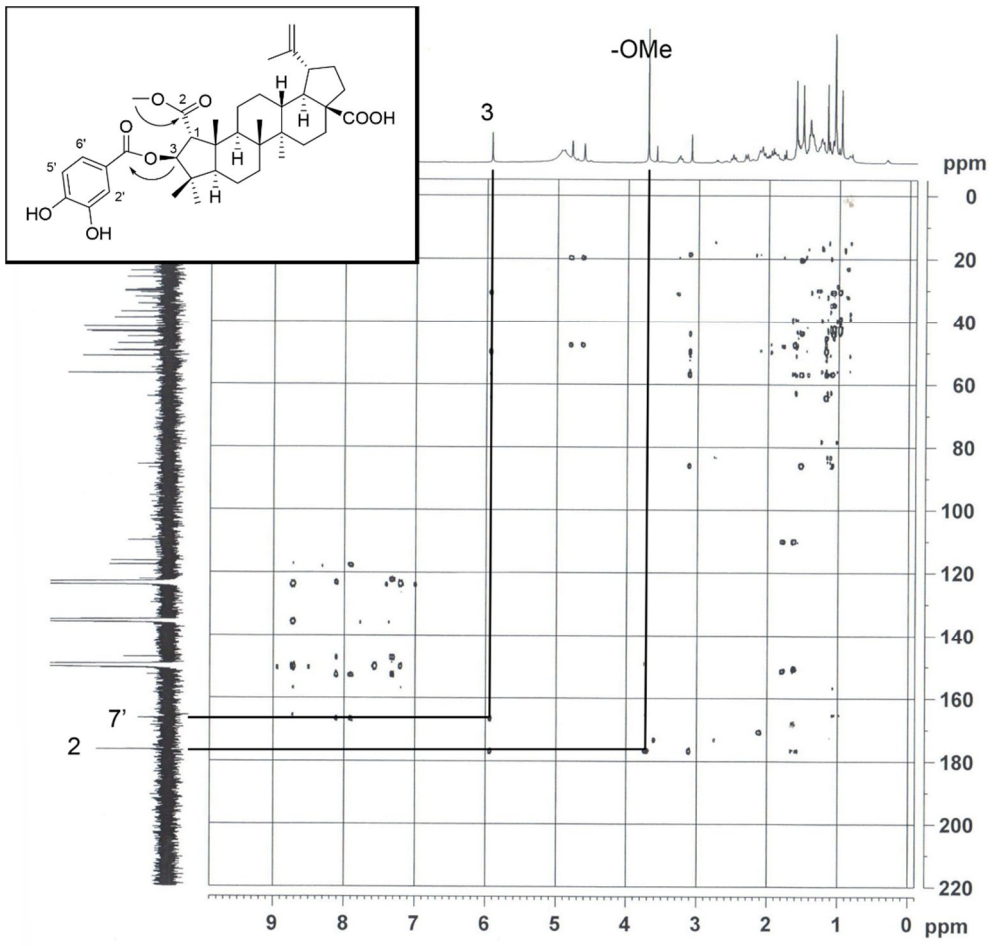

Figure 70. HMBC spectrum of compound **33** (400 MHz, pyridine-d_5)

3.3.15. Compounds **34**, **35** and **36**

Compound **34** was white amorphous powder, and its molecular formula was determined as $C_{38}H_{52}O_8$ by ESI-qTOF-MS (*m/z* 635.3594 $[M-H]^-$, calcd. for $C_{38}H_{51}O_8$, 638.3584). ^1H and ^{13}C NMR spectra of **34** were similar to those of **32**, exhibiting an isopropenyl group (δ_H 1.68, 4.67, and 4.87), five additional methyl singlets (δ_H 1.06, 1.15, 1.15, 1.27, and 1.58), two methine singlets at δ_H 3.20 (H-1) and 6.00 (H-3), aromatic protons at δ_H 7.31 (*d, J* = 8.2 Hz), 7.91 (*d, J* = 1.9), and 7.97 (*dd*, *J* =1.9, 8.2 Hz), and a methoxy singlet at δ_H 3.79 (Figure 71). These suggested that **34** is another 3-*O* aromatic moiety ester derivative of compound **14**. Chemical shifts of three aromatic protons were similar to those of compound **26**, which suggested the presence of vanilloyl moiety, and that was confirmed by the HMBC correlation of the methoxy singlet and C-3′ (δ_C 149.0). The HMBC experiment additionally confirmed the ester position at C-3 by the correlation of H-3 and C′-7 (δ_C 166.7). Therefore, compound **34** was identified as 3-*O*-vanilloyl ceanothic acid (Suksamrarn et al., 2006).

Compound **35** was isolated as yellow syrup with a molecular formula $C_{38}H_{52}O_8$, which was indicated by ESI-qTOF-MS (*m/z* 635.3594 $[M-H]^-$, calcd. for $C_{38}H_{51}O_8$, 638.3584). ^1H and ^{13}C NMR spectra of **35** resembled those of **34**, but two methine proton signals for H-1 (δ_H 3.13) and H-3 (δ_H 5.95) were doublets with *J* = 7.7 Hz, instead of singlets (Figure 72). These suggested that **35** had H-1β and H-3β orientation, such as compound **15** and **16**. The HMBC experiment exhibited correlations of the methoxy singlet (δ_H 3.70) and C-3′ (δ_C 148.3), and of H-3 and C-7′ (δ_C 166.6) (Figure 74). These confirmed the presence of a vanilloyl moiety and its ester bond position at C-3, respectively. From these spectral data, compound **35** was elucidated to be 3-*O*-vanilloyl epiceanothic acid, and it was firstly isolated from nature.

Compound **36** was obtained as yellow syrup. ESI-qTOF-MS pseudo-molecular ion peak at *m/z* 649.3737 $[M-H]^-$ (calcd. for $C_{39}H_{53}O_8$, 649.3740) suggested its

molecular formula as $C_{39}H_{54}O_8$. ^1H and ^{13}C NMR spectra of **36** were almost identical to those of **34**, but those were an additional methoxy singlet at δ_H 3.80 (Figure 73). This methoxy moiety was confirmed as the methyl ester substituent at C-2, indicated by the HMBC correlation of proton singlet of it and C-2 (δ_C 177.3) (Figure 75). The HMBC spectrum of **36** also confirmed the presence of 3-*O*-vanilloyl ester, identically to the case of compound **34**. Consequently, compound **36** was determined to be 3-*O*-vanilloyl ceanothic acid 2-methyl ester, and it was isolated for the first time from nature.

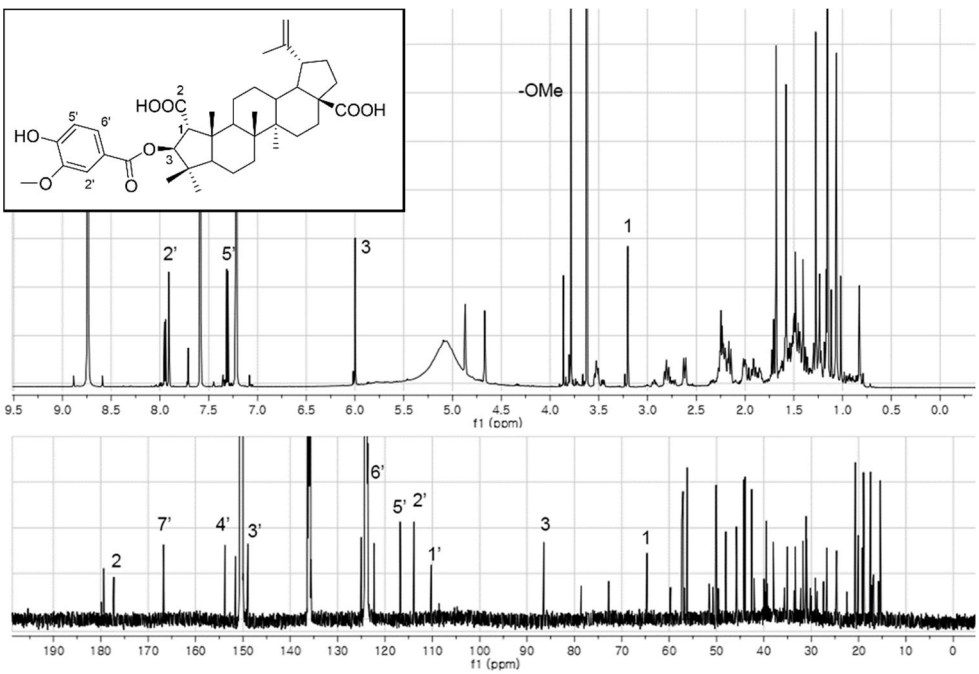

Figure 71. ^1H and ^{13}C NMR spectra of compound **34** (600 / 150 MHz, pyridine-d_5)

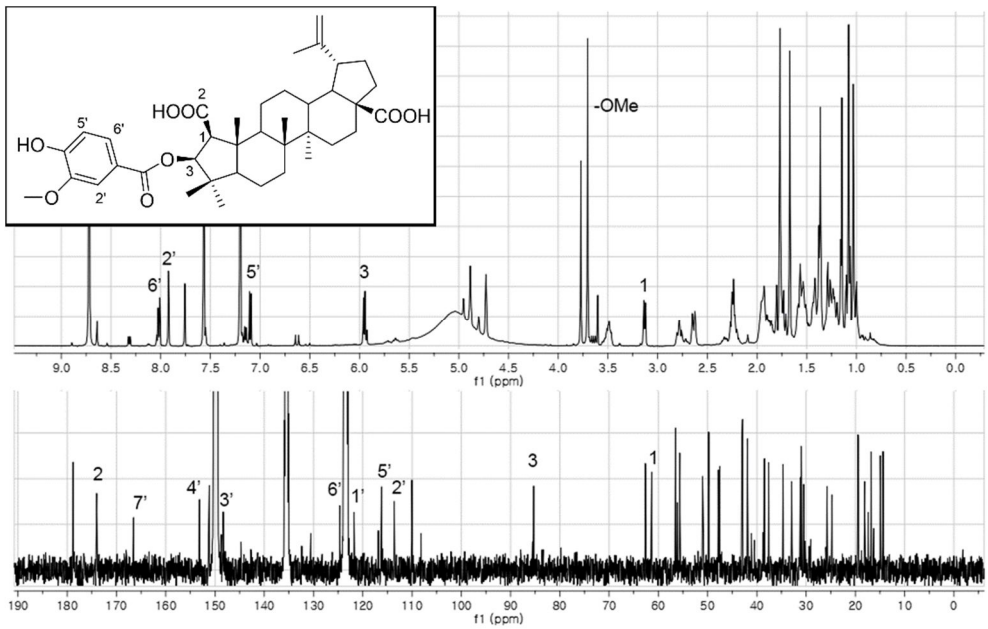

Figure 72. ^{1}H and ^{13}C NMR spectra of compound **35** (500 / 125 MHz, pyridine-d_5)

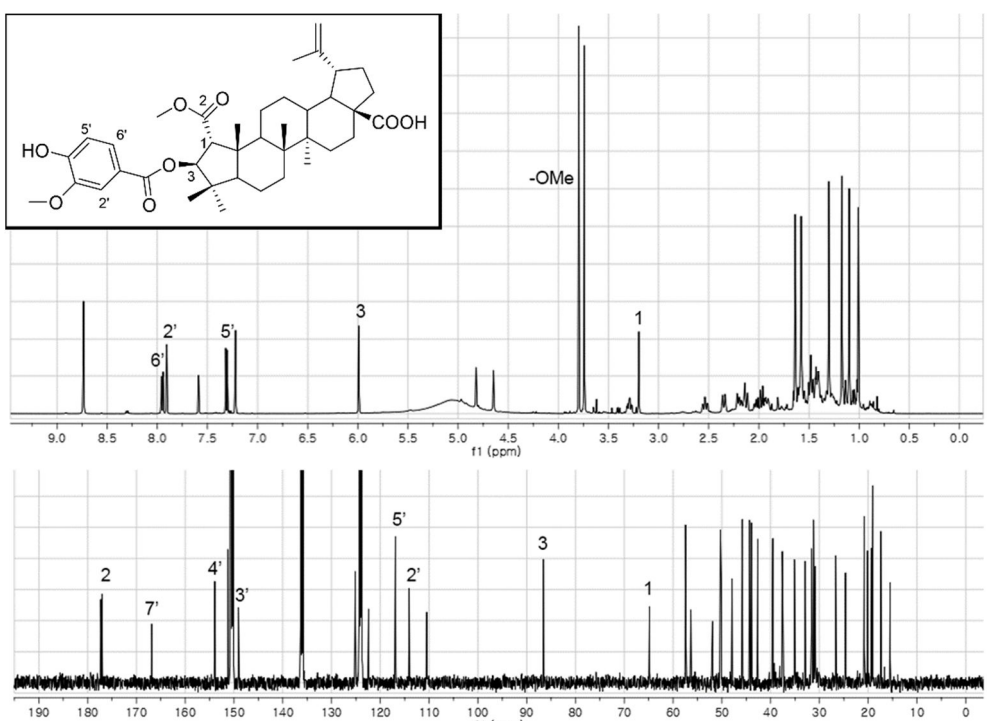

Figure 73. ^{1}H and ^{13}C NMR spectra of compound **36** (500 / 125 MHz, pyridine-d_5)

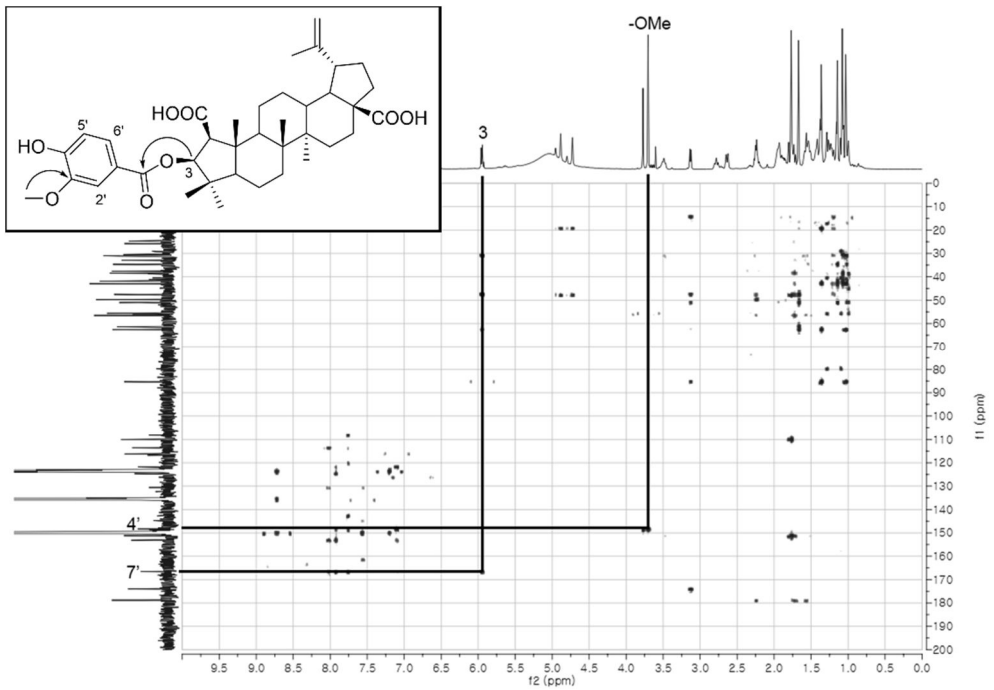

Figure 74. HMBC spectrum of compound **35** (500 MHz, pyridine-d_5)

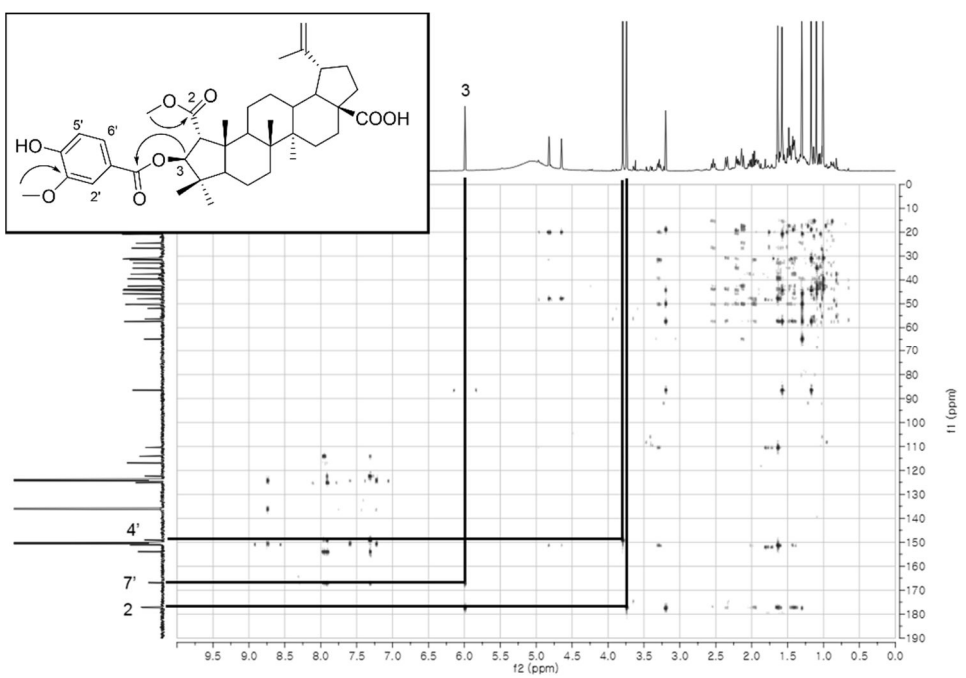

Figure 75. HMBC spectrum of compound **36** (500 MHz, pyridine-d_5)

3.3.16. Compounds **37** and **38**

Compound **37** was obtained as white amorphous powder with molecular formula of $C_{37}H_{50}O_7$, indicated by ESI-qTOF-MS pseudo-molecular ion peak at *m/z* 605.3472 $[M-H]^-$ (calcd. for $C_{37}H_{49}O_7$, 605.3468). ^1H and ^{13}C NMR spectra of **37** resembled those of compounds **32**-**36**, which suggested **37** is also an aromatic moiety ester derivative of compound **14** (Figure 76). Aromatic proton doublets in AB coupling system were observed at δ_H 7.25 and 8.27 (2H for each, *d, J* = 8.7 Hz), as same as compound **28**-**30**. These suggested the presence of *p*-hydroxybenzoyl moiety. From the singlet shapes of the methine protons at δ_H 3.18 (H-1) and δ_H 5.98 (H-3), H-1β and H-3α *trans* orientation was deduced. The ester position at C-3 was supposed by the downfielded H-3, and it was confirmed by the HMBC experiment (Figure 78). Consequently, compound **37** was determined to be 3-*O*-*p*-hydroxybenzoyl ceanothic acid, and it was isolated for the first time from nature.

Compound **38** was isolated as a pinkish amorphous powder with molecular formula of $C_{37}H_{50}O_7$, indicated by ESI-qTOF-MS pseudo-molecular ion peak at *m/z* 605.3472 $[M-H]^-$ (calcd. for $C_{37}H_{49}O_7$, 605.3468). ^1H and ^{13}C NMR spectra of **38** were almost identical to those of **37**, but methine protons at δ_H 3.51 (H-1) and δ_H 5.86 (H-3) were observed doublets with *J* = 7.8 Hz (Figure 77). H-1α and H-3α *cis* orientation was deduced from this proton-proton coupling. The HMBC spectrum confirmed the ester linkage of *p*-hydroxybenzoyl moiety to C-3 (Figure 79). Therefore, compound **38** was confirmed to be 3-*O*-*p*-hydroxybenzoyl epiceanothic acid. This compound was also isolated firstly from nature.

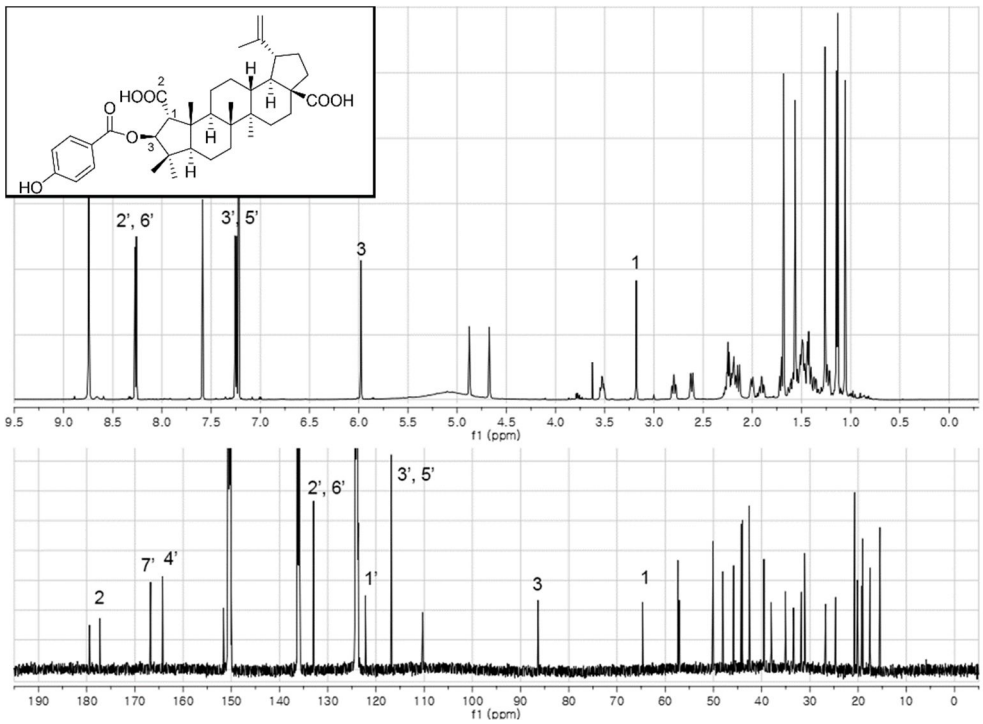

Figure 76. ^{1}H and ^{13}C NMR spectra of compound **37** (600 / 150 MHz, pyridine-d_5)

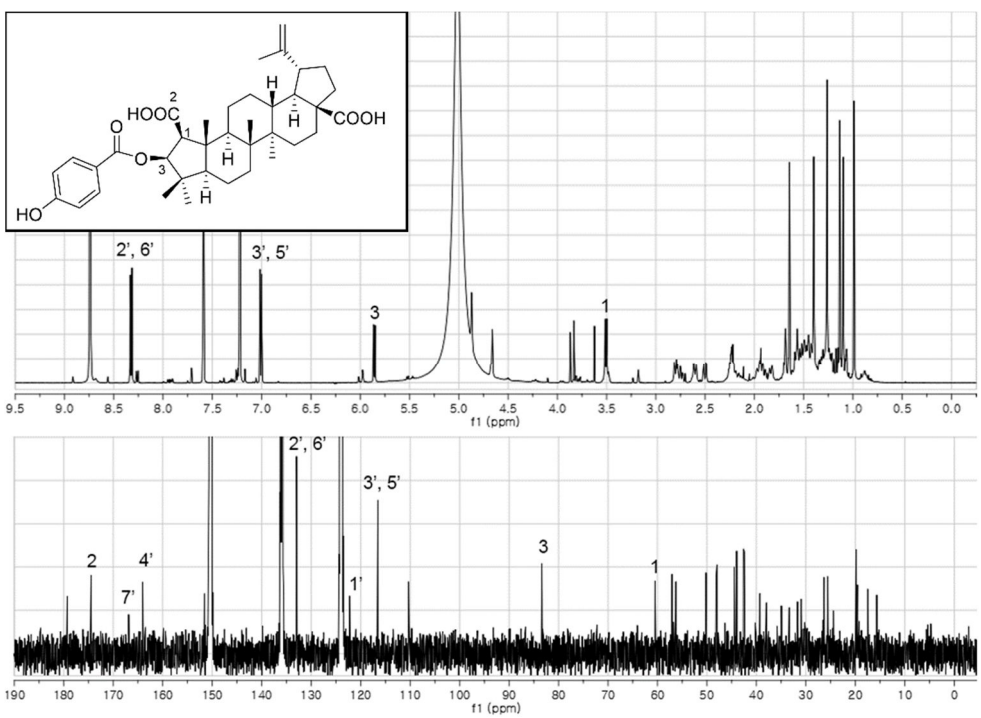

Figure 77. ^{1}H and ^{13}C NMR spectra of compound **38** (500 / 125 MHz, pyridine-d_5)

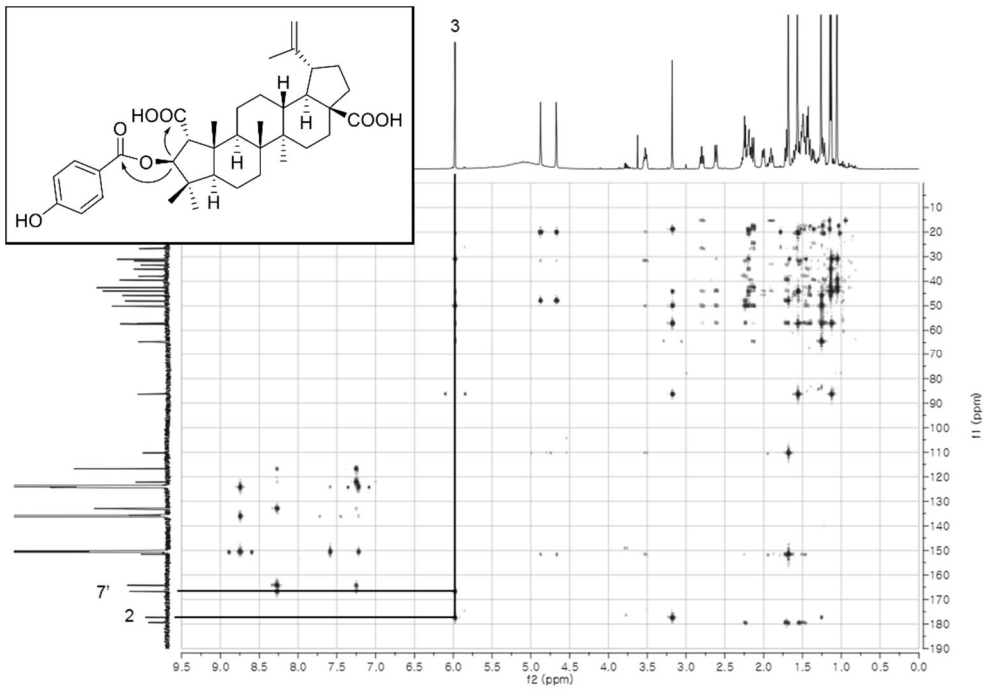

Figure 78. HMBC spectrum of compound **37** (600 MHz, pyridine-d_5)

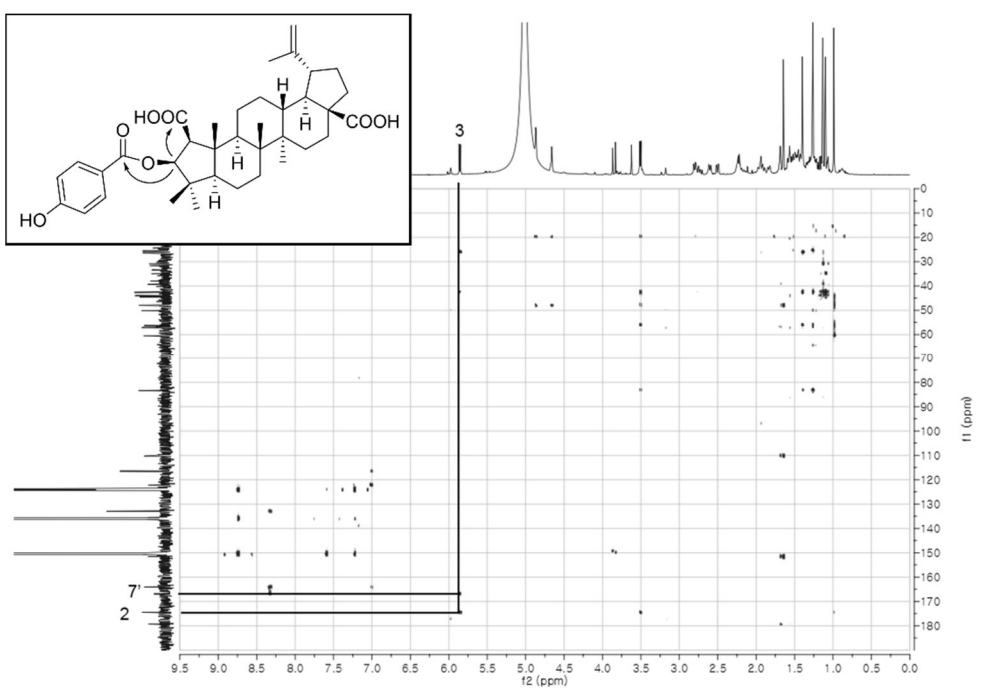

Figure 79. HMBC spectrum of compound **38** (500 MHz, pyridine-d_5)

3.3.17. Compound **39**

Compound **39** was obtained as white amorphous powder. ESI-qTOF-MS pseudo-molecular peak at *m/z* 607.3639 $[M-H]^-$ (calcd. for $C_{37}H_{51}O_7$, 607.3635) suggested the molecular formula $C_{37}H_{52}O_7$. Because of its scarce amount (0.8 mg), ^{13}C NMR spectrum was not available, so chemical shifts of carbons were deduced by multiplicity-edited HSQC and HMBC spectra. Two oxygenated methylene protons at δ_H 4.73 (*dd*, *J* = 10.0, 5.5 Hz, H-2a) and 4.46 (*dd, J* = 10.0, 8.8 Hz, H-2b), one oxygenated methine singlet at 4.37 (H-3), and three aromatic protons at δ_H 7.28 (*d, J* = 8.3 Hz), 7.90 (*dd, J* = 8.3, 1.9 Hz), and 8.22 (*d, J* = 1.9 Hz) were observed in ^1H NMR spectrum of **39** (Figure 80). ^1H-^1H COSY spectrum of **39** revealed proton couplings between H-2s and H-1 (δ_H 2.45, *dd, J* = 8.8, 5.5 Hz), and H-1 and H-3. These suggested that **39** was an aromatic ester derivative of ceanothane-type triterpene with a hydroxymethyl function at C-2, instead of a carboxy function. The HMBC experiment confirmed this structural suggestion with correlations of H-2/C-1 (δ_C 58.7), H-1/C-2 (δ_C 65.1), and H-3/C-2 (Figure 81). The presence of a protocatechuoyl moiety was deduced by the chemical shifts and coupling constants of aromatic protons. Unlike 3-*O*-ester derivatives such as **32-38**, chemical shift of H-3 of **39** was not downshifted than compound **14** or **15**. This suggested the position of protocatechuoyl ester as at C-2, and the HMBC correlation between H-2 and C-7′ (δ_C 167.7) confirmed the ester substitution at C-2. The H-1β/H-3α *trans* oriented configuration was deduced by singlet peak shape of H-3. The ROESY experiment was performed to confirm this configuration of A-ring. H-1 exhibited spatial correlation with β-oriented methyl protons of H-25 (δ_H 1.31, *s*) while H-3 correlated with α-oriented H-23 (δ_H 1.16, *s*) and H-5 (δ_H 1.55, *s*) (Figure 82). Correlations of H-2/H-5 and H-2/H-9 (δ_H 1.84, *m*) were also observed in the ROESY spectrum. Thus, from these correlations, the H-1β/H-3α configuration was confirmed in the A-ring of **39**. Based on these spectral analysis, compound **39** was

elucidated as a 2-*O*-protocatechuoyl ester derivative of the (1*S*, 3*S*)-isomer of ceanothanolic acid (Lee et al., 1997). Therefore, compound **39** was named 2-*O*-protocatechuoyl isoceanothanolic acid, and it was firstly isolated from nature.

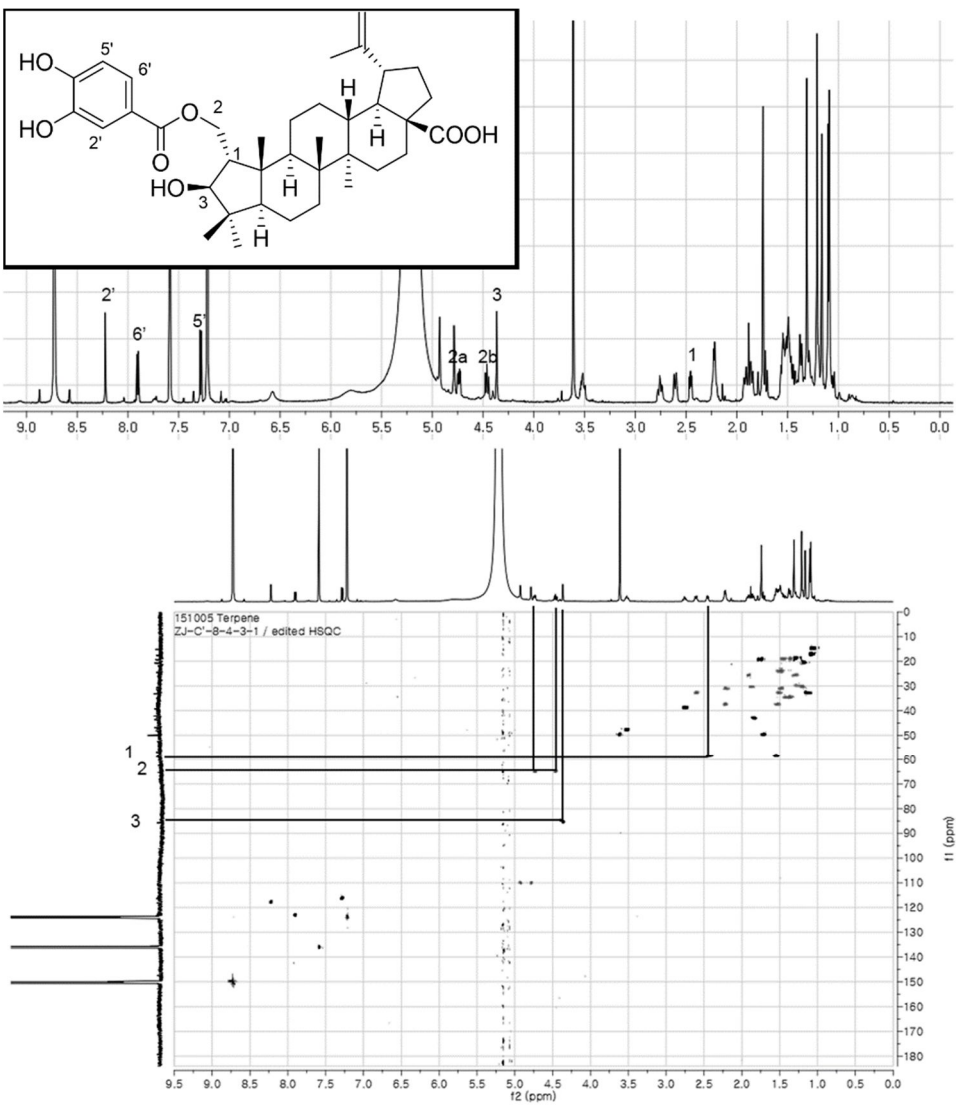

Figure 80. ^{1}H NMR and HSQC spectra of compound **39** (600 MHz, pyridine-d_5)

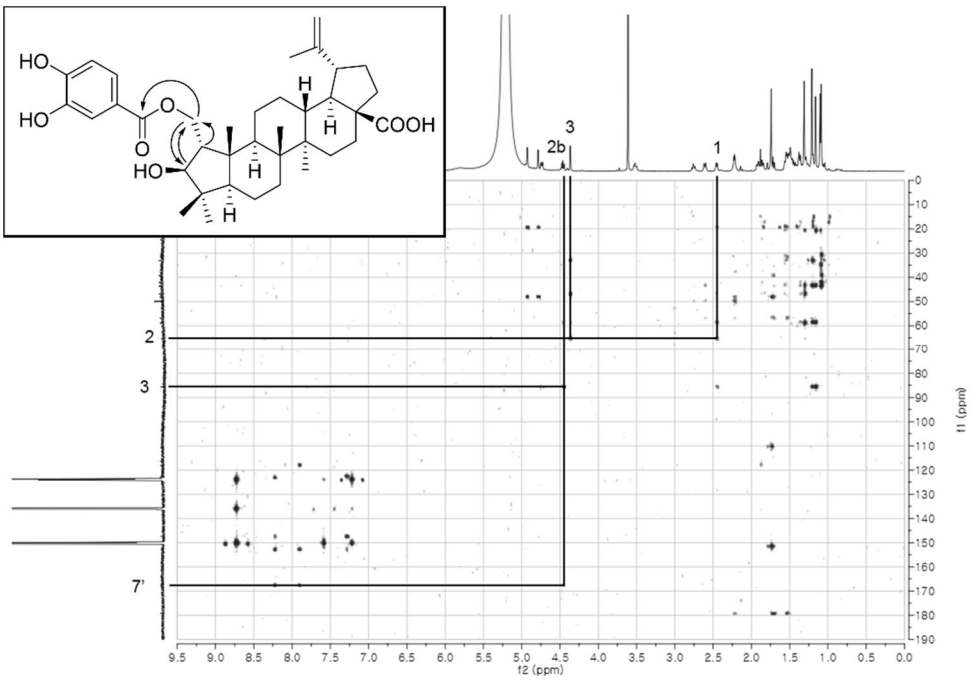

Figure 81. HMBC spectra of compound **39** (600 MHz, pyridine-d_5)

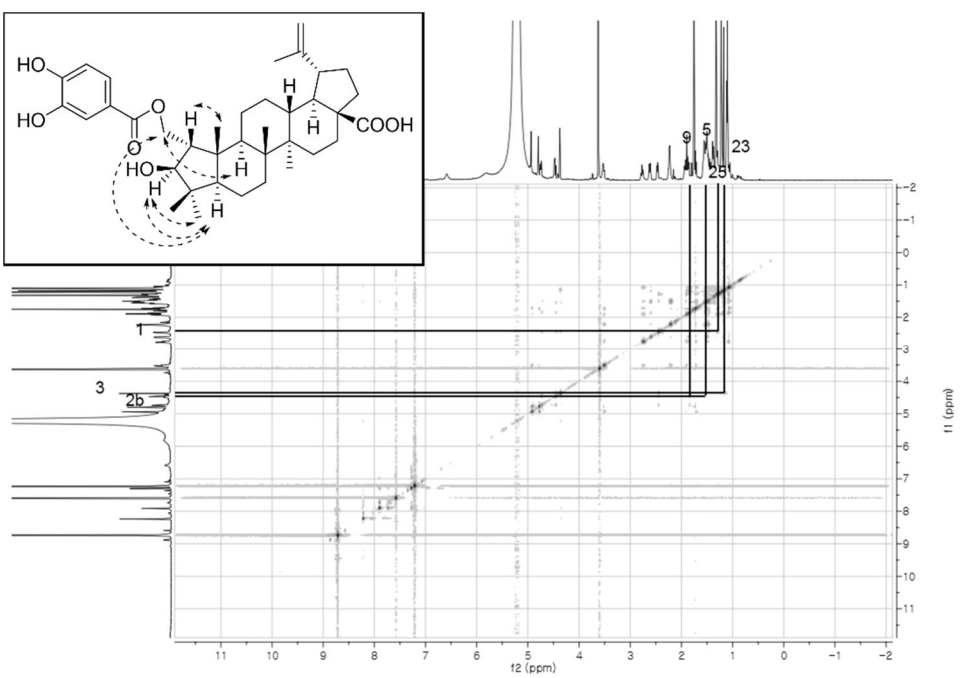

Figure 82. ROESY spectrum of compound **39** (600 MHz, pyridine-d_5)

3.3.18. Compound **40**

Compound **40** was isolated as white amorphous powder. Its molecular formula, $C_{37}H_{48}O_8$ was established by ESI-qTOF-MS (*m/z* 619.3257 $[M-H]^-$ calcd. for $C_{37}H_{47}O_8$, 619.3271). In ^1H NMR spectrum of **40**, an isopropenyl group signal (δ_H 5.49, 4.99 and 1.62), three aromatic protons at δ_H 7.40 (*d, J* = 8.3, H-5′), 7.92 (*d, J* = 8.3, H-6′), and 8.14 (*br s,* H,-2′), and two methine proton singlets at δ_H 3.14 (H-1) and 5.97 (H-3) were observed (Figure 83). In ^{13}C NMR spectrum, a tertiary carbon signal was observed at δ_C 92.9 (C-17). With the downshifted H-29s, this suggested **40** is a γ-lactone bridged derivative of **14**, similar to compound **20**. The HMBC correlations of H-29b and H-30 with C-17 confirmed the presence of the lactone bridge (Figure 84). The HMBC experiment also confirmed the position of protocatechuoyl ester as at C-3, by the correlation between H-3 and C-7′ (δ_C 167.0). H-1β/H-3α orientations were deduced from the singlet coupling of H-1 and H-3. From these spectral data, compound **40** was concluded to be 3-*O*-protocatechuoyl ceatha-28β,19β-olide, and it was first isolated from nature.

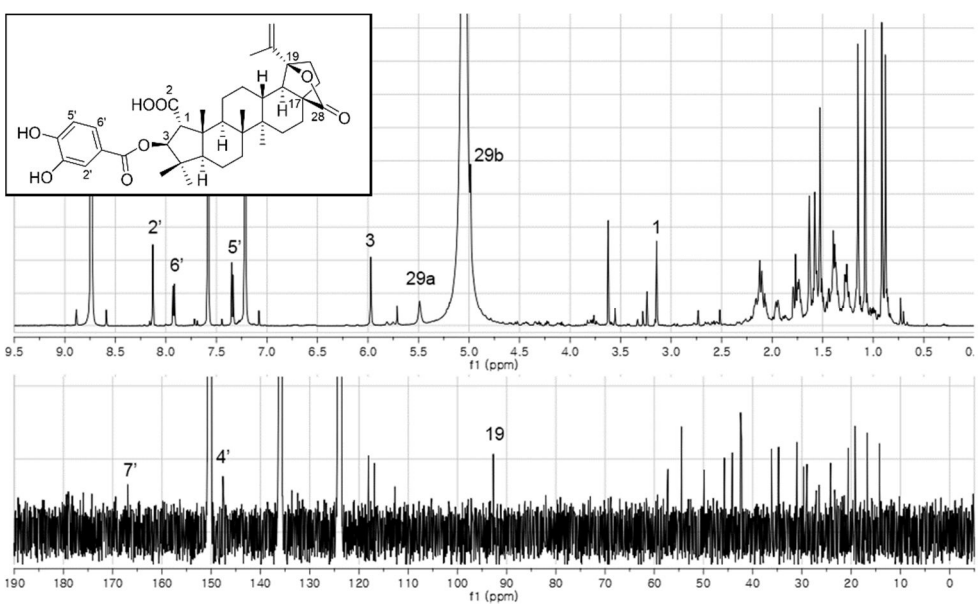

Figure 83. ^1H and ^{13}C NMR spectra of compound **40** (600 / 150 MHz, pyridine-d_5)

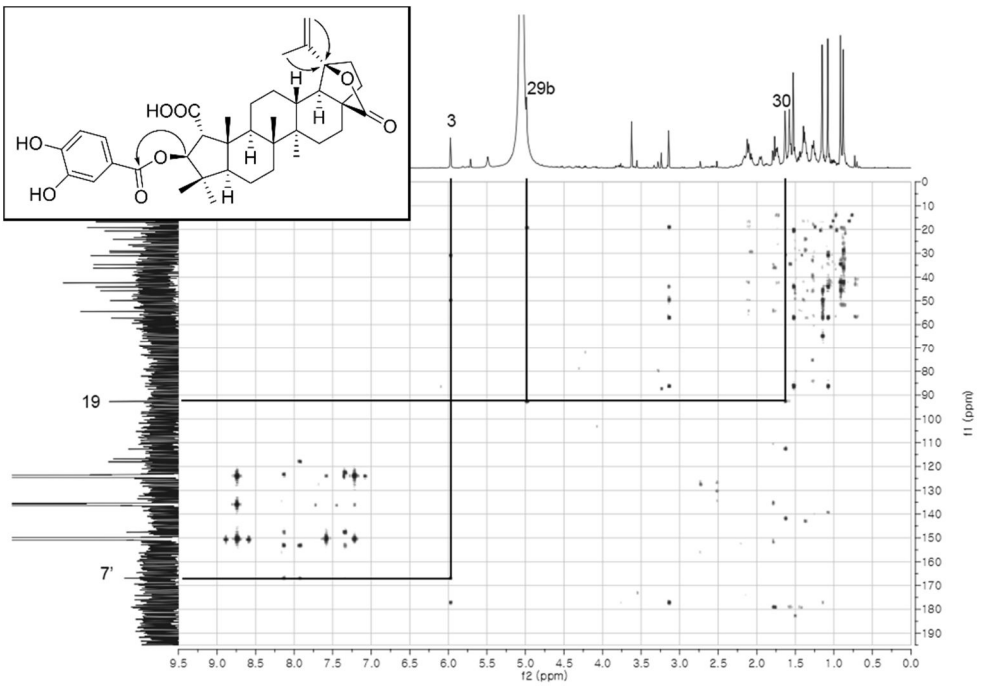

Figure 84. HMBC spectrum of compound **40** (600 MHz, pyridine-d_5)

3.3.19. Compound **41**

Compound **41** was obtained as white amorphous power. Its molecular formula was determined to be $C_{39}H_{52}O_{10}$ from the ESI-qTOF-MS pseudo-molecular ion peak at *m/z* 679.3474 (calcd. for $C_{39}H_{51}O_{10}$, 679.3482). In ^{1}H NMR spectrum of **41**, three aromatic protons [δ_H 8.01 (*dd, J* = 8.2, 1.1 Hz, H-6′), 7.97 (*d*, *J* = 1.1 Hz, H-2′), 7.20 (overlapped with solvent peak)], one oxygenated methine proton at δ_H 6.02 (*dd, J* = 10.3, 4.4 Hz, H-7), and two methoxy singlets at δ_H 3.76 and 3.78 were observed (Figure 85). In ^{13}C NMR spectrum, three carboxy carbons at δ_C 176.4 (C-2), 178.7 (C-27), and 179.8 (C-28) were observed, which indicated **41** is a derivative of **17**. By the HMBC experiment, two methoxy functions were positioned to the vailloyl moiety and the ester of C-2, respectively (Figure 86). From the HMBC cross-peak between the methine proton at δ_H 3.06 (H-13, *m*) and C-27, the presence of carboxyl group at C-27 was confirmed. The downshifted

methyl singlet at δ_H 1.63 (H-26) exhibited a HMBC correlation with the oxygenated methine carbon at δ_C 80.9, and H-7 showed the correlation with C-7′ (δ_C 165.9) of the vanilloyl moiety, which revealed the attachment of the vanilloyl ester at C-7. Downshifted chemical shifts of H-13 and H-26 suggested the β-orientation of the ester group at C-7. H-7 showed NOE correlations with α-oriented H-5 (δ_H 2.12, *m*) and H-9 (δ_H 2.21, *m*), so the relative configuration at C-7 was confirmed (Figure 87). The NOE cross-peak between H-1 (δ_H 2.71, *d*, *J* = 7.6 Hz) and H-25 (δ_H 0.99, *s*) was also observed, which determined the H-1β configuration. Consequently, compound **41** was determined to be 7β-*O*-vanilloyl-3-dehydroxy-ceanothetric acid 2-methyl ester, and it was isolated from nature for the first time.

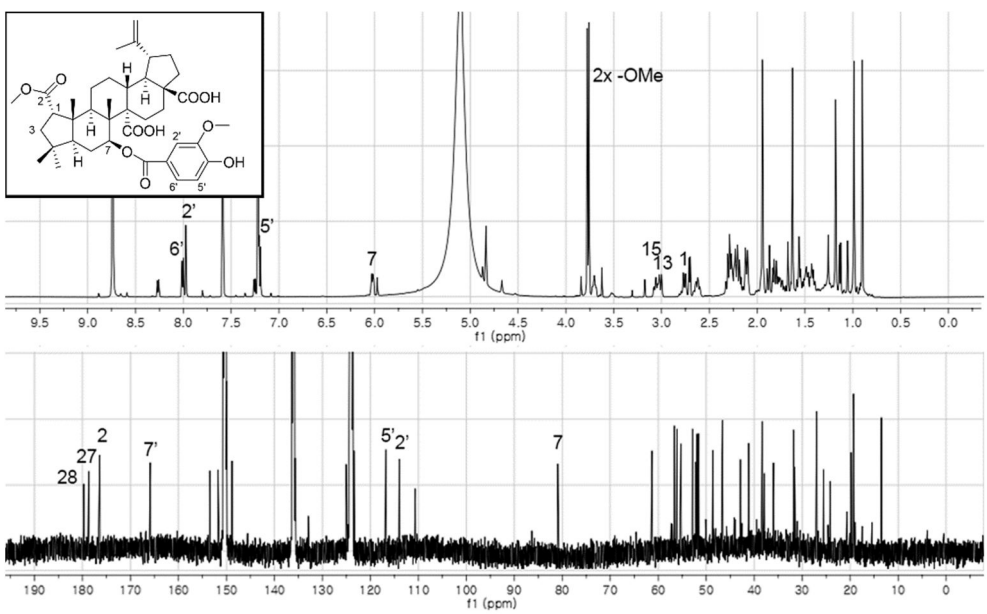

Figure 85. ^{1}H and ^{13}C NMR spectra of compound **41** (600 / 150 MHz, pyridine-d_5)

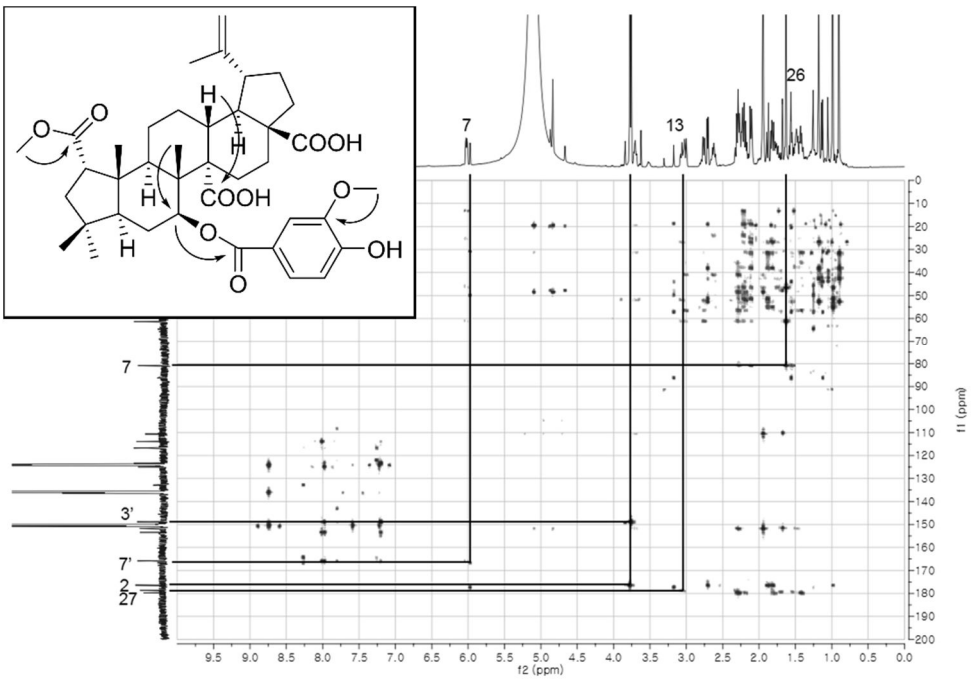

Figure 86. HMBC spectrum of compound **41** (600 MHz, pyridine-d_5)

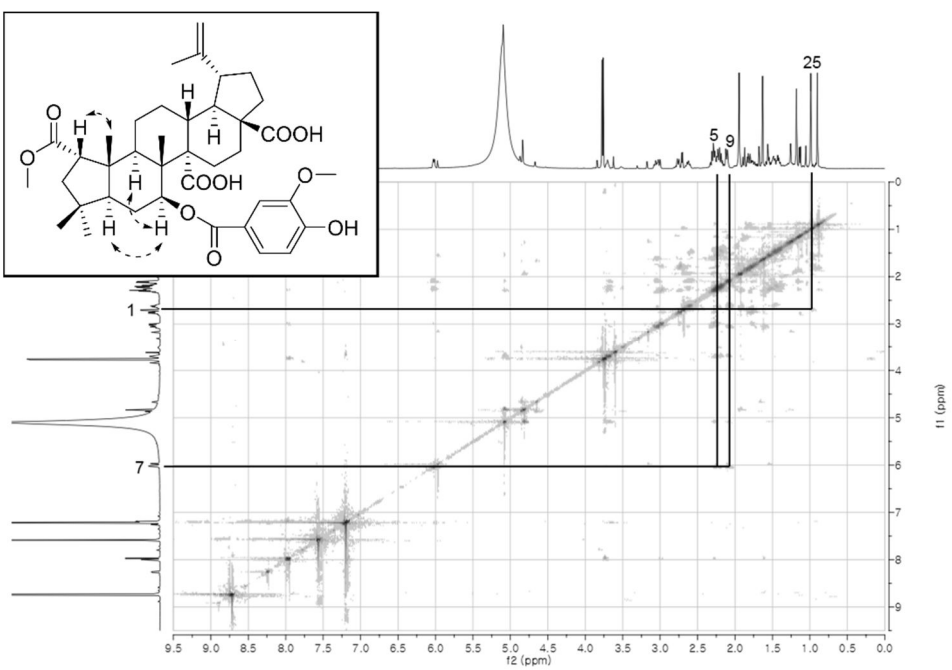

Figure 87. NOESY spectrum of compound **41** (600 MHz, pyridine-d_5)

3.3.20. Compound **42**

Compound **42** was isolated as brown syrup. The ESI-qTOF-MS of **42** exhibited a pseudo-molecular ion peak at *m/z* 739.3857 $[M-H]^-$ (calcd. for $C_{45}H_{55}O_9$, 739.3846), corresponding to a molecular formula of $C_{45}H_{56}O_9$. The ^1H NMR spectrum of **42** showed characteristic signals of an isopropenyl group [δ_H 5.10 (*br s*, H-29a), 5.02 (*br s*, H-29b), and 2.00 (*s*, H-30)]. Additionally, five additional methyl singlets and two methine singlets at δ_H 4.05 (H-1) and 3.93 (H-3) were observed (Figure 88). The methine singlets were suggested to be coupled to each other by a ^1H-^1H COSY spectrum, so compound **42** was deduced to be a derivative of **14**. In ^1H and ^{13}C NMR spectra of **42**, signals of eight protons and fifteen carbons were observed additionally. After assignment of those protons and carbons in the ceanothic acid subunit by HSQC and HMBC spectra, the residual NMR signals resembled those of (-)-epicatechin (**48**), except for the absence of a proton equivalent to H-8. The attachment between the ceanothic acid subunit and the epicatechin subunit was determined by the HMBC experiment (Figure 89). The presence of a ketone bridge at C-2 was deduced from the chemical shift of C-2 (δ_C 208.9), and HMBC correlations from H-1 to C-7′ (δ_C 155.3), C-8′ (δ_C 99.6) and C-8a′ (δ_C 154.6) indicated that the ketone bridge was attached to C-8′. In addition, the ether bond between C-3 (δ_C 87.4) and C-7′ was determined by the HMBC correlation of H-3 and C-7′.

Singlet couplings of H-1 and H-3 in cyclopentanyl A-ring of ceanothane-type triterpenoids were often occurred in H-1β/H-3α *trans* orientations only (Eade et al., 1967). However, this is only true when the cyclopentanyl ring is in a β-envelope conformation, which is more stable than α-envelope in ceanothic acid (**14**) because of the strong 10β-CH_3−4β-CH_3 interaction. In this case of **42**, C-1, C-2, and C-3 were also parts of the chromone ring structure, so it was supposed that the conformation of the cyclopentanyl ring would be different to that of **14** or its

derivatives. To validate this hypothesis, the ROESY experiment was performed, and H-1 exhibited correlations with β-oriented H-25 (δ_H 0.93, *s*) and H-11a (δ_H 2.20, *m*), while H-3 also with H-25 and H-24 (δ_H 0.86, *s*) (Figure 90). Therefore, compound **42** was deduced to have *cis* relative configuration of H-1β and H-3β, although both of them exhibited singlet signals in ^{1}H NMR spectrum. It was not so surprising, because it has been reported that *cis*-flavanonol such as (-)-epitaxifolin (Lundgren and Theander, 1988) or (2*R*,3*S*)-dihydrokaempferol (Prescott et al., 2002) exhibited small $J_{2,3}$ values as 2.8 Hz and 2.4 Hz, respectively. In *trans* epimers of these compounds, which is the major isomer in nature, $J_{2,3}$ values are often 10–12 Hz. Interestingly, aromatic protons of catechin moiety B-ring exhibited spatial couplings with protons of the isoproprenyl group. It suggested that in the stable conformer of **42**, their distance would be so close enough to give spatial effect to each other. Downshifted chemical shifts of H-29a, H-29b, H-30 supported this hypothesis.

Singlet coupling of H-2′ and H-3′ suggested their *cis* orientation. The absolute configuration of compound **42** was confirmed by the application of modified Mosher's method (Figure 91) (Hoye et al., 2007). Shielding effects by MTPA esters suggested that the absolute configuration of the catechin moiety is identical to one of (-)-epicatechin, the naturally abundant form of *cis*-catechin (Brand et al., 2007). The most stable conformer of compound **42** was calculated by molecular mechanics method and optimized with density functional theory. The distance between the epicatechin B-ring and the isopropenyl function was calculated as 2.420 Å, which could explain the presence of NOE correlation between protons of them (Figure 92). The spatial coupling between H-1 and H-11a was also rationalized by their calculated distance of 2.542 Å. Consequently, chemical structure of **42** was confirmed as shown in below figures, and it was named epicatechinoceanothic acid A.

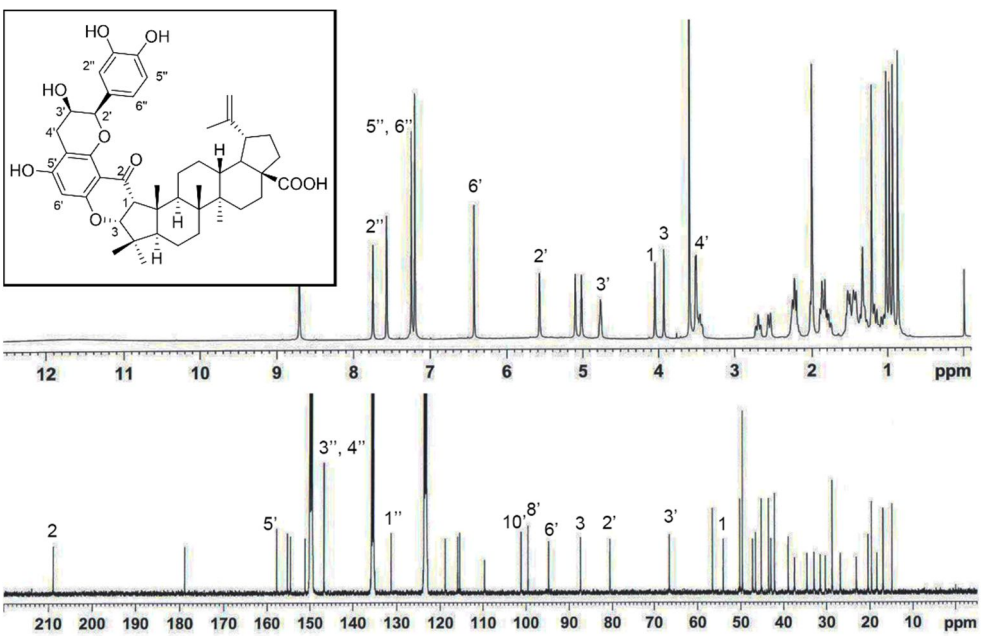

Figure 88. ^{1}H and ^{13}C NMR spectra of compound **42** (400 / 100 MHz, pyridine-d_5)

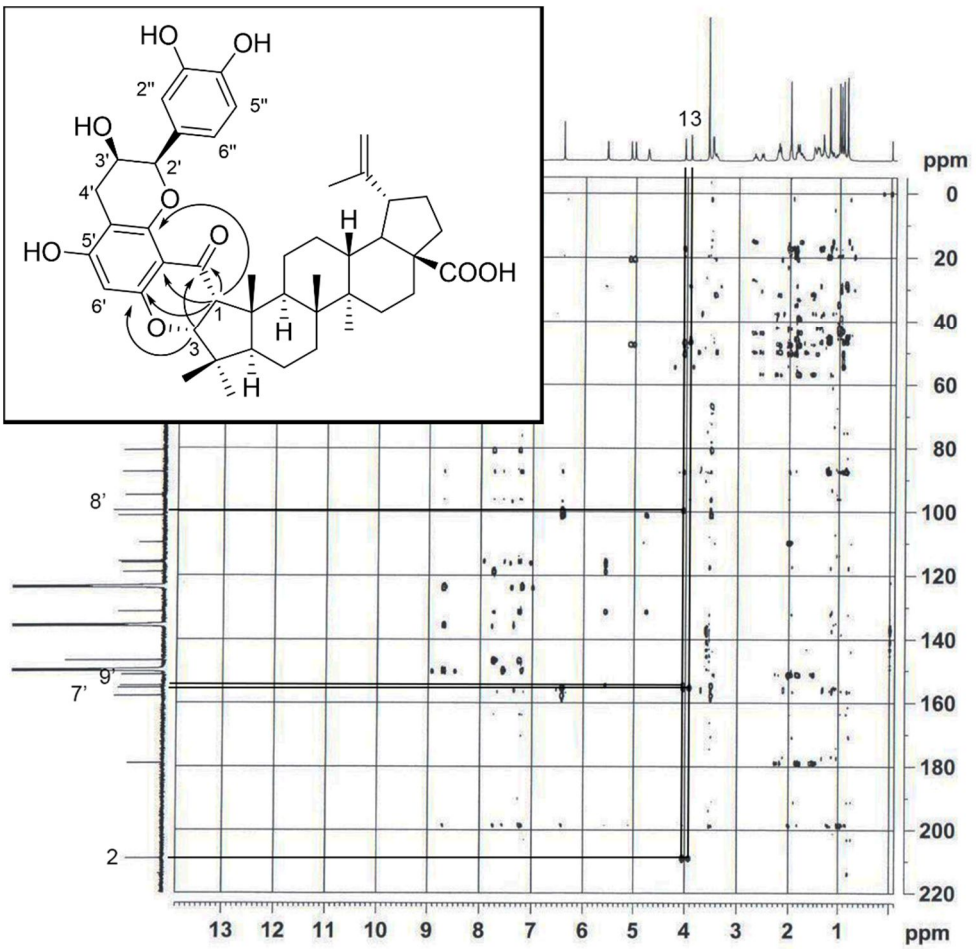

Figure 89. HMBC spectrum of compound **42** (400 MHz, pyridine-d_5)

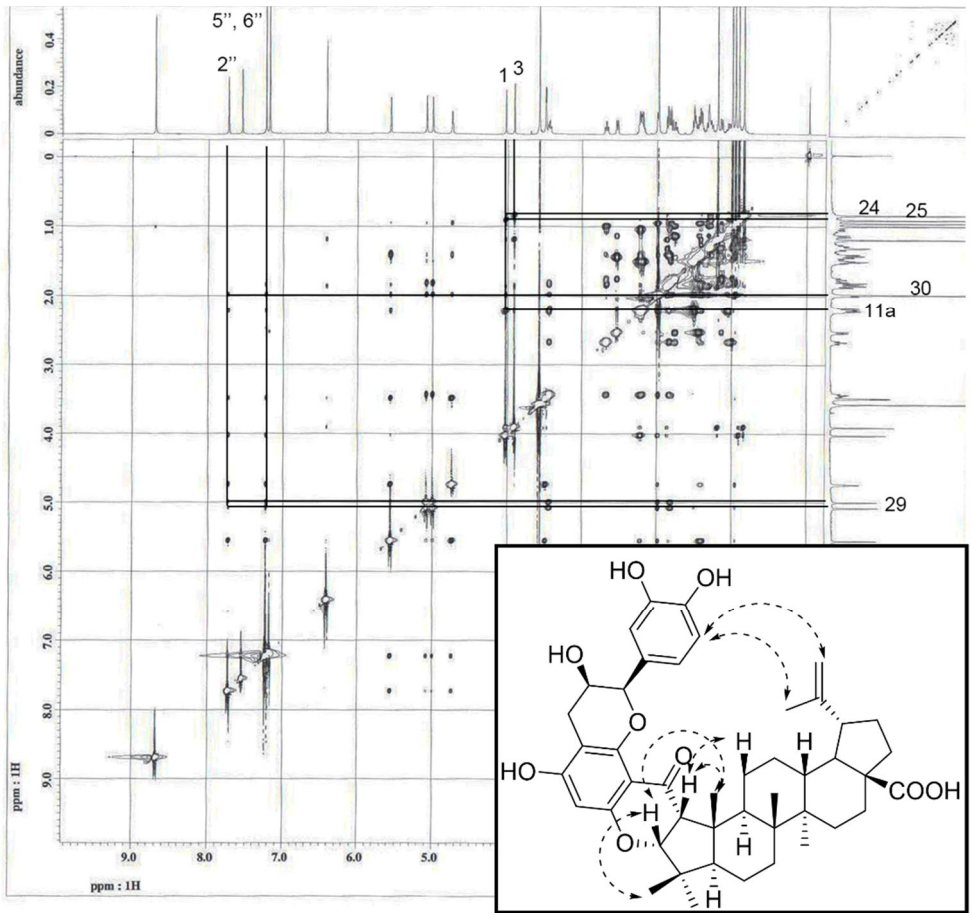

Figure 90. ROESY spectrum of compound **42** (400 MHz, pyridine-d_5)

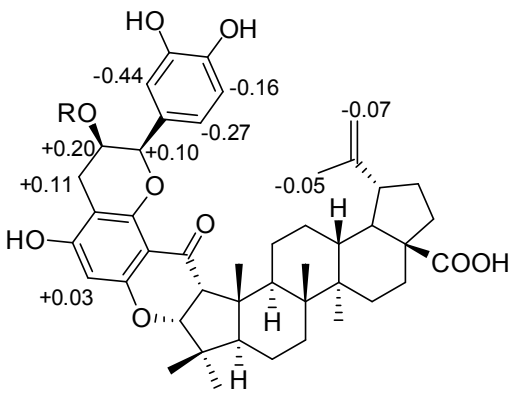

42a R = (S)-MTPA ester
42b R = (R)-MTPA ester

Figure 91. $\Delta\delta$ (δ_S-δ_R) values obtained from MTPA esters of compound **42**

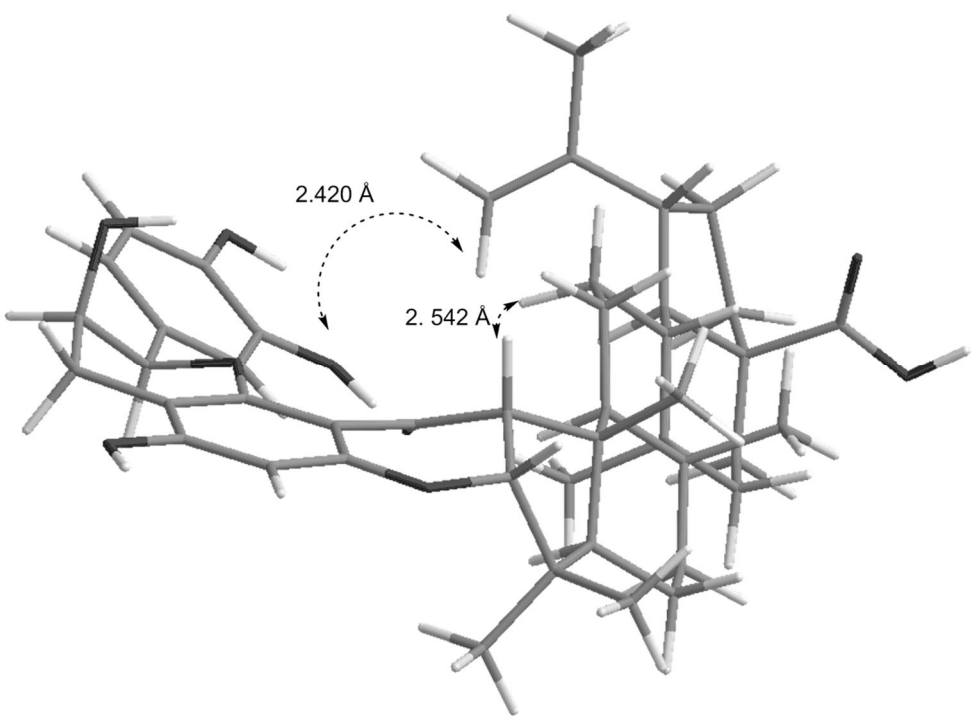

Figure 92. 3D structure of most stable conformer for compound **42**

3.3.21. Compounds **43** and **44**

Compound **43** was obtained as brown syrup. Its molecular formula $C_{45}H_{56}O_8$ was determined by ESI-qTOF-MS pseudo-molecular ion peaks at *m/z* 723.3892 $[M-H]^-$ (calcd. for $C_{45}H_{55}O_8$, 723.3897). ^1H and ^{13}C (which was deduced from the multiplicity-edited HSQC spectrum, because of scarce amount of **43**) spectra of **43** were similar to those of **42**, which indicated it is also a catechin-bound derivative of **14** (Figure 93). However, the ketone carbon signal was absent and a conjugated olefinic carbon was observed at δ_C 107.8 (C-2), instead. This carbon was coupling with an olefinic proton singlet at δ_H 6.99 (H-2) in me-HSQC spectrum. In HMBC spectrum of **43**, the olefinic proton exhibited correlations with carbons at δ_C 153.6 (C-8a′), 85.5 (C-3), and 45.5 (C-10), which suggested that this olefinic proton is H-2 (Figure 94). The HMBC cross-peak between the methyl singlet at δ_H 0.90 (H-25) and the other olefinic carbon at δ_C 146.0 (C-1) supported the presence of conjugated double bond between C-1 and C-2. Thus, compound **43** was confirmed to be a dehydrated derivative of **42**. The relative configuration at C-3 was confirmed by the ROESY experiment. H-3 exhibited spatial correlations with H-24 (δ_H 1.06) and H-25, which indicated β-orientation of H-3 (Figure 95). The *cis* orientation of H-2′ and H-3′ was assigned by their singlet coupling. However, trace amount of compound **43** did not allowed Mosher's method, so absolute configuration of **43** could not be determined. Compound **43** was named epicatechinoceanothic acid B.

Compound **44** was also isolated as brown syrup with molecular formula $C_{45}H_{56}O_8$, indicated by ESI-qTOF-MS (*m/z* 723.3892 $[M-H]^-$, calcd. for $C_{45}H_{55}O_8$, 723.3897). ^1H, me-HSQC (Figure 96) and HMBC (Figure 97) spectra of **44** were almost identical to those of **43**, so it was deduced that **44** has the same planar structure with **43**. However, in the ROESY spectrum, H-3 (δ_H 4.61, *s*) showed correlations with α-oriented H-5 (δ_H 1.37, *m*) and H-23 (δ_H 1.22, *s*), which proposed that compound **44** is a stereoisomer of **43** (Figure 98). Absolute configuration of **44** was

also unable to be confirmed because of scarce amount. Compound **44** was named epicatechinoceanothic acid C.

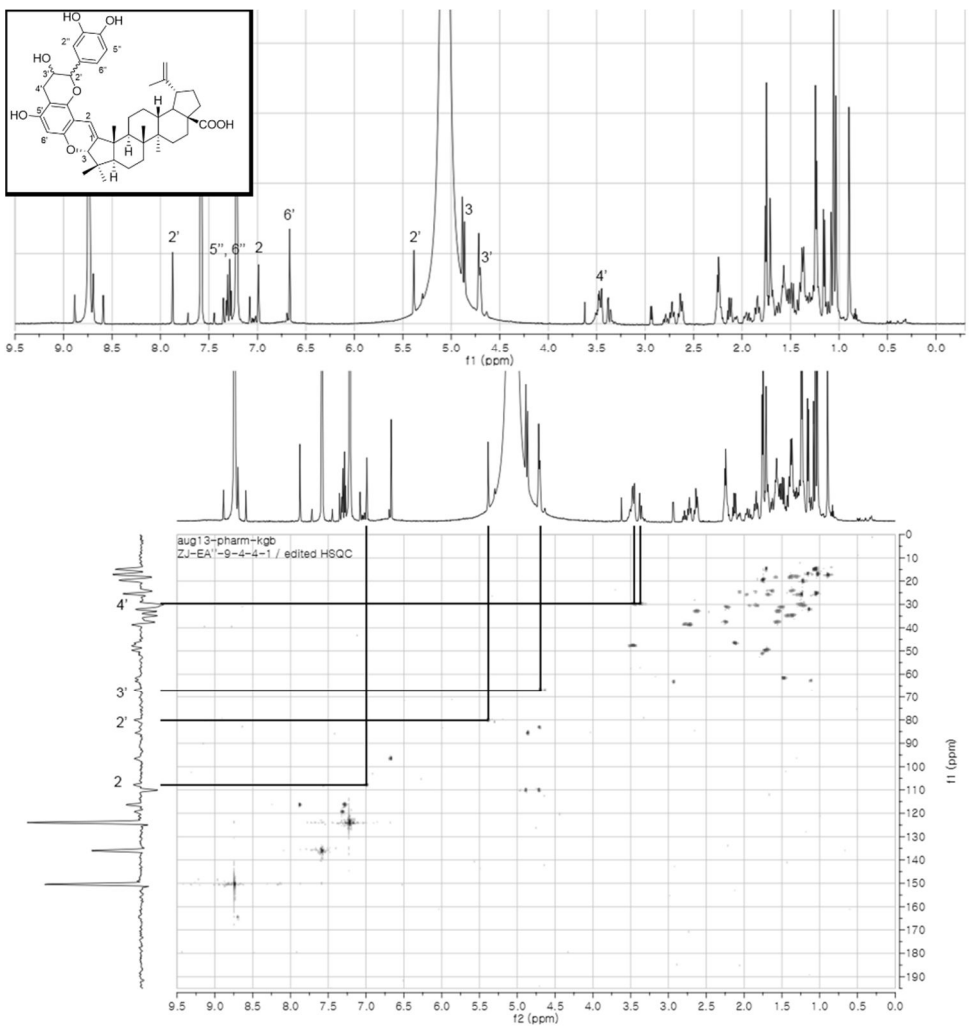

Figure 93. ^{1}H NMR and HSQC spectra of compound **43** (600MHz, pyridine-d_5)

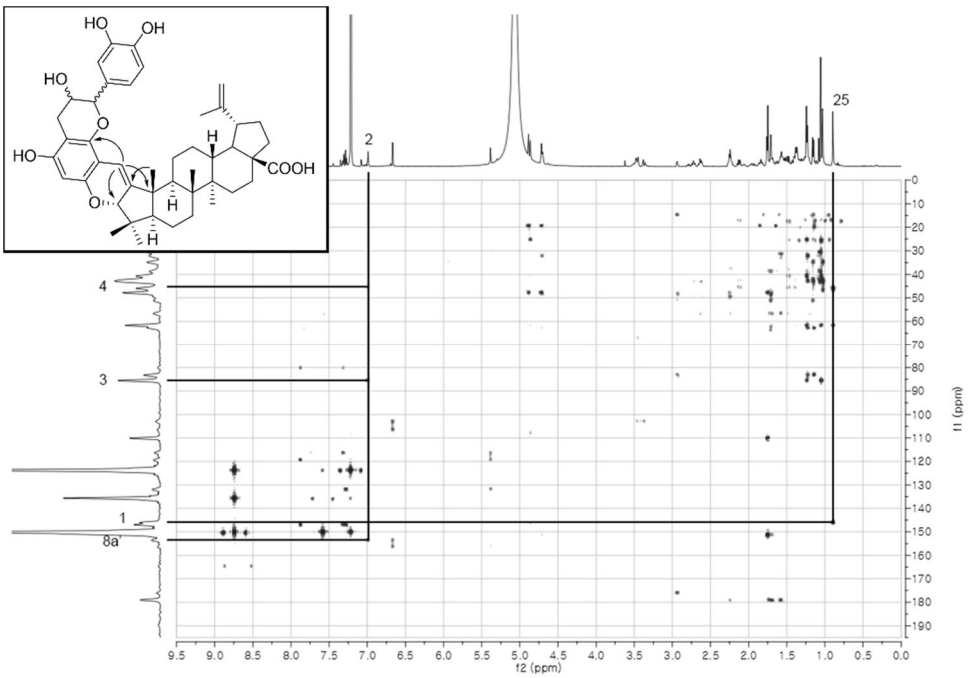

Figure 94. HMBC spectrum of compound **43** (600 MHz, pyridine-d_5)

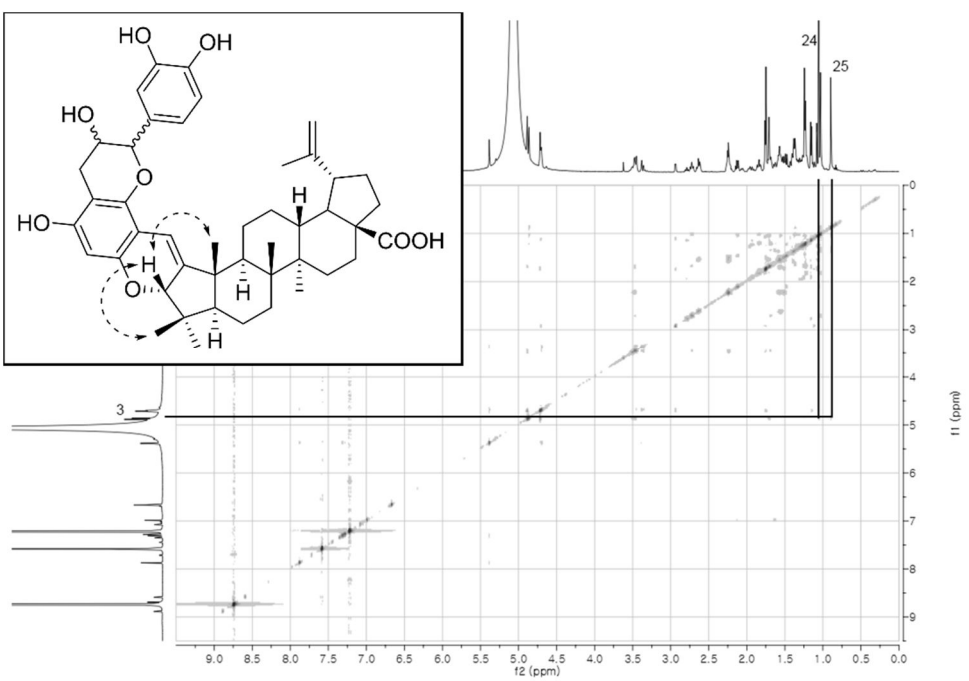

Figure 95. ROESY spectrum of compound **43** (600 MHz, pyridine-d_5)

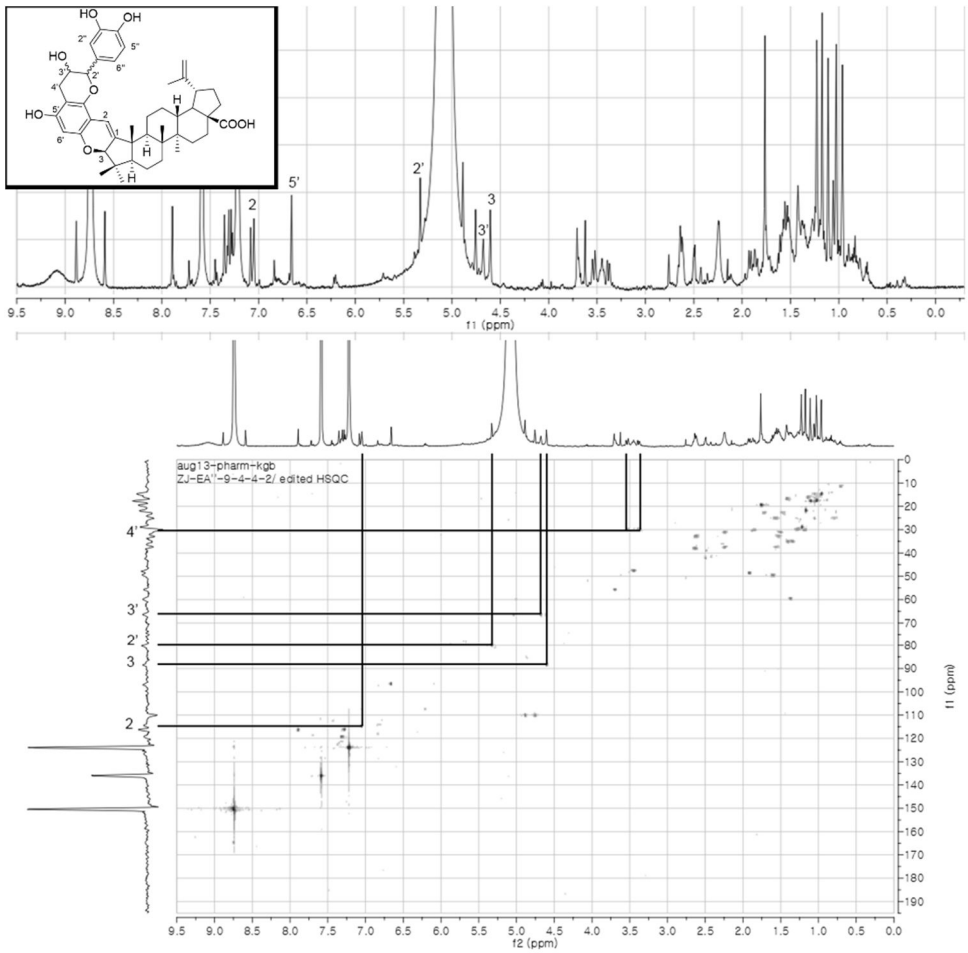

Figure 96. ^{1}H NMR and HSQC spectra of compound **44** (600 MHz, pyridine-d_5)

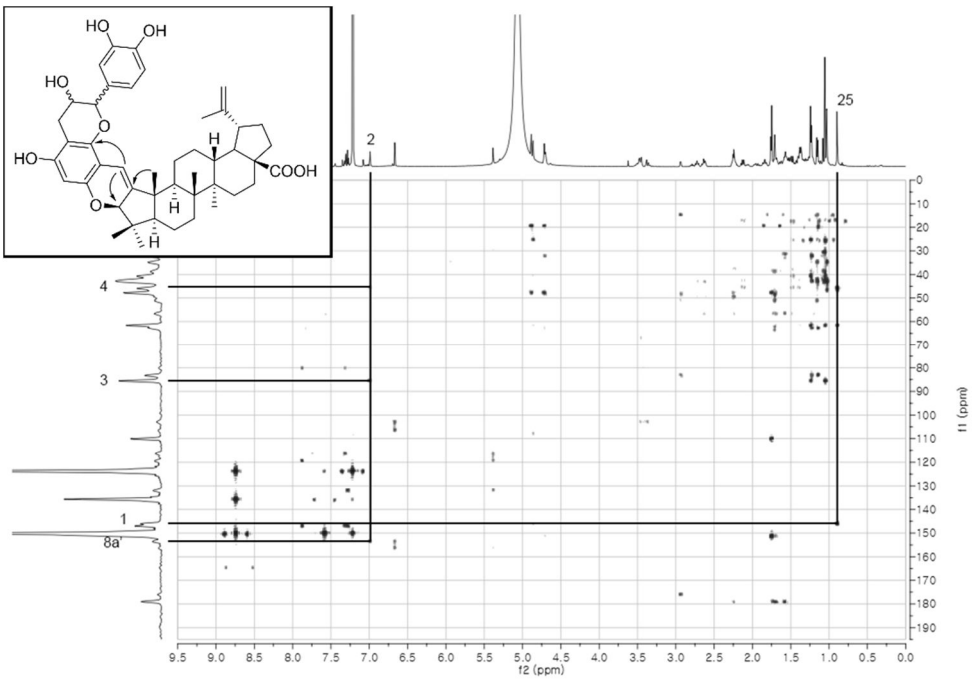

Figure 97. HMBC spectrum of compound **44** (600 MHz, pyridine-d_5)

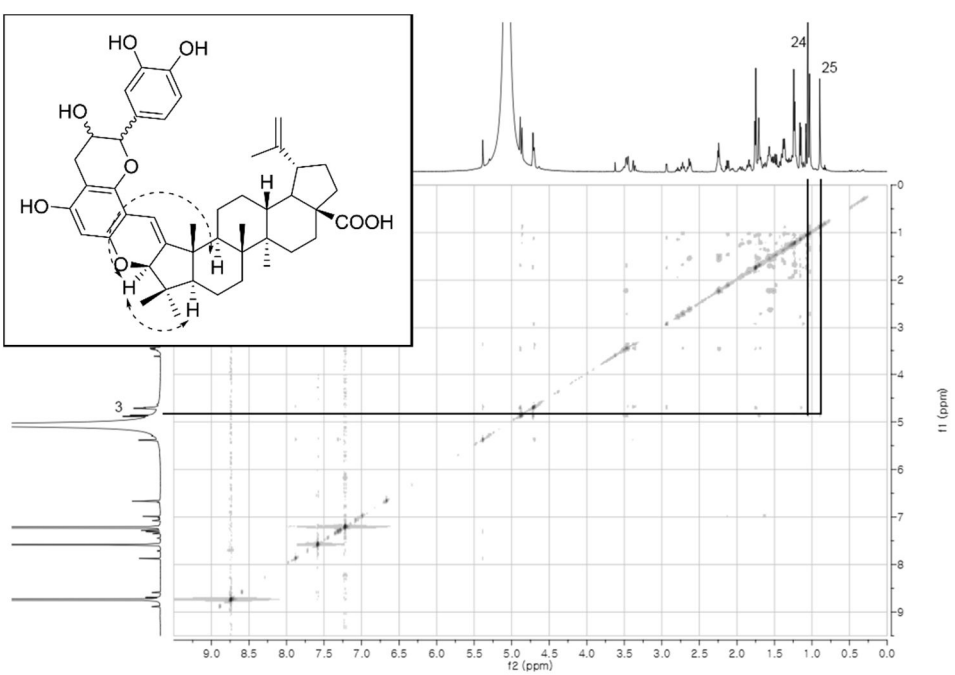

Figure 98. ROESY spectrum of compound **44** (600 MHz, pyridine-d_5)

3.3.22. Compounds **45** and **46**

Compound **45** was obtained as white amorphous powder. Its molecular formula, $C_{30}H_{48}O_4$ was established by ESI-qTOF-MS (*m/z* 471.3477 $[M-H]^-$ calcd. for $C_{30}H_{47}O_4$, 471.3477) and ^{13}C NMR spectrum. ^1H NMR spectrum of **45** displayed an olefinic proton at δ_H 5.49 (*t, J* = 3.4 Hz, H-12), two oxygenated methine protons at δ_H 4.12 (*dd, J* = 11.3, 4.5, H-2) and 3.42 (*d, J* = 9.4, H-3), and seven methyl singlets (Figure 99). These characters and the chemical shifts of two olefinic carbons at δ_C 145.3 and 122.9 suggested that compound **45** was Δ^{12} oleanane-type triterpene (Seebacher et al., 2003). The HMBC correlations indicated that two hydroxyl groups and a carboxyl group were existed at C-2, C-3, and C-28, respectively. On the basis of these spectral data and comparison with published literature, compound **45** was identified as maslinic acid (Taniguchi et al., 2002).

Compound **46** was isolated as white amorphous powder with molecular formula $C_{30}H_{48}O_5$, indicated by ESI-qTOF-MS (*m/z* 487.3417 $[M-H]^-$ calcd. for $C_{30}H_{47}O_5$, 487.3423). ^1H NMR spectrum of **46** displayed an olefinic proton at δ_H 5.56 (*br s,* H-12), two oxygenated methine protons at δ_H 4.31 (*td, J* = 3.0, 10.7, H-2) and 3.77 (*d, J* = 2.5, H-3), six methyl singlets, and one methyl doublet at δ_H 1.11 (*d, J* = 6.7, H-30) (Figure 100). The signals of ^{13}C NMR spectrum at δ_C 181.2 (C-28), 140.2 (C-13), 128.2 (C-12), 79.6 (C-3), 72.8 (C-19), and 66.4 (C-2) revealed the presence of a carboxylic carbon, two olefinic carbons, and three hydroxyl carbons, respectively. The presence of methyl doublet and chemical shifts of two olefinic carbons suggested that compound **46** is a Δ^{12} ursane-type triterpenic acid (Thuong et al., 2006). The HMBC correlations indicated that three hydroxyl groups and a carboxyl group were existed at C-2, C-3, C-19, and C-28, respectively. Coupling constants of H-3 (*J* = 2.5 Hz) indicated that hydroxyl moieties at C-2 and C-3 of **46** are oriented in the α-, α- position respectively, not the α-, β- position as 2α, 3β, 19α-trihydroxy-urs-12-en-28-oic acid (tormentic acid) (Taniguchi et al., 2002). Based on these spectral data with comparison to previously reported reference,

compound **46** was identified as euscaphic acid (Seto et al., 1984).

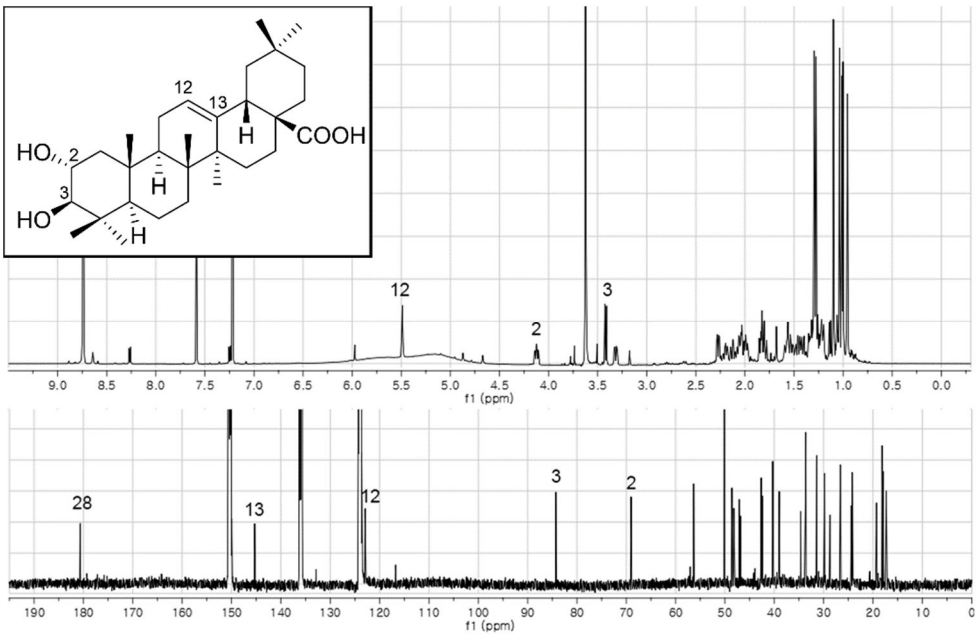

Figure 99. ^{1}H and ^{13}C NMR spectra of compound **45** (600 / 150 MHz, pyridine-d_5)

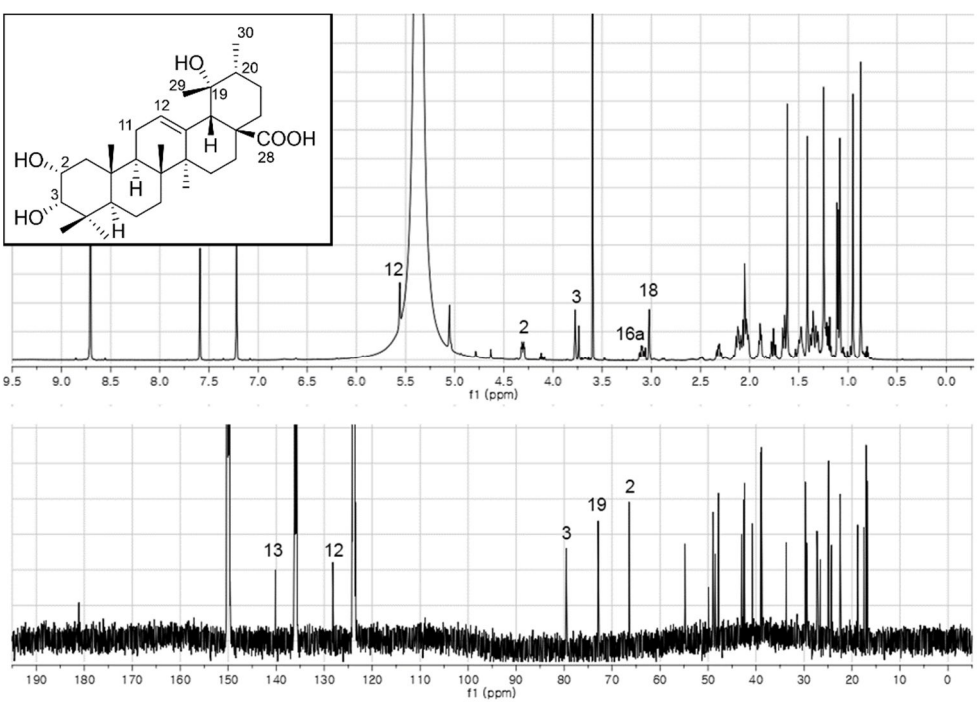

Figure 100. ^{1}H and ^{13}C NMR spectra of compound **46** (600 / 150 MHz, pyridine-d_5)

3.4. Structural identification of isolated phenolic compounds

3.4.1. Compounds **47** and **48**

Compound **47** was obtained as brown syrup, and its molecular formula $C_{15}H_{14}O_6$ was indicated by ESI-qTOF-MS 291.0870 $[M+H]^+$ (calcd. for $C_{15}H_{15}O_6$, 291.0868). In ^1H NMR spectrum of **47**, three aromatic protons at δ_H 6.88 (1H, *s*, H-2′), 6.65 (2H, *br s*, H-5′, H-6′), and two *meta* coupled aromatic protons at δ_H 5.89 (*d, J* =2.2 Hz, H-8) and 5.71 (*d, J* =2.2 Hz, H-6) were observed, which indicated **47** was a flavonoid-type compound (Figure 101). Protons at δ_H 4.71 (*s,* H-2), 3.98 (*br s,* H-3), 2.66 (*dd, J* =15.9, 4.0 Hz, H-4a), and 2.49 (*dd, J* =15.9, 4.0 Hz, H-4b) suggested 2,3-*cis* orientation of flavan-3-ol. Based on these spectral data, compound **47** was identified as (-)-epicatechin with comparison to published references (Agrawal et al., 1989).

Compound **48** was isolated as brown syrup. Molecular formula of **47** was also indicated as $C_{15}H_{14}O_6$ by ESI-qTOF-MS *m/z* 291.0870 $[M+H]^+$ (calcd. for $C_{15}H_{15}O_6$, 291.0868). ^1H and ^{13}C NMR spectra of **48** were similar to **47**, but coupling system of H-2, H-3, H-4 showed difference (Figure 102). Their proton signals were observed at δ_H 4.45 (*d, J* =7.5 Hz, H-2), 3.92 (*m,* H-3), 2.50 (*dd, J* =16.1, 5.5 Hz, H-4a), and 2.48 (*dd, J* =16.1, 5.5 Hz, H-4b), which proposed 2,3-*trans* orientation of flavan-3-ol. By these spectra data and comparison with the previously reported publication, compound **48** was identified to be (+)-catechin (Agrawal et al., 1989).

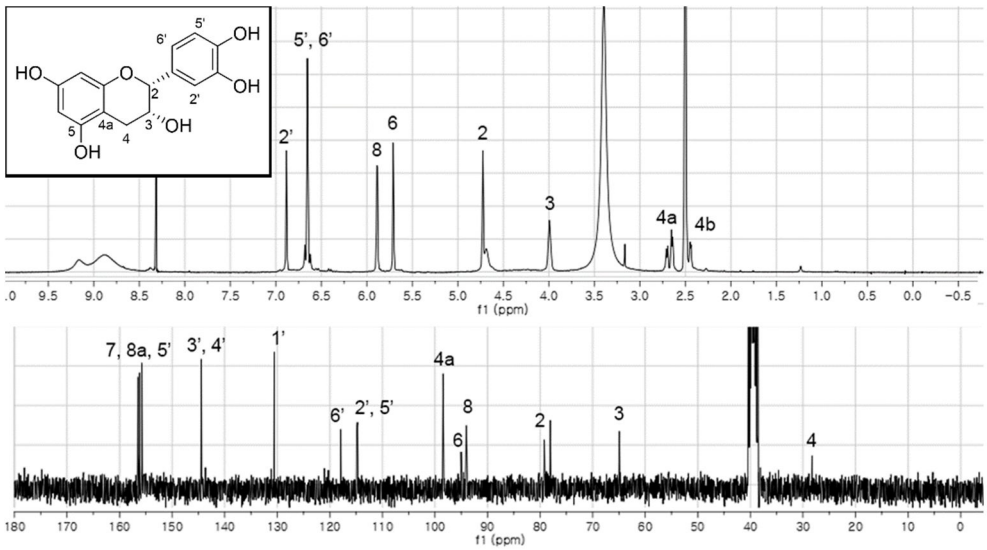

Figure 101. ^{1}H and ^{13}C NMR spectra of compound **47** (300 / 75 MHz, DMSO-d_6)

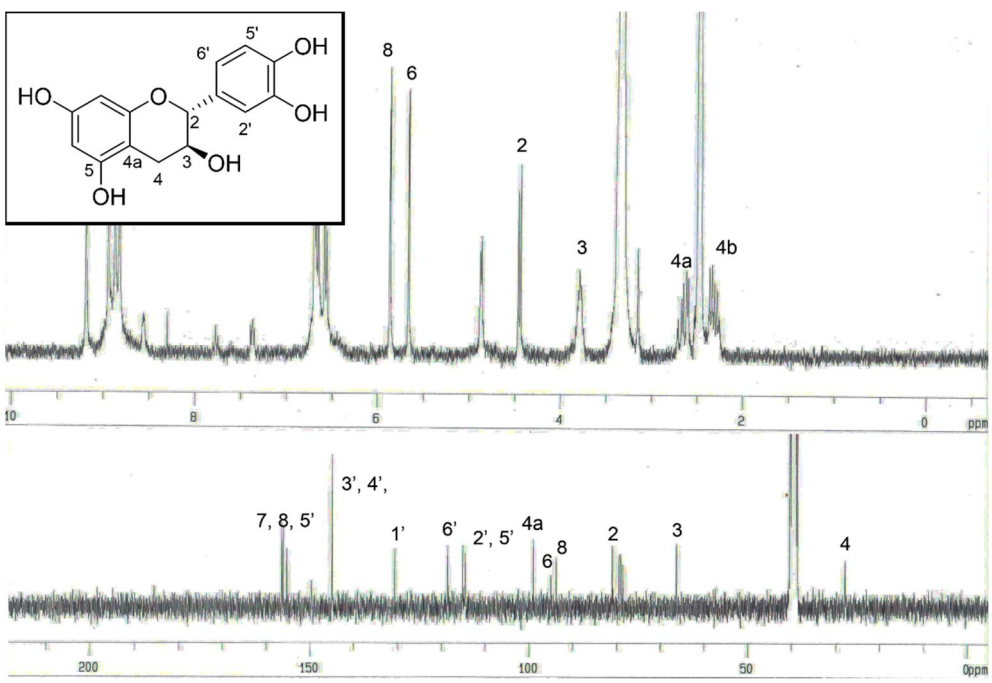

Figure 102. ^{1}H and ^{13}C NMR spectra of compound **48** (300 / 75 MHz, DMSO-d_6)

3.4.2. Compound **49**

Compound **49** was purified as white amorphous powder. Its ESI-qTOF-MS pseudo-molecular peak at *m/z* 167.0347 $[M-H]^-$ (calcd. for $C_8H_7O_4$, 167.0344) indicated the molecular formula of **49** as $C_8H_8O_4$. In ^1H NMR spectrum of compound **49**, three aromatic protons at δ_H 8.17 (*dd, J* = 8.1, 1.8 Hz, H-6), 8.08 (*d, J* = 1.8 Hz, H-2), and 7.31 (*d, J* = 8.1 Hz, H-5), and a methoxy singlet at δ_H 3.74 were observed (Figure 103). From these spectral data, compound 49 was identified as 3-methoxy-4-hydroxybenzoic acid, or vanillic acid (Yang et al., 2015).

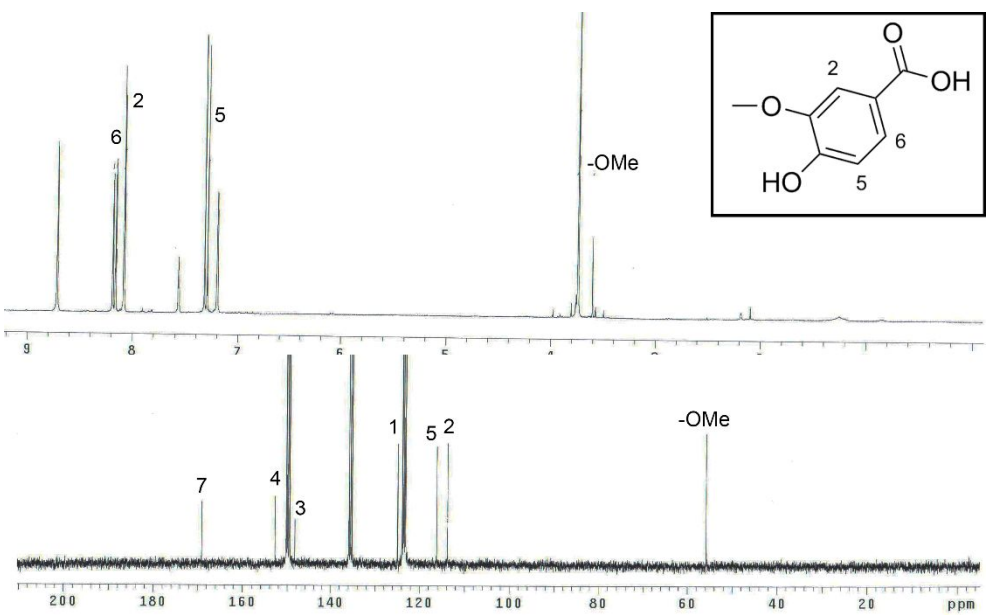

Figure 103. ^1H and ^{13}C NMR spectra of compound **49** (300 / 75 MHz, pyridine-d_5)

3.4.3. Compound **50**

Compound **50** was isolated as brown syrup. The molecular formula was determined to be $C_{21}H_{24}O_{11}$ from the ESI-qTOF-MS pseudo-molecular peak at *m/z* 451.1240 $[M-H]^-$ (calcd. For $C_{21}H_{23}O_{11}$, 451.1240). In ^1H NMR spectrum of **50**, two set of aromatic protons [δ_H 7.55 (*dd, J* = 8.2, 2.9 Hz, H-6″), 7.52 (*d, J* = 2.9 Hz, H-2″), 6.84 (*d*, *J* = 8.2 Hz, H-5″), *6*.92 (*d*, *J* = 8.7 Hz, H-6), 6.42 (*d*, *J* = 2.7 Hz, H-3),and 6.11 (*dd*, *J* = 8.2, 2.7 Hz, H-5)], two methoxy singlets at δ_H 3.77 (2-OCH_3), and 3.85 (3″-OCH_3), and one glucopyranose moiety (Figure 104). The glucose unit was determined to be attached to C-1 of the phenolic unit by the HMBC cross-peak between H-1′ (δ_H 4.70, *m*) and C-1 (δ_C 141.6). The HMBC experiment additionally confirmed positions of two methoxy, which indicated presences of a vanilloyl moiety and a 2-methoxy-4-hydroxyphenyl moiety. The attachment of the vanilloyl group to the C-6′ position was also confirmed by the HMBC correlations of H-6′a (δ_H 4.65, *dd, J* = 11.8, 6.9 Hz)/H-6′b (δ_H 4.35, *m*) and C-7″ (δ_C 168.8). Thus, compound **50** was identified as 6′-*O*-vanilloylisotachioside (Yang et al., 2007).

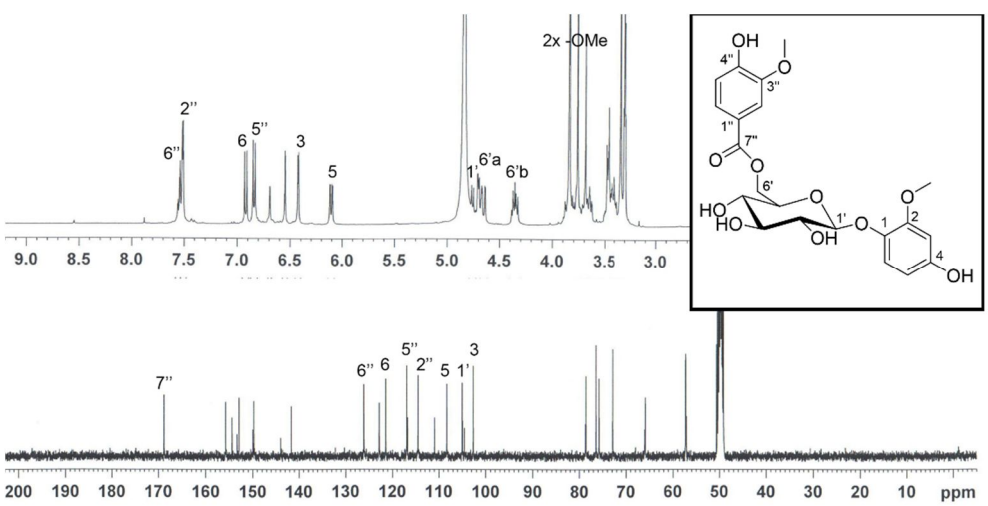

Figure 104. ^1H and ^{13}C NMR spectra of compound **50** (400 / 100 MHz, MeOD)

3.4.4. Compounds **51** and **52**

Compounds **51** and **52** were isolated as yellow syrup, in inseparable mixture. Their molecular formula were determined to be $C_{18}H_{14}O_7$ for both, by ESI-qTOF-MS (*m/z* 343.0819 $[M+H]^+$, calcd. for $C_{18}H_{15}O_7$, 343.0817), In ^1H and ^{13}C NMR spectra, it was supposed that this was a 3:1 mixture of two compounds of which chemical structures were similar, so the major compound, **51**, was identified first (Figure 105). Its ^1H NMR spectrum was similar to one of **48**, but there were additionally two conjugated olefinic protons at δ_H 8.12 (*d*, *J* = 9.5 Hz, H-10) and 6.08 (*d*, *J* = 9.5 Hz, H-9), and one of *meta*-coupling protons was absent. From these, compound **51** was deduced to be one of regioisomers of phyllocoumarin. In the HMBC spectrum, the singlet at δ_H 6.34 was assigned to be H-6 from the correlations with C-5, C-7, C-8 and C-4a, and the position of the pyranone moiety was deduced from correlations of H-9/C-7 and H-10/C-8. On the other hand, the singlet of the minor compound **52**, at δ_H 6.32, showed HMBC correlations with C-5, C-6, C-4a, and C-8a, and H-9 showed with C-5, and H-10 with C-6. Based on these spectral data and comparison with previously reported reference, compound **51** was identified as epiphyllocoumarin, while **52** was isoepiphyllocoumarin (Tang et al., 2013).

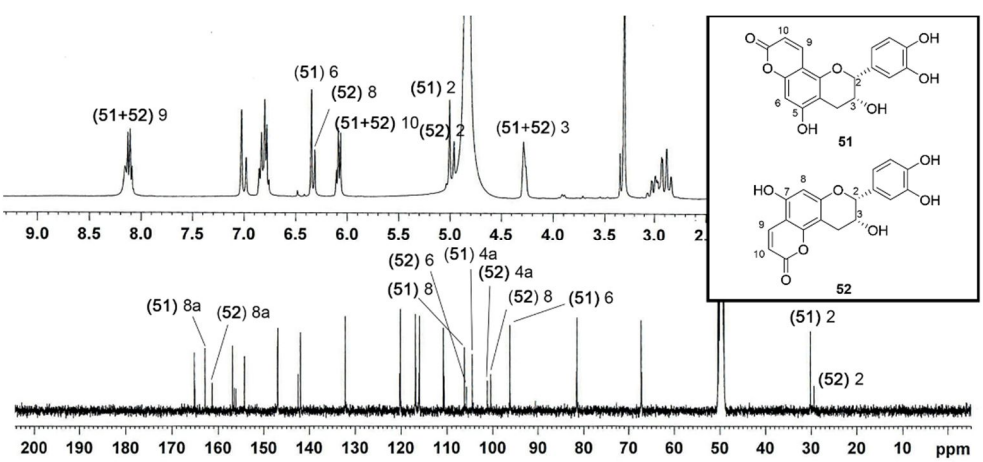

Figure 105. ^1H and ^{13}C NMR spectra of the mixture **51**/**52** (300 / 75 MHz, MeOD)

Chapter 4. Bioactivity of Isolated Compounds

4.1. Antiviral activity of isolated cyclopeptide alkaloids

Bioactivity of isolated type-Ib cyclopeptide alkaloids were evaluated. As mentioned in chapter 1, several cyclopeptide alkaloids have been reported to exhibit antibacterial, antifungal, antiplasmodial, antimycobacterial, and antimalarial effects. In the process of bioactivity screening, some of isolated cyclopeptide alkaloids have shown antiviral effect to porcine epidemic diarrhea virus (PEDV). PEDV infection in pigs causes epidemic diarrhea, dehydration, and vomiting. Most newborn piglets infected by PEDV would be dying with almost 100% mortality and pigs of all ages are also affected. Infection with this virus has caused a serious economic loss in the swine industry and recent outbreaks led to serious economic losses in many swine producing countries. Only compounds **1**, **2**, **3**, and **6** were screened for their antiviral potential against PEDV, due to the scarce amounts of other type-Ib cyclopeptide alkaloids. Compounds **2**, **3**, and **6** showed potent inhibitory effects on PEDV infected Vero cells, as shown in Table 5. Compounds **3** and **6** showed EC_{50} values at the micromolar range (EC_{50} 4.49 ± 0.67 and 6.17 ± 0.50 μM, respectively), which was potent as compared to 6-azauridine, the positive control (5.58 ± 0.53 μM). However, both compounds showed much lower cytotoxicity (CC_{50} 211.26 ± 29.64 and 165.30 ± 16.49 μM, respectively) compared to the positive control (44.47 ± 6.11 μM), so they had higher selective index (SI) values (47.11 ± 0.49 and 26.75 ± 0.54 respectively) than 6-azauridine (7.98 ± 0.37). Compound **2** showed lower potency than **3** and **6** (EC_{50} 13.41 ± 1.13 mM), but **2** also demonstrated high SI values because of the very low cytotoxicity (CC_{50} > 400 μM). To the author's knowledge, this is the first report on the antiviral activities of cyclopeptide alkaloids.

Table 5. Inhibitory effects on PEDV replication of compounds **1**, **2**, **3**, and **6**

Compounds	CC_{50} (μM)	EC_{50} (μM)	SI
1	> 400	N.A.	
2	> 400	13.41 ± 1.13	> 30.04 ± 2.74
3	211.26 ± 29.64	4.49 ± 0.67	47.11 ± 0.49
6	165.30 ± 16.49	6.17 ± 0.50	26.75 ± 0.54
6-Azauridine [a]	44.47 ± 6.11	5.58 ± 0.53	7.98 ± 0.37

[a] positive control.

4.2. Cytotoxicity of isolated triterpenoids against human liver hepatocellular carcinoma HepG2 cell line

As written in chapter 1.1.3, cytotoxicity against cancer cells is one of the most important bioactive potentials of ceanothane-type triterpenoids. Cytotoxicity of isolated triterpenoids against human hepatocarcinoma HepG2 cell line were evaluated *in vitro*. Among 37 isolated triterpenoids, compounds **10**, **11**, **14-22**, **25**, **28-37**, and **41** were treated to human hepatocarcinoma HepG2 cells, and the survival rates were measured using the MTT method (Mosmann, 1983). The result showed that compound **10** exhibited cytotoxicity against HepG2 with IC_{50} value of 5.87 μM while 5-flurouracil, a widely used anticancer agent, showed IC_{50} value of 45.41 μM, as already reported in other references (Fu et al., 2005; Zhang et al., 2015). Its 2-hydroxy derivative compound **11** did not exhibit cytotoxicity, but 2-*O*-aromatic ester derivatives of **11**, compounds **28-30,** showed more potent cytotoxicity (IC_{50} 1.97 - 2.92 μM) than compound **10** as shown in Table 6. The coumaroyl moiety at the C-3 position has been already known to have an important role for enhancing cytotoxicity of lupane-type triterpenoids (Lee et al., 2003). Our results suggested that aromatic ester substitutes at A-ring could enhance cytotoxicity of lupane-type triterpenoids regardless of their position. Most of ceanothane-type triterpenoids did not exhibit cytotoxicity against HepG2 cells, but aromatic ester derivatives with 2-methyl ester, compounds **33**, **36**, and **41** were cytotoxic to HepG2 cell lines. Compound **35** showed cytotoxicity without the presence of 2-methyl ester, while its epimeric compound **34** was not cytotoxic. Compound **22**, which have an unsaturated A-ring, was also cytotoxic to HepG2 cells, as Arai et al. and Ji et al. already reported (Arai et al., 2008; Ji et al., 2012).

Table 6. Cytotoxicity of isolated triterpenoids against HepG2 cell line

Compounds	IC_{50} (μM)	Compounds	IC_{50} (μM)
10	5.87	**33**	2.84
22	1.98	**35**	3.88
28	1.97	**36**	1.93
29	2.13	**41**	9.24
30	2.92	5-fluorouracil [a]	45.41

[a] positive control. Compounds **11**, **14-21**, **25**, **31**, **32**, **34**, **37** showed IC_{50} > 10 μM

Chapter 5. Experimental Section

5.1. Materials

5.1.1. Plant materials

Roots, twigs, leaves, and fruits of *Z. jujuba* which were used for LC-MS profiling were collected in the Herbarium of the medicinal Plant Garden, College of Pharmacy, Seoul National University, Koyang, Korea, in October 2011. *Z. jujuba* roots for macro-scaled isolations were collected in Jinju, Korea, in Apirl 2012. It was authenticated by Prof. Dr. Eun Ju Jeong (Gyeongnam National University of Science and Technology, Jinju, Korea). A voucher specimen (SUPH-1204-01) is deposited in the Herbarium of the Medicinal Plant Garden.

5.1.2. Reagents

Column chromatography was carried out with Kieselgel 60 silica gel (40–60 μm, 230–400 mesh, Merck, Darmstadt, Germany) and Sephadex LH-20 (25–100 μm, Pharmacia, Piscataway, NJ, USA). First grade solvents for extraction, fractionation, and isolation, and HPLC grade solvents were purchased from Dae Jung Pure chemical Eng. Co. Ltd., Korea. Advanced Marfey's reagent (D-FDLA and L-FDLA) and GITC were purchased from Tokyo Chemical Industry Co. Ltd. (Tokyo, Japan). The (*S*)-(+)-Phenylglycine methyl ester hydrochloride [(*S*)-(+)-PGME] reagent was purchased from Sigma–Aldrich (St. Louis, MO, USA). Dulbecco's Modified Eagle's Medium (DMEM) and fetal bovine serum (FBS) were purchased from Hyclone (Logan, UT, USA). Penicillin and streptomycin were purchased from Sigma-Aldrich.

5.1.3. Equipment

Analytical balance: Mettler AE50, Switzerland

Autoclave: Sanyo MLS 3000, Japan

Centrifuge: Effendroff centrifuge 5810, Germany

Circular dichroism: Chirascan CD Spectometer, UK

Elisa reader: Molecular Devices E_{max}, USA

Evaporator: EYELA NE, Japan

Freeze-dryer: Operon FDCF-12012

HPLC for analysis of amino acid derivatives:

Agilent 6120 quadruple MSD equipped with

1260 Infinity pump

1260 Infinity autosampler

1260 Infinity PDA detector (Agilent Technologies, Santa Clara, CA, USA)

Phenomenex column (Luna 5μ C18 (2) 100 Å New Column, 4.6 mm × 100 mm, 5 μm, Sungmoon Systech Co. Ltd., Seoul, Korea)

Openlab ChemStation (Agilent) for data acquisition and processing.

Infared spectrometer: JASCO FT/IR-4200, USA

Melting Point apparatus: Buchi B-545, Germany

NMR: JEOL JMN-LA300 Spectrometer, Japan

Bruker GPX 400 Spectrometer, Germany

Bruker AVANCE 500 Spectrometer, Germany

Bruker AMX 500 Spectrometer, Germany

Bruker AVANCE 600 Spectrometer coupled with cryoprobe, Germany

Bruker AMX 600 Spectrometer, Germany

pH meter: Phoenix PMS-500, USA

Polarimeter: JASCO P-2000, USA

Preparative HPLC:

1) Waters Delta Prep system coupled with Waters 2489 UV/vis detector,

USA

2) Gilson 321 Pump and UV/Vis-151 detector, USA

3) Waters 600 Pump coupled with Waters 486 tunable absorbance detector and Hitachi D-2500 chromato-integrator

UHPLC-ESI-qTOF-MS system:

Waters Xevo G2 qTOF mass spectrometer (Waters MS Technologies, Manchester, UK) equipped with Waters BEH C18 (100 × 2.1 mm, 1.7μm, Waters, Milford, MA, USA) column and MassLynx SCN 855 software for data acquisition and processing

Ultrasonicator: Branson 5210, UK

5.2. UHPLC-qTOF-MS analysis for cyclopeptide alkaloids

For preparation of crude MeOH extracts of roots, twigs, leaves, and fruits of *Z. jujuba,* 30.0 g of each plant part samples were macerated with MeOH (500 mL for 5 days) at rt. Crude extracts were evaporated *in vacuo* for the removal of MeOH, then their weights were measured to be 1.4 g, 0.9 g, 2.5 g, and 4.1 g, respectively. Extracts were suspended in H_2O and acidified with 1 N HCl to pH 3–4. The acidic solutions were firstly extracted with EtOAc to remove other hydrophobic metabolites, then the aqueous residues were basified with NaOH to pH 9–10. The basic solutions were extracted with $CHCl_3$ to provide alkaloid fractions of extracts. These alkaloid fractions were prepared to be 5 mg/mL in 50% aqueous MeOH, and were analyzed by UHPLC-qTOF-MS equipped with ACQUITY BEH C18 column (100 mm × 2.1 mm, 1.7 μm). The mobile phase was composed of A (H_2O) and B (MeCN), each containing 10 mM ammonium formate. A gradient (10 – 65% B) was carried out in 20.0 min, followed by an increase of B from 65% to 95% in 0.1 min, a 5.0 min isocratic step at 95% B, a decrease of B from 95% to 10% in 0.1 min, and a second 10.0 min isocratic step at 10% B for column reconditioning. The flow rate of the mobile phase was 0.3 mL/min and the column temperature was maintained at 25 °C. Analysis of each sample (2.0 μL injected in the partial loop with needle overfill mode) were performed in positive ion modes in the 100-1500 Da range with acquisition times of 0.3 seconds in the centroid mode. The ESI conditions were set as follows: capillary voltage 2500 V, con voltage 45 V, source temperature 120 °C, desolvation temperature 300 °C, cone gas flow 50 L/h, desolvation gas flow 800 L/h. MS^E methodology (Lecompte et al., 2014) was applied for MS/MS fragmentation pattern analysis. Low collision energy was set to 4V, while high collision energy ramp was set to 40 to 45 V.

5.3. Isolation of cyclopeptide alkaloids

Powdered dried roots of *Z. jujuba* (14.5 kg) were extracted through maceration with MeOH (2 × 60 L, for one week each) at rt. A crude extract (0.5 kg) resulted from extraction solvent removal *in vacuo*. The extract was fractionated with the acid-base method, as described in section 5.2, to yield the acidic EtOAc fraction (186.2 g) and the alkaloid fraction (1.7 g) (Scheme 4). The alkaloid fraction was subjected to silica gel column chromatography (CC) eluted with increasingly polar $CHCl_3$–MeOH mixture (30:1, 10:1, 5:1, 3:1 and 1:1) to yield four fractions (A1–4). Fraction A3 was further separated on Sephadex LH-20 eluted with CH_2Cl_2–MeOH (3:1) to give five subfractions (A3a–A3e). Compounds **4** (2.7 mg), **5** (2.0 mg), **7** (1.6 mg), **8** (2.0 mg), and **9** (25.1 mg) were purified by ODS silica gel HPLC eluted with 0.1% NH4Ac in 50% aqueous MeCN, while Compounds **1** (7.8 mg), **2** (53.1 mg), **3** (6.9 mg), and **6** (13.5 mg) were isolated by ODS silica gel HPLC eluted with 0.1% NH4Ac in 30% aqueous MeCN (Scheme 5).

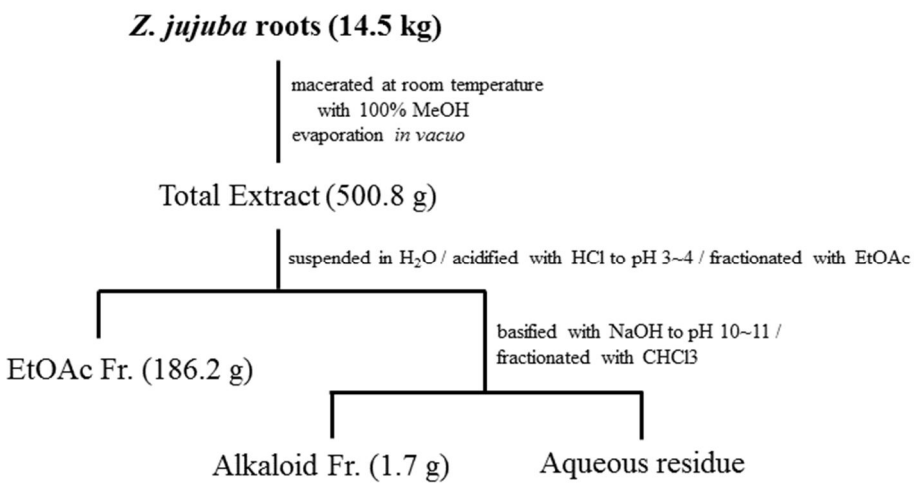

Scheme 4. Extraction and acid-base fractionation for isolation of cyclopeptide alkaloids

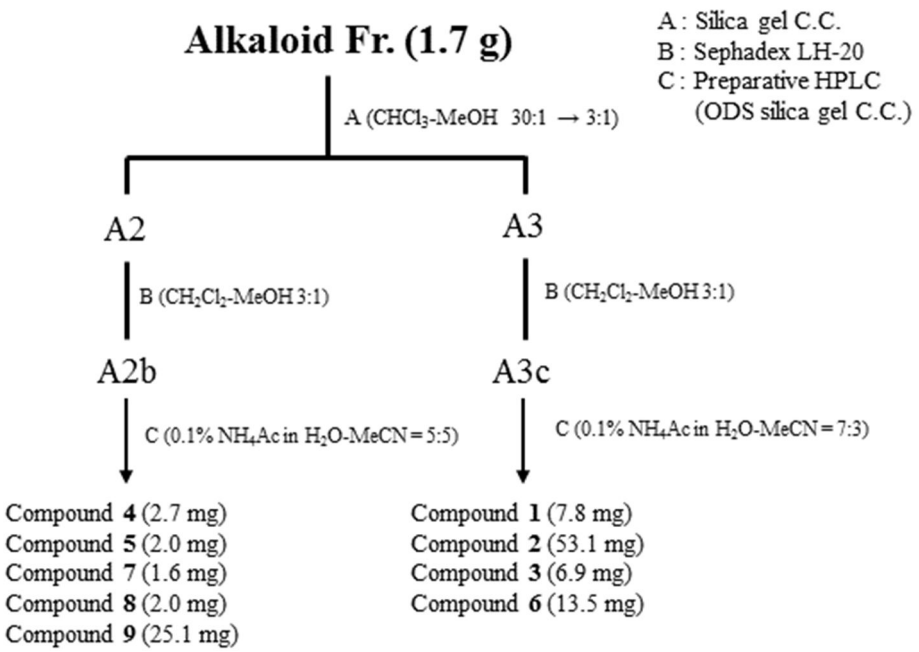

Scheme 5. Isolation of cyclopeptide alkaloids from alkaloids fraction of *Z. jujuba* roots MeOH extract

5.4. Acid hydrolysis of compounds **1-5**

Approximately 0.2 mg of **1**–**3** and 0.1 mg of **4**–**5** were hydrolyzed with 6 N HCl (100 μL) at 110 °C for 30 min with stirring. The hydrolysates were evaporated to dryness and then the dried hydrolysates were resuspended in H_2O (100 μL). The solutions were concentrated under reduced pressure.

5.4.1. Determining absolute configurations of the amino acids in compounds **1-5** by the advanced Marfey's method

Each hydrolysate (30 μg) was added to 1 M $NaHCO_3$ (200 μL) and 1% D- or L-FDLA in acetone (25 μL). The reaction vials were incubated and stirred for 30 min at 50 °C. The reactions were then quenched with 2 N HCl (100 μL). MeOH (100 μL) was added to prepare LC–MS samples. The reaction products were analyzed by HPLC–MS with a positive ion detection mode. H_2O-MeCN containing 0.05% HCO_2H was used as eluents with MeCN containing 0.05% HCO_2H increasing from 5% to 100% over 19 min at a flow rate of 0.7 mL/min. Authentic standards (200 μg) were also prepared and analyzed using the same procedure. The retention times of the hydrolysates and amino acid standard D and L-FDLA-derivatives were as follows: L-Val-D-FDLA (t_R 13.51 min, *m/z* 412 $[M+H]^+$), L-Val-L-FDLA (t_R 12.04 min, *m/z* 412 $[M+H]^+$), L-*N*-Me-Ala-L-FDLA (t_R 11.92 min, *m/z* 398 $[M+H]^+$), L-*N*-Me-Ala-D-FDLA (t_R 12.05 min, *m/z* 398 $[M+H]^+$), L-Ile/L-*allo*-Ile-L-FDLA (t_R 12.62 min, *m/z* 426 $[M+H]^+$), and L-Ile/L-*allo*-Ile-D-FDLA (t_R 14.04 min, *m/z* 426 $[M+H]^+$).

5.4.2. Determining absolute configurations of the amino acids in compounds **2-5** by GITC analysis

Each hydrolysate (30 μg) was treated with 6% trimethylamine (40 μL) and 1% GITC reagent (40 μL). After 30 min of incubation at rt, 5% acetic acid (40 μL) was added to a reaction vial to quench the reaction. MeOH (50 μL) was added to the reaction residues to prepare LC–MS samples. An authentic standard was also prepared from the same procedure. For the GITC product analysis of natural hydrolysates and standard amino acids, the following chromatographic method was used: solvent A was H_2O-MeCN with 0.1% HCO_2H (95:5, v/v), solvent B was MeCN with 0.1% HCO_2H. The LC–MS program for detecting the GITC-derivatives was set as 5% solvent B (0–7 min), 5–27% solvent B (7–12 min), 27–28.5% solvent B (12–45 min), 28.5–100% solvent B (45–46 min), and 100–100% solvent B (46–51 min) at a flow rate of 1 mL/min. The reaction products were analyzed on a positive mode with a LC–MS system. The co-injection experiments of the GITC-derivatized hydrolysates with authentic amino acid derivatives (L-Ile and L-*allo*-Ile) were established so that Ile residues in 2–5 are all L-Ile (Retention time: L-Ile-GITC (33.67 min)/L-*allo*-Ile-GITC (33.31 min)).

5.4.3. Preparing L- and D-*N,N*-dimethylalanine (Choi et al., 2012)

The L and D-alanine (8.0 mg) standards in H_2O were individually treated with HCHO (27 μL) and 10% Pd/C (10.4 mg). The mixtures were subjected to H_2 for 16 h and each reaction mixture was boiled and then dried under reduced pressure.

5.4.4. Determining absolute configurations of *N,N*-dimethylalanine in compounds **4** and **5** by PGME derivatization

Each dried L- and D-*N,N*-dimethylalanine was dissolved in tetrahydrofuran (THF,

500 μL). After adding 1-(3-dimethylaminopropyl)-3-ethylcarbodiimide (EDC, 8.8 μL) to each vial, each mixture was stored at rt and stirred for 5 min. (*S*)-(+)-PGME (10.5 mg) was added to each vial and each mixture was stirred for 6 h at rt. The reaction products were dried under N_2 gas and extracted with CH_2Cl_2. The CH_2Cl_2 soluble products were analyzed by LC–MS [same column but 150 mm length instead of 100 mm; solvent A was H_2O:MeCN with 0.05% HCO_2H (95:5, v/v), solvent B was MeCN with 0.05% HCO_2H with gradient solvent system as follows: 5% solvent B (0–2 min), 5–10% solvent B (2–12.5 min), 10–30% solvent B (12.5–15 min), flow rate 0.7 mL/min]. The authentic amides, the (*S*)-(+)-PGME product of L- and D-*N,N*-dimethylalanine (*m/z* 265 $[M+H]^+$), were eluted at 8.83 and 10.24 min, respectively. The (*S*)-(+)-PGME product of *N,N*-dimethylalanine in **4** and **5** hydrolysates were observed at 8.79 and

8.73 min, respectively, retention time for LC–MS analyses. The absolute configurations of *N,N*-dimethylalanine in **4** and **5** were identified as both L forms (*S* configuration).

5.5. UHPLC-qTOF-MS analysis for triterpenic acids

For preparation of LC-MS analysis samples, 30.0 g of roots, twigs, leaves, and fruits of *Z. jujuba* were extracted with MeOH (500 mL) at rt using an ultrasonic apparatus. MeOH extracts were evaporated *in vacuo* for the removal of MeOH, then their weights were measured to be 2.5 g, 1.6 g, 4.7 g, and 6.3 g, respectively. These extracts were resolved with 50 % aqueous MeOH to be 5 mg/mL, and then they were analyzed by UHPLC-qTOF-MS equipped with ACQUITY BEH C18 column (100 mm × 2.1 mm, 1.7 μm). The mobile phase was composed of A (H_2O) and B (MeCN), each containing 0.1% formic acid. A gradient (30 – 90% B) was carried out in 14.0 min, followed by an increase of B from 90% to 100% in 0.1 min, a 3.0 min isocratic step at 100% B, a decrease of B from 100% to 30% in 0.1 min, and a second 10.0 min isocratic step at 30% B for column reconditioning. The flow rate of the mobile phase was 0.3 mL/min and the column temperature was maintained at 25 °C. Analysis of each sample (2.0 μL injected in the partial loop with needle overfill mode) were performed in negative ion modes in the 100-1500 Da range with acquisition times of 0.3 seconds in the centroid mode. The ESI conditions were set as follows: capillary voltage 3500 V, con voltage 45 V, source temperature 120 °C, desolvation temperature 300 °C, cone gas flow 50 L/h, desolvation gas flow 800 L/h. MS^E methodology (where E represents the collision energy) was applied for MS/MS fragmentation pattern analysis (Lecompte et al., 2014). Low collision energy was set to 4 eV, while high collision energy ramp was set to 40 to 45 eV.

5.6. Isolation of triterpenoids and phenolic compounds

Pulverized, air-dried roots of *Z. jujuba* (7.5 kg) were extracted with MeOH (2 × 30 L, for 3 h each) at rt in an ultrasonic apparatus. After removal of the solvent *in vacuo,* the crude extract (630.4 g) was suspended in H_2O and successively partitioned into $CHCl_3$ fraction (103.5 g), EtOAc fraction (75.0 g), and BuOH fraction (127.3 g), respectively (Scheme 6). Among these fractions, $CHCl_3$ and EtOAc fractions showing abundant amounts of triterpenic acids in LC-MS profiles were subjected to repeated column chromatography and preparative HPLC to afford compounds **10-52**.

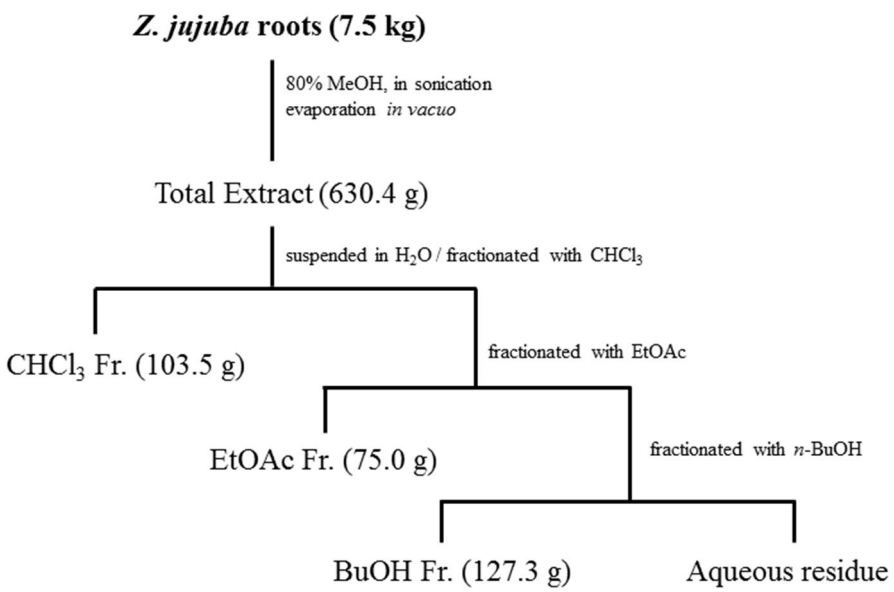

Scheme 6. Extraction and fractionation for isolation of triterpenes

The $CHCl_3$ fraction was subjected to silica gel CC eluted with mixtures of $CHCl_3$-MeOH = 100:1, 50:1, 25:1, 15:1, 10:1, 7:1, 5:1, and 3:1 to yield ten fractions (C1 – C10) (Scheme 7). C3 was further separated into six subfractions (C1a – C1f) on

silica gel CC eluted with mixtures of $CHCl_3$-MeOH = 200:1, 100:1, 70:1, 50:1, 30:1, and 20:1. Compound **13** (10.2 mg) was purified from subfraction C3b using ODS silica gel HPLC eluted with 82% aqueous MeCN. C3e was further devided into 5 subfractions (C3e1 – C3e5) by Sephadex LH-20 with a mixture of CH_2Cl_2-MeOH (3:1). Compounds **26** (1.2 mg) and **34** (1.6 mg) were isolated from C3e5 by ODS silica gel HPLC eluted with 83% aqueous MeCN. Subfraction C3f was subjected to silica gel CC eluted with mixtures of $CHCl_3$-MeOH = 200:1, 100:1, 50:1, 20:1, and 10:1 to afford six subfractions (C3f1 – C3f6). Compound **28** (124.6 mg) was isolated from C3f3 by recrystallization (MeOH). Before subjected to further isolation, MeOH-insoluble precipitation of fraction C5 was collected and purified into compound **10** (12.5 g), by recrystallization with MeOH. Rest of the fraction was subjected to silica gel CC eluted with $CHCl_3$-MeOH of increasing polarity (100:1, 50:1, 25:1, 15:1, 10:1) to give ten fractions (C5a – C5j). C5e was separated into 7 subfractions (C5e1 – C5e7) by silica gel CC with $CHCl_3$-MeOH of increasing polarity (100:1, 50:1, 25:1, 15:1, 10:1) once more again. White pellets of C5e2 which was insoluble to MeOH were filtered, and purified by recrystallization with MeOH to yield compound **18** (45.8 mg). MeOH-soluble part of C5e2 was subjected to ODS silica gel HPLC (MeCN-H_2O = 78:22) and afforded compounds **12** (2.3 mg), **22** (9.0 mg), **23** (0.7 mg), **24** (5.6 mg), **31** (11.3 mg), and **36** (10.8 mg). Compound **46** (53.4 mg) was purified from subfraction C5e6 by recrystallization (MeOH). C5g was chromatographed by ODS silica gel HPLC with 65% aqueous MeCN to yield six subfractions (C5g1 – C5g6). Compounds **11** (30.3 mg), **37** (8.5 mg), **38** (2.8 mg), **41** (3.3 mg), and **45** (2.7 mg) were isolated from C5g3 by ODS silica gel HPLC eluted with 60% aqueous MeCN. C5g5 was further isolated with ODS silica gel HPLC with 80% aqueous MeCN and yielded compounds **30** (4.2 mg) and **35** (6.4 mg). Compound **17** (45.8 mg) was isolated from MeOH-insoluble pellets of C5i by recrystallization with MeOH. Rest of C5i was further separated on Sephadex LH20 with mixture of CH_2Cl_2-MeOH (3:1) to give four subfractions (C5i1 – C5i4), and compound **20** (6.5 mg) was purified from C5i4 using ODS

silica gel HPLC eluted with 70% aqueous MeCN. C8 was separated into five subfracations (C8a – C8e) by Sephadex LH20 with 1:1 mixture of CH_2Cl_2-MeOH. Compounds **16** (12.1 mg), **25** (2.8 mg), **32** (5.8 mg), and **40** (2.3 mg) were isolated from C8c using ODS silica gel HPLC with 62% aqueous MeCN. Compounds **27** (1.0 mg) and **39** (0.8 mg) were purified from C8d by ODS silica gel HPLC with 70% aqueous MeCN. Subfraction C8e afforded compound **49** (7.4 mg) by ODS silica gel HPLC with 40% aqueous MeCN.

EtOAc fraction was subjected to silica gel column chromatography (CC) eluted with mixtures of $CHCl_3$-MeOH = 50:1, 25:1, 15:1, 10:1, 7:1, 5:1, 3:1 and 1:1 to yield fourteen fractions (E1 – E14) (Scheme 8). Three major triterpenic acids, compounds **10** (18.7g), **14** (14.5 g), and **15** (276.4 mg) were isolated from E4, E7, and E8 by recrystallization with MeOH, respectively. Compounds **18** (15.6 mg) and **46** (2.1 mg) were isolated from E6 using successive ODS silica gel HPLCs eluted with 65% aqueous MeCN, followed by 50% aqueous MeCN. Fraction E9 was further separated into four subfractions (E9a – E9d) using Sephadex LH-20 with 1:1 mixture of CH_2Cl_2-MeOH. Compound **21** (39.6 mg) was isolated from subfraction E9c using ODS silica gel HPLC eluted with 50% aqueous MeCN, while compound **44** (0.7 mg) was from E9d with 75% aqueous MeCN. E11 was subjected to silica gel CC eluted with mixture of $CHCl_3$-MeOH = 50:1, 25:1, 15:1, 10:1, 5:1, and 3:1 to yield seven fractions (E11a – E11e). Compound **33** (56.0 mg) was purified from E11d using ODS silica gel HPLC eluted with MeCN-H_2O of increasing polarity (4:6 to 9:1). Compounds **42** (34.7 mg) and **43** (2.8 mg) were isolated from E11e by ODS silica gel HPLC eluting aqueous MeCN gradiently from 65% to 90%. E13 was further fractionated into six subfractions (E13a – E13f) on silica gel CC eluted with $CHCl_3$-MeOH-H_2O = 100:4:1, 50:4:1, 25:4:1, and 15:4:1. Compound **50** and inseparable mixture of compounds **51** and **52** were isolated from E13c using ODS silica gel HPLC eluted with MeCN-H_2O of increasing polarity (15:85 to 45:55). Compounds **47** (5.6 mg) and **48** (14.2 mg) were separated from E13e by ODS silica gel HPLC with 15% aqueous MeCN.

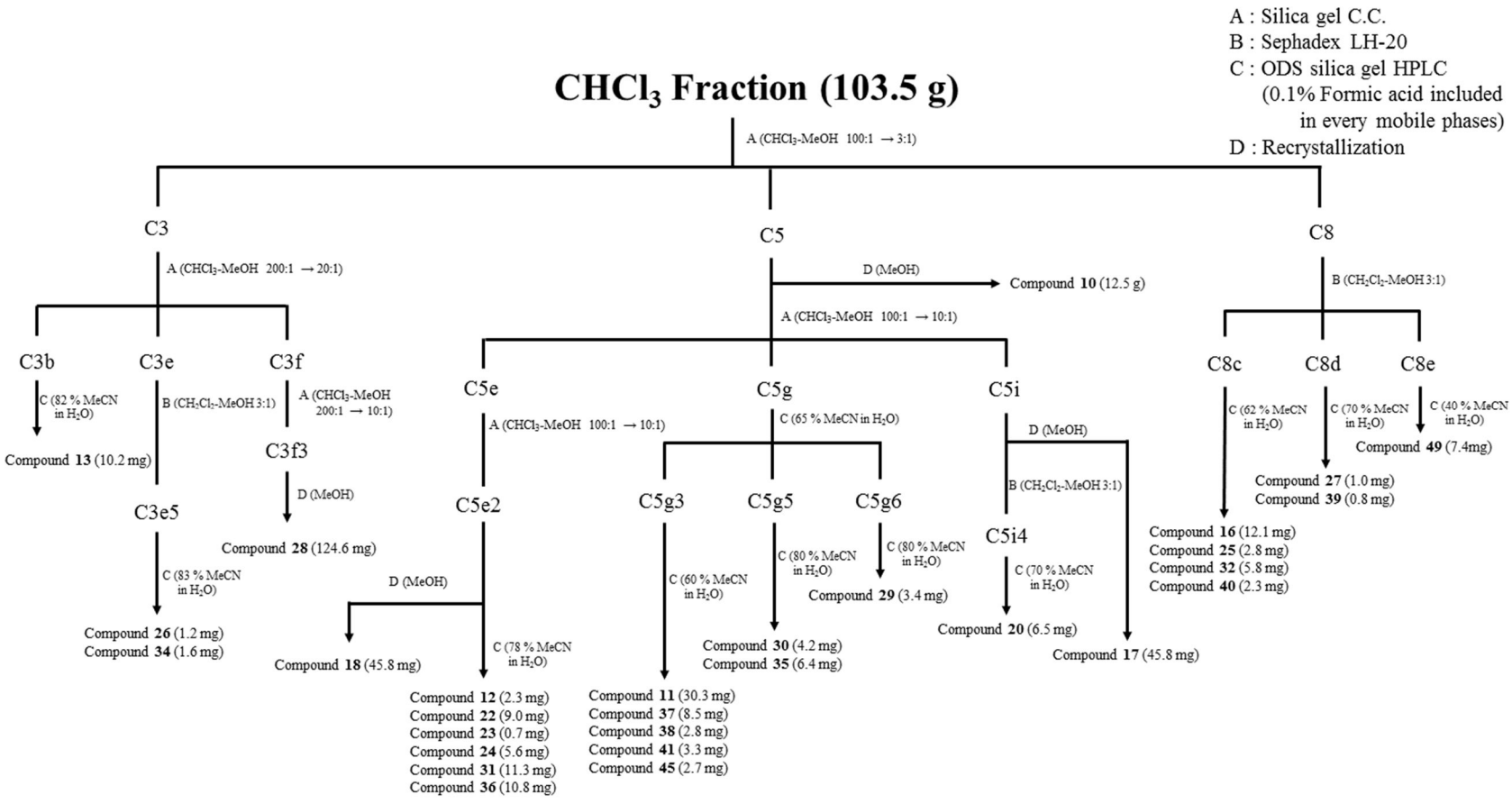

Scheme 7. Isolation of triterpenoids from $CHCl_3$ fraction of *Z. jujuba* roots MeOH extract

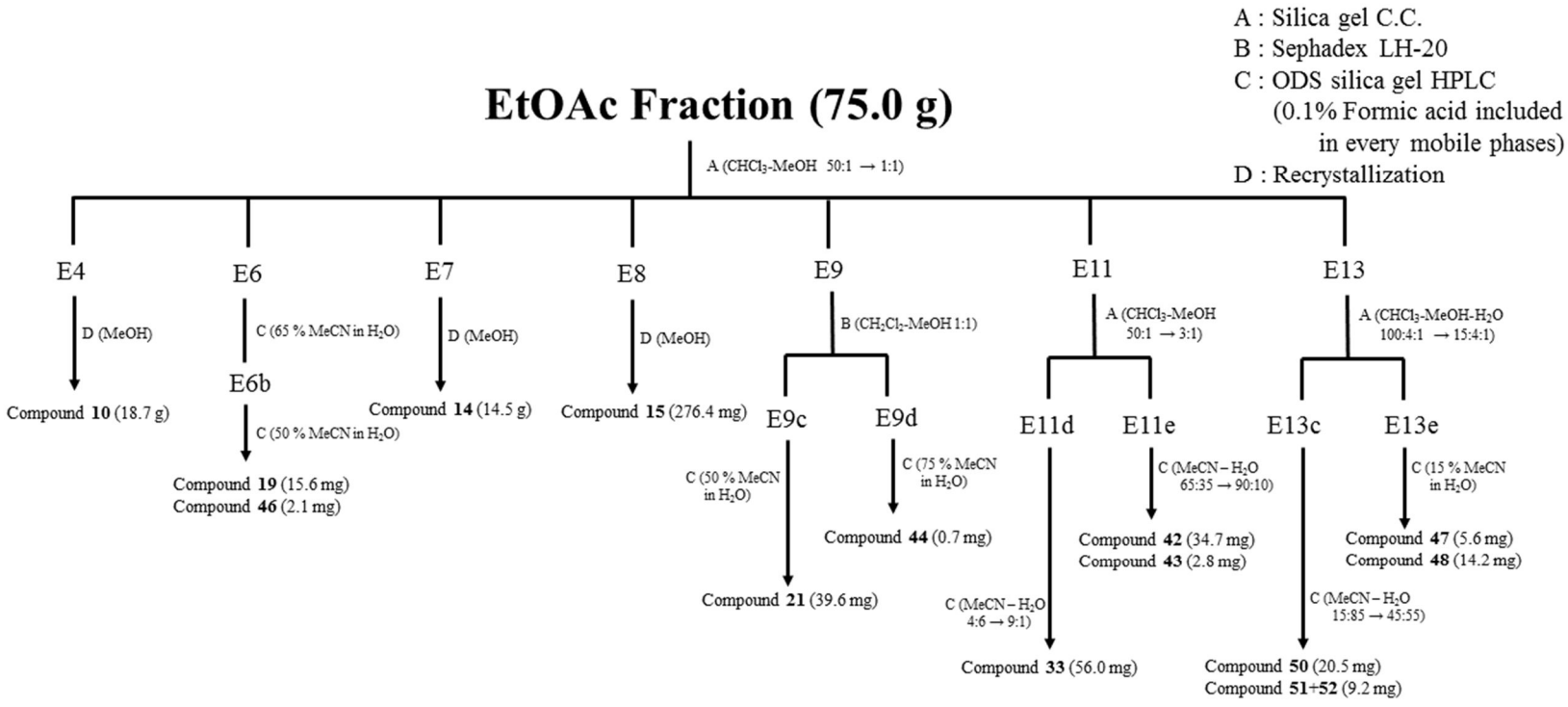

Scheme 8. Isolation of triterpenoids from EtOAc fraction of *Z. jujuba* roots MeOH extract

5.7. Preparation of (*S*)-MTPA ester and (*R*)-MTPA ester of **42**

Compound **42** (1 mg) was transferred into 5 ml glass vial and dry pyridine (100 μL) and (*R*)-(-)-α-methoxy-α-trifluromethylphenylacetyl (MTPA) chloride (20 μL) were added into the vial immediately. The vial was shaken carefully to mix the reactant. The mixture were left in rt, and TLC analysis (CH_2Cl_2-MeOH = 10:1) were peformed on every 30 min to verify for affording the (*S*)-MTPA ester derivative (**42a**). Similarly, another portion of **42** (1 mg) was reacted with (*S*)-(-)-MTPA chloride at rt to afford the (*R*)-MTPA ester derivative (**42b**).

5.8. Spectral data of isolated compounds

5.8.1. Jubanine F (**1**)

White amorphous powder

$C_{28}H_{41}N_5O_6$

$[\alpha]_D^{20}$ = - 309.8 (*c* 0.10, MeOH)

UV λmax (log ε): 276 (3.47), 323 (3.87) nm

CD (MeOH) (Δε): 321 (-2.2), 294 (-0.9), 265 (-4.4), 234 (-1.8), 213 (-5.9) nm

IR ν_{max}: 2966, 2352, 2317, 1674, 1645, 1514, 1566, 1222 cm^{-1}

ESI-qTOF-MS *m/z*: 544.3112 $[M+H]^+$ (calcd. 544.3135)

^1H (400 MHz, $CDCl_3$) NMR: See Table 7

^{13}C (100 MHz, $CDCl_3$) NMR: See Table 8

5.8.2. Jubanine G (**2**)

White amorphous powder

$C_{29}H_{43}N_5O_6$

$[\alpha]_D^{20}$ = - 247.8 (*c* 0.10, MeOH)

UV λmax (log ε): 273 (3.22), 323 (3.06) nm

CD (MeOH) (Δε): 321 (-2.5), 294 (-0.9), 264 (-4.9), 231 (-0.5), 215 (-3.7) nm

IR ν_{max}: 3332, 2964, 1643, 1513, 1446, 1222, 1186, 1038, 1027 cm^{-1}

ESI-qTOF-MS *m/z*: 558.3296 $[M+H]^+$ (calcd. 558.3292)

^1H (500 MHz, $CDCl_3$) NMR: See Table 7

^{13}C (125 MHz, $CDCl_3$) NMR: See Table 8

5.8.3. Jubanine H (**3)**

White amorphous powder

$C_{30}H_{45}N_5O_6$

$[\alpha]_D^{20}$ = - 280.9 (*c* 0.10, MeOH)

UV λmax (log ε): 271 (3.65), 323 (3.50) nm

CD (MeOH) (Δε): 321 (-4.2), 295 (-1.7), 262 (-8.9), 231 (-0.8), 215 (-6.2) nm

IR ν_{max}: 3337, 2966, 1678, 1643, 1513, 1432, 1222, 1031, 1006 cm^{-1}

ESI-qTOF-MS *m/z*: 572.3451 $[M+H]^+$ (calcd. 572.3448)

^1H (600 MHz, $CDCl_3$) NMR: See Table 7

^{13}C (150 MHz, $CDCl_3$) NMR: See Table 8

5.8.4. Jubanine I (**4)**

White amorphous powder

$C_{30}H_{45}N_5O_6$

$[\alpha]_D^{20}$ = - 64.3 (*c* 0.02, MeOH)

UV λmax (log ε): 271 (3.15), 322 (3.27) nm

CD (MeOH) (Δε): 322 (-0.8), 293 (0.0), 264 (-1.6), 236 (-0.7), 212 (-2.5) nm

IR ν_{max}: 2966, 2936, 2350, 1681, 1516, 1391, 1342, 1033, 1011 cm^{-1}

ESI-qTOF-MS *m/z*: 572.3451 $[M+H]^+$ (calcd. 572.3448)

^1H (600 MHz, DMSO-d_6) NMR: See Table 7

^{13}C (150 MHz, DMSO-d_6) NMR: See Table 8

5.8.5. Jubanine J (**5)**

White amorphous powder

$C_{31}H_{47}N_5O_6$

$[\alpha]_D^{20}$ = - 172.8 (*c* 0.10, MeOH)

UV λmax (log ε): 271 (3.13), 323 (2.82) nm

CD (MeOH) (Δε): 321 (-2.0), 296 (-0.8), 262 (-4.3), 232 (-0.4), 215 (-3.2) nm

IR ν_{max}: 3707, 2972, 2873, 2350, 1643, 1513, 1220, 1054, 1033, 1013 cm^{-1}

ESI-qTOF-MS *m/z*: 586.3597 $[M+H]^+$ (calcd. 586.3605)

^1H (600 MHz, DMSO-d_6) NMR: See Table 7

^{13}C (150 MHz, DMSO-d_6) NMR: See Table 8

Table 7. ^{1}H NMR spectroscopic data (δ (*J* in Hz)) for compounds **1-5**

	1 [c,d]	**2** [b,d]	**3** [a,d]	**4** [a,e]	**5** [a,e]
1	5.92 *d* (9.2)	5.92 *d* (9.0)	5.94 *d* (9.1)	5.84 *d* (8.9)	5.85 *d* (8.7)
2	6.93 *dd* (9.2, 11.5)	6.91 *dd* (9.0, 11.2)	6.93 *dd* (9.2, 11.5)	6.81 *dd* (8.9, 3.0)	6.82 *dd* (8.7, 3.2)
3-NH	8.42 *d* (11.5)	8.51 *d* (11.2)	8.44 *d* (11.5)	9.11 *d* (10.1)	9.09 *d* (10.1)
5	4.21 *dd* (4.6, 4.6)	4.23 *dd* (5.3, 5.3)	4.27 *dd* (4.6, 5.0)	4.46 *dd* (8.8, 8.8)	4.46 *dd* (8.3, 8.3)
6-NH	7.24 [f]	7.5 *br s*	7.19 *d* (5.0)	8.16 *d* (8.2)	7.83 *d* (8.7)
8	4.50 *d* (3.2)	4.49 *d* (3.2)	4.49 *d* (3.2)	4.52 *d* (1.8)	4.51 *d* (2.3)
9	5.52 *td* (3.2, 7.3)	5.43 *td* (3.2, 5.0)	5.53 *td* (3.2, 7.4)	5.16 *m*	5.15 *m*
12	6.70 *d* (3.2)	6.71 *d* (2.8)	6.69 *d* (2.8)	6.77 *d* (3.0)	6.73 [f]
15	6.87 *d* (9.2)	6.85 *d* (9.0)	6.87 *d* (8.7)	7.01 *d* (9.1)	7.02 *d* (9.1)
16	6.80 *dd* (3.2, 9.2)	6.80 *dd* (2.9, 9.0)	6.80 *dd* (2.8, 8.7)	6.81 *dd* (3.0, 9.0)	6.76 [f]
17	2.29, 2.59 *m*	2.32, 2.58 *m*	2.32, 2.59 *m*	2.13, 2.54 *m*	2.15, 2.53 *m*
18	3.56, 4.23 *m*	3.60, 4.30 *m*	3.55, 4.31 *m*	3.59, 4.25 *m*	3.60, 4.12 *m*
21	4.56 *dd* (7.8, 9.2)	4.60 *dd* (8.1, 8.1)	4.60 *dd* (7.3, 9.1)	4.03 *m*	4.06 *dd* (6.9, 8.7)
22-NH	7.64 *d* (9.2)	7.87 *d* (7.1)	7.60 *d* (9.1)	8.25 *d* (8.7)	8.26 *d* (8.7)
R_1 (ringbound amino acid)	Val	Val	Ile	Ile	Ile
1′	2.33 *m*	2.30 *m*	2.09 *m*	1.75 *m*	1.72 *m*
2′	0.99 *d* (6.9)	0.97 *d* (7.0)	1.11, 1.38 *m*	1.06, 1.42 *m*	1.08, 1.43 *m*
3′	0.88 *d* (7.3)	0.86 [f]	0.87 [f]	0.76 [f]	0.79 *d* (7.3)
4′			0.96 *d* (6.9)	0.67 *d* (6.6)	0.79 *d* (7.3)
R_2 (intermediate amino acid)	Val	Ile	Ile	Val	Ile
1″	1.97 *m*	1.76 *m*	1.77 *m*	1.85 *m*	1.85 *m*
2″	0.87 *d* (7.8)	1.09, 1.42 *m*	1.10, 1.44 *m*	0.80 [f]	1.18, 1.34 *m*
3″	0.85 *d* (6.9)	0.81 [f]	0.84 [f]	0.86 [f]	0.80 *d* (7.3)
4″		0.85 [f]	0.83 [f]		0.86 *d* (6.9)
R_3 (terminal amino acid)	*N*-Me Ala	*N*-Me Ala	*N*-Me Ala	*N,N*-diMe Ala	*N,N*-diMe Ala
1‴	3.11 *q* (6.8)	3.58 [f]	3.10 *q* (6.8)	2.77 *q* (10.4)	2.99 *q* (6.9)
2‴	1.30 *d* (6.8)	1.30 *d* (6.8)	1.30 *d* (6.8)	1.75 [f]	1.07 *d* (6.9)
OMe	3.78 *s*	3.77 *s*	3.78 *s*	3.16 *s*	3.74 *s*
NMe	2.37 *s*	2.43 *s*	2.37 *s*	2.17 *s*	2.17 *s*

[a] Recorded at 600 MHz [b] Recorded at 500 MHz [c] Recorded at 400 MHz [d] Recorded in $CDCl_3$ [e] Recorded in DMSO-d_6 [f] overlapped.

Table 8. ^{13}C NMR spectroscopic data (δ) for compounds **1-5**

	1 [c,d]	**2** [b,d]	**3** [a,d]	**4** [a,e]	**5** [a,e]
1	106.8	107.0	106.7	107.9	107.8
2	121.5	121.5	121.5	122.0	116.9
4	167.1	167.4	167.1	168.5	169.8
5	60.7	60.7	60.3	53.8	53.4
7	170.4	170.4	170.4	170.4	172.2
8	64.5	64.7	64.5	64.8	64.8
9	77.2	77.2	77.3	77.8	77.2
11	151.1	150.9	151.1	150.6	150.5
12	111.3	111.2	111.2	111.9	111.3
13	124.3	124.2	124.3	124.1	124.1
14	151.5	151.0	151.5	150.9	150.9
15	113.8	113.7	113.8	113.6	113.7
16	117.8	117.6	117.8	116.9	116.9
17	32.6	32.6	32.6	32.6	32.3
18	46.7	46.8	46.8	46.2	46.1
20	171.6	171.5	171.7	168.5	170.3
21	54.6	54.5	53.8	60.4	59.0
23	175.0	172.6	175.0	169.8	172.5
R_1 (ringbound amino acid)	Val	Val	Ile	Ile	Ile
1′	28.3	28.6	35.2	36.5	36.5
2′	19.7	19.6	24.5	24.3	24.1
3′	17.3	17.4	11.7	11.1	10.7
4′			16.2	15.6	14.8
R_2 (intermediate amino acid)	Val	Ile	Ile	Val	Ile
1″	31.3	37.4	37.6	34.8	34.8
2″	19.2	24.5	24.5	18.2	24.5
3″	17.6	10.8	11.0	19.4	10.5
4″		15.1	15.4		15.6
R_3 (terminal amino acid)	*N*-Me Ala	*N*-Me Ala	*N*-Me Ala	*N,N*-diMe Ala	*N,N*-diMe Ala
1‴	60.2	58.4	60.2	70.4	63.1
2‴	19.5	17.8	19.4	32.4	13.2
OMe	56.1	56.0	56.1	55.9	56.0
NMe	34.9	32.9	35.0	41.0	41.7

[a] Recorded at 150 MHz [b] Recorded at 125 MHz [c] Recorded at 100 MHz [d] Recorded in $CDCl_3$ [e] Recorded in DMSO-d_6.

5.8.6. Nummularine B (**6**)

White amorphous powder

$C_{32}H_{41}N_5O_6$

UV λmax (log ε): 270 (3.84), 320 (3.68) nm

CD (MeOH) (Δε): 321 (-6.6), 295 (-3.1), 264 (-12.5), 231 (+0.3), 217 (-9.6) nm

ESI-qTOF-MS *m/z*: 592.3107 $[M+H]^+$ (calcd. 592.3125)

^1H (400 MHz, $CDCl_3$) NMR: See Table 9

^{13}C (100 MHz, $CDCl_3$) NMR: See Table 9

5.8.7. Daechuine-S3(**7**)

White amorphous powder

$C_{34}H_{53}N_5O_6$

UV λmax (log ε): 272 (3.95), 320 (3.79) nm

CD (MeOH) (Δε): 321 (-22.7), 296 (-9.6), 263 (-49.1), 232 (-12.7), 216 (-45.0) nm

ESI-qTOF-MS *m/z*: 628.4074 $[M+H]^+$ (calcd. 628.4059)

^1H (400 MHz, DMSO-d_6) NMR: See Table 9

^{13}C (100 MHz, DMSO-d_6) NMR: See Table 9

5.8.8. Mucronine K (**8**)

White amorphous powder

$C_{28}H_{43}N_4O_5$

UV λmax (log ε): 270 (3.76), 323 (3.87) nm

CD (MeOH) (Δε): 321 (-6.3), 295 (-2.6), 264 (-12.7), 232 (+0.9), 217 (-7.1) nm

ESI-qTOF-MS *m/z*: 515.3245 $[M+H]^+$ (calcd. 515.3245)

^1H (400 MHz, DMSO-d_6) NMR: See Table 9

^{13}C (100 MHz, DMSO-d_6) NMR: See Table 9

Table 9. ^{1}H and ^{13}C NMR spectroscopic data (δ (*J* in Hz)) of compounds **6-8**

	6 [a]		**7** [b]		**8** [b]	
	δ_H	δ_C	δ_H	δ_C	δ_H	δ_C
1	5.94 *d* (9.1)	107.3	5.84 *d* (8.9)	107.8	5.85 *d* (8.9)	107.7
2	6.91 *dd* (9.0, 11.2)	121.4	6.73 [c]	121.9	6.73 *dd* (8.9, 9.9)	121.9
3-NH	8.40 *d* (11.2)		9.09 *d* (10.2)		9.12 *d* (10.2)	
4		167.2		168.5		168.5
5	4.58 *td* (4.1, .4.8)	56.7	4.04 *m*	59.0	4.04 *m*	58.9
6-NH	7.33 *d* (4.8)		8.24 *d* (8.4)		8.24 *d* (8.6)	
7		170.1		170.0		170.1
8	4.41 *d* (3.0)	64.3	4.51 *d* (2.8)	64.8	4.50 *d* (1.3)	64.9
9	5.47 *td* (7.1, 3.0)	77.2	5.16 *td* (5.3, 2.8)	77.3	5.14 *td* (6.1, 1.3)	77.3
11		151.0				150.6
12	6.67 *d* (3.0)	111.3	6.75 [c]	111.8	6.79 [c]	111.8
13		124.2				124.1
14		151.5				150.9
15	6.85 *d* (9.0)	113.9	7.01 *d* (9.0)	114.1	7.02 *d* (9.0)	113.6
16	6.77 *dd* (3.0, 9.0)	117.9	6.81 *dd* (3.0, 9.0)	116.8	6.81 [c]	116.9
17	2.26, 2.55 *m*	32.5	2.15, 2.54 *m*	32.6	2.11, 2.54 *m*	32.3
18	3.48, 4.11 *m*	46.6	3.59, 4.27 *m*	46.1	3.56, 4.06 *m*	45.6
20		171.3		171.2		169.9
21	4.51 *dd* (6.4, 9.0)	54.5	4.43 *dd* (8.8, 8.8)	53.8		
22-NH	7.52 *d* (9.0)		8.11 *d* (8.2)			
23		174.6		170.5		
R_1 (ringbound amino acid)	Phe		Ile		Ile	
1′	2.86 *dd* (9.1, 14.3) 3.24 *dd* (3.8, 14.3)	36.6	1.83 *m*	34.9	1.85 *m*	34.9
2′		135.8	1.20, 1.36 *m*	24.8	1.19, 1.35 *m*	24.6
3′	7.29 [c]	128.9	0.86 [c]	10.5	0.83 [c]	10.5
4′	7.22 [c]	129.2	0.86 [c]	15.8	0.86 [c]	15.6
5’	7.20 [c]	127.2				
R_2 (intermediate amino acid)	Val		Ile			
1″	1.78 *m*	31.0	1.75 *m*	35.7		
2″	0.59 *d* (6.7)	17.3	1.08, 1.57 *m*	24.8		
3″	0.66 *d* (6.7)	19.1	0.77 [c]	14.6		
4″			0.86 [c]	15.7		
R_3 (terminal amino acid)	*N*-Me-Ala		*N,N*-diMe-Ile		*N,N*-diMe-Leu	
1‴	3.16 *q* (6.9)	60.0	2.77 *d* (10.3)	70.5	3.35 *m*	62.3
2‴	1.31 *d* (6.9)	19.4	1.75 *m*	33.2	1.25, 1.61 *m*	33.4
			1.53, 1.56 *m*	24.7	1.35 *m*	24.9
			0.69 *d* (6.5)	15.5	0.66 *d* (6.6)	22.2
			0.80 [c]	10.3	0.82 [c]	23.1
OMe	3.77 *s*	56.1	3.77 *s*	56.1	3.75 *s*	55.9
NMe	2.41 *s*	34.6	2.19 *s*	41.3	2.22 *s*	41.0

[a] Recorded in $CDCl_3$ [b] Recorded in DMSO-d_6 [c] Overlapped.
Every data were measured at 400 MHz (^{1}H) and 100 MHz (^{13}C).

5.8.9. Adouetine X (**9)**

White amorphous powder

$C_{28}H_{44}N_4O_4$

UV λmax (log ε): 234 (3.72) nm

CD (MeOH) (Δε): 234 (-11.0), 282 (2.6) nm

ESI-qTOF-MS *m/z*: 501.3444 $[M+H]^+$ (calcd. 501.3441)

^{1}H (400 MHz, $CDCl_3$) NMR : δ 7.77 (1H, *d, J* = 10 Hz, H-20), 7.17 (1H, *dd*, *J* = 8.5, 2.0 Hz, H-13), 7.11 (1H, *dd*, *J* = 8.5, 2.0 Hz, H-15), 7.04 (1H, *m*, H-16), 7.02 (1H, *m*, H-12), 6.64 (1H, *dd*, *J* = 9.9, 7.6 Hz, H-2), 6.43 (1H, *d*, *J* = 9.9 Hz, H-3), 6.35 (1H, *d*, *J* = 7.6 Hz, H-1), 5.90 (1H, *d*, *J* = 8.0 Hz, H-6), 5.00 (1H, *dd*, *J* = 7.0, 2.0 Hz, H-9), 4.44 (1H, *dd*, *J* = 10.0, 7.0 Hz, H-8), 3.96 (1H, *dd*, *J* = 8.0, 3.5 Hz, H-5), 2.81 (1H, *dd*, *J* = 8.5, 4.4 Hz, H-22), 2.12 (1H, *m*, H-1′), 1.92 (1H, *m*, H-17), 1.78 (1H, *m*, H-2″), 1.59 (1H, *m,* H-1a″), 1.30 (1H, *m,* H-1b″), *1*.26 (3H, *d*, *J* = 6.8 Hz, H-18), 1.19 (1H, *m*, H-2a′), 0.96 (3H, *d,* J = 6.8 Hz, H-19), 0.93 (3H, *d, J* = 6.5 Hz, H-3″), 0.92 (1H, *m*, H-2b′), 0.86 (3H, *d, J* = 6.5 Hz, H-4″), 0.79 (3H, *t*, *J* = 7.3 Hz, H-3′), 0.67 (1H, *d*, *J* = 6.9 Hz, H-4′)

^{13}C (100 MHz, $CDCl_3$) NMR : δ 173.9 (C-21), 172.1 (C-4), 167.1 (C-7), 155.9 (C-11), 131.8 (C-12), 131.8 (C-14), 130.1 (C-16), 123.1 (C-15), 122.8 (C-13), 125.5 (C-2), 116.6 (C-1), 81.4 (C-9), 66.3 (C-22), 59.4 (C-5), 55.1 (C-8), 34.9 (C-1′), 34.4 (C-1″), 29.3 (C-17), 26.2 (C-2″), 23.8 (C-2′), 23.1 (C-3″), 21.7 (C-4″), 20.4 (C-18), 15.9 (C-3′), 15.0 (C-19), 11.9 (C-4′),

5.8.10. Betulinic acid (**10)**

White amorphous powder

$C_{30}H_{48}O_3$

mp: 298 – 302 °C

$[\alpha]_D^{20}$ = + 18.9 (*c* 0.10, MeOH)

IR ν_{max}: 3694, 2938, 2865, 2843, 2361, 2310, 1686, 1054, 1032, 1012 cm^{-1}

ESI-qTOF-MS *m/z*: 455.3524 $[M-H]^-$ (calcd. 455.3525)

^1H (400 MHz, pyridine-d_5) NMR: See Table 10

^{13}C (100 MHz, pyridine-d_5) NMR: See Table 11

5.8.11. Alphitolic acid (**11)**

White amorphous powder

$C_{30}H_{48}O_3$

mp: 262 – 264 °C

$[\alpha]_D^{20}$ = + 27.6 (*c* 0.10, MeOH)

IR ν_{max}: 3681, 2966, 2870, 2872, 2361, 2345, 1686, 1054, 1031, 1013 cm^{-1}

ESI-qTOF-MS *m/z*: 471.3472 $[M-H]^-$ (calcd. 471.3471)

^1H (400 MHz, pyridine-d_5) NMR: See Table 10

^{13}C (100 MHz, pyridine-d_5) NMR: See Table 11

5.8.12. Betulin (**12)**

White amorphous powder

$C_{30}H_{50}H_2$

$[\alpha]_D^{20}$ = - 5.6 (*c* 0.10, MeOH)

IR ν_{max}: 3679, 2965, 2873, 2346, 2307, 1339, 1053, 1032, 1013 cm^{-1}

ESI-qTOF-MS *m/z*: 443.3885 $[M+H]^+$ (calcd. 443.3889)

^{1}H (600 MHz, pyridine-d_5) NMR: See Table 10

^{13}C (150 MHz, pyridine-d_5) NMR: See Table 11

5.8.13. 3β-hydroxy-28-norlup-20(29)-en-17β-hydroperoxide (**13)**

Colorless amorphous solid

$C_{29}H_{48}O_3$

$[\alpha]_D^{20}$ = - 21.6 (*c* 0.10, MeOH)

IR ν_{max}: 3853, 2948, 2873, 2360, 2331, 1689, 1054, 1032, 1013 cm^{-1}

ESI-qTOF-MS *m/z*: 445.3678 $[M+H]^+$ (calcd. for $C_{29}H_{49}O_3$, 445.3682)

^{1}H (600 MHz, $CDCl_3$) NMR: See Table 10

^{13}C (150 MHz, $CDCl_3$) NMR: See Table 11

Table 10. [1]H NMR spectroscopic data (δ (*J* in Hz)) for compounds **10-13**

	10 [a, c]	**11** [a, c]	**12** [b, c]	**13** [b, d]
1a	1.66 *dt* (13.0, 3.0)	2.34 *dd* (12.5, 4.5)	1.68 *m*	1.65 *m*
1b		1.29 *m*	1.00 *m*	0.89 *m*
2	1.87 *m*	4.14 *m*	1.89 *m*	1.59 *m*
3	3.46 *t* (7.8)	3.42 *d* (9.4)	3.48 *t* (4.6)	3.17 *m*
5	0.82 *m*	1.01 *m*	0.84 *m*	0.66 *m*
6a	1.56 *m*	1.56 *m*	1.56 *m*	1.52 *m*
6b	1.41 *m*	1.43 *m*	1.41 *m*	1.40 *m*
7a	1.42 *m*	1.47 *m*	1.44 *m*	1.40 *m*
7b	1.40 *m*	1.39 *m*	1.36 *m*	
9	1.39 *m*	1.50 *m*	1.36 *m*	1.25 *m*
11a	1.42 *m*	1.52 *m*	1.41 *m*	1.37 *m*
11b	1.21 *m*	1.22 *m*	1.17 *m*	1.20 *m*
12a	1.93 *m*	1.95 *m*	1.80 *m*	1.63 *m*
12b		1.18 *m*	1.19 *m*	1.53 *m*
13	2.74 *td* (11.4, 3.2)	2.74 *td* (12.1, 3.4)	1.81 *m*	1.86 *td* (12.3, 3.3)
15a	1.90 *m*	1.88 *m*	1.93 *m*	2.18 *m*
15b	1.28 *m*	1.25 *m*	1.06 *m*	1.04 *m*
16a	2.63 *dt* (12.7, 3.0)	2.65 *m*	2.46 *m*	1.78 *m*
16b	1.56 *m*	1.56 *m*	1.34 *m*	1.05 *m*
18	1.76 *dd* (11.4, 11.4)	1.75 *dd* (11.3, 11.3)	1.72 *m*	1.67 *m*
19	3.54 *dt* (5.0, 11.4)	3.55 *dt* (4.8, 11.2)	2.65 *dt* (5.8 11.0)	2.60 *dt* (5.8, 10.8)
21a	2.24 *m*	2.24 *m*	2.17 *m*	2.04 *m*
21b	1.52 *m*	1.54 *m*	1.52 *m*	1.40 *m*
22a	2.26 *m*	2.27 *m*	2.44 *m*	2.15 *m*
22b	1.59 *m*	1.59 *m*	1.20 *m*	1.25 *m*
23	1.23 *s*	1.28 *s*	1.25 *s*	0.95 *s*
24	1.06 *s*	1.08 *s*	1.06 *s*	0.74 *s*
25	0.83 *s*	0.92 *s*	0.89 *s*	0.81 *s*
26	1.01 *s*	1.06 *s*	1.03 *s*	1.00 *s*
27	1.07 *s*	1.06 *s*	1.07 *s*	0.93 *s*
28a			4.12 *d* (10.7)	
28b			3.69 *d* (10.7)	
29a	4.95 *s*	4.95 *s*	4.91 *s*	4.68 *s*
29b	4.77 *s*	4.79 *s*	4.76 *s*	4.57 *s*
30	1.79 *s*	1.80 *s*	1.79 *s*	1.67 *s*

[a] Recorded at 400 MHz [b] Recorded at 600 MHz [c] Recorded in pyridine-d_5
[d] Recorded in $CDCl_3$

Table 11. ^{13}C NMR spectroscopic data (δ) for compounds **10-13**

	10 [a, c]	**11** [a, c]	**12** [b, c]	**13** [b, d]
1	39.5	48.6	39.7	38.8
2	28.3	69.2	28.7	27.4
3	78.1	84.1	78.5	79.0
4	39.3	40.3	39.9	38.9
5	55.9	56.4	56.2	55.4
6	18.8	19.2	19.2	18.3
7	34.8	35.1	35.1	34.4
8	41.1	41.5	41.6	40.8
9	51.0	50.1	51.2	50.6
10	37.5	37.9	37.9	37.2
11	21.2	21.7	21.5	20.9
12	26.1	26.4	26.1	25.3
13	38.6	39.0	38.0	36.7
14	42.9	43.2	43.4	42.0
15	30.3	30.6	28.0	27.3
16	32.9	33.2	30.4	27.0
17	56.6	56.9	48.9	91.6
18	49.8	50.1	49.5	49.2
19	47.8	48.6	48.7	47.9
20	151.3	151.6	151.6	150.0
21	31.2	31.5	30.4	29.5
22	37.6	38.9	35.2	32.2
23	28.7	29.6	28.7	28.0
24	16.4	17.8	16.8	15.4
25	16.4	18.0	16.7	16.2
26	16.3	16.8	16.5	16.1
27	14.9	15.2	15.3	14.0
28	178.9	179.2	59.8	
29	109.9	110.4	110.3	109.7
30	19.5	19.8	19.7	19.1

[a] Recorded at 100 MHz [b] Recorded at 150 MHz [c] Recorded in pyridine-d_5
[d] Recorded in $CDCl_3$

5.8.14. Ceanothic acid (**14)**

Pale yellowish amorphous powder

$C_{30}H_{46}O_5$

mp: 324 – 326 °C

$[\alpha]_D^{20}$ = + 38.2 (*c* 0.10, MeOH)

IR ν_{max}: 3712, 2957, 2834, 2355, 2321, 1336, 1052, 1032, 1014 cm^{-1}

ESI-qTOF-MS *m/z*: 485.3268 $[M-H]^-$ (calcd. 485.3267)

^1H (500 MHz, pyridine-d_5) NMR: See Table 12

^{13}C (125 MHz, pyridine-d_5) NMR: See Table 13

5.8.15. Epiceanothic acid (**15)**

Pale yellowish amorphous powder

$C_{30}H_{46}O_5$

mp: 310 – 312 °C

$[\alpha]_D^{20}$ = - 21.6 (*c* 0.10, MeOH)

IR ν_{max}: 3853, 2948, 2873, 2360, 2331, 1689, 1054, 1032, 1013 cm^{-1}

ESI-qTOF-MS *m/z*: 485.3268 $[M-H]^-$ (calcd. 485.3267)

^1H (600 MHz, pyridine-d_5) NMR: See Table 12

^{13}C (150 MHz, pyridine-d_5) NMR: See Table 13

5.8.16. Epiceanothic acid 2-methyl ester (**16)**

White amorphous powder

$C_{31}H_{48}O_5$

$[\alpha]_D^{20}$ = + 10.0 (*c* 0.10, MeOH)

IR ν_{max}: 3649, 2950, 2869, 2360, 2337, 1698, 1054, 1033, 1013 cm^{-1}

ESI-qTOF-MS *m/z*: 499.3420 $[M-H]^-$ (calcd. 499.3423)

^{1}H (600 MHz, pyridine-d_5) NMR: See Table 12

^{13}C (150 MHz, pyridine-d_5) NMR: See Table 13

5.8.17. 3-dehydroxy ceanothetric acid (**17)**

White amorphous powder

$C_{30}H_{44}O_6$

mp: 288 – 290 °C

$[\alpha]_D^{20}$ = + 58.6 (*c* 0.10, MeOH)

IR ν_{max}: 2966, 2869, 2361, 2322, 1698, 1456, 1054, 1033, 1014 cm^{-1}

ESI-qTOF-MS *m/z*: 499.3062 $[M-H]^-$ (calcd. 499.3060)

^{1}H (600 MHz, pyridine-d_5) NMR: See Table 12

^{13}C (150 MHz, pyridine-d_5) NMR: See Table 13

5.8.18. 3-dehydroxy ceanothetric acid 2-methyl ester (**18)**

White amorphous powder

$C_{31}H_{46}O_6$

mp: 296 – 298 °C

$[\alpha]_D^{20}$ = + 73.4 (*c* 0.10, MeOH)

IR ν_{max}: 3704, 2950, 2869, 2361, 2327, 1687, 1054, 1033, 1013 cm^{-1}

ESI-qTOF-MS *m/z*: 513.3213 $[M-H]^-$ (calcd. 513.3216)

^{1}H (600 MHz, pyridine-d_5) NMR: See Table 12

^{13}C (150 MHz, pyridine-d_5) NMR: See Table 13

5.8.19. Ceanothetric acid 2-methyl ester (**19**)

White amorphous powder

$C_{31}H_{46}O_7$

mp: 288 – 2902 °C

$[\alpha]_D^{20}$ = + 44.6 (*c* 0.10, MeOH)

IR ν_{max}: 3710, 2966, 2873, 2360, 2337, 1717, 1684, 1456, 1054, 1033, 1011 cm^{-1}

ESI-qTOF-MS *m/z*: 529.3165 $[M-H]^-$ (calcd. 529.3165)

^1H (500 MHz, pyridine-d_5) NMR: See Table 12

^{13}C (125 MHz, pyridine-d_5) NMR: See Table 13

Table 12. [1]H NMR spectroscopic data (δ (*J* in Hz)) for compounds **14-19**

	14 [a]	**15** [b]	**16** [b]	**17** [b]	**18** [b]	**19** [a]
1	3.18 *s*	2.89 *d* (7.3)	2.77 *d* (7.5)	2.88 *d* (7.3)	2.69 *d* (7.6)	3.06 *s*
3a	4.79 *s*	4.66 *d* (7.3)	2.57 *d* (7.5)	2.06 *m*	1.85 *m*	4.64 *s*
3b				1.88 *m*	1.78 *m*	
5	2.20 *m*	1.08 *m*	1.04 *m*	2.06 *m*	1.80 *m*	1.93 *m*
6a	1.41 *m*	1.57 *m*	1.56 *m*	1.35 *m*	1.31 *m*	1.44 *m*
6b	1.35 *m*	1.37 *m*	1.37 *m*	1.31 *m*		
7a	1.49 *m*	1.40 *m*	1.40 *m*	2.10 *m*	1.99 *m*	2.04 *m*
7b				1.86 *m*	1.81 *m*	1.83 *m*
9	2.19 *m*	1.73 *m*	1.62 *m*	2.65 *dd* (2.2, 12.2)	2.17 *m*	2.17 *m*
11a	2.07 *m*	2.01 *m*	1.75 *m*	2.26 *m*	1.89 *m*	1.90 *m*
11b	1.58 *m*	1.81 *m*	1.63 *m*	1.65 *m*	1.55 *m*	1.60 *m*
12a	1.85 *m*	1.93 *m*	1.98 *m*	2.83 *m*	2.62 *m*	2.59 *m*
12b	1.32 *m*	1.27 *m*	1.28 *m*	2.09 *m*	2.05 *m*	2.03 *m*
13	2.75 *dt* (3.2, 12.7)	2.75 *dt* (3.1, 11.9)	2.77 *m*	3.01 *m*	2.98 *dt* (4.8, 12.9)	2.98 *dt* (4.7, 12.7)
15a	1.89 *m*	1.90 *m*	1.92 *m*	2.54 *m*	2.50 *m*	2.51 *m*
15b	1.21 *m*	1.23 *m*	1.25 *m*	1.95 *m*	1.91 *m*	1.91 *m*
16a	2.57 *m*	2.63 *dt* (3.2, 12.8)	2.64 *m*	2.92 *m*	2.91 *m*	2.88 *m*
16b	1.50 *m*	1.52 *m*	1.52 *m*	1.97 *m*	1.95 *m*	1.91 *m*
18	1.66 *m*	1.70 *m*	1.73 *m*	2.21 *m*	2.18 *m*	2.17 *m*
19	3.47 *dt* (4.3, 10.5)	3.47 *dt* (5.5, 9.0)	3.53 *dt* (4.2, 10.2)	3.7 *dt* (4.7, 10.9)	3.71 *m*	3.68 *dt* (3.5, 10.5)
21a	2.21 *m*	2.22 *m*	2.25 *m*	2.26 *m*	2.28 *m*	2.26 *m*
21b	1.41 *m*	1.48 *m*	1.52 *m*	1.52 *m*	1.53 *m*	1.52 *m*
22a	2.20 *m*	2.22 *m*	2.26 *m*	2.29 *m*	2.29 *m*	2.28 *m*
22b	1.50 *m*	1.55 *m*	1.59 *m*	1.53*m*	1.53 *m*	1.51 *m*
23	1.40 *s*	1.12 *s*	1.11 *s*	1.24 *s*	1.17 *s*	1.22 *s*
24	1.24 *s*	1.19 *s*	1.16 *s*	0.94 *s*	0.89 *s*	1.19 *s*
25	1.36 *s*	1.67 *s*	1.62 *s*	0.98 *s*	0.89 *s*	1.37 *s*
26	1.12 *s*	1.13 *s*	1.12 *s*	1.23 *s*	1.16 *s*	1.21 *s*
27	1.04 *s*	1.05 *s*	1.06 *s*			
29a	4.83 *s*	4.85 *s*	4.93 *s*	5.03 *s*	5.08 *s*	5.05 *s*
29b	4.63 *s*	4.67 *s*	4.75 *s*	4.70 *s*	4.82 *s*	4.80 *s*
30	1.63 *s*	1.73 *s*	1.78 *s*	1.87 *s*	1.92 *s*	1.90 *s*
-OMe			3.62 *s*		3.78 *s*	3.74 *s*

[a] Recorded at 500 MHz [b] Recorded at 600 MHz. Every data were measured in pyridine-d_5

Table 13. ^{13}C NMR spectroscopic data (δ) for compounds **14-19**

	14 [a]	**15** [b]	**16** [b]	**17** [b]	**18** [b]	**19** [a]
1	67.0	63.1	63.3	56.3	55.7	66.3
2	178.0	175.6	173.6	179.1	176.8	175.7
3	84.7	83.1	83.5	43.2	42.6	84.0
4	43.8	43.0	43.4	43.2	38.6	43.6
5	57.0	62.7	63.0	56.7	56.5	57.0
6	19.1	18.4	18.8	19.4	19.1	18.9
7	34.7	34.8	35.1	38.3	38.1	37.6
8	43.5	51.1	43.5	41.9	41.7	41.4
9	45.0	42.0	51.2	46.7	46.5	46.0
10	49.7	48.1	48.4	51.6	51.6	50.3
11	24.2	24.6	25.1	24.6	24.4	24.1
12	26.2	25.9	26.2	27.2	27.2	26.8
13	39.1	38.5	38.9	41.0	40.7	40.3
14	42.1	42.9	42.3	60.8	60.8	60.5
15	30.5	30.4	30.9	29.4	29.3	28.7
16	32.9	33.0	33.4	35.9	35.8	35.3
17	56.6	56.5	57.0	57.1	57.0	56.5
18	49.6	49.8	50.2	52.8	52.7	52.3
19	47.6	47.8	48.3	48.3	48.3	47.8
20	151.1	151.1	151.7	151.6	151.6	151.1
21	31.2	31.2	31.6	31.7	31.6	31.1
22	37.5	37.6	38.1	38.2	38.1	37.6
23	31.4	32.1	32.5	32.1	31.9	31.2
24	20.3	19.9	19.9	27.5	27.0	20.2
25	18.8	14.6	15.1	20.4	19.8	18.8
26	17.0	16.9	17.2	18.5	18.5	18.1
27	15.0	14.9	15.4	179.0	178.9	178.4
28	178.8	178.8	179.3	179.8	179.8	179.3
29	109.7	110.0	110.5	110.7	110.7	110.1
30	19.5	19.4	20.3	20.0	19.8	19.3
-OMe			51.2		51.7	51.3

[a] Recorded at 125 MHz [b] Recorded at 150 MHz. Every data were measured in pyridine-d_5

5.8.20. 3-dehydroxy-ceanotha-27α-carboxy-28β,19β-olide (**20**)

White amorphous powder

$C_{30}H_{42}O_6$

mp: 246 – 248 °C

$[\alpha]_D^{20}$ = + 87.2 (*c* 0.10, MeOH)

IR ν_{max}: 2949, 2876, 2361, 2307, 1780, 1708, 1456, 1223, 1179, 1032 cm^{-1}

ESI-qTOF-MS *m/z*: 497.2897 $[M-H]^-$ (calcd. 497.2903)

^1H (600 MHz, pyridine-d_5) NMR: See Table 14

^{13}C (150 MHz, pyridine-d_5) NMR: See Table 15

5.8.21. 24-hydroxy ceanothic acid (**21**)

White amorphous powder

$C_{30}H_{46}O_6$

mp: 290 – 292 °C

$[\alpha]_D^{20}$ = + 76.0 (*c* 0.10, MeOH)

IR ν_{max}: 3680, 2965, 2866, 2360, 2331, 1685, 1507, 1054, 1033, 1013 cm^{-1}

ESI-qTOF-MS *m/z*: 501.3221 $[M-H]^-$ (calcd. 501.3216)

^1H (600 MHz, pyridine-d_5) NMR: See Table 14

^{13}C (150 MHz, pyridine-d_5) NMR: See Table 15

5.8.22. Zizyberenalic acid (**22**)

White amorphous powder

$C_{30}H_{44}O_3$

$[\alpha]_D^{20}$ = + 28.0 (*c* 0.10, MeOH)

UV λmax (log ε): 235 (4.09) nm

IR ν_{max}: 3679, 2950, 2866, 1685, 1455, 1054, 1033, 1013 cm^{-1}

ESI-qTOF-MS *m/z*: 451.3207 $[M-H]^-$ (calcd. 451.3212)

^1H (600 MHz, pyridine-d_5) NMR: See Table 14

^{13}C (150 MHz, pyridine-d_5) NMR: See Table 15

5.8.23. 3-*O*-methyl-zizyberanalic acid (**23**)

White amorphous powder

$C_{31}H_{48}O_4$

$[\alpha]_D^{20}$ = - 13.7 (*c* 0.10, MeOH)

IR ν_{max}: 2928, 2869, 2366, 2326, 1713, 1600, 1456, 1360 cm^{-1}

ESI-qTOF-MS *m/z*: 483.3484 $[M-H]^-$ (calcd. 483.3474)

^1H (600 MHz, pyridine-d_5) NMR: See Table 14

^{13}C (150 MHz, pyridine-d_5) NMR: See Table 15

5.8.24. 1,28-dinor-24-hydroxy-lup-2,17(22)-diene-27-oic acid (**24**)

Colorless solid

$C_{28}H_{40}O_3$

mp: 116 – 120 °C

$[\alpha]_D^{20}$ = + 0.61 (*c* 0.10, MeOH)

IR ν_{max}: 3393, 2938, 2867, 2322, 1689, 1455, 1054, 1033, 1014 cm^{-1}

ESI-qTOF-MS *m/z*: 423.2901 $[M-H]^-$ (calcd. 423.2889)

^1H (600 MHz, pyridine-d_5) NMR: See Table 14

^{13}C (150 MHz, pyridine-d_5) NMR: See Table 15

Table 14. [1]H NMR spectroscopic data (δ (*J* in Hz)) for compounds **20-24**

	20	**21**	**22**	**23**	**24**
1	2.87 *d* (7.9)	3.18 *s*		2.53 *dd* (4.0, 8.7)	
2			9.86 *s*	10.12 *d* (4.0)	6.24 *d* (5.7)
3a	2.05 *m*	4.87 *s*	6.51 *s*	4.03 *d* (8.7)	5.85 *d* (5.7)
3b	1.89 *m*				
5	2.05 *m*	2.23 *dd* (2.8, 11.7)	1.51 *m*	1.32 *m*	1.66 *m*
6a	1.37 *m*	1.48 *m*	1.37 *m*	1.31 *m*	1.80 *m*
6b	1.30 *m*	1.38 *m*		1.28 *m*	1.66 *m*
7a	1.56 *m*	1.39 *m*	1.39 *m*	1.36 *m*	2.31 *m*
7b	1.44 *m*	1.31 *m*	1.35 *m*	1.32 *m*	1.88 *m*
9	2.47 *m*	2.09 *dd* (2.6, 12.6)	1.99 *m*	1.75 *dd* (3.3, 12.8)	2.39 *m*
11a	2.15 *m*	2.02 *m*	1.72 *m*	1.39 *m*	1.66 *m*
11b	1.56 *m*	1.39 *m*	1.45 *m*	1.32 *m*	
12a	2.70 *m*	1.89 *m*	1.97 *m*	1.89 *m*	2.55 *m*
12b	2.13 *m*	1.22 *m*	1.26 *m*	1.23 *m*	1.97 *m*
13	1.94 *m*	2.69 *dt* (3.5, 12.7)	2.74 *dt* (3.2, 13.0)	2.68 *dt* (3.5, 13.0)	1.60 *m*
15a	2.30 *m*	1.82 *dt* (3.6, 13.4)	1.90 *m*	1.85 *m*	2.40 *m*
15b	1.76 *m*	1.11 *m*	1.18 *m*	1.19 *m*	1.48 *m*
16a	2.38 *m*	2.50 *td* (3.2, 12.8)	2.65 *m*	2.63 *m*	2.56 *m*
16b	1.96 *m*	1.39 *m*	1.56 *m*	1.54 *m*	
18	2.46 *d* (10.8)	1.62 *m*	1.69 *m*	1.69 *t* (11.2)	3.01 *t* (8.6)
19		3.42 *dt* (4.7, 10.7)	3.52 *dt* (4.7, 10.7)	3.50 *m*	2.77 *dd* (8.4, 16.6)
21a	2.00 *m*	2.15 *m*	2.25 *m*	2.24 *m*	2.58 *m*
21b	1.56 *m*	1.38 *m*	1.51 *m*	1.52 *m*	2.22 *m*
22a	2.16 *m*	2.14 *m*	2.24 *m*	2.25 *m*	5.33 *s*
22b	1.77 *m*	1.44 *m*	1.56 *m*	1.57 *m*	
23	1.24 *s*	1.73 *s*	1.08 *s*	1.06 *s*	1.31 *s*
24a	0.95 *s*	4.56 *d* (10.6)	0.87 *s*	1.00 *s*	4.03 *d* (10.6)
24b		3.62 *d* (10.6)			3.84 *d* (10.6)
25	0.94 *s*	1.39 *s*	1.12 *s*	0.94 *s*	1.16 *s*
26	1.01 *s*	1.05 *s*	1.09 *s*	0.97 *s*	1.16 *s*
27		0.98 *s*	1.00 *s*	1.00 *s*	
29a	5.54 *s*	4.79 *s*	4.92 *s*	4.94 *s*	5.04 *s*
29b	5.02 *s*	4.60 *s*	4.76 *s*	4.78 *s*	4.84 *s*
30	1.72 *s*	1.59 *s*	1.78 *s*	1.78 *s*	1.79 *s*
-OMe				3.30 *s*	

Every data were measured in 600 MHz, pyridine-d_5

Table 15. ^{13}C NMR spectroscopic data (δ) for compounds **20-24**

	20	**21**	**22**	**23**	**24**
1	56.2	66.2	158.2	72.4	
2	178.8	177.4	191.7	205.6	143.4
3	43.2	85.6	164.2	91.4	137.7
4	38.8	48.3	44.2	41.2	52.3
5	56.5	57.0	63.9	63.4	63.7
6	19.6	18.3	17.5	18.6	19.2
7	29.7	35.0	35.9	34.9	39.2
8	42.0	41.8	43.4	42.7	42.5
9	46.6	45.1	48.2	50.7	49.5
10	51.4	49.5	52.9	49.2	51.6
11	23.9	24.1	25.1	25.5	24.3
12	26.2	26.0	26.2	26.0	27.1
13	38.4	38.9	38.9	38.9	49.1
14	55.1	43.3	43.8	43.5	59.5
15	28.0	30.3	30.9	30.8	31.5
16	25.5	32.7	33.5	33.3	27.9
17	55.1	56.4	56.9	56.8	146.1
18	58.3	49.8	50.2	50.1	51.5
19	92.9	47.4	48.2	48.2	54.3
20	142.3	150.1	151.6	151.7	150.7
21	35.2	31.1	31.7	31.6	39.7
22	37.7	37.4	38.1	38.1	120.1
23	32.1	25.5	28.6	25.8	25.3
24	27.2	66.4	20.9	26.9	67.1
25	20.2	18.8	19.7	15.4	21.8
26	17.8	16.8	18.5	17.4	18.7
27	177.9	14.9	15.3	15.2	178.5
28	179.3	178.7	179.4	179.4	
29	112.4	109.6	110.5	110.5	110.9
30	19.3	19.4	19.9	19..9	21.3
-OMe				60.0	

Every data were measured in 150 MHz, pyridine-d_5

5.8.25. 2-*O*-protocatechuoyl alphitolic acid (**25**)

White amorphous powder

$C_{37}H_{52}O_7$

$[\alpha]_D^{20}$ = - 4.9 (*c* 0.10, MeOH)

UV λmax (log ε): 296 (3.76), 261 (3.96) nm

IR ν_{max}: 3652, 2972, 2866, 2360, 1055, 1033, 1013 cm^{-1}

ESI-qTOF-MS *m/z*: 607.3644$[M-H]^-$ (calcd. 607.3635)

^1H (600 MHz, pyridine-d_5) NMR: See Table 16

^{13}C (150 MHz, pyridine-d_5) NMR: See Table 17

5.8.26. 2-*O*-vanilloyl alphitolic acid (**26**)

White amorphous powder

$C_{38}H_{54}O_7$

$[\alpha]_D^{20}$ = + 29.5 (*c* 0.10, MeOH)

UV λmax (log ε): 292 (3.61), 262 (3.80) nm

IR ν_{max}: 3811, 2939, 2866, 2360, 1682, 1054, 1032, 1013 cm^{-1}

ESI-qTOF-MS *m/z*: 621.3787 $[M-H]^-$ (calcd. 621.3791)

^1H (600 MHz, pyridine-d_5) NMR: See Table 16

^{13}C (150 MHz, pyridine-d_5) NMR: See Table 17

5.8.27. 3-*O*-protocatechuoyl alphitolic acid (**27**)

White amorphous powder

$C_{37}H_{52}O_7$

$[\alpha]_D^{20}$ = + 19.8 (*c* 0.10, MeOH)

UV λmax (log ε): 296 (3.63), 256 (3.86) nm

IR ν_{max}: 3631, 2971, 2864, 2360, 1510, 1055, 1033, 1013 cm^{-1}

ESI-qTOF-MS *m/z*: 607.3630 $[M-H]^-$ (calcd. 607.3635)

^1H (600 MHz, pyridine-d_5) NMR: See Table 16

^{13}C (150 MHz, pyridine-d_5) NMR: See Table 17

5.8.28. 2-*O*-*trans*-*p*-coumaroyl alphitolic acid (**28**)

White amorphous powder

$C_{39}H_{54}O_6$

mp: 246 – 248 °C

$[\alpha]_D^{20}$ = + 12.7 (*c* 0.10, MeOH)

UV λmax (log ε): 311 (3.88) nm

IR ν_{max}: 3648, 2971, 2843, 2360, 1507, 1054, 1032, 1013 cm^{-1}

ESI-qTOF-MS *m/z*: 617.3848 $[M-H]^-$ (calcd. 617.3842)

^1H (600 MHz, pyridine-d_5) NMR: See Table 16

^{13}C (150 MHz, pyridine-d_5) NMR: See Table 17

5.8.29. 2-*O*-*cis*-*p*-coumaroyl alphitolic acid (**29**)

White amorphous powder

$C_{39}H_{54}O_6$

$[\alpha]_D^{20}$ = - 80.7 (*c* 0.10, MeOH)

UV λmax (log ε): 309 (4.09) nm

IR ν_{max}: 3648, 2971, 2866, 2360, 1698, 1507, 1055, 1033, 1013 cm^{-1}

ESI-qTOF-MS *m/z*: 617.3848 $[M-H]^-$ (calcd. 617.3842)

^1H (600 MHz, pyridine-d_5) NMR: See Table 16

^{13}C (150 MHz, pyridine-d_5) NMR: See Table 17

5.8.30. 2-*O*-*p*-hydroxybenzoyl alphitolic acid (**30**)

White amorphous powder

$C_{37}H_{52}O_6$

$[\alpha]_D^{20}$ = - 16.5 (*c* 0.10, MeOH)

UV λmax (log ε): 257 (4.12) nm

IR ν_{max}: 3649, 2939, 2865, 2360, 2326, 1684, 1055, 1033, 1013 cm^{-1}

ESI-qTOF-MS *m/z*: 591.3678 $[M-H]^-$ (calcd. 591.3686)

^1H (600 MHz, pyridine-d_5) NMR: See Table 16

^{13}C (150 MHz, pyridine-d_5) NMR: See Table 17

5.8.31. 2-*O*-benzoyl alphitolic acid (**31**)

White amorphous powder

$C_{37}H_{52}O_5$

$[\alpha]_D^{20}$ = - 18.5 (*c* 0.10, MeOH)

UV λmax (log ε): 228 (4.24) nm

IR ν_{max}: 3649, 2966, 2866, 2360, 2327, 1698, 1507, 1055, 1032, 1013 cm^{-1}

ESI-qTOF-MS *m/z*: 575.3735 $[M-H]^-$ (calcd. 575.3736)

^1H (600 MHz, pyridine-d_5) NMR: See Table 16

^{13}C (150 MHz, pyridine-d_5) NMR: See Table 17

Table 16. ^{1}H NMR spectroscopic data (δ (*J* in Hz)) for compounds **25-31**

	25	**26**	**27**	**28**	**29**	**30**	**31**
1a	2.34 *dd* (4.5, 12.3)	2.36 *dd* (4.7, 12.3)	2.39 *dt* (4.1, 12.8)	2.25 *m*	2.29 *m*	2.35 *m*	2.32 *m*
1b	1.16 *m*	1.20 *m*	1.35 *m*	1.08 *m*	1.10 *m*	1.17 *m*	1.18 *m*
2	5.72 *dt* (4.5, 10.8)	5.78 *dt* (4.7, 10.7)	4.31 *m*	5.59 *dt* (4.6, 11.1)	5.60 *dt* (4.6, 11.1)	5.74 *dt* (4.7, 11.1)	5.74 *dt* (4.6, 11.1)
3	3.68 *d* (9.9)	3.72 *d*	5.34 *d* (9.8)	3.60 *d* (9.9)	3.61 *d* (10.0)	3.71 *d* (9.9)	3.70 *d* (9.9)
5	1.00 *m*	1.01 *m*	1.04 *m*	0.92 *m*	0.96 *m*	1.01 *m*	1.03 *m*
6a	1.56 *m*	1.56 *m*	1.43 *m*	1.48 *m*	1.52 *m*	1.55 *m*	1.56 *m*
6b	1.43 *m*	1.39 *m*	1.35 *m*	1.31 *m*	1.39 *m*	1.40 *m*	1.41 *m*
7a	1.45 *m*	1.46 *m*	1.35 *m*	1.37 *m*	1.44 *m*	1.46 *m*	1.48 *m*
7b		1.39 *m*		1.28 *m*	1.35 *m*	1.39 *m*	1.40 *m*
9	1.43 *m*	1.43 *m*	1.47 *m*	1.38 *m*	1.41 *m*	1.44 *m*	1.44 *m*
11a	1.24 *m*	1.27 *m*	1.50 *m*	1.38 *m*	1.29 *m*	1.26 *m*	1.28 *m*
11b	1.16 *m*	1.18 *m*	1.23 *m*	1.18 *m*	1.18 *m*	1.17 *m*	1.19 *m*
12a	1.94 *m*	1.92 *m*	1.94 *m*	1.86 *m*	1.91 *m*	1.92 *m*	1.93 *m*
12b	1.17 *m*	1.16 *m*	1.21 *m*	1.10 *m*	1.17 *m*	1.16 *m*	1.19 *m*
13	2.73 *dt* (3.2, 9.7)	2.74 *m*	2.75 *dt* (3.5, 12.7)	2.66 *dt* (3.2, 11.7)	2.73 *m*	2.74 *m*	2.74 *dt* (3.3, 12.1)
15a	1.89 *m*	1.87 *m*	1.86 *m*	1.81 *m*	1.86 *m*	1.90 *m*	1.89 *m*
15b	1.26 *m*	1.26 *m*	1.26 *m*	1.18 *m*	1.23 *m*	1.26 *m*	1.26 *m*
16a	2.66 *m*	2.64 *m*	2.65 *m*	2.57 *m*	2.63 *m*	2.26 *m*	2.64 *m*
16b	1.59 *m*	1.56 *m*	1.56 *m*	1.49 *m*	1.54 *m*	1.57 *m*	1.57 *m*

18	1.77 *m*	1.78 *m*	1.76 *m*	1.70 *m*	1.77 *m*	1.77 *m*	1.78 *m*
19	3.56 *dt* (4.7, 10.7)	3.56 *dt* (4.8, 10.7)	3.56 *dt* (4.3, 9.9)	3.49 *dt* (4.9, 10.9)	3.55 *dt* (4.7, 10.8)	3.56 *dt* (4.8, 10.8)	3.55 *dt* (4.8, 10.8)
21a	2.26 *m*	2.26 *m*	2.26 *m*	2.49 *m*	2.26 *m*	2.27 *m*	2.27 *m*
21b	1.57 *m*	1.54 *m*	1.53 *m*	1.45 *m*	1.53 *m*	1.54 *m*	1.55 *m*
22a	2.25 *m*	2.26 *m*	2.27 *m*	2.20 *m*	2.27 *m*	2.28 *m*	2.27 *m*
22b	1.60 *m*	1.59 *m*	1.59 *m*	1.51 *m*	1.56 *m*	1.59 *m*	1.59 *m*
23	1.30 *s*	1.31 *s*	1.00 *s*	1.23 *s*	1.27 *s*	1.31 *s*	1.31 *s*
24	1.11 *s*	1.13 *s*	0.99 *s*	1.04 *s*	1.10 *s*	1.02 *s*	1.12 *s*
25	1.00 *s*	1.02 *s*	1.05 *s*	0.93 *s*	1.00 *s*	1.12 *s*	1.02 *s*
26	1.13 *s*	1.04 *s*	0.92 *s*	0.96 *s*	1.07 *s*	1.09 *s*	1.05 *s*
27	1.09 *s*	1.09 *s*	1.07 *s*	1.01 *s*	1.03 *s*	1.04 *s*	1.11 *s*
29a	4.97 *s*	4.97 *s*	4.95 *s*	4.90 *s*	4.97 *s*	4.97 *s*	4.97 *s*
29b	4.82 *s*	4.82 *s*	4.78 *s*	4.74 *s*	4.82 *s*	4.82 *s*	4.82 *s*
30	1.83 *s*	1.82 *s*	1.79 *s*	1.74 *s*	1.82 *s*	1.82 *s*	1.83 *s*
2´	8.29 *d* (1.7)	7.99 *d* (1.9)	8.21 *d* (1.8)	7.50 *d* (8.6)	8.16 *d* (8.7)	8.34 *d* (8.6)	8.30 *d* (7.1)
3´				7.10 *d* (8.6)	7.16 *d* (8.7)	7.21 *d* (8.6)	7.42 *dd* (7.1, 7.4)
4´							7.52 *t* (7.4)
5´	7.3 *d* (8.2)	7.28 *d* (8.3)	7.31 *d* (8.2)	7.10 *d* (8.6)	7.16 *d* (8.7)	7.21 *d* (8.6)	7.42 *dd* (7.1, 7.4)
6´	7.97 *dd* (1.7, 8.2)	8.06 *dd* (1.9, 8.3)	7.97 *dd* (1.9, 8.2)	7.50 *d* (8.6)	8.16 *d* (8.7)	8.34 *d* (8.6)	8.30 *d* (7.1)
8´				7.89 *d* (15.9)	6.92 *d* (12.9)		
9´				6.58 *d* (15.9)	6.07 *d* (12.9)		
-OMe´		3.72 *s*					

Every data were measured in 600 MHz, pyridine-d_5

Table 17. ^{13}C NMR spectroscopic data (δ) for compounds **25-31**

	25	**26**	**27**	**28**	**29**	**30**	**31**
1	45.4	45.5	49.3	44.8	45.3	45.5	45.3
2	74.3	74.6	67.0	73.6	74.1	74.5	75.2
3	80.1	80.1	85.6	79.6	80.1	80.2	80.2
4	40.9	41.0	40.5	40.3	40.9	41.0	41.0
5	56.0	56.2	56.0	55.5	56.1	56.1	56.2
6	19.1	19.2	18.9	18.6	19.2	19.2	19.2
7	35.0	35.1	35.0	34.5	35.1	35.1	35.1
8	41.4	41.5	41.5	40.9	39.2	41.5	41.6
9	51.1	51.3	51.2	50.6	51.2	51.4	51.3
10	38.9	39.2	38.9	38.6	41.5	43.3	39.1
11	21.6	21.7	21.7	21.1	21.7	21.7	21.8
12	26.3	26.5	26.4	25.8	26.4	26.5	26.5
13	39.0	39.0	39.0	38.4	39.0	39.0	39.3
14	43.2	43.3	43.1	42.7	43.3	43.3	43.4
15	30.5	30.7	30.5	30.0	30.6	30.7	30.7
16	33.2	33.3	33.2	32.7	33.3	33.3	33.3
17	56.9	57.0	57.0	56.3	57.0	57.0	57.0
18	50.1	50.1	50.1	49.5	50.2	50.1	50.3
19	48.1	48.2	48.2	49.6	48.2	48.2	48.2
20	151.7	151.8	151.7	151.2	150.7	151.8	151.8
21	31.5	31.6	31.6	30.9	31.6	31.6	31.6
22	38.1	38.1	38.0	37.4	38.1	38.1	38.1
23	29.4	29.6	29.2	28.9	29.5	29.5	29.5
24	17.8	17.9	18.5	17.2	17.9	17.8	17.8
25	17.7	17.9	16.8	17.3	17.8	17.9	17.8
26	16.6	16.7	17.9	16.1	15.3	15.3	16.8
27	15.2	15.3	15.3	14.7	16.7	16.7	15.3
28	179.3	179.3	179.4	178.7	179.3	179.3	179.3
29	110.4	110.5	110.8	109.9	110.5	110.5	110.4
30	19.7	19.8	19.8	19.2	19.8	19.8	19.9
1′	123.3	123.2	123.5	126.0	127.0	123.0	133.5
2′	118.3	113.9	118.3	130.4	134.1	132.9	130.4
3′	152.8	148.8	152.7	116.7	116.4	116.5	129.2
4′	147.4	153.5	147.5	161.2	161.1	163.9	132.2
5′	116.4	116.6	116.7	116.7	116.4	116.5	129.2
6′	123.4	125.2	123.5	130.4	134.1	132.9	130.4
7′	167.4	167.2	167.8	144.6	144.4	167.2	167.1
8′				115.8	117.3		
9′				167.4	167.3		
-OMe′		56.2					

Every data were measured in 150 MHz, pyridine-d_5

5.8.32. 3-*O*-protocatechuoyl ceanothic acid (**32**)

Yellowish powder

$C_{37}H_{50}O_8$

mp: 124 – 126 °C

$[\alpha]_D^{20}$ = - 17.8 (*c* 0.10, MeOH)

UV λmax (log ε): 297 (3.75), 256 (4.07) nm

IR ν_{max}: 36493, 2971, 2866, 2360, 2332, 1689, 1507, 1055, 1033, 1013 cm^{-1}

ESI-qTOF-MS *m/z*: 621.3442 $[M-H]^-$ (calcd. 621.3427)

^1H (300 MHz, pyridine-d_5) NMR: See Table 18

^{13}C (75 MHz, pyridine-d_5) NMR: See Table 19

5.8.33. 3-*O*-protocatechuoyl ceanothic acid 2-methyl ester (**33**)

Pale yellowish powder

$C_{38}H_{52}O_8$

$[\alpha]_D^{20}$ = - 4.2 (*c* 0.10, MeOH)

UV λmax (log ε): 295 (3.56), 262 (3.71) nm

IR ν_{max}: 3648, 2972, 2866, 2360, 2327, 1698, 1507, 1055, 1033, 1013 cm^{-1}

ESI-qTOF-MS *m/z*: 635.3580 $[M-H]^-$ (calcd. 635.3584)

^1H (400 MHz, pyridine-d_5) NMR: See Table 18

^{13}C (100 MHz, pyridine-d_5) NMR: See Table 19

5.8.34. 3-*O*-vanilloyl ceanothic acid (**34**)

Yellow amorphous powder

$C_{38}H_{52}O_8$

$[\alpha]_D^{20}$ = + 1.2 (*c* 0.10, MeOH)

UV λmax (log ε): 291 (3.83), 263 (4.01) nm

IR ν_{max}: 3648, 2972, 2866, 2360, 2327, 1698, 1507, 1055, 1033, 1013 cm^{-1}

ESI-qTOF-MS *m/z*: 635.3594 $[M-H]^-$ (calcd. 635.3584)

^1H (400 MHz, pyridine-d_5) NMR: See Table 18

^{13}C (100 MHz, pyridine-d_5) NMR: See Table 19

5.8.35. 3-*O*-vanilloyl epiceanothic acid (**35**)

Yellow amorphous powder

$C_{38}H_{52}O_8$

mp: 250 – 252 °C

$[\alpha]_D^{20}$ = - 31.2 (*c* 0.10, MeOH)

UV λmax (log ε): 292 (3.88), 262 (4.00) nm

IR ν_{max}: 3649, 2972, 2866, 2360, 2322, 1698, 1507, 1055, 1033, 1013 cm^{-1}

ESI-qTOF-MS *m/z*: 635.3565 $[M-H]^-$ (calcd. 635.3584)

^1H (500 MHz, pyridine-d_5) NMR: See Table 18

^{13}C (125 MHz, pyridine-d_5) NMR: See Table 19

5.8.36. 3-*O*-vanilloyl ceanothic acid 2-methyl ester (**36**)

Yellowish amorphous powder

$C_{39}H_{54}O_8$

$[\alpha]_D^{20}$ = + 7.0 (*c* 0.10, MeOH)

UV λmax (log ε): 292 (3.76), 262 (4.06) nm

IR ν_{max}: 3649, 2972, 2866, 2360, 2327, 1698, 1507, 1055, 1033, 1013 cm^{-1}

ESI-qTOF-MS *m/z*: 649.3737 $[M-H]^-$ (calcd. 649.3740)

^1H (500 MHz, pyridine-d_5) NMR: See Table 18

^{13}C (125 MHz, pyridine-d_5) NMR: See Table 19

5.8.37. 3-*O*-*p*-hydroxybenzoyl ceanothic acid (**37**)

White amorphous powder

$C_{37}H_{50}O_7$

$[\alpha]_D^{20}$ = - 2.1 (*c* 0.10, MeOH)

UV λmax (log ε): 257 (4.13) nm

IR ν_{max}: 3647, 2972, 2866, 2322, 1698, 1507, 1055, 1033, 1013 cm^{-1}

ESI-qTOF-MS *m/z*: 605.3472 $[M-H]^-$ (calcd. 605.3468)

^1H (600 MHz, pyridine-d_5) NMR: See Table 18

^{13}C (150 MHz, pyridine-d_5) NMR: See Table 19

5.8.38. 3-*O*-*p*-hydroxybenzoyl epiceanothic acid (**38**)

Pinkish amorphous powder

$C_{37}H_{52}O_7$

$[\alpha]_D^{20}$ = + 20.0 (*c* 0.10, MeOH)

UV λmax (log ε): 255 (3.67) nm

IR ν_{max}: 3649, 2971, 2864, 2317, 1684, 1507, 1055, 1033, 1012 cm^{-1}

ESI-qTOF-MS *m/z*: 605.3484 $[M-H]^-$ (calcd. 605.3468)

^1H (500 MHz, pyridine-d_5) NMR: See Table 18

^{13}C (125 MHz, pyridine-d_5) NMR: See Table 19

5.8.39. 2-*O*-protocatechuoyl isoceanothanolic acid (**39**)

White amorphous powder

$C_{37}H_{52}O_7$

$[\alpha]_D^{20}$ = + 34.9 (*c* 0.10, MeOH)

UV λmax (log ε): 298 (3.74), 262 (3.91) nm

IR ν_{max}: 3649, 2966, 2865, 2321, 1684, 1507, 1055, 1032, 1012 cm^{-1}

ESI-qTOF-MS *m/z*: 607.3639 $[M-H]^-$ (calcd. 607.3635)

^{1}H (600 MHz, pyridine-d_5) NMR: See Table 18

^{13}C (150 MHz, pyridine-d_5) NMR: See Table 19

5.8.40. 3-*O*-protocatechuoyl-ceanotha-28β,19β-olide (**40**)

White amorphous powder

$C_{37}H_{48}O_8$

$[\alpha]_D^{20}$ = - 1.4 (*c* 0.10, MeOH)

UV λmax (log ε): 297 (3.91), 262 (4.12) nm

IR ν_{max}: 3853, 2972, 2866, 2844, 2310, 1698, 1507, 1055, 1033, 1013 cm^{-1}

ESI-qTOF-MS *m/z*: 619.3257 $[M-H]^-$ (calcd. 619.3271)

^{1}H (600 MHz, pyridine-d_5) NMR: See Table 18

^{13}C (150 MHz, pyridine-d_5) NMR: See Table 19

5.8.41. 7β-*O*-vanilloyl-3-dehydroxy ceanothetric acid 2-methyl ester (**41**)

White amorphous powder

$C_{39}H_{52}O_{10}$

$[\alpha]_D^{20}$ = + 79.9 (*c* 0.10, MeOH)

UV λmax (log ε): 289 (3.91), 261 (4.30) nm

IR ν_{max}: 3649, 2972, 2866, 2360, 2332, 1684, 1507, 1055, 1033, 1013 cm^{-1}

ESI-qTOF-MS *m/z*: 679.3474 $[M-H]^-$ (calcd. 679.3482)

^{1}H (600 MHz, pyridine-d_5) NMR: See Table 18

^{13}C (150 MHz, pyridine-d_5) NMR: See Table 19

Table 18. ^{1}H NMR spectroscopic data (δ (*J* in Hz)) for compounds **32-41**

	32 [a]	**33** [b]	**34** [b]	**35** [c]	**36** [d]	**37** [c]	**38** [d]	**39** [c]	**40** [c]	**41** [c]
1	3.09 *s*	3.11 *s*	3.20 *s*	3.13 *d* (7.7)	3.20 *s*	3.18 *s*	3.51 *d* (7.8)	2.45 *dd* (5.5, 8.8)	3.14 *s*	2.71 *d* (7.6)
2a								4.46 *dd* (8.8, 10.0)		
2b								4.73 *dd* (5.5, 10.0)		
3a	5.82 *s*	5.93 *s*	6.00 *s*	5.95 *d* (7.7)	5.99 *s*	5.98 *s*	5.86 *d* (7.8)	4.37 *s*	5.97 *s*	1.87 *m*
3b										1.83 *m*
5	2.16 *m*	2.15 *m*	2.22 *m*	1.21 *m*	2.20 *m*	2.20 *m*	2.79 *m*	1.55 *m*	2.16 *m*	2.12 *m*
6a	1.39 *m*	1.41 *m*	1.51 *m*	1.55 *m*	1.48 *m*	1.44 *m*	1.44 *m*	1.44 m	1.39 *m*	2.28 *m*
6b		1.15 *m*	1.45 *m*	1.37 *m*				1.36 *m*		1.55 *m*
7a	1.47 *m*	1.40 *m*	1.51 *m*	1.43 *m*	1.48 *m*	1.49 *m*	1.57 *m*	1.41 *m*	1.58 *m*	6.02 *dd*
7b	1.38 *m*		1.42 *m*		1.41 *m*	1.41 *m*	1.42 *m*	1.37 *m*		(4.4, 10.3)
9	2.11 *m*	2.08*m*	2.16 *m*	1.76 *m*	2.14 *m*	2.13 *m*	1.29 *m*	1.84 *m*	2.11 *m*	2.21 *m*
11a	2.13 *m*	2.14 *m*	2.18 *m*	1.93 *m*	2.17 *m*	2.18 *m*	1.83 *m*	1.48 *m*	2.13 *m*	1.95 *m*
11b	1.56 *m*	1.58 *m*	1.61 *m*	1.86 *m*	1.59 *m*	1.61 *m*	1.53 *m*		1.55 *m*	1.74 *m*
12a	1.97 *m*	1.90 *m*	2.00 *m*	1.97 *m*	1.91 *m*	2.00 *m*	1.94 *m*	1.92 *m*	1.94 *m*	2.62 *m*
12b	1.33 *m*	1.30 *m*	1.37 *m*	1.28 *m*	1.30 *m*	1.35 *m*	1.31 *m*	1.29 *m*	1.25 *m*	2.10 *m*
13	2.78 *dt* (3.4, 12.6)	2.52 *dt* (3.4, 12.7)	2.80 *dt* (3.5, 12.7)	2.79 *m*	2.54 *dt* (3.5, 12.7)	2.80 *dt* (3.4, 12.7)	2.74 *m*	2.75 *m*	1.73 *m*	3.06 *m*
15a	1.88 *m*	1.89 *m*	1.91 *m*	1.94 *m*	1.58 *m*	1.90 *m*	1.91 *m*	1.88 *m*	1.74 *m*	3.00 *m*
15b	1.20 *m*	1.27 *m*	1.22 *m*	1.27 *m*	1.15 *m*	1.21 *m*	1.23 *m*	1.19 *m*	1.17 *m*	2.30 *m*
16a	2.58 *m*	2.33 *m*	2.62 *m*	2.63 *m*	2.34 *m*	2.61 *m*	2.59 *m*	2.59 *m*	2.07 *m*	2.76 *m*

16b	1.46 *m*	1.38 *m*	1.50 *m*	1.57 *m*	1.40 *m*	1.49 *m*	1.23 *m*	1.51 *m*	1.37 *m*	1.79 *m*
18	1.68 *m*	1.62 *m*	1.70 *m*	1.73 *m*	1.63 *m*	1.70 *m*	1.67 *m*	1.71 *m*	1.77 *m*	2.29 *m*
19	3.48 *dt* (4.6, 10.6)	3.27 *dt* (4.8, 10.7)	3.52 *dt* (4.8, 10.6)	3.50 *dt* (4.2, 10.9)	3.29 *dt* (4.2, 10.9)	3.52 *dt* (4.8, 10.7)	3.49 *m*	3.52 *m*		3.71 *dt* (4.5, 11.0)
21a	2.22 *m*	2.01 *m*	2.24 *m*	2.22 *m*	2.01 *m*	2.25 *m*	2.24 *m*	2.22 *m*	1.55 *m*	2.24 *m*
21b	1.46 *m*	1.42 *m*	1.50 *m*	1.48 *m*	1.43 *m*	1.49 *m*	1.48 *m*	1.48 *m*		1.48 *m*
22a	2.21 *m*	1.96 *m*	2.16 *m*	2.25 *m*	1.97 *m*	2.24 *m*	2.23 *m*	2.23 *m*	1.58 *m*	2.20 *m*
22b	1.50 *m*	1.42 *m*	1.55 *m*	1.57 *m*	1.43 *m*	1.54 *m*	1.52 *m*	1.54 *m*		1.42 *m*
23	1.50 *s*	1.52 *s*	1.58 *s*	1.36 *s*	1.58 *s*	1.57 *s*	1.40 *s*	1.16 *s*	1.53 *s*	1.18 *s*
24	1.05 *s*	1.17 *s*	1.15 *s*	1.03 *s*	1.17 *s*	1.13 *s*	1.26 *s*	1.21 *s*	1.08 *s*	0.90 *s*
25	1.14 *s*	1.07 *s*	1.27 *s*	1.67 *s*	1.30 *s*	1.26 *s*	0.99 *s*	1.31 *s*	1.15 *s*	0.99 *s*
26	1.12 *s*	1.07 *s*	1.15 *s*	1.15 *s*	1.10 *s*	1.14 *s*	1.10 *s*	1.10 *s*	0.91 *s*	1.63 *s*
27	1.03 *s*	0.97 *s*	1.06 *s*	1.08 *s*	1.01 *s*	1.06 *s*	1.13 *s*	1.09 *s*	0.88 *s*	
29a	4.83 *s*	4.80 *s*	4.87 *s*	4.89 *s*	4.85 *s*	4.87 *s*	4.87 *s*	4.93 *s*	5.49 *s*	5.09 *s*
29b	4.63 *s*	4.63 *s*	4.67 *s*	4.73 *s*	4.65 *s*	4.67 *s*	4.66 *s*	4.79 *s*	4.99 *s*	4.84 *s*
30	1.65 *s*	1.62 *s*	1.68 *s*	1.77 *s*	1.64 *s*	1.68 *s*	1.65 *s*	1.74 *s*	1.62 *s*	1.95 *s*
2′	8.08 *d* (2.3)	8.10 *d* (1.8)	7.91 *d* (1.9)	7.92 *br s*	7.91 *d* (1.9)	8.27 *d* (8.7)	8.32 *d* (8.7)	8.22 *d* (1.9)	8.14 *br s*	7.97 *d* (1.1)
3′						7.25 *d* (8.7)	7.01 *d* (8.7)			
5′	7.29 *d* (8.2)	7.32 *d* (8.3)	7.31 *d* (8.2)	7.10 *d* (8.2)	7.31 *d* (8.2)	7.25 *d* (8.7)	7.01 *d* (8.7)	7.28 *d* (8.3)	7.4 *d* (8.3)	7.20 [e]
6′	7.88 *dd* (2.3, 8.2)	7.90 *dd* (1.8, 8.3)	7.95 *dd* (1.9, 8.2)	8.02 *d* (8.2)	7.95 *dd* (8.2, 1.9)	8.27 *d* (8.7)	8.32 *d* (8.7)	7.90 *dd* (1.9, 8.3)	7.92 *d* (8.3)	8.01 *dd* (8.2, 1.1)
-OMe		3.72 *s*			3.74 *s*					3.78 *s*
-OMe′			3.79 *s*	3.70 *s*	3.80 *s*					3.76 *s*

[a] Recorded at 300 MHz [b] Recorded at 400 MHz [c] Recorded at 600 MHz [d] Recorded at 500 MHz [e] overlapped. Every data were measured in pyridine-d_5

Table 19. ^{13}C NMR spectroscopic data (δ) for compounds **32-41**

	32 [a]	**33** [b]	**34** [b]	**35** [c]	**36** [d]	**37** [c]	**38** [d]	**39** [c]	**40** [c]	**41** [c]
1	64.2	64.1	64.7	61.4	64.8	64.7	60.5	58.7	64.8	55.3
2	174.7	176.5	177.3	174.0	177.3	177.3	174.5	65.1	177.3	176.4
3	85.8	85.8	86.5	85.3	86.6	86.4	83.4	85.4	86.2	42.9
4	43.7	43.7	44.2	43.1	44.3	44.2	42.4	43.5	44.0	38.3
5	56.8	56.8	57.3	62.6	57.5	57.4	56.3	58.5	57.2	52.8
6	18.7	18.7	19.0	18.1	19.3	19.2	19.6	19.0	19.0	25.6
7	34.6	34.5	35.1	34.7	35.1	35.1	35.0	34.5	35.2	80.9
8	42.4	43.4	44.0	41.9	42.6	42.6	42.6	42.4	42.5	46.6
9	45.3	45.2	45.8	51.0	45.8	45.8	44.5	43.1	45.7	46.7
10	49.5	49.5	50.1	47.6	50.3	50.1	48.2	46.9	49.7	51.6
11	24.2	24.1	24.6	24.7	24.7	24.7	24.4	24.0	23.8	24.2
12	26.2	26.1	26.7	25.8	26.7	26.7	26.5	25.6	26.4	27.0
13	39.0	39.0	39.5	38.5	39.6	39.5	39.3	38.9	36.1	41.2
14	42.1	42.0	42.6	42.9	43.9	44.0	44.0	43.3	42.3	61.3
15	30.5	30.3	31.0	30.5	30.9	31.1	31.0	30.3	28.8	31.5
16	32.9	32.4	33.3	32.9	32.9	33.4	33.4	32.9	34.7	36.0
17	56.6	56.8	57.1	56.5	57.4	57.1	57.1	56.8	54.5	56.6
18	49.7	49.7	50.1	49.8	50.3	50.1	50.2	49.7	55.9	52.2
19	47.6	47.3	48.0	47.8	47.9	48.1	48.0	47.8	92.7	48.6

20	151.1	150.7	151.6	151.2	151.2	151.6	151.6	151.5	141.8	151.8
21	31.3	31.0	31.7	31.2	31.6	31.8	31.7	31.0	24.2	31.6
22	37.6	37.0	38.0	37.6	37.6	38.0	38.0	37.5	29.6	37.9
23	30.6	30.6	31.1	31.0	31.2	31.1	25.6	32.8	30.9	31.8
24	20.2	20.2	20.7	19.5	20.8	20.7	26.3	20.4	20.6	27.0
25	18.5	18.4	19.0	14.4	19.1	19.1	19.8	18.9	19.1	19.3
26	17.0	16.8	17.5	16.8	17.4	17.5	17.5	17.2	16.7	13.5
27	15.0	14.9	15.4	15.0	15.5	15.5	15.7	14.8	14.2	178.7
28	179.0	176.5	179.4	178.8	177.0	179.4	179.3	179.4	179.1	179.8
29	109.7	109.9	110.3	110.0	110.5	110.3	110.3	110.1	112.7	110.7
30	19.6	19.6	20.7	19.5	20.2	20.2	19.9	19.3	19.6	19.8
1′	122.2	122.2	122.3	121.8	122.5	122.2	122.2	123.3	123.4	123.4
2′	117.6	117.6	113.9	113.6	114.1	132.9	133.0	117.9	118.1	114.0
3′	152.7	152.5	149.0	148.3	149.2	116.8	116.5	152.9	153.2	148.8
4′	147.1	147.1	153.8	153.2	153.9	164.2	164.1	147.5	147.5	153.5
5′	116.8	116.4	116.8	116.2	116.9	116.8	116.5	116.1	116.8	116.8
6′	122.7	123.5	125.0	124.7	125.1	132.9	133.0	123.0	123.5	125.0
7′	166.5	166.5	166.7	166.6	166.9	166.7	166.9	167.7	167.0	165.9
-OMe		51.4			51.9					51.9
-OMe′			56.2	55.6	56.4					56.1

[a] Recorded at 75 MHz [b] Recorded at 100 MHz [b] Recorded at 150 MHz [b] Recorded at 125 MHz. Every data were measured in pyridine-d_5

5.8.42. Epicatechinoceanothic acid A (**42**)

White amorphous powder

$C_{31}H_{48}O_5$

$[\alpha]_D^{20}$ = - 6.1 (*c* 0.10, MeOH)

UV λmax (log ε): 326 (3.18), 257 (3.67) nm

CD (MeOH) (Δε): 327 (-8.5), 258 (6.9), 216 (-22.3), 202 (34.2) nm

ESI-qTOF-MS *m/z*: 739.3839 $[M-H]^-$ (calcd. 739.3846)

^1H (600 MHz, pyridine-d_5) NMR: See Table 20

^{13}C (150 MHz, pyridine-d_5) NMR: See Table 20

(*S*)-MTPA-ester of **42** (**42a**): ^1H NMR (600 MHz, pyridine-d_5): δ 7.53 (1H, *s*, H-2″), 7.24 (1H, *s*, H-6″), 7.23 (1H, *s*, H-5″), 6.97 (1H, *s*, H-6′), 6.23 (1H, *m*, H-3′), 5.80 (1H, *m*, H-2′), 4.84 (2H, *s*, H-29), 2.56 (2H, *m*, H-4′), 1.77 (3H, *s*, H-30)

(*R*)-MTPA-ester of **42** (**42b**): ^1H NMR (600 MHz, pyridine-d_5): δ 7.97 (1H, *s*, H-2″), 7.51 (1H, *s*, H-6″), 7.39 (1H, *s*, H-5″), 6.94 (1H, *s*, H-6′), 6.03 (1H, *m*, H-3′), 5.70 (1H, *m*, H-2′), 4.84 (2H, *s*, H-29), 2.45 (2H, *m*, H-4′), 1.82 (3H, *s*, H-30)

5.8.43. Epicatechinoceanothic acid B **(43**)

White amorphous powder

$C_{31}H_{48}O_5$

$[\alpha]_D^{20}$ = - 24.1 (*c* 0.10, MeOH)

UV λmax (log ε): 287 (3.84), 236 (3.62) nm

CD (MeOH) (Δε): 284 (12.3), 236 (-11.9), 202 (15.2) nm

ESI-qTOF-MS *m/z*: 723.3892 $[M-H]^-$ (calcd. 723.3897)

^1H (600 MHz, pyridine-d_5) NMR: See Table 20

^{13}C (150 MHz, pyridine-d_5) NMR: See Table 20

5.8.44. Epicatechinoceanothic acid C **(44)**

White amorphous powder

$C_{31}H_{48}O_5$

$[\alpha]_D^{20}$ = -23.1 (*c* 0.10, MeOH)

UV λmax (log ε): 285 (3.52), 243 (3.45) nm

CD (MeOH) (Δε): 321 (-1.4), 291 (-0.4), 248 (-3.3), 229 (-0.5), 216 (-2.3) nm

ESI-qTOF-MS *m/z*: 723.3892 $[M-H]^-$ (calcd. 723.3897)

^1H (600 MHz, pyridine-d_5) NMR: See Table 20

^{13}C (150 MHz, pyridine-d_5) NMR: See Table 20

Table 20. ^{1}H and ^{13}C NMR spectroscopic data (δ (*J* in Hz)) of compounds **42-44**

	42		**43**		**44**	
	δ_H	δ_C	δ_H	δ_C	δ_H	δ_C
1	4.05 *s*	54.1		146.0		146.7
2		208.9	6.99 *s*	107.8	7.05 *s*	114.6
3	3.93 *s*	87.4	4.86 *s*	85.6	4.61 *s*	88.5
4		45.2		40.7		41.2
5	1.89 *m*	46.6	1.47 *m*	62.6	1.37 *m*	59.7
6a	1.48 *m*	18.4	1.39 *m*	18.2	1.41 *m*	16.9
6b	1.33 *m*		1.30 *m*			
7a	1.41 *m*	34.6	1.42 *m*	34.8	1.40 *m*	35.1
7b	1.37 *m*		1.36 *m*		1.34 *m*	
8		42.1		42.5		43.5
9	2.01 *m*	43.0	2.11 *m*	46.7	1.92 *m*	48.7
10		50.3		45.5		45.6
11a	2.09 *m*	23.1	1.63 *m*	24.3	1.72 *m*	22.9
11b	1.60 *m*		1.36 *m*		1.48 *m*	
12a	1.95 *m*	26.9	1.96 *m*	26.0	1.56 *m*	25.1
12b	1.41 *m*		1.27 *m*		0.80 *m*	
13	2.70 *dt* (3.0, 11.0)	39.0	2.72 *m*	38.7	2.63 *m*	38.1
14		43.5		43.1		43.3
15a	1.79 *m*	30.3	1.93 *m*	30.5	1.85 *m*	30.3
15b	1.15 *m*		1.23 *m*		1.19 *m*	
16a	2.55 *m*	33.0	2.23 *m*	31.3	2.24 *m*	31.2
16b	1.48 *m*		1.50 *m*		1.51 *m*	
17		56.6		56.6		56.7
18	1.82 *m*	49.7	1.72 *m*	49.6	1.60 *m*	49.7
19	3.45 *dt* (3.8, 10.0)	47.3	3.47 [a]	47.7	3.44 *m*	47.8
20		151.2		151.2		151.0
21a	2.22 *m*	31.5	2.63 *m*	32.9	2.63 *m*	32.9
21b	1.52 *m*		1.55 *m*		1.53 *m*	
22a	2.20 *m*	37.5	2.24 *m*	37.6	2.24 *m*	37.5
22b	1.55 *m*		1.57 *m*		1.56 *m*	
23	1.21 *s*	28.7	1.25 *s*	25.8	1.22 *s*	29.1
24	0.86 *s*	19.7	1.06 *s*	14.9	1.10 *s*	17.8
25	0.93 *s*	17.0	0.90 *s*	17.4	1.17 *s*	22.0
26	1.02 *s*	17.0	1.05 *s*	25.4	1.03 *s*	17.7
27	0.97 *s*	14.9	1.03 *s*	17.1	0.96 *s*	14.7
28		178.9		179.0		178.9
29a	5.10 *s*	109.7	4.88 *s*	110.1	4.88 *s*	110.1
29b	5.02 *s*		4.72 *s*		4.76 *s*	

30	2.00 *s*	20.5	1.75 *s*	19.5	1.76 *s*	19.6
2′	5.58 *s*	80.6	5.38 *s*	80.1	5.33 *s*	80.0
3′	4.76 *br s*	66.6	4.69 *br s*	66.9	4.68 *br s*	66.5
4′a	3.51 *d* (4.36)	28.7	3.45 [a]	29.7	3.53 *m*	30.0
4′b			3.36 *dd* (4.2, 16.1)		3.37 *dd* (4.5, 16.0)	
4a′		101.2		106.4		108.0
5′		157.8		156.2		
6′	6.43 *s*	94.8	6.67 *s*	96.7	6.66 *s*	96.7
7′		155.3		146.0		155.1
8′		99.6		103.1		103.0
8a′		154.6		153.6		
1′′		131.6		131.8		131.9
2′′	7.75 *s*	155.5	7.88 *s*	116.5	7.89 *s*	116.3
3′′		146.8		150.0		
4′′		146.8		146.9		146.8
5′′	7.25 *s*	116.0	7.31 *d* (8.1)	119.3	7.31 [a]	119.3
6′′	7.25 *s*	118.9	7.28 *d* (8.1)	116.3	7.28 [a]	116.3

[a] overlapped. Every data were measured at 600 MHz (^{1}H) and 150 MHz (^{13}C)

5.8.45. Maslinic acid (**45**)

White amorphous powder

$C_{30}H_{48}O_4$

mp: 228 – 230 °C

$[\alpha]_D^{20}$ = + 45.7 (*c* 0.10, MeOH)

ESI-qTOF-MS *m/z*: 471.3477 $[M-H]^-$ (calcd. 471.3477)

^{1}H (600 MHz, pyridine-d_5) NMR: δ 5.49 (1H, *t*, *J* = 3.4 Hz, H-12), 4.12 (1H, d*t*, *J* = 4.5, 11.3 Hz, H-2), 3.42 (1H, *d*, 9.4 Hz, H-3), 3.32 (1H, *dt*, *J* = 4.2, 13.8 Hz, H-18), 2.26 (1H, *m*, H-1a), 2.18 (1H, *m*, H-15a), 2.12 (1H, *m*, H-16a), 2.06 (1H, *m*, H-22a), 2.03 (2H, *m*, H-11), 1.99 (1H, *m*, H-16b), 1.85 (1H, *m*, H-22b), 1.83 (1H, *m*, H-9), 1.80 (1H, *m*, H-19a), 1.59 (1H, *m*, H-6a), 1.53 (1H, *m*, H-21a), 1.46 (1H, *m*, H-7a), 1.41 (1H, *m*, H-6b), 1.34 (1H, *m*, H-21b), 1.32 (1H, *m*, H-1b), 1.29 (1H, *m*, H-19b), 1.29 (1H, *s*, H-23), 1.28 (1H, *s*, H-27), 1.21 (1H, *m*, H-15b), 1.21 (1H, *m*, H-7b), 1.11 (1H, *s*, H-24), 1.05 (1H, *m*, H-5), 1.04 (1H, *s*, H-26), 1.01 (1H, *s*, H-30), 1.00 (1H, *s*, H-25), 0.96 (1H, *s*, H-29)

^{13}C (150 MHz, pyridine-d_5) NMR: δ 180.7 (C-28), 145.3 (C-13), 122.9 (C-12), 84.3 (C-3), 69.0 (C-2), 56.4 (C-5), 48.6 (C-9), 48.2 (C-1), 47.1 (C-17), 46.9 (C-19), 42.7 (C-14), 42.4 (C-18), 40.3 (C-4), 40.2 (C-8), 39.0 (C-10), 34.7 (C-7), 33.6 (C-21), 33.7 (C-29), 33.6 (C-22), 31.4 (C-20), 29.8 (C-23), 28.7 (C-15), 26.6 (C-27), 24.4 (C-11), 24.2 (C-30), 24.1 (C-16), 19.3 (C-6), 18.2 (C-24), 17.9 (C-26), 17.3 (C-25)

5.8.46. Euscaphic acid (**46**)

White amorphous powder

$C_{30}H_{48}O_5$

$[\alpha]_D^{20}$ = + 11.1 (*c* 0.10, MeOH)

ESI-qTOF-MS *m/z*: 487.3417 $[M-H]^-$ (calcd. 487.3423)

^1H (600 MHz, pyridine-d_5) NMR: δ 5.56 (1H, *s,* H-12), 3.41 (1H, *td, J* = 3.0, 10.7, H-2), 3.77 (1H, *d, J* = 2.5 Hz, H-3), 3.09 (1H, *dt, J* = 4.5, 13.1 Hz, H-16a), 3.02 (1H, *s,* H-18), 2.31 (1H, *m,* H-15a), 2.12 (1H, *m,* H-11a), 2.11 (1H, *m,* H-21a), 2.06 (1H, *m,* H-22a), 2.05 (1H, *m,* H-9), 2.05 (1H, *m,* H-21b), 2.03 (1H, *m,* H-11b), 2.02 (1H, *m,* H-16b), 1.87 (1H, *m,* H-1a), 1.75 (1H, *m,* H-1b), 1.65 (1H, *m,* H-5), 1.64 (1H, *m,* H-7a), 1.61 (3H, *s,* H-27), 1.48 (1H, *m,* H-6a), 1.47 (1H, *m,* H-20), 1.41 (3H, *s,* H-29), 1.36 (1H, *m,* H-7b), 1.32 (1H, *m,* H-6b), 1.30 (1H, *m,* H-12b), 1.25 (3H, *s,* H-23), 1.24 (1H, *m,* H-15b), 1.11 (3H, *d, J* = 6.7 Hz, H-30), 1.08 (3H, *s,* H-26), 0.95 (3H, *s,* H-25), 0.87 (3H, *s,* H-24)

^{13}C (150 MHz, pyridine-d_5) NMR: δ 181.2 (C-28), 140.2 (C-13), 128.2 (C-12), 79.6 (C-3), 72.8 (C-19), 66.4 (C-2), 54.9 (C-18), 49.0 (C-5), 48.5 (C-17), 47.8 (C-9), 43.0 (C-1), 42.6 (C-20), 42.4 (C-14), 40.8 (C-8), 39.1 (C-4), 38.9 (C-10), 38.8 (C-11), 33.7 (C-7), 29.7 (C-23), 29.3 (C-15), 27.3 (C-29), 27.2 (C-22), 26.6 (C-16), 24.9 (C-27), 24.3 (C-21), 22.5 (C-24), 18.8 (C-6), 17.5 (C-26), 17.0 (C-30), 16.9 (C-25)

5.8.47. (-)-epicatechin (**47**)

Brown syrup

$C_{15}H_{14}O_6$

$[\alpha]_D^{20}$ = -11.4 (*c* 0.10, MeOH)

ESI-qTOF-MS *m/z*: 291.0870 $[M+H]^+$ (calcd. 291.0868)

^1H (300 MHz, DMSO-d_6) NMR: δ 6.88 (1H, *s,* H-2′), 6.65 (2H, *br s,* H-5′, H-6′), 5.89 (1H, *d, J* =2.2 Hz, H-8), 5.71 (1H, *d, J* =2.2 Hz, H-6), 4.71 (1H, *s*, H-2), 3.98

(1H, *br s*, H-3), 2.66 (1H, *dd*, *J* =15.9, 4.0 Hz, H-4a), 2.49 (1H, *dd, J* =15.9, 4.0 Hz, H-4b)

^{13}C (75 MHz, DMSO-d_6) NMR: δ 156.5 (C-8), 156.2 (C-8a), 155.8 (C-7), 144.5 (C-3′), 144.4 (C-4′), 130.6 (C-1′), 117.9 (C-6′), 114.9 (C-2′), 114.8 (C-5′), 98.5 (C-4a), 95.0 (C-6), 94.0 (C-8), 78.1 (C-2), 64.9 (C-3), 28.3 (C-4)

5.8.48. (+)-catechin (**48**)

Brown syrup

$C_{15}H_{14}O_6$

$[\alpha]_D^{20}$ = +10.7 (*c* 0.10, MeOH)

ESI-qTOF-MS *m/z*: 291.0870 $[M+H]^+$ (calcd. 291.0868)

^{1}H (300 MHz, DMSO-d_6) NMR: δ 6.69 (1H, *d, J* = 1.8 Hz, H-2′), 6.68 (1H, *d, J* = 8.1 Hz, H-5′), 6.59 (1H, *dd, J* = 8.1, 1.8 Hz, H-6′), 5.86 (1H, *d, J* =2.4 Hz, H-8), 5.66 (1H, *d, J* =2.4 Hz, H-6), 4.45 (1H, *d, J* =7.5 Hz, H-2), 3.92 (1H, *m*, H-3), 2.50 (1H. *dd, J* =16.1, 5.5 Hz, H-4a), 2.48 (1H, *dd, J* =16.1, 5.5 Hz, H-4b)

^{13}C (75 MHz, DMSO-d_6) NMR: 156.4 (C-8), 156.2 (C-8a), 155.3 (C-7), 144.8 (C-3′), 144.8 (C-4′), 130.6 (C-1′), 118.4 (C-6′), 115.0 (C-2′), 114.5 (C-5′), 99.0 (C-4a), 95.1 (C-6), 93.8 (C-8), 80.9 (C-2), 66.3 (C-3), 27.9 (C-4)

5.8.49. Vanillic acid (**49**)

White amorphous powder

$C_8H_8O_4$

ESI-qTOF-MS *m/z*: 167.0347 $[M-H]^-$ (calcd. 167.0344)

^{1}H (300 MHz, pyridine-d_5) NMR: δ 8.17 (*dd*, *J* = 1.8, 8.1 Hz, H-6), 8.08 (*d, J* = 1.8 H-2), 7.31 (*d, J* = 8.1 Hz, H-5), 3.74 (*s,* OCH_3)

^{13}C (75 MHz, pyridine-d_5) NMR: δ 169.1 (C-7), 152.7 (C-3), 148.3 (C-4), 124.9 (C-1), 122.9 (C-6), 116.2 (C-2), 113.8 (C-5), 55.8 (OCH_3)

5.8.50. 6′-*O*-vanilloylisotachioside (**50**)

Brown syrup

$C_{21}H_{24}O_{11}$

ESI-qTOF-MS *m/z*: 451.1240 $[M-H]^-$ (calcd. 451.1240)

^{1}H (400 MHz, MeOD) NMR: δ 7.55 (1H, *dd, J* = 8.2, 2.9 Hz, H-6″), 7.52 (1H, *d, J* = 2.9 Hz, H-2″), 6.84 (1H, *d, J* = 8.2 Hz, H-5″), 6.92 (1H, *d, J* = 8.7 Hz, H-6), 6.42 (1H, *d, J* = 2.7 Hz, H-3), 6.11 (1H, *dd, J* = 8.2, 2.7 Hz, H-5), 4.70 (1H, *m*, H-1′), 4.65 (1H, *dd, J* = 6.9, 11.8 Hz, H-6′a), 4.35 (1H, *m*, H-6′b) 3.85 (3H, *s*, 3″-OCH_3), 3.77 (3H, *s,* 2-OCH_3), 3.65 (1H, *m,* H-5′), 3.47 (1H, *m*, H-3′), 3.46 (1H, *m*, H-2′), 3.39 (1H, *m*, H-4′)

^{13}C (100 MHz, MeOD) NMR: δ 168.8 (C-7″), 155.8 (C-4), 154.4 (C-3″), 152.9 (C-2), 149.7 (C-4″), 141.6 (C-1), 126.1 (C-6″), 122.8 (C-1″), 121.4 (C-6), 116.9 (C-5″), 114.5 (C-2″), 108.3 (C-5), 102.6 (C-3), 105.0 (C-1′), 78.4 (C-3′), 76.4 (C-5′), 75.8 (C-2′), 72.9 (C-4′), 65.9 (C-6′), 57.3 (2-OCH_3), 57.3 (3″-OCH_3)

5.8.51. Epiphyllocoumarin (**51**)

Yellow syrup

$C_{18}H_{15}O_7$

ESI-qTOF-MS *m/z*: 343.0819 $[M+H]^+$ (calcd. 343.0817)

^{1}H (400 MHz, MeOD) NMR: δ 8.12 (1H, *d, J* = 9.5 Hz, H-9), 7.05 (1H, *s,* H-2′), 6.84 (1H, overlapped, H-6′), 6.79 (1H, overlapped, H-5′), 6.34 (1H, *s,* H-6), 6.08

(1H, *d, J* = 9.5, H-10), 5.04 (1H, *s*, H-2), 4.29 (1H, *br s*, H-3), 2.94 (1H, *m,* H-4a), 2.87 (1H, *m,* H-4a)

^{13}C (100 MHz, MeOD) NMR: δ 165.1 (C-11), 162.8 (C-8a), 156.8 (C-7), 154.2 (C-5), 146.9 (C-3′), 146.8 (C-4′), 141.9 (C-9), 132.1 (C-1′), 120.1 (C-6′), 116.9 (C-5′), 116.0 (C-2′), 110.8 (C-10), 106.2 (C-8), 104.5 (C-4a), 96.2 (C-6), 81.5 (C-2), 67.3 (C-3), 30.1 (C-4)

5.8.52. Isoepiphyllocoumarin (**52**)

Yellow syrup

$C_{18}H_{15}O_7$

ESI-qTOF-MS *m/z*: 343.0819 $[M+H]^+$ (calcd. 343.0817)

^{1}H (400 MHz, MeOD) NMR: δ 8.10 (1H, *d, J* = 9.5 Hz, H-9), 6.98 (1H, *s,* H-2′), 6.82 (1H, overlapped*,* H-6′), 6.77 (1H, overlapped*,* H-5′), 6.32 (1H, *s,* H-8), 6.10 (1H, *d, J* = 9.5, H-10), 5.01 (1H, *s*, H-2), 4.28 (1H, *br s*, H-3), 3.03 (1H, *m,* H-4a), 2.94 (1H, *m,* H-4a)

^{13}C (100 MHz, MeOD) NMR: δ165.0 (C-11), 161.3 (C-8a), 156.5 (C-7), 156.1 (C-5), 146.9 (C-3′), 146.8 (C-4′), 142.4 (C-9), 132.1 (C-1′), 120.2 (C-6′), 116.8 (C-5′), 116.1 (C-2′), 110.6 (C-10), 105.8 (C-6), 101.2 (C-4a), 100.4 (C-8), 81.6 (C-2), 67.1 (C-3), 29.3 (C-4)

5.9. Evaluation of antiviral effects of cyclopeptide alkaloids against pocrine epidemic diarrhea virus

5.9.1. Cell culture and virus stock

Vero cells (African green monkey kidney cell line; ATCC CCR-81) were provided by the American Type Culture Collection (ATCC, Manassas, VA, USA) and maintained in Dulbecco's Modified Eagle's Medium with 100 U/mL penicillin, 100 μg/mL streptomycin (Sigma) and 10% fetal bovine serum (FBS, Hyclone, Logan, UT, USA). PEDV was obtained from Choong Ang Vaccine Laboratory, Korea. The virus stock was kept at - 80 °C before use.

5.9.2. Cytotoxicity assay

The cell viability was calculated using a MTT (3-(4,5-dimethyl-2-thiazolyl)-2,5-diphenyl-2H-tetrazolium bromide) assay. Vero cells were adhered at 1×10^5 cells per well in 96-well plates and grown for 24 h before treatment. The cells were treated with various concentrations of compounds. To avoid solvent toxicity, the final DMSO concentration was maintained under 0.05% (v/v) in the culture medium. After incubating further for 48 h, MTT solution (2 mg/mL, 20 μL) was added to each well and kept for 4 h. After removing the supernatant, DMSO (100 μL) was added to solubilize formazan crystals. Consequently, the absorbance was measured at 550 nm. The percentage cell viability is the absorbance in the experiment well compared to that in the control wells and compound toxicity is the percentage cell viability. Regression analysis was used to calculate 50% cytotoxic concentration (CC_{50}).

5.9.3. Cytopathic effect (CPE) inhibition assay

Vero cells were seeded onto 96-well plates at 1×10^5 cells per well. The medium was removed a day later and washed with phosphate buffered saline (PBS). PEDV at 0.01 MOI was inoculated onto near-confluent Vero cell monolayers for 2 h. The media was replaced by DMEM with various concentrations of compounds. After incubating for 72 h at 37 °C under 5% CO_2 atmosphere, cells were replaced with DMEM and MTT (2 mg/mL, 20 μL) to each well and incubated for 4 h at 37 °C. The 50% effective concentration (EC_{50}) was calculated using regression analysis, and the formula $SI = CC_{50}/EC_{50}$ determined the selective index (SI).

5.10. Evaluation of cytotoxicity of triterpenoids

5.10.1. Cell culture

HepG2 cells (human hepatocellular carcinoma cell line; ATCC HB-8065) were purchased by Korean Cell Line Bank (KCLB, Korea). HepG2 cells were cultured in DMEM medium, supplemented with 10% fetal bovine serum and 100 U/mL penicillin, 100 μg/mL streptomycin in a humidified atmosphere environment with 5% CO_2 at 37 °C.

5.10.2. Cytotoxicity assay

Each cytotoxicity assay was conducted according to the MTT method in 96-well microplates. Briefly, 200 μL adherent cells were seeded into 96-well microculture plates and allowed to adhere for 12 h before drug addition, with an initial density of 5×10^4 cells/mL in 200 μL medium. HepG2 cells were then exposed to samples dissolved in DMSO at four concentrations of 1, 5, 10 and 25 μM, with 5-fluorouracil as a positive control. After incubation for 48 h under growth conditions, MTT was added, and the incubation of cells was continued for another 4 h. After removing the supernatant, DMSO (100 μL) was added to solubilize formazan crystals. Consequently, the absorbance was measured at 550 nm. The percentage cell viability is the absorbance in the experiment well compared to that in the control wells and compound toxicity is the percentage cell viability. Regression analysis was used to calculate IC_{50}. The experiments were conducted for three independent replicates.

Chapter 6. Conclusions

The aim of this research was the discovery of bioactive cyclopeptide alkaloid and triterpenoid constituents of *Z. jujuba* using LC-MS based dereplication strategy. For this objective, analytical methods were developed and optimized for rapid LC-MS profiling of cyclopeptide alkaloids and triterpenic acids. Each analytical method could analyze target compounds specifically within 20 minutes.

With the optimized analytical methods, cyclopeptide alkaloids of roots, twigs, leaves, and fruits of *Z. jujuba* were analyzed by LC-MS at first. The root extract was the most abundant in cyclopeptide alkaloids among extracts of the four plant parts, so it was selected to be further separated. Tentative identification prior to isolation was not possible because of a lack of chemical database for cyclopeptide alkaloids. Nine cyclopeptide alkaloids (compounds **1**-**9**) were isolated by MS-guided fractionation and their chemical structures were elucidated. Compounds **1**-**5** were firstly isolated from nature. Isolated compounds were analyzed by the analytical method, and their retention time, MS, MS/MS, and UV spectra were matched to nine major chromatographic peaks in the LC-MS profile of the root extract. Some of characteristic spectral properties were found to be applied for further profiling and dereplication studies of cyclopeptide alkaloids.

Triterpenic acids of root, twig, leaf, and fruit extracts of *Z. jujuba* were also analyzed by the optimized LC-MS analytical method. Among the observed 52 chromatographic peaks, 30 peaks were identified tentatively based on their relative retention time and spectral data with consideration of chemotaxonomy. In this dereplication process, it was found that ceanothane-type triterpenoids could be distinguished from lupane- or oleanane-type triterpenoids by MS/MS fragmentation patterns. In addition, it was found that UV and MS/MS spectra also provide structural information about aromatic ester moieties.

Many unidentified chromatographic peaks were observed in the LC-MS profile of

the root extract, so it was determined to be further separated for searching of unknown triterpenic chemical entities. As a result, 37 triterpenoids (compounds **10-46**) and 6 phenolic compounds (**47-52**) were isolated from the root extract. Compounds **16-20**, **23**, **24**, **26**, **27**, **30**, **33**, **35-44** were isolated from nature for the first time. Within these new compounds, several compounds showed uncommon structural properties. Compounds **20** and **40** were a ceanothane-type triterpenic latone and its ester derivative, and compound **24** was a dinorlupane derivative with cyclopentenyl A-ring. Compound **41** has its aromatic *O*-ester substituent at C-7 position. Compounds **42-44** showed unique backbones which were built by a C-C bond between a ceanothane-type triterpene and a catechin moiety. By injection of isolated triterpenoids into LC-MS, it was validated that structures of isolated triterpenoids matched to predicted structures in the dereplication process.

Bioactivity screening was performed for isolated constituents of *Z. jujuba*. Isolated cyclopeptide alkaloids, **2**, **3**, **6** showed antiviral effects against PEDV, and triterpenoid compounds **10**, **22**, **28-30**, **33**, **35**, **36**, **41** exhibited potent cytotoxicity against HepG2 cell line. Therefore, it has been proven that dereplication based on LC-MS is an excellent strategy for the efficient discovery of bioactive phytochemicals with novel chemical structures.

References

Abdel Bar, F. M., Zaghloul, A. M., Bachawal, S. V., Sylvester, P. W., Ahmad, K. F., El Sayed, K. A., 2008. Antiproliferative triterpenes from *Melaleuca ericifolia*. *J Nat Prod* 71, 1787-1790.

Agrawal, P. K., Thakur, R. S., Bansa;, M. C., 1989. Flavonoids. In: Agrawal, P. K. (Ed.), Carbon ^{13}C NMR of flavonoids. Elservier, Amsterdam.

Aldini, G., Regazzoni, L., Pedretti, A., Carini, M., Cho, S. M., Park, K. M., Yeum, K. J., 2011. An integrated high resolution mass spectrometric and informatics approach for the rapid identification of phenolics in plant extract. *J Chromatogr A* 1218, 2856-2864.

Arai, M. A., Tateno, C., Hosoya, T., Koyano, T., Kowithayakorn, T., Ishibashi, M., 2008. Hedgehog/GLI-mediated transcriptional inhibitors from *Zizyphus cambodiana*. *Bioorg Med Chem* 16, 9420-9424.

Barboni, L., Gariboldi, P., Torregiani, E., Verotta, L., 1994. Cyclopeptide alkaloids from *Ziziphus mucronata*. *Phytochemistry* 35, 1579-1582.

Beutler, J. A., Alvarado, A. B., Schaufelberger, D. E., Andrews, P., McCloud, T. G., 1990. Dereplication of phorbol bioactives: *Lyngbya majuscula* and *Croton cuneatus*. *J Nat Prod* 53, 867-874.

Branch, G. B., Burgess, D. V., Mack, J. P. G., Dunstan, P. J., Taylor, W. C., Foo, L. Y., Ritchie, E., Green, G. H., 1972. Constituents of *Alphitonia* species 3. Alphitexolide, a New Triterpene, and Other Extractives. *Aust J Chem* 25, 2209-2216.

Brand, D. J., Steenkamp, J. A., Brandt, E. V., Takeuchi, Y., 2007. Conformational studies of (-)-epicatechin-Mosher ester. *Tetrahedron Lett* 48, 2769-2773.

Chen, Z. Z., Tong, L., Peng, Y. L., Wu, J. Z., Zhao, X. Y., Ruan, H. L., Pi, H. F., Zhang, P., 2015. Ursane-type nortriterpenes with a five-membered A-ring from *Rubus innominatus*. *Phytochemistry* 116, 329-336.

Choi, H., Mevers, E., Byrum, T., Valeriote, F. A., Gerwick, W. H., 2012. Lyngbyabellins K-N from two palmyra atoll collections of the marine cyanobacterium *Moorea bouillonii*. *Eur J Org Chem*, 5141-5150.

Cichewicz, R. H., Kouzi, S. A., 2004. Chemistry, biological activity, and chemotherapeutic potential of betulinic acid for the prevention and treatment of cancer and HIV infection. *Med Res Rev* 24, 90-114.

de Lima, R. B., Giulietti, A. M., 2014. Synonymies and typification of the Rhamnaceae of Brazil. *Acta Bot Bras* 28, 376-381.

Devi, S., Pandey, V. B., Singh, J. P., Shah, A. H., 1987. Peptide alkaloids from *Zizyphus* species. *Phytochemistry* 26, 3374-3375.

Dominguez-Carmona, D. B., Escalante-Erosa, F., Garcia-Sosa, K., Ruiz-Pinell, G., Gutierrez-Yapu, D., Chan-Bacab, M. J., Moo-Puc, R. E., Veitch, N. C., Gimenez-Turba, A., Pena-Rodriguez, L. M., 2011. Metabolites from roots of *Colubrina greggii* var. *yucatanensis* and evaluation of their antiprotozoan, cytotoxic and antiproliferative activities. *J Brazil Chem Soc* 22, 1279-1285.

Eade, R. A., Grand, P. K., McGrath, M. J. A., Simes, J. J. H., Wootton, M., 1967. The stereochemistry of ceanothic acid. *Chem Commun*, 1204-1206.

Erazo, S., Backhouse, N., Delporte, C., Negrete, R., Munoz, O., Lopez-Perez, J. L., San Feliciano, A., 1998. Colubrinic acid isolated from a pharmacological active extract of *Trevoa trinervis* Miers. *Bol Soc Chil Quim* 43, 297-302.

Fotie, J., Bohle, D. S., Leimanis, M. L., Georges, E., Rukunga, G., Nkengfack, A. E., 2006. Lupeol long-chain fatty acid esters with antimalarial activity from *Holarrhena floribunda*. *J Nat Prod* 69, 62-67.

Fu, L., Zhang, S., Li, N., Wang, J., Zhao, M., Sakai, J., Hasegawa, T., Mitsui, T., Kataoka, T., Oka, S., Kiuchi, M., Hirose, K., Ando, M., 2005. Three new triterpenes from *Nerium oleander* and biological activity of the isolated compounds. *J Nat Prod* 68, 198-206.

Fujii, K., Ikai, Y., Oka, H., Suzuki, M., Harada, K., 1997. A nonempirical method using LC/MS for determination of the absolute configuration of constituent

amino acids in a peptide: Combination of Marfey's method with mass spectrometry and its practical application. *Anal Chem* 69, 5146-5151.

Fujiwara, Y., Hayashida, A., Tsurushima, K., Nagai, R., Yoshitomi, M., Daiguji, N., Sakashita, N., Takeya, M., Tsukamoto, S., Ikeda, T., 2011. Triterpenoids isolated from *Zizyphus jujuba* inhibit foam cell formation in macrophages. *J Agric Food Chem* 59, 4544-4552.

Ganapaty, S., Thomas, P. S., Ramana, K. V., Karagianis, G., Waterman, P. G., 2006. Dammarane and ceanothane triterpenes from *Zizyphus glabrata*. *Z Naturforsch B* 61, 87-92.

Gao, Q. H., Wu, C. S., Wang, M., 2013. The Jujube (*Ziziphus Jujuba* Mill.) fruit: A review of current knowledge of fruit composition and health benefits. *J Agric Food Chem* 61, 3351-3363.

Gao, Q. H., Wu, P. T., Liu, J. R., Wu, C. S., Parry, J. W., Wang, M., 2011. Physico-chemical properties and antioxidant capacity of different jujube (*Ziziphus jujuba* Mill.) cultivars grown in loess plateau of China. *Sci Hortic* 130, 67-72.

Gaudencio, S. P., Pereira, F., 2015. Dereplication: racing to speed up the natural products discovery process. *Nat Prod Rep* 32, 779-810.

Giacomelli, S. R., Maldaner, G., Stucker, C., Marasciulo, C., Schmidt, J., Wessjohann, L., Dalcol, II, Morel, A. F., 2007. Triterpenoids from *Gouania ulmifolia*. *Planta Med* 73, 499-501.

Giacomelli, S. R., Missau, F. C., Mostardeiro, M. A., da Silva, U. F., Dalcol, II, Zanatta, N., Morel, A. F., 2001. Cyclopeptides from the bark of *Discaria americana*. *J Nat Prod* 64, 997-999.

Gomez-Romero, M., Segura-Carretero, A., Fernandez-Gutierrez, A., 2010. Metabolite profiling and quantification of phenolic compounds in methanol extracts of tomato fruit. *Phytochemistry* 71, 1848-1864.

Gournelis, D. C., Laskaris, G. G., Verpoorte, R., 1998. Cyclopeptide alkaloids. In: Herz, W., Falk, H., Kirby, G. W., Moore, R. E., Tamm, C. H. (Eds.), Progress in the Chemistry of Organic Natural Products, vol. 75. Springer-Verlag/Wein,

New York, pp. 1-179.

Grishko, V. V., Galaiko, N. V., Tolmacheva, I. A., Kucherov, II, Eremin, V. F., Boreko, E. I., Savinova, O. V., Slepukhin, P. A., 2014. Functionalization, cyclization and antiviral activity of A-secotriterpenoids. *Eur J Med Chem* 83, 601-608.

Grishko, V. V., Tolmacheva, I. A., Pereslavtseva, A. V., 2015. Triterpenoids with a Five-Membered A-Ring: distribution in nature, transformations, synthesis, and biological activity. *Chem Nat Compd* 51, 1-21.

Guo, S., Duan, J. A., Tang, Y. P., Qian, D. W., Zhu, Z. H., Qian, Y. F., Shang, E. X., Su, S. L., 2011a. UHPLC-TOFMS coupled with chemometric method as a powerful technique for rapid exploring of differentiating components between two *Ziziphus* species. *J Sep Sci* 34, 659-666.

Guo, S., Duan, J. A., Tang, Y. P., Qian, Y. F., Zhao, J. L., Qian, D. W., 2011b. Triterpenoids from the fruits of *Ziziphus jujuba* var. *spinosa*. *Biochem Syst Ecol* 39, 880-882.

Guo, S., Duan, J. A., Tang, Y. P., Qian, Y. F., Zhao, J. L., Qian, D. W., Su, S. L., Shang, E. X., 2011c. Simultaneous qualitative and quantitative analysis of triterpenic acids, saponins and flavonoids in the leaves of two *Ziziphus* species by HPLC-PDA-MS/ELSD. *J Pharmaceut Biomed* 56, 264-270.

Guo, S., Duan, J. A., Tang, Y. P., Su, S. L., Shang, E. X., Ni, S. M., Qian, D. W., 2009a. High-performance liquid chromatography-Two wavelength detection of triterpenoid acids from the fruits of *Ziziphus jujuba* containing various cultivars in different regions and classification using chemometric analysis. *J Pharmaceut Biomed* 49, 1296-1302.

Guo, S., Duan, J. A., Tang, Y. P., Yang, N. Y., Qian, D. W., Su, S. L., Shang, E. X., 2010. Characterization of triterpenic acids in fruits of *Ziziphus s*pecies by HPLC-ELSD-MS. *J Agric Food Chem* 58, 6285-6289.

Guo, S., Tang, Y. P., Duan, J. A., Su, S. L., Ding, A. W., 2009b. Two new terpenoids from fruits of *Ziziphus jujuba*. *Chinese Chem Lett* 20, 197-200.

Han, J., Ji, C. J., He, W. J., Shen, Y., Leng, Y., Xu, W. Y., Fan, J. T., Zeng, G. Z., Kong, L. D., Tan, N. H., 2011. Cyclopeptide alkaloids from *Ziziphus apetala*. *J Nat Prod* 74, 2571-2575.

Hanka, L. J., Kuentzel, S. L., Martin, D. G., Wiley, P. F., Neil, G. L., 1978. Detection and assay of antitumor antibiotics. *Recent Results Cancer Res* 63, 69-76.

Hao, J., Zhang, X. L., Zhang, P., Liu, J., Zhang, L. Y., Sun, H. B., 2009. Efficient access to isomeric 2,3-dihydroxy lupanes: first synthesis of alphitolic acid. *Tetrahedron* 65, 7975-7984.

He, C., Peng, B., Dan, Y., Peng, Y., Xiao, P., 2014. Chemical taxonomy of tree peony species from China based on root cortex metabolic fingerprinting. *Phytochemistry* 107, 69-79.

He, X. F., Wang, X. N., Yin, S., Dong, L., Yue, M. M., 2009. Ring A modified Novel Triterpenoids from *Dysoxylum hainanense*. *Eur J Org Chem*, 4818-4824.

Hess, S., Gustafson, K. R., Milanowski, D. J., Alvira, E., Lipton, M. A., Pannell, L. K., 2004. Chirality determination of unusual amino acids using precolumn derivatization and liquid chromatography-electrospray ionization mass spectrometry. *J Chromatogr A* 1035, 211-219.

Hoye, T. R., Jeffrey, C. S., Shao, F., 2007. Mosher ester analysis for the determination of absolute configuration of stereogenic (chiral) carbinol carbons. *Nat Prot* 2, 2451-2458.

Jagadeesh, S. G., Krupadanam, G. L. D., Srimannarayana, G., 2000. A new triterpenoid from *Zizyphus xylopyrus* stem wood. *Indian J Chem B* 39, 396-398.

Ji, C. J., Zeng, G. Z., Han, J., He, W. J., Zhang, Y. M., Tan, N. H., 2012. Zizimauritic acids A-C, three novel nortriterpenes from *Ziziphus mauritiana*. *Bioorg Med Chem Lett* 22, 6377-6380.

Jiang, J. G., Huang, X. J., Chen, J., Lin, Q. S., 2007. Comparison of the sedative

and hypnotic effects of flavonoids, saponins, and polysaccharides extracted from Semen Ziziphus jujube. *Nat Prod Res* 21, 310-320.

Jou, S. J., Chen, C. H., Guh, J. H., Lee, C. N., Lee, S. S., 2004. Flavonol glycosides and cytotoxic triterpenoids from *Alphitonia philippinensis*. *J Chin Chem Soc-Taip* 51, 827-834.

Julian, P. L., Pikl, J., Dawson, R., 1938. The constituents of *Ceanothus Americanus* I Ceanothic acid. *J Am Chem Soc* 60, 77-79.

Kang, Y. F., Liu, C. M., Kao, C. L., Chen, C. Y., 2014. Antioxidant and anticancer constituents from the leaves of *Liriodendron tulipifera*. *Molecules* 19, 4234-4245.

Kang, K. B., Ming, G., Kim, G. J., Ha, T., Choi, H., Oh, W. K., Sung, S. H., 2015. Jubanines F–J, cyclopeptide alkaloids from the roots of *Ziziphus jujuba*. *Phytochemistry* 119, 90-95.

Kawai, K., Nozawa, Y., Ogihara, Y., 1977. Biochemical studies on peptide alkaloids - induction of ion-selective mitochondrial swelling. *Experientia* 33, 1454-1454.

Khokhar, I., Ahmed, A., Kashmiri, M., 1994. Alkaloidal studies of medicinal plants of Pakistan from the root bark of *Zizyphus jujuba* mill. *J Natur Sci Math* 34, 159-163.

Kim, W. I., Zhao, B. T., Zhang, H. Y., Lee, J .H., Son, J. K., Woo, M. W., 2014. Quantitaive and pattern recognition analyses of magnoflorine, spinosin, 6″-feruloyl spinosin and jujuboside A by HPLC in Zizyphi Semen. *Arch Pharm Res* 37, 1139-1147.

Koehn, F. E., Carter, G. T., 2005. The evolving role of natural products in drug discovery. *Nat Rev Drug Discov* 4, 206-220.

Kojima, H., Ogura, H., 1989. Constituents of the Labiatae plants 4. Configurational studies on hydroxy-groups at C-2 C-3 and C-23 or C-24 of oleanene and ursene-type triterpenes by NMR-Spectroscopy. *Phytochemistry* 28, 1703-1710.

Kundu, A. B., Barik, B. R., Mondal, D. N., Dey, A. K., Banerji, A., 1989.

Zizyberanalic acid, a pentacyclic triterpenoid of *Zizyphus jujuba*. *Phytochemistry* 28, 3155-3158.

Kurihara, Y., Ookubo, K., Tasaki, H., Kodama, H., Akiyama, Y., Yagi, A., Halpern, B. 1988, Studies on the taste modifers. I. Purification and structure determination of sweetness inhibiting substance in leaves of *Ziziphus jujuba*. *Tetrahedron*, 44, 61-66.

Lecompte, Y., Rosset, M., Richeval, C., Humbert, L., Arpino, P., 2014. UPLC-ESI-Q-TOF-MS^E identification of urinary metabolites of the emerging sport nutrition supplement methoxyisoflavone in human subjects. *J Pharm Biomed Anal* 96, 127-134.

Lagarias, J. C., Houghten, R. A., Rapoport, H., 1978. Cyclopeptide alkaloids - synthesis of ring-system and its ton affinity. *J Am Chem Soc* 100, 8202-8209.

Leal, I. C., dos Santos, K. R., Junior, II, Antunes, O. A., Porzel, A., Wessjohann, L., Kuster, R. M., 2010. Ceanothane and lupane type triterpenes from *Zizyphus joazeiro* - an anti-staphylococcal evaluation. *Planta Med* 76, 47-52.

Lecompte, Y., Rosset, M., Richeval, C., Humbert, L., Arpino, P., 2014. UPLC-ESI-Q-TOF-MS^E identification of urinary metabolites of the emerging sport nutrition supplement methoxyisoflavone in human subjects. *J Pharm Biomed Anal* 96, 127-134.

Lee, S. M., Min, B. S., Lee, C. G., Kim, K. S., Kho, Y. H., 2003. Cytotoxic triterpenoids from the fruits of *Zizyphus jujuba*. *Planta Med* 69, 1051-1054.

Lee, S. M., Park, J. G., Lee, Y. H., Lee, C. G., Min, B. S., Kim, J. H., Lee, H. K., 2004. Anti-complementary activity of triterpenoides from fruits of *Zizyphus jujuba*. *Biol Pharm Bull* 27, 1883-1886.

Lee, S. S., Chen, W. C., Huang, C. F., Su, Y., 1998. Preparation and cytotoxic effect of ceanothic acid derivatives. *J Nat Prod* 61, 1343-1347.

Lee, S. S., Lin, B. F., Liu, K. C., 1996. Three triterpene esters from *Zizyphus jujuba*. *Phytochemistry* 43, 847-851.

Lee, S. S., Lin, C. J., Liu, K. C., 1992. 2 Triterpenes from *Paliurus ramosissimus*. *J*

Nat Prod 55, 602-606.

Lee, S. S., Shy, S. N., Liu, K. C. S., 1997. Triterpenes from *Paliurus hemsleyanus*. *Phytochemistry* 46, 549-554.

Lee, S. S., Su, W. C., Liu, K. C., 1991. 2 New triterpene glucosides from *Paliurus ramosissimus*. *J Nat Prod* 54, 615-618.

Lee, S. S., Su, W. C., Liu, K. C. S. C., 2001. Cyclopeptide alkaloids from stems of *Paliurus ramossisimus*. *Phytochemistry* 58, 1271-1276.

Li, J. W., Fan, L. P., Ding, S. D., Ding, X. L., 2007a. Nutritional composition of five cultivars of chinese jujube. *Food Chem* 103, 454-460.

Li, L. M., Liao, X., Peng, S. L., Ding, L. S., 2005. Chemical constituents from the seeds of *Ziziphus jujuba* var. *spinosa* (Bunge) Hu. *J Integr Plant Biol* 47, 494-498.

Li, W. H., Zhang, X. M., Tian, R. R., Zheng, Y. T., Zhao, W. M., Qiu, M. H., 2007b. A new anti-HIV lupane acid from *Gleditsia sinensis* Lam. *J Asian Nat Prod Res* 9, 551-555.

Li, X. C., Cai, L., Wu, C. D., 1997. Antimicrobial compounds from *Ceanothus americanus* against oral pathogens. *Phytochemistry* 46, 97-102.

Lin, H. Y., Chen, C. H., Liu, K. C. S. C., Lee, S. S., 2003. 14-membered cyclopeptides from *Paliurus ramosissimus* and *P. hemsleyanus*. *Helv Chim Acta* 86, 127-138.

Lin, H. Y., Chen, C. H., You, B. J., Liu, K. C., Lee, S. S., 2000. Cyclopeptide alkaloids from *Paliurus ramossisimus*. *J Nat Prod* 63, 1338-1343.

Liu, J. J., Chen, B., Yao, S. Z., 2007. Simultaneous analysis and identification of main bioactive constituents in extract of *Zizyphus jujuba* var. *sapinosa* (Zizyphi spinosi semen) by high-performance liquid chromatography-photodiode array detection-electrospray mass spectrometry. *Talanta* 71, 668-675.

Liu, Y. P., Cai, X. H., Feng, T., Li, Y., Li, X. N., Luo, X. D., 2011. Triterpene and sterol derivatives from the roots of *Breynia fruticosa*. *J Nat Prod* 74, 1161-

1168.

Lundgren, L. N., Theander, O., 1988. The Constituents of conifer needles 14. *Cis*-dihydroquercetin and *trans*-dihydroquercetin glucosides from needles of *Pinus sylvestris*. *Phytochemistry* 27, 829-832.

Maldaner, G., Marangon, P., Ilha, V., Caro, M. S., Burrow, R. A., Dalcol, II, Morel, A. F., 2011. Cyclopeptide alkaloids from *Scutia buxifolia* Reiss. *Phytochemistry* 72, 804-809.

Meng, Y. J., Zhang, Y. W., Jiang, H. Y., Bao, Y. L., Wu, Y., Sun, L. G., Yu, C. L., Huang, Y. X., Li, Y. X., 2013. Chemical constituents from the roots of *Zizyphus jujuba* Mill. var. *spinosa*. *Biochem Syst Ecol* 50, 182-186.

Mosmann, T., 1983. Rapid colorimetric assay for cellular growth and survival: application to proliferation and cytotoxicity assays. *J Immunol Methods* 65, 55-63.

Mun, D., Jeong, J., 2006. A Herbological study on the plants of Rhamnaceae in Korea. *Kor J Herbology* 21, 21-33.

Mostardeiro, M. A., Ilha, V., Dahmer, J., Caro, M. S. B., Dalcol, I. I., da Silva, U. F., Morel, A. F., 2013. Cyclopeptide Alkaloids: Stereochemistry and Synthesis of the Precursors of Discarines C and D and Myrianthine A. *J Nat Prod* 76, 1343-1350.

Nielsen, K. F., Mansson, M., Rank, C., Frisvad, J. C., Larsen, T. O., 2011. Dereplication of microbial natural products by LC-DAD-TOFMS. *J Nat Prod* 74, 2338-2348.

Outlaw, W. H., Zhang, S. Q., Riddle, K. A., Womble, A. K., Anderson, L. C., Outlaw, W. M., Outlaw, N. N., Outlaw, E. C., Thistle, A. B., 2002. The jujube (*Ziziphus jujuba* Mill.), a multipurpose plant. *Econ Bot* 56, 198-200.

Pandey, M. B., Singh, A. K., Singh, J. P., Singh, V. P., Pandey, V. B., 2008. Three new cyclopeptide alkaloids from *Zizyphus* species. *J Asian Nat Prod Res* 10, 709-713.

Panseeta, P., Lomchoey, K., Prabpai, S., Kongsaeree, P., Suksamrarn, A.,

Ruchirawat, S., Suksamrarn, S., 2011. Antiplasmodial and antimycobacterial cyclopeptide alkaloids from the root of *Ziziphus mauritiana*. *Phytochemistry* 72, 909-915.

Pawlowska, A. M., Camangi, F., Bader, A., Braca, A., 2009. Flavonoids of *Zizyphus jujuba* L. and *Zizyphus spina-christi* (L.) Willd (Rhamnaceae) fruits. *Food Chem* 112, 858-862.

Plastina, P., Bonofiglio, D., Vizza, D., Fazio, A., Rovito, D., Giordano, C., Barone, I., Catalano, S., Gabriele, B., 2012. Identification of bioactive constituents of *Ziziphus jujube* fruit extracts exerting antiproliferative and apoptotic effects in human breast cancer cells. *J Ethnopharmacol* 140, 325-332.

Prescott, A. G., Stamford, N. P. J., Wheeler, G., Firmin, J. L., 2002. In vitro properties of a recombinant flavonol synthase from *Arabidopsis thaliana*. *Phytochemistry* 60, 589-593.

Quiroz, S., Cespedes, C. L., Alderete, J. B., Alarcon, J., 2015. Ceanothane and oleanane-type triterpenes from *Talguenea quinquenervia* have insecticidal activity against *Cydia pomonella*, *Tenebrio molitor* and *Drosophila melanogaster*. *Ind Crop Prod* 74, 759-766.

Schmidt, U., Lieberknecht, A., Bokens, H., Griesser, H., 1983. Total synthesis of zizyphine-a - synthesis of peptide alkaloids & amino-acids and peptides. *J Org Chem* 48, 2680-2685.

Schmidt, U., Lieberknecht, A., Haslinger, E., 1985. In The Alkaloids - Chemistry and Pharmacology. vol. 26. Academic Press, New York, pp. 299-326.

Seebacher, W., Simic, N., Weis, R., Saf, R., Kunert, O., 2003. Complete assignments of H-1 and C-13 NMR resonances of oleanolic acid, 18 alpha-oleanolic acid, ursolic acid and their 11-oxo derivatives. *Magn Reson Chem* 41, 636-638.

Sekar, K., Parthasarathy, S., Kundu, A. B., Barik, B. R., 1992. Structure of dimethyl ceanothate. *Acta Crystallogr C* 48, 2251-2253.

Seto, T., Tanaka, T., Tanaka, O., Naruhashi, N., 1984. Beta-glucosyl esters of 19-

alpha-hydroxyursolic acid-derivatives in leaves of *Rubus* Species. *Phytochemistry* 23, 2829-2834.

Shao, Z. Y., Zhu, D. Y., Guo, Y. W., 2002. Two new triterpene esters from *Daphniphyllum oldhami. Chin Chem Lett* 13, 1181-1184.

Suksamrarn, S., Panseeta, P., Kunchanawata, S., Distaporn, T., Ruktasing, S., Suksamrarn, A., 2006. Ceanothane- and lupane-type triterpenes with antiplasmodial and antimycobacterial activities from *Ziziphus cambodiana. Chem Pharm Bull* 54, 535-537.

Suksamrarn, S., Suwannapoch, N., Aunchai, N., Kuno, M., Ratananukul, P., Haritakun, R., Jansakul, C., Ruchirawat, S., 2005. Ziziphine N, O, P and Q, new antiplasmodial cyclopeptide alkaloids from *Ziziphus oenoplia* var. *brunoniana. Tetrahedron* 61, 1175-1180.

Tadic, V. M., Jeremic, I., Dobric, S., Isakovic, A., Markovic, I., Trajkovic, V., Bojovic, D., Arsic, I., 2012. Anti-inflammatory, gastroprotective, and cytotoxic effects of *Sideritis scardica* extracts. *Planta Med* 78, 415-427.

Tan, N. H., Zhou, J., 2006. Plant cyclopeptides. Chemical reviews 106, 840-895.

Tang, W. J., Zhang, Y. L., Xiao, Q. P., Huang, C., Jin, Y., Li, J., 2013. Four flavanocoumarins from the leaves of *Litsea coreana* LEVL. *Chem Biodivers* 10, 1128-1132.

Taniguchi, S., Imayoshi, Y., Kobayashi, E., Takamatsu, Y., Ito, H., Hatano, T., Sakagami, H., Tokuda, H., Nishino, H., Sugita, D., Shimura, S., Yoshida, T., 2002. Production of bioactive triterpenes by *Eriobotrya japonica* calli. *Phytochemistry* 59, 315-323.

Thuong, P. T., Min, B. S., Jin, W. Y., Na, M., Lee, J., Seong, R., Lee, Y. M., Song, K., Seong, Y., Lee, H. K., Bae, K., Kang, S. S., 2006. Anti-complementary activity of ursane-type triterpenoids from *Weigela subsessilis*. *Biol Pharm Bull* 29, 830-833.

Trevisan, G., Maldaner, G., Velloso, N. A., Sant'Anna Gda, S., Ilha, V., Velho Gewehr Cde, C., Rubin, M. A., Morel, A. F., Ferreira, J., 2009.

Antinociceptive effects of 14-membered cyclopeptide alkaloids. *J Nat Prod* 72, 608-612.

Tripathi, M., Pandey, M. B., Jha, R. N., Pandey, V. B., Tripathi, P. N., Singh, J. P., 2001. Cyclopeptide alkaloids from *Zizyphus jujuba*. *Fitoterapia* 72, 507-510.

Tschesche, R., Hillebrand, D., 1977. Alkaloide aus Rhamnaceen 30. Scutianine-G, additional cyclopeptide alkaloid from *Scutia buxifolia*. *Phytochemistry* 16, 1817-1818.

Tschesche, R., Hillebrand, D., Wilhelm, H., Ammermann, E., Eckhardt, G., 1977. Alkaloids from Rhamnaceae 29. Hysodricanine-a, scutianine-F, mauritine-H and aralionine-C - 4 additional cyclopeptide alkaloids from *Ziziphus*, *Scutia* and *Araliokhamnus*. *Phytochemistry* 16, 1025-1028.

Tschesche, R., Khokhar, I., Wilhelm, H., Eckhardt, G., 1976. Alkaloids from Rhamnaceae 27. Jubanine-a and jubanine-B, new cyclopeptide alkaloids from *Ziziphus jujuba*. *Phytochemistry* 15, 541-542.

Um, S., Choi, T. J., Kim, H., Kim, B. Y., Kim, S. H., Lee, S. K., Oh, K. B., Shin, J., Oh, D. C., 2013. Ohmyungsamycins A and B: cytotoxic and antimicrobial cyclic peptides produced by *Streptomyces* sp. from a volcanic island. *J Org Chem* 78, 12321-12329.

Wei, X. H., Yang, S. J., Liang, N., Hu, D. Y., Jin, L. H., Xue, W., Yang, S., 2013. Chemical constituents of *Caesalpinia decapetala* (Roth) Alston. *Molecules* 18, 1325-1336.

Wolfender, J. L., Marti, G., Thomas, A., Bertrand, S., 2015. Current approaches and challenges for the metabolite profiling of complex natural extracts. *J Chromatogr A* 1382, 136-164.

Yagi, A., Okamura, N., Haraguchi, Y., Noda, K., Nishioka, I., 1978. Studies on the constituents of Zizyphi Fructus 1. Structures of three new *p*-coumaroylates of alphitolic acid. *Chem Pharm Bull* 26, 1798-1802.

Yang, B., Yang, H. S., Chen, F., Hua, Y. L., Jiang, Y. M., 2013. Phytochemical analyses of *Ziziphus jujuba* Mill. var. *spinosa* seed by ultrahigh performance

liquid chromatography-tandem mass spectrometry and gas chromatography-mass spectrometry. *Analyst* 138, 6881-6888.

Yang, X. Q., Peng, T. F., Yang, Y. B., Li, W., Xiong, J., Zhao, L. X., Ding, Z. T., 2015. Antimicrobial and antioxidant activities of a new benzamide from endophytic *Streptomyces* sp. YIM 67086. *Nat Prod Res* 29, 331-335.

Yang, X. W., Wang, J. S., Ma, Y. L., Xiao, H. T., Zuo, Y. Q., Lin, H., He, H. P., Li, L., Hao, X. J., 2007. Bioactive phenols from the leaves of *Baccaurea ramiflora*. *Planta Med* 73, 1415-1417.

Yili, A., Mutalipu, Aisa, H. A., Isaev, M. I., 2009. Betulinic acid and sterols from *Astragalus altaicus*. *Chem Nat Compd* 45, 592-594.

Yoshikawa, K., Kondo, Y., Kimura, E., Arihara, S., 1998. A lupane-triterpene and a 3(2→1)abeolupane glucoside from *Hovenia trichocarea*. *Phytochemistry* 49, 2057-2060.

Yu, L., Jiang, B. P., Luo, D., Shen, X. C., Guo, S., Duan, J. A., Tang, Y. P., 2012. Bioactive components in the fruits of *Ziziphus jujuba* Mill. against the inflammatory irritant action of Euphorbia plants. *Phytomedicine* 19, 239-244.

Zhang, D. M., Xu, H. G., Wang, L., Li, Y. J., Sun, P. H., Wu, X. M., Wang, G. J., Chen, W. M., Ye, W. C., 2015. Betulinic acid and its derivatives as potential antitumor agents. *Med Res Rev* 35, 1127-1155.

Zhang, P., Xu, L., Qian, K., Liu, J., Zhang, L., Lee, K. H., Sun, H., 2011. Efficient synthesis and biological evaluation of epiceanothic acid and related compounds. *Bioorg Med Chem Lett* 21, 338-341.

Zhang, X. Y., Cai, X. H., Luo, X. D., 2012. Chemical constituents of Allophylus longipes. *Chin J Nat Med* 10, 36-39.

국문초록

대추나무 (*Ziziphus jujuba* Mill.) 는 갈매나무과 (Rhamnaceae) 에 속하는 다년생 낙엽수로서 남부 유럽과 아시아에 걸쳐 널리 분포되어 있다. 대추나무의 열매는 예전부터 말린 상태로 식용되어 왔으며, 또한 열매와 종자는 여러 문화권의 전통 의학에서 약물로서 다양한 용도로 오래 전부터 사용되어 왔다.

대추나무로부터 분리 보고된 성분들 중 cyclopeptide alkaloid 와 ceanothane-type triterpenoid 류 물질은 갈매나무과 식물들에서 특이적으로 관찰되는 화합물이다. Cyclopeptide alkaloid는 α-amino acid와 styrylamine이 결합하여 13, 14, 또는 15원환을 형성하는 구조의 화합물로서 진정 작용, 항균, 항진균, 항말라리아 등의 다양한 생리 활성이 보고되어 있는 화합물 군이다. Ceanothane-type triterpene은 식물에서 보다 흔하게 관찰되는 lupane-type triterpene의 A-ring이 5원환으로 transformation된 화합물 구조군으로서 현재까지 28 종의 화합물만이 보고되어 있으며 대부분 갈매나무과 식물에서 분리 보고된 바 있다. 이들 물질 또한 암세포에 대한 세포 독성과 HIV에 대한 항바이러스 효과와 같은 생리 활성이 보고된 바 있다.

최근의 분석 기술 발전으로 등장한 UHPLC-qTOF-MS는 식물 추출물과 같은 복잡한 혼합물을 단시간에 분석 가능한 플랫폼으로 주목을 받았으며, 이를 이용하여 혼합물로부터 기존에 알려진 화합물 구조를 식별하는 dereplication 기술은 천연물 연구에 있어 빼놓을 수 없는 기술이 되어가고 있다. 본 연구에서는 UHPLC-qTOF-MS를 이용하여 대추나무로부터 갈매나무과의 특이적 성분군인 cyclopeptide alkaloid 및 ceanothane-type triterpene에 속하는 신규 화합물을 효율적으로 분리

하고 그 생리 활성을 규명하는 것을 주요 목적으로 하였다.

대추나무의 뿌리, 가지, 잎, 열매를 채집하여 메탄올 추출물을 수득한 후 각각의 cyclopeptide alkaloid와 triterpenic acid를 분석하는 UHPLC-qTOF-MS 프로파일링 조건을 확립하였다. 또한 확립된 프로파일링 조건 하에서 얻어진 UV, MS 및 MS/MS 데이터를 이용하여 cyclopeptide alkaloid 와 triterpenic acid의 구조를 예측하는 dereplication 방법을 개발하였다. 그 결과 대추나무의 뿌리 추출물에서 이전에 분리 보고되지 않은 것으로 여겨지는 cyclopeptide alkaloid 및 triterpenic acid 의 chromatographic peak를 다수 확인하여 신규 화합물 분리에 적합한 후보 추출물임을 확인하였다. UHPLC-qTOF-MS 크로마토그램을 이용하여 기존에 밝혀지지 않은 molecular formula를 갖는 신규 화합물을 추적하여 분리하는 targeted isolation 전략을 활용하여 대추나무 뿌리 추출물로부터 각 성분의 분리를 수행하였다. 그 결과 9종의 cyclopeptide alkaloids (**1-9**), 37종의 triterpenoids (**10-46**), 6종의 phenolic compounds (**47-52**) 를 분리 및 구조동정 하였다. 분리한 37종의 triterpenoids 중 11종은 lupane-type, 1종은 oleanane-type, 1종은 ursane-type triterpene이었으며 나머지 24종은 기존에 목표하였던 ceanothane-type의 triterpenoid 임을 밝혔다. 분리한 52종의 화합물 중 화합물 **1-5**, **16-20**, **23**, **24**, **26**, **27**, **30**, **33**, **35-43**의 26종은 천연에서 처음으로 분리보고 되는 물질로, 각각 jubanine F-J (**1-5**), epiceanothic acid 2-methyl ester (**16**), 3-dehydroxy ceanothetric acid (**17**), 3-dehydroxy ceanothetric acid 2-methyl ester (**18**), ceanothetric acid 2-methyl ester (**19**), 3-dehydroxy-ceanotha-27α-carboxy-28β,19β-olide (**20**), 3-*O*-methyl-zizyberanalic acid (**23**), 1,28-dinor-24-hydroxy-lup-2,17(22)-diene-27-oic acid (**24**), 2-*O*-

vanilloyl alphitolic acid (**26**), 3-*O*-protocatechuoyl alphitolic acid (**27**), 2-*O*-*p*-hydroxybenzoyl alphitolic acid (**30**), 3-*O*-protocatechuoyl ceanothic acid 2-methyl ester (**33**), 3-*O*-vanilloyl epiceanothic acid (**35**), 3-*O*-vanilloyl ceanothic acid 2-methyl ester (**36**), 3-*O*-*p*-hydroxybenzoyl ceanothic acid (**37**), 3-*O*-*p*-hydroxybenzoyl epiceanothic acid (**38**), 2-*O*-protocatechuoyl epiceanothanolic acid (**39**), 3-*O*-protocatechuoyl-ceanotha-28β,19β-olide (**40**), 7-*O*-vanilloyl-3-dehydroxy ceanothetric acid 2-methyl ester (**41**), epicatechinoceanothic acid A-C (**42-44**) 로 명명하였다. 분리한 화합물들중 dereplication 과정에서 그 구조가 예측된 물질들은 실제 구조가 예측된 구조와 일치함을 확인하였으며, 대추나무 뿌리, 가지, 잎, 열매 추출물의 성분 프로파일 상의 peak들과 일치함을 확인하였다.

분리된 화합물을 대상으로 세포 독성, 항바이러스, 항염증 등의 약리활성에 대한 스크리닝을 수행하였다. Cyclopeptide alkaloid 계열 화합물 **2**, **3**, **6**은 porcine epidemic diarrhea virus에 대하여 선택적인 저해 활성을 보였다. Triterpenoid 화합물 중 **10**, **22**, **28-30**, **33**, **35**, **36**, **41**은 인간 유래 간암세포주인 HepG2에 대한 강한 세포 독성을 보였다.

이상의 실험 결과로부터 UHPLC-qTOF-MS를 활용한 dereplication은 천연물로부터 생리 활성을 갖는 새로운 화합물 발견에 효율적인 방법임을 확인하였다. 또한 본 실험에서 확립된 dereplication 조건을 활용하여 갈매나무과의 타 종 식물들로부터 추가적인 신규 생리활성 화합물의 발견이 가능할 것으로 전망된다.

주요어 : 대추나무, dereplication, UHPLC-qTOF-MS, cyclopeptide alkaloid, triterpenoids,

학번 : 2012-3045